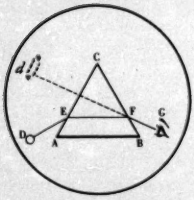

optics and spectroscopy

volume vii
number 4
october 1959

OPTICAL SOCIETY OF AMERICA

RUSSIAN EDITORIAL STAFF

Editor: S. E. FRISH

Assistant Editor: P. P. FEOFILOV
Corresponding Secretary: L. S. SAZONOV

Associate Editors:

M. M. GUREVICH M. A. EL'IASHEVICH A. A. LEBEDEV V. P. LINNIK
S. L. MANDEL'SHTAM I. V. OBREIMOV V. K. PROKOF'EV
N. N. SOBOLEV A. N. TERENIN A. I. TUDOROVSKII

Translated on the Initiative of
THE OPTICAL SOCIETY OF AMERICA, INC.
With a Grant-in-Aid from
THE NATIONAL SCIENCE FOUNDATION

TRANSLATION EDITORIAL STAFF

Scientific Editors

FRED W. BEHNKE, *Perkin-Elmer Corp.*

CYRUS FELDMAN, *Oak Ridge National Laboratory*

GEORGE HERRMAN, *Columbia University*

Administrative Editor: PATRICIA R. WAKELING, *OSA*

Published monthly by the Optical Society of America, Inc. Executive office: 1155 Sixteenth Street, N.W., Washington, D.C. Subscriptions for one year to members of the Society: Associates $13.00; Regular members and Fellows $17.00. Subscriptions for non-members of the Society: One year U. S. and Possessions, $25.00; Foreign $28.00. Back numbers: $3.00 per copy. Subscriptions, changes of address and undeliverable copies should be referred to the Executive offices in Washington, D.C. The office of publication is 2500 South State Street, Ann Arbor, Michigan. Second class postage paid at Ann Arbor, Michigan.

Printed in the U.S.A. by Edwards Brothers, Inc., Ann Arbor, Michigan.

THE CLASSIFICATION OF SECONDARY RADIATION

B. I. Stepanov and P. A. Apanasevich

Received 24 January 1959

A quantum-electrodynamical analysis of the transformation of light by matter yields a systematic classification of secondary radiation, justifying its division into scattering or photoluminescence, depending on the absence or presence of intermediate processes between the disappearance and appearance of photons. The limits of adapting the criteria for duration and decay suggested by Vavilov are clarified.

1. As a rule, the propagation of light is accompanied by luminescence of the medium. Depending on the observed characteristics, this secondary radiation is classified as photoluminescence (fluorescence and phosphorescence) or induced emission (Rayleigh and Raman scattering, reflection, etc.). Such a division is based on the criterion of duration (or the closely connected criterion of decay), proposed by Vavilov[1] for classifying nonequilibrium emissions.*

*According to Wiedemann[2] and Vavilov,[1] by nonequilibrium emission we understand emission of the substance in excess of its thermal emission.

Vavilov's criterion represents a generalization of several experimental facts—a practical convenience, but as yet without a theoretical basis. The limits of its application are not entirely clear.

According to the criterion of duration, luminescence is defined as nonequilibrium radiation having a long afterglow (longer than the period of the light fluctuation) and therefore capabable of decaying. Induced emission is that part of the luminescence which disappears (appears) practically instantaneously after the cessation (beginning) of the outside excitation. It is assumed that the forced emission does not decay.

Application of the criteria of duration and decay allowed Vavilov to classify nonequilibrium emissions accurately in two cases: the clarification of the Vavilov-Cherenkov radiation[3, 4]* and the demonstration that the

*Here other properties of the radiation were considered.

"universal" blue luminescence of pure solutions appears to be due to organic impurities. This criterion is useful in daily practice, e.g., for the elimination of photoluminescence in scattering observations.

Applying the criterion of duration to resonance emission meets with serious difficulties. On this basis, resonance emission should be classified as photoluminescence, because it possesses a long afterglow and a clearly defined decay behavior. At the same time, when the density of the luminescent vapor increases, the diffuse resonance radiation turns into a specular reflection,[5-9] which demonstrates its coherence with the incident radiation. The coherence of resonance emission also follows from theory.[10, 11] Thus, resonance emission has properties which are not included among the ordinary properties of luminescence, and are characteristic only of induced processes.

Although much theoretical and experimental work has been devoted to resonance emission, in the literature one finds most inconsistent explanations of its nature. Some authors call it resonance fluorescence;[10-12] others —resonance scattering.[13-16] Several authors have attempted to point out the nature of this type of radiation, and following Wood,[17] have called it resonance emission.[18] According to Vavilov,[1] when the frequency of the exciting light approaches the absorption frequency, "the conversion of scattering to resonance emission is not a gradual one," and these phenomena always coexist. At the same time, according to Pringsheim,[12] varying the frequency of the illuminating light may bring about a continuous transition from Rayleigh scattering to resonance emission.

Thus, the question of classifying secondary radiation demands a detailed theoretical analysis.

Experimentally, both scattering and photoluminescence are observed in primary and secondary radiation beams, and represent phenomena of the same type. Both phenomena show different and for the most part coexisting aspects of a single phenomenon—the transformation of radiation by matter. Thus, in theory we must regard them jointly from a single point of view. Only in this manner can we find out the essential differences among them and connect them with a mechanism of the light-transformation process, and hence give a proper theoretical and fundamental classification of secondary radiation.

An over-all treatment of all the diverse aspects of secondary emission is evidently not, in general, possible within the framework of classical theory. The general theory of the classical dipole gives a good description of many properties of scattering and of resonance emission, but does not explain the existence of photoluminescence under stationary illumination conditions, and therefore cannot systematically resolve the question of classifying secondary radiation. In addition, we should note that the criterion of duration does not agree with the results of the classical theory. Investigations of scattering and resonance emission, treated by the classical theory as emission caused by forced vibration of a dipole, show that they decay and have prolonged afterglow.[19-21]

As shown in references 20, 22-24, in contrast to classical theory, quantum electrodynamics permits a systematic treatment of all the various secondary radiations and an investigation of the dependence of their properties on those of the excitation, as well as on the properties of the matter that transforms the light.

In the present work, the results obtained in references 22-24 are utilized for classifying secondary radiation. Some aspects of the question of classification have already been briefly considered in references 19 and 25.

2. In quantum electrodynamics, the transformation of light is considered as the result of the interaction of quantized electromagnetic field with matter. This interaction is described by a system of equations of the type*:[22, 20]

*Equation (1) represents Schrödinger's equations including interactions. In the derivation interactions proportional to the square of the vector potential are not

taken into account. This part of the interaction of fields and matter leads to scattering. Quantitatively it is small. It must be taken into account to explain the proportionality between the intensity and the fourth power of the frequency of the scattered light.[14]

$$i\hbar\frac{\partial c_{i(n_\chi)}}{\partial t} = -\sum_{j,\chi'}\frac{(P_{\chi'})_{ij}\sqrt{n_{\chi'}+1}}{\sqrt{V\omega_{\chi'}}}e^{i(\omega_{ij}-\omega_{\chi'})t}c_{j(n_\chi+1_{\chi\chi'})} - \sum_{j,\chi'}\frac{(P^+_{\chi'})_{ij}\sqrt{n_{\chi'}}}{\sqrt{V\omega_{\chi'}}}e^{i(\omega_{ij}+\omega_{\chi'})t}c_{j(n_\chi-1_{\chi\chi'})} + \sum_j M_{ij}e^{i\omega_{ij}t}c_{j(n_\chi)} \quad (1)$$

Here $c_{i(n_\chi)}$ is the amplitude of the probability of finding the matter in state i and the field in state (n_χ). The index $(n_\chi) = n_1, n_2 \ldots n_\chi \ldots$ designates a set of numbers of photons; $\omega_{\chi'}$ is the frequency of photon χ'; ω_{ij} is an eigenfrequency of the material; $(p_{\chi'})_{ij}$ and $(p^+_{\chi'})_{ij}$ are the matrix elements of the interaction between matter and field; and M_{ij} are the matrix elements of the interaction between molecule and environment (assuming that the matter consists of a molecule interacting with light and the environment) and the interactions among various degrees of freedom inside the molecule.

The two first terms of the right-hand side of Eq. (1) indicate a change in $c_{i(n_\chi)}$ as a result of optical transitions (changes in the states of field and matter). Changes of $c_{i(n_\chi)}$, due to nonoptical transitions are described by the third term. As seen from (1), for optical transitions the state of the field changes only by one photon $(\pm\delta_{\chi\chi'})$. Therefore any process of light transformation, e.g., the process of the disappearance of incident photons and the appearance of new secondary photons, can occur only with the help of an intermediate state. In such a process at least two molecular transitions are involved: a transition in which an incident photon disappears from the field, and a transition accompanied by the appearance of a new photon. These transitions can occur either one immediately after the other, or separately, when some intermediate process intervenes, converting the system from one state of excitation to another. For example, as a result of the disappearance of an incident photon χ' (because the levels are broad, the photon frequency may be arbitrary) the system can change from some initial level i to an intermediate level k. From level k, by means of optical or nonoptical transitions, it may enter other excited k' or unexcited j levels. For optical transitions $k - k'$ or $k - j$ a photon χ'' appears in the field. Here we have a process which transforms photon χ' into photon χ'', and involves a single intermediate state (and not an intermediate transition). If, however, as a result of the transition $k - k'$ the system enters the excited level k', then with optical transitions new photons χ'' can arise from it too. The appearance of these photons is separated from the disappearance of the incident photon χ' by the intermediate (optical or nonoptical) transition $k - k'$. In an analogous way we may distinguish processes of light transformation which take place with the help of two or more intermediate transitions. The secondary radiation of atoms and molecules usually observed experimentally is the resultant of the joint action of all such processes of light transformation.

Thus, the transformation of light by matter can be theoretically represented as a combination of simple molecular processes, which take place with and without the help of various numbers of intermediate transitions.*

*Usually only a process of light transformation occurring without redistribution is considered (a two-photon process). In this way, it is true, scattering and resonance emission are investigated separately.[10-15, 28] All types of luminescence, including photoluminescence, are usually treated from the point of view of a single-photon process as emitted light occurring when excitation ceases.[10, 14] In references 19, 20, 22-25, in addition to processes occurring without intermediate transitions, other processes of light transformation are also considered.

Defining the properties of each of them on the basis of Eq. (1), we can determine their similarities and differences, and consequently resolve the problem of classifying secondary radiation.

For each partial process we may introduce the concept of its own quantum yield. The quantum yield of the entire process of light transformation is defined by the ratio of the number of secondary photons $N_{sec.}$, appearing per unit time, to the number of photons $N_{abs.}$ disappearing from the primary beam in the same time. The number of secondary photons may be represented as the sum $N_{sec.} = \Sigma N_m$, where N_m is the number of photons transformed with the help of m (m = 0, 1, 2 ...) intermediate transitions. The number of photons disappearing from the field is equal to

$$N_{abs.} = N_0 + N_{nonrad.} + N_{redist.},$$

where $N_{nonrad.}$ and $N_{redist.}$ are the numbers of photons absorbed by matter which do not return to the field as the result of nonradiative transitions and redistribution among excited levels. From this, for the quantum yield B, we have

$$B = \frac{\sum_{m=0}^{\infty} N_m}{N_{abs.}} = \sum_{m=0}^{\infty} B_m. \quad (2)$$

Introducing the following quantity into (2)

$$B_m = \frac{N_m}{N_0 + N_{nonrad.} + N_{redist.}} \quad (3)$$

gives the quantum yield of a part of the process of light transformation occurring with the help of m intermediate transitions.

Let us examine briefly the characteristics of the separate phases of a secondary emission.

3. Solving Eq. (1) for steady-state illumination under the conditions $n_\chi = n^0_\chi = \text{const.}$ and $|c_{i(n_\chi)}|^2 = a_i = \text{const.}$, it is easily shown[10, 23-26] that a transformation of light occurring without the aid of intermediate processes, can be described by the expression*

*Equation (4) is a generalization of Eqs. (11), (12), and (27) of reference 22. In its derivation the width of the final level $2\gamma_j$ is not taken into account.

$$I_{i\to j}(\omega'\to\omega'') = \frac{\omega''^2 I_0(\omega')}{2\pi^2\hbar^2 c^4\omega'^2}\left|\sum_k\left[\frac{(p^+_{\chi'})_{jk}(p_{\chi''})_{ki}}{-i\gamma_k+\omega_{ki}-\omega'}+\frac{(p_{\chi''})_{jk}(p^+_{\chi'})_{ki}}{\omega_{ki}+\omega''}\right]\right|^2 \times |a_i|^2\,\delta(\omega_{ij}-\omega'+\omega''), \quad (4)$$

where $I_{i\to j}(\omega'-\omega'')$ is the intensity of the secondary radiation at frequency ω'', which arises from transition of the system from state i to state j; $I_0(\omega')$ is the intensity of the incident light; $|a_i|^2$ is the probability that the system remains at the initial level i. The quantities $2\gamma_k$ represent the widths of the intermediate levels k, or, in other words, the probabilities that the system will leave these levels. In the usual case they consist of three parts: the probability of optical transitions $2\gamma_k^{opt.}$, the probability of nonradiative transitions $2\gamma_k^{nonrad.}$ (nonoptical transitions in nonexcited states), and the probability of redistribution $2\gamma_k^{redist.}$ (nonoptical transitions to other excited levels), that is

$$\gamma_k = \gamma_k^{(\text{opt.})} + \gamma_k^{(\text{nonrad.})} + \gamma_k^{(\text{redist.})} \qquad (5)$$

As indicated by the δ-function, the transformation of light described in (4) occurs either with conservation of frequency (i = j) or with its conversion to an eigenfrequency of the material ω_{jj} (i ≠ j). The power of this portion of the secondary radiation is obtained from (4) by integration with respect to ω′:

$$I_{i\to j}(\omega'') = \frac{\omega''^2 I_0(\omega''+\omega_{ji})}{4\pi^2\hbar^2c^4(\omega''+\omega_{ji})^2}\left|\sum_k\left[\frac{(p_{v'}^+)_{jk}(p_{v''})_{ki}}{-i\gamma_k+\omega_{kj}-\omega''}+\frac{(p_{v''})_{jk}(p_{v'}^+)_{ki}}{\omega_{ki}+\omega''}\right]\right|^2|a_i|^2. \qquad (6)$$

The spectral composition of secondary radiation (6) depends essentially on the spectral composition of the primary radiation $I_0(\omega''+\omega_{ji})$. When a material is illuminated by nonresonance lines which are not too broad (when $|\omega_{kj}-\omega''| \gg \gamma_k$) it is possible in (6) to neglect the dependence of all factors on ω″ except $I_0(\omega''+\omega_{ji})$. In this case the shape and location of the lines of secondary radiation are determined by the spectral composition of the illumination.

For resonance illumination, one may neglect all the nonresonance components in (6) in comparison with the resonance components (it is assumed that the distance between the various ω_{kj} is larger than γ_k). As a result we obtain

$$I_{i\to j}(\omega'') = \frac{\omega''^2 I_0(\omega''+\omega_{ji})}{4\pi^2\hbar^2c^4(\omega''+\omega_{ji})^2}\frac{\left|(p_{v'}^+)_{jk}\right|^2\left|(p_{v''})_{ki}\right|^2}{\gamma_k^2+(\omega_{kj}-\omega'')^2}|a_i|^2. \qquad (6a)$$

In this case it is necessary to consider the ω″-dependence not only of the quantity $I_0(\omega''+\omega_{ji})$ but of the denominator as well. For illumination by narrow resonance lines ($\Delta\omega \ll \gamma_k$) just as in the absence of resonance, the shapes and locations of lines of secondary radiation are determined solely by the quantity $I_0(\omega''+\omega_{ji})$. On the other hand, for illumination by wide ($\Delta\omega \gg \gamma_k$) resonance lines they do not depend on $I_0(\omega''+\omega_{ji})$ but are determined rather by the properties of the material. In this case, the lines of secondary emission look like the natural lines of the material emitted, e.g., by thermal excitation, although the transformation of radiation by this mechanism occurs in the same way as for exposure by narrow lines, or for the absence of resonance. All light transformations which occur without intermediate transitions show a strong correlation of frequencies between the secondary and primary light.

The quantum yield of a light transformation, occurring without the aid of intermediate transitions, is determined by expression (3) with m = 0. It is possible to show[20] that the ratios among N_0, $N_{\text{nonrad.}}$ and $N_{\text{redist.}}$ are of the same order of magnitude as the corresponding ratios of transitions probabilities, averaged in some way over all possible transitions. Therefore the order of magnitude of the quantum yield B_0 may be characterized by the relation

$$B_0 \approx \frac{\gamma_{\text{opt.}}}{\gamma_{\text{opt.}}+\gamma_{\text{nonrad.}}+\gamma_{\text{redist.}}}, \qquad (7)$$

where $\gamma_{\text{opt.}}$, $\gamma_{\text{nonrad.}}$, and $\gamma_{\text{redist.}}$ represent respectively $\gamma_k^{(\text{opt.})}$, $\gamma_k^{(\text{nonrad.})}$, and $\gamma_k^{(\text{redist.})}$, averaged over all sublevels k.

As the probability of nonoptical transitions $2(\gamma_{\text{nonrad.}}+\gamma_{\text{redist.}})$ increases, the quantum yield B_0 decreases, i.e., the secondary radiation described in (6) decays. However, as seen from (6), the decrease of B_0 is not always accompanied by a corresponding decrease in the intensity of this radiation. With nonresonance illumination, the intensity of radiation (6) actually does not depend on the quantity γ_k. It may be shown that in this case the decrease of B_0 is caused by the increasing absorption.*

*Exactly the same connection among yield, intensity of emission, and absorption occurs in the classical theory of induced emission.[18, 20, 25]

In resonance transformation of light the increase of $\gamma_{\text{nonrad.}}+\gamma_{\text{redist.}}$ leads to decreased quantum yield and radiation intensity. By varying the frequency of the exposing light it is possible to bring about a continuous transition from one case to the other and to satisfy one's self that the change which occurs this way is purely quantitative in nature.

4. Let us examine the properties of light transformed with the help of intermediate processes. On the basis of Eq. (1) it may be shown that the intensity of secondary radiation occurring with m intermediate transitions, for stationary illumination conditions, be described by the expression:*

*Equation (8) represents a generalization of Eqs. (13) and (34) in reference 22. For more detailed analysis see reference 24.

$$I_{k\to j}^{(m)}(\omega'') = \frac{\omega''^2}{8\pi^2c^2\hbar}\frac{\left|(p_{v''}^+)_{jk}\right|^2\left|Q_k^{(m)}(\omega')\right|^2}{\gamma_k^2+(\omega_{kj}-\omega'')^2}, \qquad (8a)$$

where $|Q_k^{(m)}(\omega')|^2$ is the probability that after m redistributions the system will find itself at the level k. This probability depends on both the properties of the system transforming the light, and those of the illumination conditions.

As seen from (8a), the secondary radiation occurring with intermediate processes consists of lines whose shapes and locations do not depend at all on the spectral composition of the illumination. Only the integral of the line intensities depends on the illumination conditions (through $Q_k^{(m)}(\omega')$). These, the natural lines of the material, have a dispersive shape with half-width γ_k.

Portions of the secondary radiation corresponding to different m comprise the same lines, coinciding in shape and location. They are impossible to separate experimentally, and therefore must be regarded as a single radiation. Superimposed one on the other, they constitute a luminescence with the intensity

$$I_{k\to j}^{(\text{tot.})}(\omega'') = \frac{\omega''^2}{8\pi^2c^2\hbar}\frac{\left|(p_{v''}^+)_{kj}\right|^2\sum_{m=1}^{\infty}\left|Q_k^{(m)}(\omega')\right|^2}{\gamma_k^2+(\omega_{kj}-\omega'')^2} \qquad (8b)$$

and a quantum yield[20, 24]

$$B_1 = \sum_{m=1}^{\infty} B_m \approx \frac{\gamma_{\text{redist.}}}{\gamma_{\text{opt.}}+\gamma_{\text{nonrad.}}+\gamma_{\text{redist.}}}\cdot\frac{\gamma_{\text{opt.}}}{\gamma_{\text{opt.}}+\gamma_{\text{nonrad.}}}. \qquad (9)$$

An increase in the probability of nonradiative transitions $2\gamma_{\text{nonrad.}}$ always leads to a decrease of B_1, satisfying the following relation

$$\frac{B_1}{B_0} \sim \frac{\gamma_{\text{redist.}}}{\gamma_{\text{opt.}}+\gamma_{\text{nonrad.}}}. \qquad (10)$$

An increase in the probability of redistribution $2\gamma_{\text{redist.}}$, on the other hand, leads to an increase of the quantum yield of emission occurring with the participation of intermediate processes. Under the condition $\gamma_{\text{redist.}} \gg \gamma_{\text{opt.}}+\gamma_{\text{nonrad.}}$, which is satisfied, e.g., in complex molecules, B_1 is represented by the well-known formula usually obtained for the quantum yield of lum-

inescence[27] (the first factor in (9) equal to 1). In this case B_0, as seen from (7), is vanishingly small, i.e. transformations of light without redistribution is practically absent. In contrast to a transformation of light which occurs without the intermediate processes, a change of quantum yield B_1, is always accompanied by a corresponding variation of intensity (8b).

We have examined above the properties of the separate lines of secondary radiation. Experimentally, narrow lines are only observed for transformations of light by simple systems (in rarefied atomic vapors and simple molecules). In the case of complex systems the frequencies ω_{kl} and ω_{lj} are close to each other, and therefore the separate lines strongly overlap, forming more or less wide bands. The shape and location of these bands can depend in a complex way on the properties of the material as well as on the conditions of illumination. In the limiting case of very complex systems, e.g., in complex molecules, in which redistributions of excitation energy among vibration sublevels occur very rapidly, and therefore most of the radiation is emitted after the establishment of equilibrium,[27] the shape of the emission bands within wide limits does not depend on the frequency of the exposing light.

5. If exposure ceases instantaneously at a certain time $t = t_e$, the radiation described in (6) and (8b) also disappears practically instantaneously. However, after this, the atoms and molecules excited during the steady-state illumination will revert to the normal state, which leads to the production of afterglow. The properties of the afterglow can be determined from the solution of Eq. (1), provided that at the initial instant of time photons are absent from the field and the distribution of the system among its energy levels corresponds to the steady state. Calculations show[20, 23, 25] that afterglow occurs in any case of radiation transformation. Independently of the spectral composition of the exciting light, it consists of the natural lines of the material. The decay time of the afterglow is also independent of the conditions of excitation. It is determined only the the properties of the system illuminated (expressed by the coefficients $\gamma_k^{(opt.)}$, $\gamma_k^{(nonrad.)}$ and $\gamma_k^{(redist.)}$).

To each process of light transformation in steady-state operation, there corresponds a specific fraction of the afterglow. Comparing the spectrum of secondary radiation, transformed with the participation of intermediate processes, with the spectrum of its afterglow, we are easily convinced that the spectra completely coincide with one another in the location of lines as well as in their shapes. On the other hand, light transformed without intermediate processes generally does not coincide in its spectral composition with the corresponding afterglow. Only for resonance exposure by light of a wide spectral composition, when the steady-state radiation has the appearance of natural lines, do both spectra coincide with each other. However, this coincidence is clearly superficial.

6. From the point of view of quantum electrodynamics, transformations of light represent a process of disappearance of primary and appearance of secondary photons. In this connection there is no difference between photoluminescence and scattering, between scattering and resonance emission, etc. The differences in the mechanism of light-transformation processes consist only in whether the disappearance and appearance of photons follow one directly after the other, or whether intermediate transitions intervene. The theoretical basis for classifying secondary radiation certainly must take these differences into account. As shown in the preceding sections, it has been established, based on the mechanism of radiation transformation, that all secondary radiation may be consistently and unambiguously divided into two classes, showing essential differences in their properties.

If, between the events of the disappearance of primary photons and the appearance of secondary photons, there occur intervening processes, the secondary emission is characterized by the following properties: (a) the shape and positions of its lines do not depend on the conditions of excitation (natural lines of the material); (b) changes in the quantum yield are always accompanied by a corresponding change in the intensity of the radiation (a proportional change, for constant absorption); (c) the spectrum of the radiation under stationary illumination conditions coincides with the spectrum of the afterglow. It is well known that all types of luminescence excited by nonoptical means have such characteristics. Therefore, in strict accord with generally accepted concepts, secondary radiation which occurs with the help of intermediate processes must be regarded as photoluminescence.

Intermediate processes, which participate in the transformation of radiation, lead to a loss of connection (correlation) between the properties of the primary and secondary photons. As a result of this, the excitation of a material and the emission of radiation are taken as independent processes and can be considered separately. The usual treatment of photoluminescence (see reference 4) coincides exactly with such a representation of the light-transformation process.

If the disappearances of photons are not separated from each other by intermediate processes, then the light transformation occurs with a strong correlation between the frequencies of primary and secondary photons, and therefore is sometimes taken as a single-photon process.*

*In particular, Weisskopf[11] and Heitler[15] take this view in discussing single-photon emission.

Secondary radiation, which is transformed without the help of intermediate processes possesses the following characteristic properties: (a) the shape and position of its lines depend on the spectral composition of the illuminating light; (b) variation of yield does not indicate variation of radiation intensity; (c) the spectrum in the steady state does not coincide with the spectrum of the corresponding afterglow. Only in one special case (often realized experimentally), namely, illumination with wide resonance lines, does the indicated property not appear externally, and the radiation under consideration possesses properties practically coincident with the properties of radiation aided by intermediate processes. However, as already noted, this case does not in fact differ from light transformation with illumination by narrow lines or in the absence of resonance.

Equation (6), describing this part of secondary radiation, represents a generalization of the Kramers-Heisenberg formula, which doubtless applies to scattering, to include resonance. For $i = j$ it characterizes Rayleigh scattering and resonance emission, and completely coincides with the classic expression for induced radiation of a dipole. For $i \neq j$ Eq. (6) describes Raman scattering. In the case of resonance this radiation is usually called fluorescence, although according to its nature it represents resonance Raman scattering.

Without exception, radiation transformed without intermediate processes must be considered as Rayleigh and Raman scattering.

Thus, theoretical analysis indicates that classification of secondary radiation in principle cannot be based on the criteria of duration* and decay, because any radi-

*The limitations of the duration criterion are shown in another way by Ovander.[15]

ation is accompanied by a lasting afterglow and possesses a quantum yield which decreases with increasing probability of nonradiative transitions. Moreover, there is no single experimentally observed quantity which could serve as a universal criterion for a theoretically sound classification of secondary radiation. The practical discrimination of scattering from photoluminescence must be carried out with account taken of the many properties of the radiation.

However, it does not follow from the above that duration and decay cannot be utilized for practical classification. As seen from (10), when the probability of nonradiative transitions increases, the quantum yield of photoluminescence decreases considerably faster than the quantum yield of scattering. Therefore in many cases it is possible to suppress photoluminescence almost completely in comparison with scattering. This possibility is often utilized experimentally in observing scattering. In this sense, decay has a good theoretical basis as a criterion.

As noted, in the absence of resonance the intensity of scattering, in practice, does not depend on the probability of nonradiative transitions, and the steady-state spectrum is situated in a frequency region different from that of the afterglow spectrum. Therefore, by measuring only the intensity of nonresonance scattering, it is impossible to detect its decay; noncoincidence of the spectra of the stationary state and the afterglow can be taken as absence of afterglow, however. In this sense, duration and extinction also preserve their practical significance as criteria for nonresonance illumination, and can be utilized successfully for classification. Direct application of them to the case of resonance is difficult because of the discrepancy between the variation of quantum yield and the intensity of scattering, and also because the noncoincidence of steady-state emission and afterglow spectra demands minute investigation, which with overlapping lines is generally impossible.

The present work studies the possibility of using for classification such properties of radiation as decay, duration, and dependence of spectral composition on the conditions of illumination. The properties of coherence and polarization are not considered here. As noted by Vavilov[1] they cannot serve as a basis for classifying secondary radiation.

According to both experiment and theory, only Rayleigh scattering and resonance emission are coherent with the primary radiation. Within the framework of quantum electrodynamics, coherence of resonance emission has been demonstrated by Weisskopf[11] and investigated in detail by Heitler.[10] Raman scattering and photoluminescence are not coherent, as is well known.

The connection between the polarization of secondary and primary light can take many forms. It is determined not only by the nature of the illuminated molecules and the properties of the illuminating light, but also by the orientation of the molecules in space, which is dependent on the presence of external fields or crystalline structure. Introduction of a tensor connecting the polarization factors of emitted and exciting light permits consideration of the polarization of various types of secondary radiation from a single point of view. Preliminary calculations show no essential difference between the polarization of photoluminescence and scattering.

REFERENCES

1. S. I. Vavilov. Sobr. soch. t.2, staty 20, 28, and 29. Izd. Akad. Nauk SSSR, 1952.
2. E. Wiedemann. Wied. Ann. 34, 446 (1889); Wied. Ann. 37, 177 (1889).
3. P. A. Cherenkov. Doklady Akad. Nauk SSSR 2, 451 (1934).
4. S. I. Vavilov. Doklady Akad. Nauk SSSR 2, 257, (1934).
5. R. Wood. Physik. Z. 10, 425 (1909); Physik. Z. 13, 353 (1912); Phil. Mag. 23, 689 (1912); Phil. Mag. 44, 1105 (1922).
6. W. Rump. Z. Physik 29, 196 (1924).
7. O. Schnettler. Z. Physik. 65, 55 (1930).
8. M. Spitzer. C. R. Acad. Sci. 241, 631 (1955); C. R. Acad. Sci. 244, 2036 (1957).
9. J. A. Galt and H. L. Welsh. Canad. J. Phys. 35, 114 (1957).
10. B. Gaitler (Heitler). "Kvantovaya teoriya izlucheniya." (Quantum Theory of Radiation), IL, Moscow, 1956.
11. V. Weisskopf. Ann. Physik. 9, 23 (1931).
12. P. Pringsheim. "Fluorescenciya i fosforescenciya." (Fluorescence and Phosphorescence), IL, Moscow, 1951.
13. G. Plachek. "Releevskoye rasseyanie i raman-effekt." (Rayleigh Scattering and the Raman-Effect), Khar'kov, 1935.
14. A. I. Akheizer and B. V. Berestetskii. "Kvantovaya electrodinamika." (Quantum Electrodynamics), GITTL, 1955.
15. L. N. Ovander. Opt. i Spektr. 5, 10 (1958).
16. R. Lennuier. C. R. Acad. Sci. 218, 665 (1944); C. R. Acad. Sci. 224, 1022 (1957).
17. R. W. Wood. Phil. Mag. 10, 513 (1905); Phil. Mag. 10, 521 (1905).
18. A. Mitchel and M. Zemanskii. "Rezonancnoe izluchenie i vozbuzhdennie atomy." (Resonance Emission and Excited Atoms), GNTI, 1937.
19. B. I. Stepanov and P. A. Apanasevich. Izv. Akad. Nauk SSSR, Ser. Fiz. 22, 1380 (1958).
20. P. A. Apanasevich. Dissertatsiya. (Dissertation), Minsk, Belgosuniversitet, 1958.
21. S. I. Vavilov. Sobr. Soch., t. 1, Paper No. 37, Izd. Akad. Nauk SSSR, 1954.
22. P. A. Apanasevich. Opt. i Spektr. 5, 97 (1958).
23. P. A. Apanasevich. Tr. Inst. Fiz. Mat. Akad. Nauk SSSR 2, 55 (1957).
24. P. A. Apanasevich. Tr. Inst. Fiz. Mat. Akad. Nauk SSSR v. 3, 72 (1958).
25. B. I. Stepanov and P. A. Apanasevich. Doklady Akad. Nauk SSSR 116, 772 (1957).
26. L. N. Ovander. Opt. i. Spektr. 2, 781 (1957); Opt. i Spektr. 3, 221 (1957); Opt. i Spektr. 4, 555 (1958).
27. B. I. Stepanov. "Liuminestsentsiya slozhnykh molekul." (Luminescence of Complex Molecules), Izd. Akad. Nauk SSSR, Minsk, 1956.

DEPENDENCE OF THE INTENSITY OF SOME HELIUM LINES ON PRESSURE

V. E. Yakhontova and M. I. Kliot-Dashinskii

Received 26 February 1959

The pressure dependence of the intensity of the 5016 A and 3965 A lines of helium in a discharge tube is examined theoretically. It is shown that in the general case, the emission intensity and the gas pressure are related by a nonlinear expression which depends upon the existence in the discharge of self-absorption effects.

It is shown that the theoretical relationships obtained are in quantitative agreement with the experimental results.

1. In the study of the gaseous discharge by optical methods, one frequently encounters a process by which the radiation emitted by a gas at some wavelength is absorbed by the same gas, and then is re-radiated in the form of light of a different wavelength. In the present work we will examine the influence of this effect on the pressure dependence of the intensity of certain helium lines.

We will examine a cylindrical tube of radius R, containing helium at a pressure p, which can be changed. We will pass a narrow parallel beam of electrons of a given velocity along the axis of this tube, thereby exciting the gas. The radius of the electron beam is r_0; the beam current is made so small that we can ignore collisions between excited atoms and beam electrons. The pressure of the gas in the tube is made so low that collisions between excited and normal atoms, which might result in energy exchange, can also be ignored. In this case, as follows from reference 1, the flux of energy emitted at frequency ν_{jk} per unit length of the beam is

$$F_{jk} = \frac{A_{jk}}{\sum_{i=1}^{j-1} A_{ji}} N \frac{i}{e} \sum_{i=1}^{j-1} Q_{ji} h\nu_{ji}. \qquad (1)$$

where A_{jk} is the probability of transition with radiation from level j to level k, N is the number of helium atoms per unit volume, i is the beam current, e is the charge of an electron, and Q_{jk} is the effective excitation cross section of the line (corresponding to the transition from level j to level k) excited by a collision with an electron.

If direct excitation of atoms by collisions with electrons is the only source of radiation of the line under consideration, and if absorption of the line by the gas within the tube is insignificant and can be neglected, the intensity of that line will be proportional to F_{jk}, and consequently proportional to pressure.

Direct proportionality between intensity and pressure can be confirmed by experiment for a number of helium lines.[2] However, for certain lines which do not experience absorption (in particular, for the 5016 A line) the dependence of intensity upon pressure cannot be expressed by a linear law. This shows that in the excitation of such lines, along with direct excitation of atoms by electronic collisions, an essential role is also played by other processes.

A qualitative explanation of the phenomenon for the 5016 A line has been given by Lees and Skinner.[3] It consists of the following. From the 3^1P level, transition is possible either to the 2^1S level, with emission of the 5016 A line, or to the normal 1^1S level with emission of the 537 A line.* Since under the conditions being considered most of the gas atoms are in the normal state, the 5016 A radiation will pass through the tube almost without being absorbed, but the 537 A radiation is absorbed to a considerable extent. Atoms, excited to the 3^1P level, will therefore appear even outside the electron beam; these atoms will then emit light at 537 A and 5016 A. Thus the tube becomes a volume source of radiation, the brightness of which varies with distance from the axis of the tube, and is distributed along the radius in a manner dependent upon the pressure.

*The transition $3^1S - 3^1P$ is also possible, but extremely improbable. We do not consider it.

2. We will examine a surface in the form of a cylinder of radius $r \leq R$, coaxial with the tube. The energy flux per unit length passing through this surface will be $F_1(r)$ for the short wavelength radiation 537 A, and $F_2(r)$ for the long wavelength radiation 5016 A. We will define the dependence of these fluxes upon r. In order to simplify the problem we will consider the tube to be infinitely long.

We will concern ourselves first with the short wavelength radiation. Together with the idea of energy flux $F_1(r)$, we introduce the concepts of incident and emergent fluxes, $F_{1\downarrow}(r)$ and $F_{1\uparrow}(r)$ respectively, defining them by the equations

$$F_{1\downarrow}(r) = 2\pi r \int_0^{2\pi} d\varphi \int_0^{\pi/2} I(r, \vartheta, \varphi) \cos\vartheta \sin\vartheta d\vartheta, \qquad (2)$$

$$F_{1\uparrow}(r) = 2\pi r \int_0^{2\pi} d\varphi \int_{\pi}^{\pi/2} I(r, \vartheta, \varphi) \cos\vartheta \sin\vartheta d\vartheta. \qquad (3)$$

Here $I(r, \theta, \phi)$ is the intensity of the energy flux of short wavelength radiation at the point M, situated at a distance r from the axis of the tube and corresponding to a direction MN characterized by angles θ and ϕ.* It is obvious that $F_1 = F_{1\downarrow} - F_{1\uparrow}$.

*The angles θ and ϕ are defined in the following manner. From the point M a perpendicular MM' is erected to the axis of the tube. Angle θ is the angle between perpendicular MM' and direction MN. Angle ϕ is in plane P perpendicular to segment MM', and is reckoned from line MK, parallel to the axis of the tube, to line MN', which is the projection of MN upon plane P.

We will consider the change of the emergent flux on going from a surface of radius r to a surface of radius r + dr

$$dF_{1\uparrow}(r) = -\chi\alpha(r) F_{1\uparrow}(r) dr + \beta(r) dr. \qquad (4)$$

Here χ is the coefficient of absorption of helium at 537 A, and $\alpha(r)dr$ is the average path length for the rays between the cylindrical surfaces of radii r and r + dr. The quantity $\beta(r)dr$ expresses the increase in flux caused

by emission by the medium. Considering change in incident flux, we obtain analogously

$$dF_{1\downarrow}(r) = \varkappa_3(r)\,F_{1\downarrow}(r)\,dr - \beta(r)\,dr. \qquad (5)$$

Let us define the quantity $\beta(r)dr$. This is half the energy of the short wavelength radiation emitted by an annulus of unit length and limited by the two cylindrical surfaces of radii r and r + dr. If $\epsilon_1(r)$ is the coefficient of emission of the medium at 537 A, then

$$\beta(r)\,dr = \frac{1}{2}\cdot 2\pi r\cdot 4\pi\cdot \varepsilon_1(r)\,dr.$$

In order to define the quantity $\epsilon_1(r)$ we will consider the source of the radiation described by this function. Let $f = A_2/(A_1 + A_2)$, where A_1 is the probability of the transition with emission of the line 537 A, and A_2 is the analogous quantity for the line 5016 A. The short wavelength radiation is absorbed in passing through the helium atmosphere in the tube, and then a portion of the absorbed energy equal to $1 - f$ is re-emitted at the same wavelength. This process can be considered as scattering, with the coefficient $\chi(1 - f)$ and a spherical index of scattering. In addition, when $r \leqslant r_0$ true emission takes place, originating as a result of the excitation of the gas by the electron beam. Thus[4]

$$\varepsilon_1(r) = (1-f)\,\varkappa\int I(r,\,\vartheta,\,\varphi)\,\frac{d\omega}{4\pi} + \varepsilon_{01}(r), \qquad (6)$$

where $\epsilon_{01}(r)$ is the coefficient of true radiation of the medium.

Let Q_1 and Q_2 be the effective cross sections of excitation of 537 A and 5016 A; let ν_1 and ν_2 be the frequencies of these lines; and let $\delta(r)$ be a function equal to 1 for $r \leqslant r_0$, and to 0 for $r > r_0$. Then $\epsilon_{01}(r) = \mu_{01}\delta(r)$, where, corresponding to formula (1),

$$\mu_{01} = N\,\frac{i}{e}\,\frac{Q_1+Q_2}{4\pi^2 r_0^2}\,(1-f)\,h\nu_1. \qquad (7)$$

We will expand the quantity $I(r, \vartheta, \phi)$ into a Fourier series as a function of the angle ϕ, given over the interval $[0, 2\pi]$. Taking into account the conditions of symmetry $I(\phi) = I(-\phi) = I(\pi - \phi)$, we obtain

$$I(r,\,\vartheta,\,\varphi) = a_0(r,\,\vartheta) + a_2(r,\,\vartheta)\cos 2\varphi + a_4(r,\,\vartheta)\cos 4\varphi + \ldots \qquad (8)$$

If this transformation is substituted in formulas (2), (3), and (6), and integration is performed with respect to ϕ, then only the coefficient $a_0(r, \vartheta)$ will appear in the expressions for the quantities $F_{1\downarrow}(r)$, $F_{1\uparrow}(r)$, and $\epsilon_1(r)$. Transforming this coefficient into a Fourier cosine series in the interval $[0, \pi]$, and limiting it to the first two members of the series

$$a_0(r,\,\vartheta) = A(r) + B(r)\cos\vartheta, \qquad (9)$$

we will have

$$F_{1\downarrow}(r) = \frac{2}{3}\,\pi^2 r\,[3A(r) + 2B(r)], \quad F_{1\uparrow}(r) = \frac{2}{3}\,\pi^2 r\,[3A(r) - 2B(r)], \qquad (10)$$

$$F_1(r) = F_{1\downarrow}(r) - F_{1\uparrow}(r) = \frac{8}{3}\,\pi^2 r B(r), \qquad (11)$$

$$\varepsilon_1(r) = \varkappa(1-f)\,A(r) + \varepsilon_{01}(r). \qquad (12)$$

Substituting Eqs. (10) and (12) into Eqs. (4) and (5), we receive a system of equations for definition of A and B

$$3A' + 2B' + 3A\left(\frac{1}{r} + k\right) + 2B\left(\frac{1}{r} + \varkappa\right) = 6\varepsilon_{01},$$
$$3A' - 2B' + 3A\left(\frac{1}{r} - k\right) - 2B\left(\frac{1}{r} - \varkappa\right) = -6\varepsilon_{01}, \qquad (13)$$

where $k = \chi\alpha - 2\chi(1 - f)$.

In solving the system (13) we make the approximation that the quantity α is a constant.*[3] Then

*It can be shown that if the intensity $I(r, \vartheta, \phi)$ is defined by the series (8) and (9), then $\alpha(r)$ lies within the limits $1.75 \leqslant \alpha \leqslant 2$ and consequently depends only slightly upon r.

$$3A(r) = [c_1 - \delta(r)\,\sigma_1]\,\frac{e^{-r\sqrt{k\varkappa}}}{r} + [c_2 - \delta(r)\,\sigma_2]\,\frac{e^{r\sqrt{k\varkappa}}}{r} + \frac{6\varepsilon_{01}(r)}{k},$$

$$2B(r) = \sqrt{\frac{k}{\varkappa}}\left\{[c_1 - \delta(r)\,\sigma_1]\,\frac{e^{-r\sqrt{k\varkappa}}}{r} - [c_2 - \delta(r)\,\sigma_2]\,\frac{e^{r\sqrt{k\varkappa}}}{r}\right\} - \frac{6\varepsilon_{01}(r)}{k\varkappa r}, \qquad (14)$$

where σ_1 and σ_2 are constants, the values of which are found from the conditions of continuity of the functions A(r) and B(r) at the point r_0

$$\sigma_1 = \frac{3\mu_{01}\,(r_0\sqrt{k\varkappa} - 1)}{k\sqrt{k\varkappa}}\,e^{r_0\sqrt{k\varkappa}}, \quad \sigma_2 = \frac{3\mu_{01}\,(r_0\sqrt{k\varkappa} + 1)}{k\sqrt{k\varkappa}}\,e^{-r_0\sqrt{k\varkappa}},$$

and c_1 and c_2 are constants defined by the boundary conditions $F_{1\downarrow}(R) = 0$ and $F_1(0) = 0$:

$$c_1 = \frac{\dfrac{6\mu_{01}}{k\sqrt{k\varkappa}} + \sigma_1 - \sigma_2}{1 + \dfrac{1-\sqrt{\frac{k}{\varkappa}}}{1+\sqrt{\frac{k}{\varkappa}}}\,e^{-2R\sqrt{k\varkappa}}}, \quad \frac{c_2}{c_1} = -\frac{1-\sqrt{\frac{k}{\varkappa}}}{1+\sqrt{\frac{k}{\varkappa}}}\,e^{-2R\sqrt{k\varkappa}}.$$

The constant α may be defined by the law of conservation of energy. The energy radiated in a unit of time within a cylinder of unit length and radius r is equal to the energy flux through the surface of this cylinder, plus the energy absorbed in its volume. In a unit of volume, the quantity of energy absorbed in a unit of time is equal to $\chi f \int I d\omega = 4\pi\chi f A$. Consequently, the condition of conservation of energy assumes the form

$$4\pi^2\rho^2\mu_{01} = F_1(r) + 8\pi^2\varkappa f\int_0^r A(r)\,r\,dr \quad (0 \leqslant r \leqslant R), \qquad (15)$$

where $\rho = r$ when $r \leqslant r_0$, and $\rho = r_0$ when $r \geqslant r_0$. Carrying out the indicated calculation, we find that the relationship (15) is fulfilled if $\alpha = 2$.

Taking into account the meanings of the constants σ_1, σ_2, c_1, c_2, and α of the formulas (11) and (14), it is easy to obtain a final expression for flux $F_1(r)$. In particular, when $r_0 \leqslant r \leqslant R$ we have

$$F_1(r) = \frac{8\pi^2\mu_{01}}{\gamma}\cdot\frac{1+\gamma_0 h\gamma_0 - ch\gamma_0}{1+\frac{1-\sqrt{f}}{1+\sqrt{f}}\,e^{-2\gamma R}}\left[e^{-\gamma r} + \frac{1-\sqrt{f}}{1+\sqrt{f}}\,e^{-\gamma(2R-r)}\right], \qquad (16)$$

where $\gamma = 2\chi\sqrt{f}$.

We will now examine the long wavelength radiation. It consists of radiation directly excited by the electron beam, and of radiation from the gas in the entire volume of the tube brought about by the transformation of short wavelength radiation into long wavelength radiation. We will indicate by $\Delta F_2(r)$ that part of the flux $F_2(r)$ which is a result of transformation of radiation. Then, outside the region occupied by the electron beam ($r \geqslant r_0$),

$$F_2(r) = 4\pi\mu_{02}\cdot\pi r_0^2 + \Delta F_2(r), \qquad (17)$$

where μ_{02} is the coefficient of true radiation of the medium at 5016 A which is determined from formula (1), analogous to the coefficient of true radiation given by (7)

$$\mu_{02} = N \frac{i}{e} \frac{Q_1 + Q_2}{4\pi^2 r_0^3} f h\nu_2. \tag{18}$$

Let us find the quantity $\Delta F_2(r)$. The quantity of short wavelength radiation absorbed in one second in the volume of a cylinder of unit length and radius $r (r \geq r_0)$ is equal to

$$E(r) = 4\pi\mu_{01} \cdot \pi r_0^2 - F_1(r).$$

This quantity of energy corresponds to $E(r)/h\nu_1$ elementary absorption events. Since each of these leads to a single emission of a quantum of frequency ν_2(5016 A), then

$$\Delta F_2(r) = \frac{E(r)}{h\nu_1} \cdot h\nu_2 = \left[4\pi^2 r_0^3 \mu_{01} - F_1(r)\right] \frac{\nu_2}{\nu_1}. \tag{19}$$

From formulas (17), (18), (19), and (16) it follows that outside the region occupied by the electron beam we have

$$F_2(r) = N \frac{i}{e} (Q_1 + Q_2) h\nu_2 \left\{ 1 - \frac{2(1-f)}{(\gamma r_0)^2} \cdot \frac{1 + \gamma r_0 \operatorname{sh} \gamma r_0 - \operatorname{ch} \gamma r_0}{1 + \frac{1-\sqrt{f}}{1+\sqrt{f}} e^{-2\gamma r}} \left[e^{-\gamma r} + \frac{1-\sqrt{f}}{1+\sqrt{f}} e^{-\gamma(2R-r)} \right] \right\}, \tag{20}$$

where $\gamma = 2\chi\sqrt{T}$, and the coefficient of absorption χ is defined by the equation $\chi = \tau_\alpha N$. Here τ_α is the atomic coefficient of absorption of the line 537 A, $N = p/KT$, K is the Boltzmann constant, and T is the temperature of the gas. Thus $\gamma = 2\sqrt{T}(\tau_\alpha/KT)p$ so that for any fixed r, the quantity $F_2(r)$ is a nonlinear function of pressure.

3. Let us compare our theoretical conclusions with our experimental results. A measurement of the pressure dependence of the intensity of helium lines was performed by Yakhontova on an apparatus described in reference 2.

The optical portion of this apparatus consisted of a tube, a condensing lens, and a monochromator. The image of the electron beam was focussed on the plane of the entrance slit of the monochromator by means of the condenser lens, and intersected the slit at right angles, halfway up its long dimension. The illumination conditions of the entrance slit and the width of the exit slit of the monochromator were chosen such that all the light falling on the entrance slit would pass through the exit slit and strike the detector.

Light from a certain portion of the volume of the tube falls on the monochromator (Fig. 1). In order to determine the shape of this portion we will construct the image of the entrance slit of the monochromator, which is formed by the condensing lens in the plane P_1, which passes through the axis of the tube perpendicularly to the optic axis. If from each point of this image we construct a cone whose apex is that point and whose base is the condensing lens, then the volume delineated by the envelope of these cones and the wall of the tube will give us half the desired volume. The other half is symmetrical with the first, and is situated on the other side of the plane P.

To determine the extent to which the various portions of the tube contribute to the intensity of the line 5016 A, we compute the energy $(dF_2(r)/dr)dr$ radiated in one second by an annulus having unit length and bounded by cylindrical surfaces with radii r and r + dr. According to formula (20), this energy is proportional to $e^{-\gamma r}$, so that the emission in an annulus of thickness dr decreases rapidly with increasing r. In addition, if the diameter of

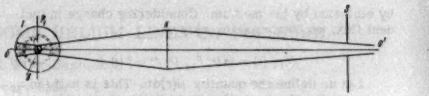

Fig. 1. Arrangement for the illumination of the monochromator slit. T—tube, K—condenser, S—plane of the slit, OO'—optic axis of the system.

the ring, 2r, is greater than the height of the image of the slit, then, as can be seen from the figure, light from only a portion of the annulus will fall on the monochromator; the larger r is made, the smaller this portion becomes. All this leads to the fact that the basic role in determining the intensity of a line, as observed in the monochromator, is played by the radiation emitted by a cylinder coaxial with the tube, whose length is equal to its width and whose diameter is equal to the height of the slit image. It can be shown that the contribution of the remaining part of

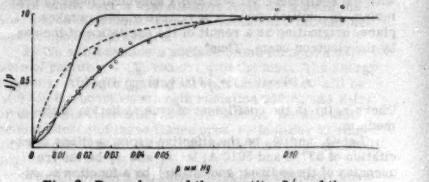

Fig. 2. Dependence of the quantity J/p of the line 5016 A upon pressure. 1—experimental curve; 2—Curve constructed according to formula (21); 3—Curve constructed according to formula (22).

the volume is not greater than 5% when $r_0 = 0.1$ cm, $p \geq 0.035$ mm Hg, and the height of the slit image $2b \geq 0.28$ cm.

Let Φ be the light flux of wavelength 5016 A falling on the monochromator. In the indicated approximation it is obviously equal to

$$\Phi = 2a \frac{\omega_0}{4\pi} F_2(b),$$

where 2a is the width, 2b the altitude of the slit image, and ω_0 the solid angle within which the condenser is seen from the center of the tube. The observed intensity of the line is proportional to Φ. Consequently, in accordance with (20), the ratio of intensity of the line to pressure is proportional to the quantity

$$\frac{J}{p} \sim 1 - \frac{2(1-f)}{(\gamma r_0)^2} \cdot \frac{1 + \gamma r_0 \operatorname{sh} \gamma r_0 - \operatorname{ch} \gamma r_0}{1 + \frac{1-\sqrt{f}}{1+\sqrt{f}} e^{-2\gamma R}} \times \left[e^{-\gamma b} + \frac{1-\sqrt{f}}{1+\sqrt{f}} e^{-\gamma(2R-b)} \right]. \tag{21}$$

Fig. 2 shows the experimental dependence of J/p on pressure, as obtained by Yakhontova (curve 1), and also a theoretical curve constructed according to formula (21) (curve 2). The experimental curve was obtained under the conditions indicated at the beginning of Section 1. The ordinates of both curves are in relative units. In the construction of the theoretical curve it was assumed (in accordance with the experimental conditions) that b = 0.14

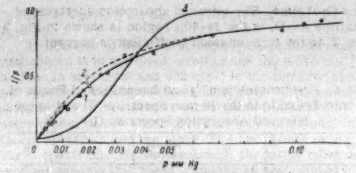

Fig. 3. Dependence of the quantity J/p for He 3965 A on pressure. 1—Experimental curve, 2—Curve constructed according to formula (21), 3—Curve constructed according to formula (22).

cm, R = 2.5 cm, r = 0.1 cm. The coefficient of absorption χ and the quantity f were calculated on the basis of data on the oscillator strengths of helium.[5] (This reference is absent from the bibliography of the original paper—translator's note.) In connection with this it has been shown that $\chi = 2056$ p cm^{-1} (p in mm Hg), and f = 0.019. It can be seen from the sketch that although the theoretical curve lies a little higher than the experimental, they have the same general shape. For example, if we take $\chi = 1028$ p cm^{-1} (half the calculated value), the curves will coincide almost perfectly.

Approximate theoretical computation of the dependence of the intensity of He 5016 A on pressure was performed also by Lees and Skinner.[3] However these authors assumed (in order to simplify the problem greatly and to avoid mathematical difficulties) that after absorption of short wavelength radiation, re-emission takes place along the axis of the tube (this greatly magnifies the role of absorption) and that all the radiation is propagated in a radial direction (this decreases the role of absorption). They also assumed that the radius of the tube was infinite. According to the calculations of Lees and Skinner

$$F_2(r) = \frac{N\frac{i}{e}(Q_1 + Q_2)fh\nu_2}{1 - (1-f)(1-e^{-\chi r})}$$

and consequently,

$$\frac{J}{P} \approx \frac{f}{1 - (1-f)(1-e^{-\chi b})}. \qquad (22)$$

Curve 3 of Fig. 2 is calculated according to formula (22), with b = 0.14 cm and $\chi = 2056$ p cm^{-1}. Clearly, the character of this curve differs from the experimental one, so that the two could not be made to coincide with any value of χ.

We remark in conclusion that He 3965 A also does not yield a linear dependence of intensity upon pressure. This is explained by the same reasoning as for the He 5016 A. Thus the intensity of He 3965 A is described by the same formula (21) where, however, $\chi = 770$ p cm^{-1} and f = 0.027. The corresponding curves, experimental (1) and theoretical, constructed according to formulas (21) (curve 2) and (22) (curve 3) are shown in Fig. 3.

REFERENCES

1. G. Messi and E. Barkhop. "Elektronnye i ionnye stolkovenniya." (Electron and Ion Collisions), I.L., Moscow, 1958.
2. V. E. Yakhontova. Vestnik, L.G.U. (Bulletin Leningrad State Univ.) 10, 27 (1959).
3. J. H. Lees and H. W. Skinner. Proc. Roy. Soc. A 137, 186 (1932).
4. V. V. Sobolev. "Perenos luchistoi energii v atmosfepakh zvezd i planet." (The Transfer of Radiant Energy in the Atmospheres of Stars and Planets), GITTL, Moscow, 1956.

VIBRATIONAL SPECTRUM AND THE STRUCTURE OF THE ARSENIC TRIOXIDE MOLECULE

V. P. Cheremisinov

Received 9 February 1959

The Raman spectrum of crystalline arsenic trioxide was studied and eleven lines were found, of which the most intense line was 365 cm^{-1}. An investigation of the infrared spectrum was carried out in the region 2.5-40μ. In this region six absorption bands were found, of which four were very intense. Analysis of the Raman spectrum and infrared absorption showed that they agreed well with an As_4O_6 molecular species which belongs to the symmetry point group T_d. This conclusion was found in agreement with the x-ray investigation of arsenic trioxide. An interpretation of the vibrational spectrum of As_2O_3 was presented.

INTRODUCTION

According to the results of Zachariasen,[1] all vitreous oxides which form single component glasses must have a coordination structure. However, it is possible to foresee that this is not likely at the melting point of these oxides in crystalline and vitreous states.

Actually it was established by the x-ray method for the crystalline modifications of P_2O_5, As_2O_3, and Sb_2O_3[2] and by spectroscopic methods for liquid P_2O_5, crystalline P_2O_5, and vitreous B_2O_3[3-7] that these substances, which have a comparatively low melting point, have a molecular structure.

Arsenic trioxide in the solid state exists in three modifications: two crystalline and one vitreous.[8] The low temperature crystalline form (octahedral) is converted into a high temperature monoclinic form when heated to ~275°C. The octahedral form has a molecular lattice.[2] The structure of the monoclinic form has not been definitely established up to this time. Investigation by electron diffraction of arsenic trioxide in the gas phase[9] showed that As_2O_3 consists of dimeric molecules As_4O_6 which beling to the point group T_d.

Borisov and Gorshtein[10] assumed that the vitreous form of As_2O_3, as distinct from the low temperature crystalline form, is an "irregular, extended atomic lattice" which would confirm the hypothesis of Zachariasen. But the fact that the vitreous form converts into the octahedral form on devitrification gives proof of the similarity of their structures. Also, investigations of the in-

frared absorption spectrum of vitreous arsenic trioxide[11] showed it has a great resemblance to the infrared absorption spectrum of the octahedral form. This similarity of the infrared spectra provides a still stronger basis for confirmation of the similarity of the vitreous and low-temperature crystalline form. Thus, it is possible to be confident that a study of the structure of the low temperature form of arsenic trioxide using data about its vibrational spectrum will not only give an opportunity to confirm the x-ray and chemical data, but will also assist in the study of the structure of vitreous arsenic trioxide since the x-ray method does not give reliable results in this case.

EXPERIMENTAL METHOD

The Raman spectrum of As_2O_3 was obtained by the powder method with the exciting light passing through a layer of the substance being studied, the thickness of which was selected experimentally (1 mm). A diagram of the equipment is shown in Fig. 1. A low pressure mercury lamp was used as the source of excitation. The spectra were photographed on othochromatic plates—Raman-Plate AlFA. The slit width was 0.05 mm. Excitation of the spectrum was by the mercury line at 4358 A. Filters which were used in the investigation of the Raman spectrum of vitreous boron trioxide[3] were adapted as crossed filters. The investigations were carried out using a three prism spectograph ISP-51 with camera (f = 270 mm). The exposure times varied from 20 to 50 hr. Investigations of the infrared spectrum of crystalline As_2O_3 were performed by the method of powders mixed with paraffin oil, using a double-beam infrared spectrophotometer ПИАНе.[12] In order to obtain spectra in the 2.5-40μ region, prisms of NaCl, KBr, and KRS-5 were used. Pure crystalline arsenic trioxide was obtained for the investigation.

EXPERIMENTAL RESULTS

The Raman spectrum of arsenic trioxide contained 11 lines. It should be noted that determination of the frequencies of the weak lines in the region up to 360 cm^{-1} was difficult because of the scattering background of the exciting mercury line λ = 4358 A, in spite of the filters

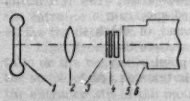

Fig. 1

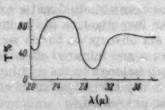

Fig. 2

Fig. 1. Diagram of the apparatus for obtaining the spectra of crystalline powders. 1—low pressure mercury lamp; 2—condensor; 3, 5—filters; 4—layer of material being studied; 6—spectograph.
Fig. 2. Infrared absorption spectrum of crystalline As_2O_3 in the 24-40μ region.

The frequencies of the lines with approximate strengths of their intensities are presented in Table 1.

Also in this table are presented data from the infrared absorption spectrum. In the 2.5-24μ region they agree well with the data of Sidorov[11] (with the exception of the wide band at 488 cm^{-1} which in our spectrum is at 479 cm^{-1}). Results in the 24-40μ region were obtained for the first time. The infrared absorption spectrum of crystalline As_2O_3 in the 24-40μ region is shown in Fig. 2 where T is the transmission coefficient in percent.

Table 1. Frequencies (cm^{-1}) and Intensities of Bands of Arsenic Trioxide in the Raman Spectrum (I) and in the Infrared Absorption Spectrum (II)

Spectral band no.	I	II	Spectral band no.	I	II
1	270 (s.)		8	559 (s.)	
2	306 (w.)		9	780 (av.)	
3	?	340 (s.)	10	815 (w.)	802 (v.s.)
4	365 (v.s.)		11	840 (s.)	842 (s.)
5	415 (s.)		12	1037 (v.w.)	1061 (w.)
6	473 (w.)	479 (s.)	13		1152 (v.w.)
7	515 (w.)				

Note: v.w.—very weak; w.—weak; av.—average; s.—strong; v.s.—very strong.

DISCUSSION OF RESULTS

From analysis of the x-ray data, it is known that arsenic trioxide has a molecular structure. Therefore, in the discussion of results, the vibrational spectra will be examined in terms of a molecular representation.

As is seen from Table 1, six absorption bands were found in the infrared absorption spectrum, investigated in the 2.5-40μ region; of these four bands (ν = 340, 479, 802, and 842 cm^{-1}) were considered strong, and the remaining two weak. It is evident that the four strongest bands can be assigned as frequencies of fundamental vibrations; and the weak bands, combination or overtone frequencies.

It should be noted that three strong frequencies of the infrared spectrum agree within the experimental limits of error with the frequencies of the Raman spectrum (ν = 473, 815, 840 cm^{-1}). Regarding the fourth strong band of the infrared spectrum (ν = 340 cm^{-1}) it is difficult to say if it occurs in the Raman spectrum in view of the significant background from the exciting line. It is also necessary to point out the poor agreement of frequencies 802 and 815 cm^{-1}—a difference of 13 cm^{-1}. This is explained, evidently, by the poor accuracy of frequency measurement of the 815 cm^{-1} line in the Raman spectrum, since it is rather weak. Below we shall check this question in detail, and also point out why the line ν = 340 cm^{-1} is absent from the Raman spectrum. In addition to the three previously mentioned frequencies, all the frequencies which were considered strong or average can be taken as fundamental frequencies in the Raman spectrum. It is also possible that fundamental frequencies can be weak in intensity. Thus, in the Raman spectrum there are 8-10 frequencies of fundamental vibrations. On the basis of comparison and calculation of all frequencies in the Raman spectrum and infrared absorption spectrum, it is possible to select (as was done in references 4-7) a possible species of crystalline arsenic trioxide.

First of all, the following characteristics should be noticed in the comparison of the spectra.

1. The number of lines of the Raman spectrum (8-10) greatly exceeds the number of fundamentals in the infrared spectrum (4). From this fact, it follows that the molecule being analyzed cannot belong to point groups of C_s, C_3, C_3, C_{3v}, $C_{\infty v}$ symmetry for which lines are active in both spectra.

2. There are lines which are present in both spectra. This characteristic suggests that the molecule being analyzed cannot belong to those point groups of symmetry for which lines of the Raman spectrum are forbidden in the infrared absorption spectrum, and vice versa.

Thus, the following point groups are excluded: C_1,

C_{2h}, $D_{2h} \equiv V_h$, S_6, C_{4h}, C_{6h}, $D_{4d} \equiv S_{8v}$, $D_{4d} \equiv S_{8v}$, D_{4h}, D_{5h}, $D_{\infty h}$, O_h.

3. Because of the comparatively large difference in frequencies it is not clear whether the lines 815 cm^{-1} in the Raman spectrum and 802 cm^{-1} in the infrared absorption spectrum belong to the same type of vibration or whether they are related to vibrations of different symmetry types, one of which (815 cm^{-1}) is active only in the Raman spectrum and the other (802 cm^{-1}) only in the infrared spectrum. We shall examine the latter case; i.e., we shall assume that these frequencies are related to different types of symmetry and also we shall consider that the frequency $\nu = 340$ cm^{-1} is present only in the infrared absorption spectrum. Then the molecule must belong to one of the following groups of symmetry: D_3, D_4, D_5, D_6, C_{3h}, C_{5h}, D_{3h}.

Table 2 shows the results of a calculation of the number of frequencies active both in the infrared spectrum and the Raman spectrum for each of the point groups of symmetry for B_2O_3 using data in references 4 and 5.

Table 2. Selection Rules for Species of a Molecule Belonging to Different Groups of Symmetry

Symmetry group	Molecular formula	Number of frequencies active only in IR	Total number of frequencies active in IR	Number of frequencies active in R
D_3	As_3O_9	3	11	13
D_4	As_4O_{12}	5	15	24
D_5	As_5O_{15}	4	13	23
C_{3h}	As_3O_6	3	8	11
D_{3h}	As_3O_9	1	3	5
D_{5h}	As_5O_5	2	7	12
Experiment	—	—	4	8—10

Note: IR—infrared absorption spectrum; R—Raman spectrum.

For each symmetry group we selected only such molecular species which give a minimum number of frequencies in the infrared absorption spectrum.

As is seen from the table, the closest agreement with experiment is for the species of symmetry group D_{3h}. But they differ rather significantly from the experimental data in the number of frequencies. As a consequence of this, these models are hardly acceptable. Therefore, one must assume that, first, the frequencies 815 and 802 cm^{-1} are related to one type of vibration and the difference between them is caused by experimental inaccuracies in the determination of their numerical value and, second, that the frequency 340 cm^{-1} is present in the Raman spectrum but is masked by the background from the excitation line.

A calculation of the number of frequencies for species of symmetry groups D_5 and C_{5h} was not carried out because of the absence of appropriate tables in the book by Hertzberg.[13] Since the number of atoms for species of these groups increases in comparison with species of D_3 and C_{3h} and the symmetry increases only slightly, then the number of frequencies for species of D_5 and C_{5h} will be no smaller than for species of D_3 and C_{3h}, which also leads to a strong discrepancy with the experiment.

Thus, it should be taken into account that all four fundamental frequencies of the infrared spectrum are present in the Raman spectrum. Therefore a molecule of arsenic trioxide must belong to one of the following groups of symmetry: C_{2v}, $D_2 \equiv V$, C_4, C_5, C_6, S_4, C_{4v}, C_{5v}, C_{6v}, $D_{2d} \equiv V_d \equiv S_{4v}$, T, T_d. For these point groups appropriate calculations were carried out in the work of Sidorov and Sobolev for a molecule of boron trioxide.[4, 5]

Table 3. Selection Rules for Different Structural Models of a Molecule of Arsenic Trioxide

Symmetry group	Molecular formula	Number of frequencies active in IR	Number of frequencies active in R	Symmetry group	Molecular formula	Number of frequencies active in IR	Number of frequencies active in R
C_{2v}	As_2O_3	8	9	C_{3v}	As_3O_6	12	15
$D_2 \equiv V$	As_2O_3	7	9	C_{3v}	As_3O_6	10	13
C_4	As_4O_6	12	18	D_{3d}	As_3O_6	10	17
C_5	As_5O_8	12	15	T	As_4O_{12}	13	23
C_6	As_6O_6	10	13	T_d	As_4O_6	4	8
S_4	As_4O_6	12	17	T_d	As_4O_{12}	9	17
C_{4v}	As_4O_6	11	17	Experiment	—	4	(8—10)

Note: For IR and R see Table 2.

An examination of Table 3 for arsenic trioxide, which has the same structure as boron trioxide, shows that the closest agreement with experiment is obtained for the As_4O_6 species belonging to the point group of T_d symmetry.

INTERPRETATION OF THE VIBRATIONAL SPECTRUM OF THE ARSENIC TRIOXIDE MOLECULE

As was shown above, an As_4O_6 species belonging to point group T_d agrees well with experiment. Selection rules for the vibrations of a molecule of this point group are given in Table 4.[13] From an examination of Table 4 it is seen that a molecule of As_4O_6 of symmetry T_d must

Table 4. Selection Rules for Point Group T_d

Type	Selection		Number of vibrations
	Raman	IR	
A_1	alw.	for.	2
A_2	for.	for.	0
E	alw.	for.	2
F_1	for.	for.	2
F_2	alw.	alw.	4

Note: alw.—allowed; for.—forbidden; IR—infrared absorption spectrum.

have two totally symmetric and completely polarized vibrations of type A_1 active only in the Raman spectrum, two triply degenerate vibrations of type E active only in the Raman spectrum, two triply degenerate vibrations of type F_1, forbidden in both spectra, and four triply degenerate vibrations of type F_2, active in both Raman and infrared spectra.

Unfortunately, it is impossible to obtain data about the polarization of separate lines using the method of "filtration"; this makes an interpretation of the vibrational spectrum of arsenic trioxide difficult. Nonetheless it is possible to carry out the assignment of the fundamental frequencies. Since totally symmetric lines evidently have a high intensity, the 365 cm^{-1} line, considered as very strong, can be assigned to one of the two totally symmetric vibrations of type A_1. Frequencies of the Raman spectrum 473, 815, and 840 cm^{-1} can be assigned to the triply degenerate vibrations of type F_2, since they are active in the infrared spectrum. The frequency 340 cm^{-1} can likewise be assigned to a vibration of type F_2, since for point group T_d only frequencies of vibration F_2 are present in the infrared spectrum.

The Raman spectrum frequencies of 270 and 780 cm^{-1}, which are absent in the infrared spectrum, can be assigned to vibrations of type E. It is rather improbable that frequency 270 cm^{-1} can be related to a vibration of type A_1, since totally symmetric vibrations are seldom found at such low frequencies. Therefore, we assign the

frequency 550 cm^{-1}, considered strong, to the second vibration of type A_1. The weak frequencies 306, 415, 1041, 1152 cm^{-1} can be interpreted as combination frequencies or as overtones of fundamental vibrations, or as frequencies of type F_1 which appear as the result of a violation of the selection rules. Interpretation of all frequencies of the Raman and infrared spectra are presented in Table 5. The correctness of assigning the weak frequency 515 cm^{-1} to a fundamental vibration of type F_1 is confirmed by the satisfactory interpretation of frequency 1041 cm^{-1} which is present in both spectra. The remaining weak frequencies are satisfactorily interpreted as difference and sum frequencies, although it is not excluded that they could be interpreted by some other method.

It should be noted that the presented interpretation cannot be considered entirely well-defined for all lines in view of the absence of polarization measurements, although for some lines (for instance, triply degenerate and nondegenerate totally symmetric) it is entirely well-defined.

Table 5. Interpretations of the Vibrational Spectrum of Arsenic Trioxide (Frequencies in cm^{-1})

Raman spectrum	Infrared absorption spectrum	Interpretation	Computed frequencies	Symmetry type of the upper vibrational state
270 (s.)		ν_4		E
306 (w.)		$\nu_3 - \nu_5$	304	$F_1 + F_2$
?	340 (s.)	ν_{10}		F_2
365 (v.s.)		ν_2		A_1
415 (w.)		$\nu_3 - \nu_7$	415	E
473 (s.)	479 (s.)	ν_5		F_2
515 (w.)		ν_9		F_1
550 (s.)		ν_1		A_1
780 (sv.)		ν_6		E
815 (w.)	802 (v.s.)	ν_8		F_2
840 (w.)	842 (s.)	ν_8		F_2
1037 (v.w.)	1041 (v.w.)	$2\nu_5$	1030	$A_1 + E + F_2$
	1152 (v.w.)	$\nu_3 + \nu_9$	1167	F_2

Note: For abbreviation definitions see Table I.

CONCLUSION

The present investigations of the vibrational spectrum of crystalline arsenic trioxide shows that it is satisfactorily interpreted by assuming an As_4O_6 species which belong to the point group T_d. This conclusion is found in agreement with the x-ray analyses of arsenic trioxide. On the basis of the similarity in infrared spectra to the vitreous and the low temperature crystalline form, it is possible to make the statement that the vibrational spectrum of the vitreous form of As_2O_3 must be interpreted in the same way as the vibrational spectrum of the crystalline form. Therefore there is reason to believe that a molecular structure of an analogous type persists in the vitreous state.

In conclusion, I offer profound thanks to N. N. Sobolev and T. A. Sidorov for valuable meetings during the preparation of the paper.

REFERENCES

1. W. H. Zachariasen. J. Am. Chem. Soc., 54, 3841 (1932).
2. B. F. Ormont. "Struktura Neorganicheskikh Veshchestv." (Structure of Inorganic Substances), M-L, 1950.
3. E. J. Lotkova, V. V. Obukhov, N. N. Sobolev, and V. P. Cheremisinov. Opt. i Spektr. 1, 772 (1956).
4. T. A. Sidorov and N. N. Sobolev. Opt. i Spektr. 3, 560 (1957).
5. T. A. Sidorov and N. N. Sobolev. Opt. i Spektr. 4, 9 (1958).
6. T. A. Sidorov and N. N. Sobolev. Opt. i Spektr. 2, 710 (1957).
7. T. A. Sidorov and N. N. Sobolev. Opt. i Spektr. 2, 717 (1957).
8. L. R. Maxwell, S. B. Hendricks and L. S. Demping. J. Chem. Soc. 5, 626 (1937).
9. J. H. Schulman. J. Am. Chem. Soc. 65, 878 (1943).
10. V. M. Borisov and M. G. Gorshtein. Zhur. Obshch. Khim. 22, 1903 (1952).
11. T. A. Sidorov. Thesis. Fiz. Inst. Akad. Nauk, 1957.
12. V. I. Malishev, M. N. Markov, and A. A. Shubin. Doklady Akad. Nauk SSSR, 86, 273 (1952).
13. G. Herzberg. "Kolebatel' ni invrashchatel' ni spektri mnoguatomnikh molekul." (Infrared and Raman Spectra of Polyatomic Molecules), IL, Moscow, 1949.

CALCULATIONS AND INTERPRETATIONS OF VIBRATIONAL SPECTRA OF NAPHTHENES II. METHYLCYCLOPROPANE AND 1,1-DIMETHYLCYCLOPROPANE

L. M. Sverdlov and E. P. Krainov

Received 12 January 1959

The vibrational frequencies are calculated and a complete interpretation is given of the infrared absorption and Raman spectra of methylcyclopropane and 1,1-dimethylcyclopropane. The characteristic frequencies of monoalkyl-substituted cyclopropane and of 1,1-dimethyl-substituted cyclopropane are determined.

1. In a preceding paper of this series,[1] we have calculated the vibrational frequencies and the constants of the potential energy of cyclopropane. Thus it becomes possible to calculate the vibrational spectra of the simplest alkyl-substituted cyclopropanes of various types: methyl-cyclopropane, 1,1-dimethylcyclopropane, cis- and trans-1,2-dimethylcyclopropane 1,2,3,-trimethyl-cyclopropane, 1,1,2,2-tetramethylcyclopropane, and hexamethylcylopropane.

Calculations of this kind are of considerable interest, because in recent years papers have appeared in increasing numbers dealing with the vibrational spectra of the substituted cyclopropanes of various types, and the vibrational spectra of complex compounds with the three-member carbon rings.

For the interpretation of spectra of these compounds, a theoretical calculation is necessary of the simplest alkyl-substituted cyclopropanes; this will permit also the determination of the characteristic frequencies of the various substitution types.

The mechanics of vibrations of cyclic systems has a number of features which considerably complicate the calculations of the vibrational spectra. The main difficulty is caused by the large number of redundancy relations between the coordinates; the matrix elements of the potential energy are represented by complex combinations of force coefficients, and all calculations become very cumbersome. Probably, this fact explains why no rigorous calculations of even relatively simple compounds, such as alkylcyclopropanes, were published up to now.

In the present work, the vibrational frequencies are calculated by using the method of El'iashevitch and Stepanov,[2] and the interpretation of the vibrational spectra is given for methylcyclopropane and 1,1-dimethylcyclopropane.

2. The molecules of methylcyclopropane and of 1,1-dimethylcyclopropane belong to the symmetry groups C_s and C_{2v}, respectively. For C_4H_8, there are vibrations of the following symmetry types: $\Gamma = 17\,A' + 13\,A''$, for C_5H_{10} $\Gamma = 12A_1 + 10B_1 = 9B_2 = 8A_2$. All vibrations are active both in the Raman and in the infrared spectra, with the exception of vibrations of the symmetry type A_2 which are forbidden in the infrared spectrum.

For calculation, we introduce the internal coordinates—changes of bond lengths and of the angles. Methylcyclopropane: Q_a, Q_b, Q_c, Q_d; $q_i (i = 1-9;\ i \neq 2)$; γ_{ac}, γ_{ab}, γ_{bc}, γ_{cd}, γ_{ad}; α_{24}, α_{28}, α_{78}, α_{79}, α_{89}; β_{a1}, β_{c1}, β_{a3}, β_{a4}, β_{b3}, β_{b4}, β_{b5}, β_{b6}, β_{c5}, β_{c6}, β_{d1}, $\beta_i (i = 7-9)$(see Fig. 1). There are altogether 36 coordinates with 7 redundancy relations. 1,1-dimethylcyclopropane: Q_a, Q_b, Q_c, Q_d, Q_e; $q_i (i = 3-12)$; α_{24}, α_{58}, α_{78}, α_{79}, α_{89}, $\alpha_{10,11}$, $\alpha_{10,12}$, $\alpha_{11,12}$; β_{a3}, β_{a4}, β_{b3}, β_{b4}, β_{b5}, β_{b6}, β_{c5}, β_{c6}, $\beta_i (i = 7-12)$; γ_{de}, γ_{ab}, γ_{ac}, γ_{bc}, γ_{ad}, γ_{ae}, γ_{cd}, γ_{ce} (see Fig. 2). Altogether 45 coordinates* with 8 redundancy relations.

*Coordinates describing the hindered rotation of the CH_3 group around the C—C bond, are not considered in the calculation.

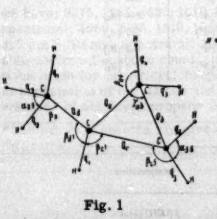

Fig. 1

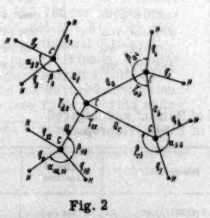

Fig. 2

Next we introduce the total symmetry coordinates (types C_s and C_{2v}) and the higher symmetry coordinates (types D_{3h} and C_{3v}), some of which are identical with the symmetry coordinates of cyclopropane.

For the calculation of kinematic coefficients, the geometric parameters of cyclopropane[1] and those of the paraffins were used. The anharmonicity was taken into consideration according to the method of "spectroscopic mass."[3]

For the calculation of the matrices of potential energy, the force coefficients used were those determined in the calculation of cyclopropane[1] and of the paraffins.[2]

The secular equations of the 17th, 12th, 12th, 10th, 8th, and 7th powers were solved by iterated diagonalization, as well as with the help of an electronic computer* (in the case of methylcyclopropane).

*We take the opportunity to express our gratitude to A. N. Bogomolov for solving the equation with the electronic computer.

The results of frequency calculations, and the interpretation of the Raman and infrared spectra, are given in Tables 1 and 2. The good agreement between the calculated and observed frequencies (mean error 14 cm^{-1}, maximum error 39 cm^{-1}) confirms the validity of the suggested interpretation. On the basis of the given assignment of the fundamental frequencies, the rest of the observed lines can be considered as overtones or as combination frequencies (Tables 3 and 4).

It should be mentioned that several lines were assigned erroneously by authors who attempted a partial interpretation of spectra. For instance, Mecke[4] assigned the Raman line 759 cm^{-1} in the spectrum of methylcyclopropane to the vibration C—C of the carbon ring, the line 292 cm^{-1} to the representation A′, and 368 cm^{-1} to A″. The lines 326, 356, 392, 778, and 1319 cm^{-1} in the Raman spectrum of 1,1-dimethylcyclopropane, Mecke also interpreted erroneously. Cleveland[5] erroneously attributed the Raman line 658 cm^{-1} (which is an overtone, according to our data) and the infrared line 842 cm^{-1} to the vibrations of the carbon skeleton; the lines 2733, 2840, and 2863 cm^{-1} belong to the fundamental frequencies.

Table 1. Calculation and Interpretation of the Vibrational Spectrum of Methylcyclopropane (Frequencies in cm^{-1})

Interpretation	Symmetry	Calculated frequencies	Raman scattering (liquid)[4]	Infrared absorption (gas)[5]
q_{CH_2} (C—H) (Δ) *	A′	3100	—	—
q_{CH} (C—H) (Δ)	A′	3055	—	—
$q^+_{CH_2}$ (C—H) (Δ)	A′	3017	2998 (w.)	—
q^- (C—H) (CH_3) **	A′	2976	2957 (m.)	—
q^+ (C—H) (CH_3)	A′	2898	2874 (m.)	—
α (HCH) (Δ)	A′	1488	1462 (w.)	—
α^- (HCH) (CH_3)	A′	1474		—
β_{a1} (CCH) (Δ)	A′	1387	1390 (v. w.)	1389 (v. w.)
α^+ (HCH) (CH_3)	A′	1380	1363 (v. w.)	1372 (v. w.)
Q (C—C) (Δ) (Q^{A_1})***	A′	1202	1207 (s.)	
Q (C—C) (Δ) ($Q^{E'1}$)	A′	1047	—	1030 (s.)
β^- (CCH) (CH_3)	A′	1021	—	1017 (m.)
Q_d (C—C)	A′	968	982 (s.)	—
β (CCH) (Δ)	A′	911	930 (w.)	931 (m.)
β (CCH) ($\Delta\beta^{E'12a}$)	A′	804	—	785 (s.)
β (CCH) ($\Delta\beta^{E'11a}$)	A′	758	759 (m.)	755 (c)
γ_d (CCC)	A′	349	368 (m.)	—
q^- (C—H) ($\Delta q^{E'1}$)	A″	3079	3074 (m.)	—
q^+ (C—H) ($\Delta q^{E'1}$)	A″	3017	3015	—
q^- (C—H) (CH_3)	A″	2976	2957 (m.)	—
ε (HCH) (CH_3)	A″	1465	—	1457 (v. s.)
ε (HCH) ($\Delta\varepsilon^{E'1}$)	A″	1419	—	1410 (v. w.)
β (CCH) (Δ)	A″	1111	—	1060 (w.)
β (CCH) (CH_3)	A″	1072	—	1076 (w.)
β (CCH) ($\Delta\beta^{E'12b}$)	A″	1016	—	1002 (m.)
β (CCH) (Δ)	A″	983	—	979 (m.)
Q (C—C) ($\Delta Q^{E'1}$)	A″	889	851 (m.)	850 (s.)
β (CCH) (Δ)	A″	810	—	807 (m.)
γ_d (CCC)	A″	291	292 (w.)	—

Notes: s. – strong; m. – medium; w. – weak; v. w. – very weak; v. s. – very strong; * – Δ vibration belonging to the group C; ** – CH_3 vibration belonging to the group CH_3; *** – symmetry coordinate of cyclopropane, identical with that of methylcyclopropane.

Table 2. Calculation and Interpretation of the Vibrational Spectrum of 1,1-Dimethylcyclopropane (Frequencies in cm^{-1})

Interpretation	Symmetry	Calculated frequencies	Raman scattering (liquid)[a]	Infrared absorption (gas)[a]
ν_1 (C—H) (A)	A_1	3018	2993 (10) p	—
ν_2 (C—H) (CH_2)	A_1	2977	2930 (5) d	—
ν_3 (C—H) (CH_3)	A_1	2866	2892 (5) p	—
α (HCH) (A)	A_1	1502	—	1470 (s.)
α (HCH) (CH_2)	A_1	1484	—	1460 (v. s.)
α^s (HCH) (CH_3)	A_1	1381	1382 (2)	1385 (m.)
Q (C—C) (ΔQ^{A_1})	A_1	1358	1319 (8) p	1335 (m.)
Q (C—C) ($\Delta Q^{E'11}$)	A_1	1070	1056 (5) p	1056 (w.)
β (CCH) ($\Delta\beta^{E'11a}$)	A_1	987	—	1007 (v. s.)
β (CCH) (CH_3)	A_1	930	928 (10) p	928 (v. s.)
Q^a (C—H)	A_1	675	678 (7) p	—
γ (CCC)	A_1	331	336 (3) d	—
ν_4 (C—H) ($\Delta\varepsilon^{E'11}$)	A_2	3089	3061 (4) d	—
ν_5 (C—H) (CH_2)	A_2	2978	2950 (5) d	—
α (HCH) (CH_2)	A_2	1466	1465 (4) d	—
β (CCH) (A)	A_2	1050	—	1042 (m.) ?
β (CCH) (A)	A_2	995	—	—
γ (CCH) ($\Delta\beta^{E'11b}$)	A_2	964	—	—
γ (CCC)	A_2	290	326 (1)	—
ν^s (C—H) (A)	B_1	3099	—	3075 (m.)
ν_6 (C—H) (CH_2)	B_1	2975	2950 (5) d	—
ν_7 (C—H) (CH_3)	B_1	2899	—	2890 (v. s.)
α^s (HCH) (CH_2)	B_1	1470	1465 (4) d	—
α^{as} (HCH) (CH_3)	B_1	1378	—	1380 (m.)
Q^a (C—C)	B_1	1281	—	1310 (m.)
β (CCH) (CH_3)	B_1	970	—	970 (v. w.)
β (CCH) (A)	B_1	866	—	842 (v. s.)
β (CCH) ($\Delta\beta^{E'11a}$)	B_2	731	778 (1)	766 (w.)
γ (CCC)	B_2	369	392 (1)	—
ν_8 (C—H) ($\Delta\varepsilon^{E'1}$)	B_2	3018	—	2985 (m.)
ν_9 (C—H) (CH_2)	B_2	2976	2950 (5) d	—
α^{as} (HCH) (CH_3)	B_2	1468	1465 (4) d	—
α (HCH) ($\Delta\varepsilon^{E'1}$)	B_2	1418	1433 (4) d	1420 (m.)
β (CCH) (A)	B_2	1162	1124 (2)	1127 (m.)
β (CCH) (A)	B_2	983	—	976 (v. w.)
Q (C—C) ($\Delta Q^{E'1}$)	B_2	844	836 (5) d	830 (m.)
γ (CCC)	B_2	314	328 (1)	—

Notes: p – polarized; d – depolarized (the rest of notes are the same as in Table 1).

Table 3. Interpretation of Overtones and Combination Frequencies in Methylcyclopropane

Infrared spectrum	Interpretation	Infrared spectrum	Interpretation
748 (w.)	1030 − 292 = 738	941 (w.)	859 + 362 − 292 = 935
772 (w.)	1076 − 292 = 784	970 (w.)	1002 + 1002 − 1030 = 974
821 (w.)	917 + 917 − 783 = 829	1180 (w.)	807 + 368 = 1175
859 (m.)	1207 − 368 = 839	1343 (v. w.)	979 + 368 = 1347
921 (w.)	1207 − 292 = 915	1353 (v. w.)	982 + 368 = 1350

Table 4. Interpretation of Overtones and Combination Frequencies in 1,1-Dimethylcyclopropane

Infrared spectrum	Interpretation	Infrared spectrum	Interpretation
724 (w.)	392 + 326 = 718	1940 (v. w.)	970 + 970 = 1940
754 (w.)	392 + 356 = 748	1955 (v. w.)	978 + 978 = 1952
758 (w.)	1433 − 678 = 755	2030 (w.)	1056 + 976 = 2032
785 (w.)	392 + 392 = 784	2060 (v. w.)	1056 + 1007 = 2061
1112 (m.)	786 + 356 = 1122	2070 (v. w.)	1310 + 766 = 2076
	1433 − 326 = 1107	2285 (w.)	1481 + 830 = 2290
1137 (m.)	1460 − 326 = 1134	2460 (w.)	1460 + 1037 = 2487
1163 (w.)	786 + 392 = 1158	2580 (w.)	1127 + 1430 = 2557
1180 (v. w.)	830 + 356 = 1186	2720 (m.)	1380 + 1310 = 2690
1240 (w.)	842 + 392 = 1234	2840 (m.)	1460 + 1380 = 2840
1270 (v. w.)	928 + 356 = 1284	3240 (w.)	2890 + 356 = 3246
1340 (w.)	976 + 356 = 1332	Raman scattering	
1395 (m.)	1007 + 392 = 1399	658 (1)	326 + 326 = 652
1420 (w.)	1058 + 336 = 1412	1158 (1)	830 + 326 = 1156
1785 (w.)	1007 + 786 = 1773	2733 (3)	1310 + 1430 = 2740
1850 (w.)	928 + 928 = 1856	2863 (6)	1430 + 1430 = 2860
1930 (v. w.)	1007 + 928 = 1935	2926 (7)	1460 + 1460 = 2920

Notes as in Table 1.

Table 5

Cyclopropane	Methylcyclopropane	1,1-dimethyl cyclopropane	Cyclopropane	Methylcyclopropane	1,1-dimethyl cyclopropane
Q (C—C) A_1' 1188	1207 (A')	1319 (A_1)	β (CCH) E''_{1a} 741	807 (A'')	1042 (A_2)
Q (C—C) $E'11$ 1029	1030 (A')	1056 (A_1)	β (CCH) E''_{1b} 1050	1002 (A'')	964 (A_2)
Q (C—C) $E'1$ 1029	859 (A'')	830 (B_2)			
β (CCH) E''_{1a} 866	785 (A'')	1007 (A_1)	β (CCH) A_1' 1125	1090 (A')	995 (A_2)
β (CCH) E''_{1a} 866	—	1127 (B_2)	β (CCH) A_2'' 854	931 (A')	842 (B_1)
β (CCH) E''_{1a} 741	755 (A')	766 (B_1)	β (CCH) A_2' 975	979 (A'')	978 (B_2)

Table 6. Interpretation of Raman[a] and Infrared Absorption Spectra[a] of Ethylcyclopropane

Raman spectrum	Interpretation	Raman spectrum	Interpretation	Infrared spectrum	Interpretation
290 (2)	γ (CCC) A''	1107 (7)	β (CCH) (A) A''	746 (m.)	β (CCH) (A) A'
317 (2)	$\gamma_{C_2H_5}^{CH_3}$ A''	1124 (1)	747 + 370 = 1117	813 (s.)	β (CCH) (A) A''
331 (2)	768 − 441 = 327	1170 (5)	890 + 290 = 1180	917 (s.)	β (CCH) (A) A'
347 (2)	1329 − 983 = 346	1198 (110)	Q (C—C) (A) A'	1005 (v. s.)	β (CCH) (A) A''
370 (13)	γ (CCC) A'	1215 (4)	768 + 441 = 1209	1107 (w.)	β (CCH) (A) A''
441 (25)	γ (CCC) A'	1241 (3)	957 + 290 = 1247	1176 (w.)	890 + 290 = 1180
488 (1)	768 − 290 = 478	1273 (5)	β_{CH_2}(CCH) A''	1290 (m.)	superposition β_{CH_2} (A'') 1273
624 (1)	918 − 290 = 628	1310 (6)	β_{CH_2}(CCH) A'		and β_{CH_2} (A') 1310
661 (1)	370 + 290 = 660	1329 (2)	δ_{CH_2} (CCH) (A) A'	1370 (m.)	$\alpha_{CH_3}^{s}$(HCH) A'
673 (1)	1427 − 747 = 680	1383 (16)	$\alpha_{CH_3}^{s}$(HCH) A'	1449 (s.)	α_{CH_3}(HCH) A'
709 (1)	1088 − 370 = 718	1427 (19)	α_{CH_2}(HCH) (A) A''	1818 (v. w.)	1005 + 813 = 1818
727 (3)	441 + 290 = 731	1444 (29)	α_{CH_3}(HCH) A'	1980 (v. w.)	1005 + 983 = 1988
747 (48)	β (CCH) (A) A'	1460 (30)	$\alpha_{CH_3}^{s}$(HCH) (A) A' and $\alpha_{CH_3}^{as}$(HCH) (A' and A'')	2174 (w.)	1088 + 1088 = 2176
768 (5)	β (CCH) (A) A''; $\beta_{CH_3}^{(CCH)}$ A''	2858 (50)	1427 + 1427 = 2854	2899 (v. s.)	$\nu_{CH_2}^{s}$(C—H) A'
817 (22)	β (CCH) (A) A''	2878 (70)	1444 + 1444 = 2888	4170 (w.)	3080 + 1088 = 4168

Table 6. (continued)

Raman spectrum	Interpretation	Raman spectrum	Interpretation	Infrared spectrum	Interpretation
890 (41)	Q (C—C) (Δ) A''	2901 (50)	1460 + 1444 = 2904		
918 (65)	β (CCH) (Δ) A''	2909 (90)	$\tilde{\nu}_{CH_2}$(C—H) A'		
941 (0)	β_{CH_2} (CCH) A''	2936 (100)	$\tilde{\nu}_{CH_2}$(C—H) A'		
957 (1)	β (CCH) (Δ) A''	2965 (80)	$\tilde{\nu}_{CH_3}$ (CH) A' and A''; $\tilde{\nu}_{CH_3}$ (CH) A''		
983 (4)	Q_s (C—C) A'	3006 (190)	$\tilde{\nu}_{CH_2}$(C—H) (Δ) A' and A''		
1012 (1)	β (CCH) (Δ) A''	3069 (50)	$\tilde{\nu}_{CH_2}$(C—H) (Δ) A''; ν_{CH} (Δ) A'		
1029 (11)	Q (C—C) (Δ) A'	3080 (50)	$\tilde{\nu}_{CH_2}$(C—H) (Δ) A'		
1041 (4)	β_{CH_2} (CCH) A''				
1088 (17)	Q (C—C) A'				

Notes as in Table 1.

The comparison of the spectra of cyclopropane, methylcyclopropane, and of 1,1-dimethylcyclopropane shows that the kind of the alkyl-substitution exerts a very strong influence on the type of spectrum. This is true with respect to the frequencies Q(C—C) of the three-member ring, as well as to the frequencies (CCH) connected with the ring. Table 5 gives frequencies Q(C—C) and (CCH) of cyclopropane and the corresponding frequencies of C_4H_8 and C_5H_{10} (by considering the alteration of the symmetry types).

Furthermore, the calculation permits establishment of the characteristic frequencies of alkyl-substituted cyclopropane of the type

$$RHC\langle^{CH_2}_{CH_2} \quad \text{and} \quad R_2C\langle^{CH_2}_{CH_2}.$$

For the monoalkyl-substituted cyclopropane the following frequencies are characteristic: 3080, 1020, 980, 810, 720 cm^{-1} (infrared spectrum); 3080, 3065, 3000, 1200, 920, 750, 370, 290 cm^{-1} (Raman spectrum). For the dialkyl-substituted of the type

$$\begin{matrix} R \\ R \end{matrix}\rangle C\langle^{CH_2}_{CH_2}$$

we have: 3075, 2985, 1335, 1010, 850, 785 cm^{-1} (infrared spectrum); 3060, 2995, 1319, 1056, 836, 778, 678, 390, 360, 325 cm^{-1} (Raman spectrum). Experimental data available confirm the above conclusions.[7, 8] Finally, calculations made for methylcyclopropane permit a complete interpretation of the Raman and the infrared absorption spectra* of ethylcyclopropane (see Table 6). This molecule belongs to the symmetry group C_s and has frequencies of the following symmetry groups: Γ = 22 A′ + 17 A″. We have interpreted 38 frequencies as fundamental and the rest as combination frequencies and overtones. The large number of combination frequencies that appear in the Raman scattering should be noted.

*The infrared spectra are given in reference 8 only in diagrams.

REFERENCES

1. L. M. Sverdlov and E. P. Krainov. Opt. i Spektr. 3, 54 (1957).
2. M. V. Vol'kenshtein, M. A. El'iashevitch and B. I. Stepanov. "Kolebaniia molecul." (Vibrations of Molecules), GITTL, Moscow, Vol. 1, 1949.
3. M. Bourguel et al. Bull. Soc. chim. de France 51, 400 (1932).
4. F. E. Coudan and E. Smith. J. Am. Chem. Soc. 69, 965 (1947).
5. F. Cleveland, M. Murray, and W. Gallaway. J. Chem. Phys. 15, 742 (1947).
6. Landolt-Boernstein. "Molecules." Vol. I, Part 2, 1951.
7. V. A. Slably. J. Am. Chem. Soc. 76, 3604 (1954).
8. J. Delfer et al. J. Am. Chem. Soc. 71, 2482 (1949).
9. G. S. Landsberg, P. A. Bazhulin, and M. M. Sushchinskii. "Osnovnye parametry spectrov kombinatsionnogo rasseianiia uglevodorodov." (The Fundamental Parameters of the Raman Spectra of the Hydrocarbons), Akad. Nauk USSR, Moscow, 1956.

ROTATIONAL STRUCTURE OF (1-1) AND (0-1) BANDS IN THE SPECTRUM OF THE CARBON MONOCHLORIDE MOLECULE

Yu. Ya. Kuzyakov and V. M. Tatevsky

Received 9 February 1959

The rotational analysis of two bands in the spectrum of the CCl molecule (2713-2927 A region) is presented, and the value of the rotational constants corresponding to the ground and excited states are determined.

The spectrum of the carbon monochloride molecule (CCl) contains a group of bands in the λ = 2713-2927 A region. In all papers available in the literature concerned with a study of the spectrum of the CCl molecule[1-3] only a vibrational analysis of the investigated bands had been examined. In the present paper, for the first time, a rotational analysis is presented of two bands of the spectrum of the CCl molecule; and the values of the rotational constants corresponding to the ground and excited states are found.

The bands of the spectrum of the CCl molecule were obtained with diffraction spectograph DFC-3 (dispersion of 2 A/mm in the first order). These spectograms indicate that of all the spectrum, which consists of four sequences with $\Delta v = -1, 0, +1, +2$, only two sequences ($\Delta v = 0, +1$) are suitable for performing a rotational analysis. The rotational spectrum of the bands of the two other sequences is either strongly overlapped by the rotational structure of the intense bands of the C_2 molecule (sequence $\Delta v = +2$) or has a small intensity and the rotational structure is hard to measure because of a continuous background, the nature of which is not clear at the present time (sequence $\Delta v = -1$). In sequence $\Delta v = 0$, the (1 – 1) band was freest from superposition of other bands and was used to carry out the rotational analysis. In sequence $\Delta v = +1$, the (0 – 1) band was used for the same reason.

By analogy with isoelectronic molecules of CF, SiF, NO, the given system of bands can be related to a transition of the $^2\Sigma - ^2\Pi$ type. A vibrational analysis of these bands has been carried out by us,[4] from which it was seen that the doublet splitting of the ground $^2\Pi$– state is approximately equal to 120 cm^{-1}.

Due to the large doublet splitting the sub-bands formed by different components of the $^2\Pi$- state are located with respect to one another in such a way that the rotational structure of one sub-band is slightly overlapped by lines of the rotational structure of the other sub-band. For a rotational analysis the most suitable of the sub-bands is $^2\Sigma - ^2\Pi_{3/2}$, since in it there is an open beginning of $Q_2(1, 1)$ which significantly facilitates the determination of absolute numeration, while in sub-band $^2\Sigma - ^2\Pi_{1/2}$ the presence of an intense band head in the Q_1 branch does not give such an opportunity. Figure 1 is a photograph of the bands of sequence $\Delta v = 0$. The open beginning in the $^2\Sigma - ^2\Pi_{3/2}$ components of the (1 – 1) band is clearly seen, designated as $Q_2(1, 1)$.

Owing to the small differences in the values of the rotational constants of the upper and lower electronic states (this follows from an examination of the changes in distance between the band heads from band to band[4,5] many lines appear at the band head formed by the Q_1 branch. The latter leads to the conclusion that in the best-resolved parts of the sub-band $^2\Sigma - ^2\Pi_{1/2}$ there is only one intense branch R_1. It is very difficult to pick out branch P_1 (see Fig. 1) of the $^2\Sigma - ^2\Pi_{1/2}$ sub-band since

Fig. 1. Spectra of the CCl molecule ($\Delta v = 0$). 1—band head of branch $^{\circ}P_{21}(1, 1)$; 2—$P_2(0, 0)$; 3—$Q_2(0, 0)$, $P_2(1, 1)$; 4—$Q_2(1, 1)$; 5—$P_1(1, 1)$; 6—$Q_1(0, 0)$; 7—$Q_1(1, 1)$. °The lower index in the branch designation correspond to: 1—sub-band $^2\Sigma - ^2\Pi_{1/2}$; 2—sub-band $^2\Sigma - ^2\Pi_{3/2}$.

it is overlapped with lines from the rotational structure of the $^2\Sigma - ^2\Pi_{3/2}$ sub-bands. For the $^2\Sigma - ^2\Pi_{3/2}$ components the best-resolved parts contain two intense branches, Q_2 and R_2, the beginnings of which give an opportunity to calculate the rotational constants. This facilitates the choice for rotational analysis, namely, the $^2\Sigma - ^2\Pi_{3/2}$ component. All discussion here about the rotational structure of the (1 – 1) bands pertains equally to the rotational structure of the (0 – 1) bands.

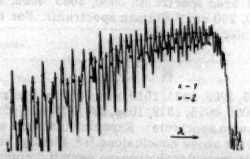

Fig. 2. Microphotometer trace of part of the (1 – 1) band of the $^2\Sigma - ^2\Pi_{3/2}$ component. 1—line of branch R_2; 2—line of branch Q_2.

While carrying out the rotational analysis of the $^2\Sigma - ^2\Pi_{3/2}$ components of the (1 – 1) and the (0 – 1) bands an accurate measurement of the position of lines in the P_2 branches seemed impossible owing to insufficient resolution. Therefore we were limited to a choice of branches Q_2 and R_2 and to a determination of absolute numeration of the rotational lines of the spectrum. In Fig. 2 a microphotometer trace is presented of parts of the (1 – 1) band with marks relating the lines to branches.

In distinguishing the branches, we assumed that the $^2\Pi$– state is similar to that described by Asundi, which in the first place follows from the value of its doublet splitting, equal to 120 cm^{-1}. Thanks to Mulliken,[5] equations for the R and Q branches of the $^2\Sigma - ^2\Pi_{3/2}$ component have the following form:

$$R_2(J) = \nu_{02} + \frac{15}{4}B' + \left(4B' - B_3''\right)J + \left(B' - B_3''\right)J^2, \qquad (1)$$

$$Q_2(J) = \nu_{02} + \frac{3}{4}B' + \left(2B' - B_3''\right)J + \left(B' - B_3''\right)J^2. \qquad (2)$$

where ν_{02} is the zero line of the $^2\Sigma - {}^2\Pi_{3/2}$ sub-band.

Equations (1) and (2) are presented without the cubic terms in the expression for the rotational energy, since an estimate of the D_v coefficient for this term derived from the theoretical equation[6] $D_v = 4B^3/\omega^2$, where ω = 860 cm^{-1} and B = 0.6 cm^{-1}, indicates that D_v has a value of the order of 10^{-6} cm^{-1}. Therefore, for values of the rotational quantum number of the order of 30, as in our case, the cubic term with D_v in general does not make a change in the value of the rotational term exceeding the experimental error.

Accuracy of relating lines to branches was verified by agreement of the first combination terms $\Delta_1F''(J) = R(J) - Q(J+1)$, calculated for the lower vibrational level $v'' = 1$, which is common for the investigated bands. The values of the frequency of the lines of the two branches, the values of the experimental combination relations, and those calculated from an assumed rotational constant are presented in Tables 1 and 2. All values are given in cm^{-1}.

Table 1. Band (1 – 1) of the $^2\Sigma - {}^2\Pi_{3/2}$ Component of the CCl Molecule

J	$P_1(J)$	$Q_1(J)$	$R_1(J) - Q_1(J) = \Delta_1F''(J)$	$R_1(J) - Q_1(J+1) = \Delta_1F''(J)$	$\Delta_1F''(J)$ calculated from Eq. (3)
1.5	35875.50				
2.5	75.37	35870.21	5.16	4.81	4.53
3.5	77.00	70.56	6.44	5.90	5.82
4.5	78.88	71.10	7.78	7.21	7.11
5.5	80.79	71.67	9.12	8.18	8.40
6.5	82.90	72.61	10.29	9.40	9.70
7.5	84.77	73.50	11.27	10.99	10.99
8.5	87.20	73.78	13.42	11.83	12.28
9.5	89.28	75.37	13.91	13.08	13.58
10.5	91.62	76.19	15.43	14.62	14.87
11.5	94.16	77.90	17.16	16.18	16.16
12.5	95.52	77.98	17.54	16.64	17.46
13.5	98.08	78.88	19.20	18.28	18.74
14.5	35900.85	79.80	21.05	20.06	20.04
15.5	35903.11	80.79	22.32	21.35	21.33
16.5	05.50	81.76	23.74	22.80	22.63
17.5	07.72	82.90	24.82	23.94	23.92
18.5	10.21	83.78	26.43	25.44	25.21
19.5	12.42	84.77	27.65	26.78	26.51
20.5	14.82	85.64	29.18	27.64	27.80
21.5	17.43	87.20	30.23	29.22	29.09
22.5	19.92	88.21	31.71	30.64	30.39
23.5	22.34	89.28	33.06	31.84	31.68
24.5	24.82	90.50	34.32	33.20	32.97
25.5	27.56	91.62	35.94	34.40	34.26
26.5	30.08	93.16	36.92	35.88	35.56
27.5	35932.48	35894.20	38.28	36.96	36.85
28.5	35.22	95.52	39.70	38.54	38.14
29.5	37.66	96.68	40.98	39.78	39.44
30.5	40.32	97.88	42.44	39.84	
31.5	43.04	35900.48	42.56	40.98	
32.5	45.68	02.06	43.62	42.69	
33.5	48.47	02.99	45.48	43.77	
34.5	51.00	04.70	46.30	45.36	
35.5	54.13	05.64	48.49	46.74	
36.5	56.74	07.39	49.35	47.82	
37.5	59.52	08.92	50.60	49.31	
38.5	62.40	10.21	52.19	49.98	
39.5	65.24	12.42	52.82	51.77	
40.5	68.17	13.47	54.70	53.35	
41.5		14.82			
42.5		16.16			
43.5		17.68			
44.5		19.23			
45.5		20.86			
46.5		22.44			
47.5		24.01			
48.5		25.07			

The rotational constants for the excited and ground states are calculated from the first combination relations $\Delta_1F'(J)$ and $\Delta_1F''(J)$, where

$$\Delta_1F''(J) = 2B_v''(J+1), \tag{3}$$

$$\Delta_1F'(J) = 2B_v'\left(J+\frac{1}{2}\right). \tag{4}$$

Calculated values of the rotational constants are:

state $^2\Pi_{3/2}$ $B_1'' = 0.6465 \pm 0.0032$;

state $^2\Sigma$ $B_0' = 0.6589 \pm 0.0038$; $B_1' = 0.6551 \pm 0.0026$.

The values of B are given in cm^{-1} with mean quadratic error. The zero lines of the investigated bands were calculated from the first lines of the Q_R branch: $\nu_{02}(1-1)$ = 35868.90 cm^{-1}, $\nu_{02}(0-1)$ = 35007.25 cm^{-1}. The value of the vibrational quanta $\Delta G_{1/2}'$ = 861.65 cm^{-1} derived from the zero lines, agrees with the value $\Delta G_{1/2}'$ = 860 cm^{-1} which was obtained in the vibrational analysis of the band heads.[4]

Table 2. Band (0 – 1) of the $^2\Sigma - {}^2\Pi_{3/2}$ Component of the CCl Molecule

J	$P_1(J)$	$Q_1(J)$	$R_1(J) - Q_1(J) = \Delta_1F''(J)$	$R_1(J) - Q_1(J+1) = \Delta_1F''(J)$	$\Delta_1F''(J)$ calculated from Eq. (3)
1.5	35012.01				
2.5	13.88				
3.5	15.90	35006.28	6.81	5.26	5.82
4.5	18.07	35010.73	7.34	7.03	7.11
5.5	20.57	11.04	9.53	8.56	8.40
6.5	22.87	12.71	10.86	10.13	9.70
7.5	25.06	12.74	12.22	11.18	10.99
8.5	26.95	13.88	13.07	11.96	12.28
9.5	29.62	14.99	14.83	13.83	13.58
10.5	31.60	15.99	15.61	14.80	14.87
11.5	34.02	16.80	17.22	15.95	16.16
12.5	36.95	18.07	18.88	17.29	17.46
13.5	39.52	19.06	19.86	18.93	18.74
14.5	41.80	20.57	21.03	19.86	20.04
15.5	44.45	21.74	22.71	21.58	21.33
16.5	46.78	22.97	23.80	22.85	22.63
17.5	49.18	24.11	25.08	23.82	23.92
18.5	51.78	25.36	26.42	24.83	25.21
19.5	55.05	26.95	28.10	26.47	26.51
20.5	57.41	28.63	28.78	27.79	27.80
21.5	61.00	29.62	31.38	29.85	29.09
22.5	62.92	31.15	31.77	30.22	30.39
23.5	65.83	32.70	32.93	31.81	31.68
24.5	68.26	34.02	34.24	32.40	32.97
25.5	71.86	35.96	35.90	34.02	34.26
26.5	35074.92	35037.84	37.08	35.40	35.56
27.5	77.77	39.52	38.25	36.58	36.85
28.5	80.87	41.19	39.69	37.78	38.14
29.5	83.76	43.09	40.67	39.31	39.44
30.5		44.45			

As is seen from the derived data, it is impossible to determine the value of α and to calculate B_v for the upper state, since the errors of determining the absolute values of the rotational constants is larger than the absolute value of α, equal to $B_1' - B_0'$. From the empirical equation $\omega_e\chi_e/\omega_e \sim 1.4\alpha_e/B_e$,[6] when ω_0 = 860 cm^{-1}, $\omega_e\chi_e$ = 5.0 cm^{-1}, and B_1' = 0.646 cm^{-1},[4] it is possible to see that α for the ground state will be of the order of several thousandths, i.e., the value of the rotational constant at zero vibrational level of the ground state will be approximately equal to the value of the rotational constant at the first vibrational level within the limits of error of the determination of B_1''.

REFERENCES

1. R. K. Asundi and S. M. Karim. Proc. Ind. Acad. Sci. 6A, 328 (1937).
2. T. Horie. Phys. Math. Soc. Japan 21, 143 (1939).
3. P. Venkateswarlu. Phys. Rev. 77, 1 (1950).
4. Yu. Ya. Kuzyakov and V. M. Tatevsky. "Nauchnie Dokladi, Vysshei Shkol." (Scientific Reports from Universities), 1959.
5. R. S. Mulliken. Rev. Mod. Phys. 3, 89 (1931).
6. G. Gertsberg. "Spectri i Stroenie Dvuatomnikh Molecul." (Spectra and Constructions of Bi-Atomic Molecules), Moscow, 1949.

STUDY OF THE TEMPERATURE DEPENDENCE OF THE INTENSITY OF INFRARED ABSORPTION BANDS IN SOLUTIONS

V. N. Smirnov

Received 12 January 1959

The temperature dependence of the intensity of infrared absorption bands has been measured for a series of substances in solutions. An influence of the nature of the solvent on the temperature variations of the intensity was discovered. The influence of the solvent on the intensity of the bands at a given temperature was studied. A discussion of the results obtained is presented.

Study of the temperature dependence of the intensity of infrared absorption bands in gases[1] has shown that the negative* effect observed in the liquid state[2] is, to all appearances, brought about by intermolecular interactions which are specific for the condensed state of the substance. However, the mechanism of the influence of molecular forces on the vibrations of the molecules— the mechanism which leads to the deviation of the observed temperature variations of the intensity from the results of statistical theory—is not yet clear. For the clarification of this question, temperature studies in solutions have an undoubted interest in connection with the possibility of changing the character of the internal field within wide limits by changing the nature of the solvent. Measurements in solutions permit us to take systematic account of the various properties of the medium; that is, of the various surroundings of the molecules under study.

*We designate as a negative temperature effect a diminution of the integrated intensity of the band with an increase in the temperature of the substance. A positive effect corresponds to an increase in intensity.

The present work is devoted in particular to a study of the influence of the permanent dipole moment of the solvent molecules on the temperature dependence of the intensity of infrared absorption bands. The experimental data obtained for liquids[2] show that the polarity of the molecules to some degree determines the magnitude of the effect under consideration: the temperature variations for polar molecules are, in general, larger than for nonpolar ones, although there are a number of exceptions. At the same time, in the investigation of the temperature dependence of the intensity of Raman lines, it has been recorded[3-5] that the observed deviation from theory was not found to be influenced by the polarity of the molecules under study.

It must be noted that, up to the present time, there are in the literature no reports devoted to a systematic study of the temperature effect in connection with a variation of the nature of the solvent. Studies of the influence of the solvent on the intensity of infrared bands at a given temperature have, to be sure, been carried out repeatedly.[6-16]

The experimental setup and the procedure for treating the results of the measurements corresponded completely with those described in reference 2 for the study of liquids.

The measurements were carried out on an IKS-2 double-beam infrared spectrometer. As before, four corrections for the integrated absorption coefficient were introduced: for the width due to the apparatus function, for the wings of the band, for the elastic deformation of the cell, and for the density of the substance studied. The first two corrections are, to a certain extent, connected with the assumption of the dispersive character of the actual profile of the bands studied. A special check, however, showed that the actual form of the bands in solutions, as in liquids, is sufficiently near the dispersion form. The correction for deformation of the cell was calculated from the temperature dependence of the vapor pressure of the solvent. In most cases this correction was insignificant, since the cell thicknesses used for solutions generally exceeded 0.02-0.04 mm.

In the case of dilute solutions, which were used in this work, one may suppose that the temperature variation of the density is determined by the coefficient of cubical expansion of the solvent. The error introduced by the latter assumption is not large, if we take into account that the coefficients of cubical expansion of most organic liquids are close together. Likewise, it is permissible to neglect the change in volume concentration which results from the deviation of the actual volume of the mixture from the mechanical sum of the volumes of the initial components.[17]

Inasmuch as the solutions studied were not azeotropic mixtures, a number of precautions were taken to avoid evaporation of the liquid under study at elevated temperatures; among these were provision for hermetic closure of the cell and for the indispensable complete filling of the cell passages with solution. On the other hand, the low concentrations and the sufficient solubility of the components of the mixtures made it possible to avoid phase separation of the liquids while using lowered temperatures. Possible small variations in background during temperature surveys (as a result of slight clouding of the windows and the cells, etc.) were always taken into account as a corresponding shift in the 100%-transmission line. To check the reproducibility of the experimental results, measurements were made both with falling and with rising temperature within the temperature interval studied, while for each temperature about three to four curves were generally recorded. The total random error in the value of the observed integrated absorption coefficient, found from the sum of the errors in the values of the cell thickness, the concentration of the substance, and the recorded area of the band, amounted to about 15-20%. The relative variation in intensity with temperature was determined, on the average, with an accuracy of 5%.

As objects of study a number of liquids were chosen for which we have presented temperature determinations in the liquid[2] or gaseous[1] state. The choice of bands was limited to some degree by the difficulty of isolating them, and also by the transparency of the solvents on hand. If the solvent had a slight absorption in the spectral region being studied, it was eliminated with the help of a compensating cell with pure solvent at the corresponding temperature.

In order to have the possibility of observing the in-

Temperature Dependence of the Intensity of the Infrared Absorption Bands of a Series of Substances in Inert and Polar Solvents

Substance*	Form of vibration	Concentration (%)	Inert solvents (P = 0) Solvent	t° C	ν_0 (cm^{-1})	$\Delta\nu_D$ (cm^{-1})	$k_\infty \times 10^{-4}$ cm^2/mole sec	$(k_\infty)_t/(k_\infty)_{t_0}$ (for 100°C)	Polar solvents (P ≠ 0) Solvent*	t° C	ν_0 (cm^{-1})	$\Delta\nu_D$ (cm^{-1})	$k_\infty \times 10^{-4}$ cm^2/mole sec	$(k_\infty)_t/(k_\infty)_{t_0}$ (for 100°C)	$(k_\infty)_{polar}/(k_\infty)_{inert}$ (at +25° C)
Chloroform $CHCl_3$ 1.15	ν(CCl)	5	CS_2	−80	746	10	530	1.22	Acetone 2.73	−80	749	17	670	1.22	1.28
				+25	747	11	430		CH_3CN 3.94	+25	747	19	550		
	δ(HCCl)	5	CS_2	−80	1230	9	91	0.99		−35	1235	22	122	1.07	1.12
				+25	1231	11	92		$SOCl_2$ 1.60	+25	1233	21	103		
	ν(CH)	5	CCl_4	−15	3023	11	15	1.09		−15	3028	31	41	1.45	2.08
				+70	3026	13	14			+70	3029	30	30		
Acetone $(CH_3)_2CO$ 2.73	ν(CC)	4	CS_2	−75	1224	6	170	0.95	CH_3CN 3.94	−30	1224	7	200	0.99	1.10
				+25	1222	10	180			+70	1221	10	200		
	ν(CO)	3	C_2Cl_4	−15	1726	18	540	0.94	Butyl chloride 2.12	−90	1718	10	580	0.96	1.10
				+115	1728	27	580			+60	1722	21	620		
Acetonitrile CH_3CN 3.94	ν(CN)	10	C_2Cl_4	−15	2216	4	17	1.16		−75	2216	4	26	1.28	1.30
				+80	2216	9	15			+25	2217	8	21		
Carbon disulfide CS_2	ν(CS)	4	C_2Cl_4	−15	1530	22	220	0.88	$CHCl_3$ 1.15	−50	1527	20	230	0.97	1.01
				+85	1528	26	250			+50	1526	24	240		
					Average . .			1.03			Average . .			1.14	1.28

*The number under the designation of the substance (solvent) corresponds to the magnitude of its permanent dipole moment P (in D units). The absence of a number indicates that P = 0.

fluence of the solvent on the intensity of corresponding bands* together with the temperature measurements,

*The ratio of the integrated absorption coefficients of the bands of the substances studied, in a polar and in an inert solvent, is shown in the last column of the table.

each pair of solutions was studied in one and the same cell and at one and the same volume concentration. Strictly speaking, the use of equal volume concentrations is not sufficient in the sense of keeping a constant ratio between the number of molecules of the substance under study and the number of solvent molecules, which characterizes the effective action of the medium. However, the change in the indicated ratio on going from one solvent to another at low concentrations is not significant. For example, for a 5% solution of chloroform in CS_2, acetonitrile, and acetone, the ratio between the number of molecules of the substance studied and the number of solvent molecules equals 1:25, 1:29, 1:21 respectively; for a 4% solution of acetone in CS_2 and CH_3CN, 1:30, 1:34; etc.

The calculation of the integrated absorption coefficient was carried out with the help of the expression:

$$k_\infty = k'_\infty \cdot \frac{cM}{C_v \rho_T} \quad \frac{\text{cm}^2}{\text{mole sec}},$$

where k'_∞ is the measured integrated absorption coefficient (in cm^{-2}), c is the velocity of light, M is the molecular weight, C_v is the volume concentration, and ρ_T is the density of the substance being studied at the given temperature T.

In the table are given the fundamental results of the measurements for a series of substances studied in polar and nonpolar solvents. The values of the integrated absorption coefficient k_∞ are given for the two extreme temperatures, although measurements were carried out at several points of the temperature interval studied. To characterize the value of the relative variation of k_∞, the intensity of the bands at the highest temperature studied was always taken as 1. For the sake of ease of comparison, relative intensity variations are everywhere reduced (using linear extrapolation as an approximation) to an interval of 100°C. To illustrate the variations observed, the spectrograms of the 3025 cm^{-1} band of chloroform, recalculated to optical density, are shown in the figure.

In the table are also given the positions of the band maxima ν_0 and their width on the optical density scale $\Delta\nu_D$ (with a precision of ±1 cm^{-1}) as a function of the temperature and the nature of the solvent. The band widths have been corrected for the final slit width by the same method as in reference 2. As can be seen from the

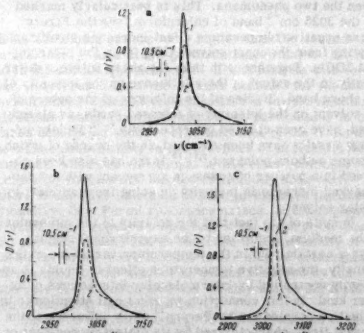

Influence of temperature and nature of the solvent on the intensity of the 3025 cm^{-1} absorption band of chloroform. a—5% solution in the inert solvent CCl_4; curve 1, −15°C; curve 2, +70°C. Cell thickness 1 mm. b—5% solution in the polar solvent $SOCl_2$; curve 1, −15°C; curve 2, +70°C. Cell thickness 0.57 mm. c—5% solutions in CCl_4 (1) and $SOCl_2$ (2) at room temperature. Cell thickness 1 mm.

table, the vibration frequencies are the least sensitive parameter. On the other hand, the influence of external disturbances on the band widths is significant. With an increase in temperature, as a rule, there is observed a broadening of the infrared absorption bands (see Figs. a and b). The change from an inert to a polar solvent is accompanied by a marked increase in the band width only in the case of chloroform (see Fig. c); for the rest of the substances investigated, the polarity of the solvent molecules has, for practical purposes, little influence on $\Delta\nu_D$. It has not yet been possible to establish any clear connection between the observed shifts and broadenings of the bands and the temperature behavior of the intensity.

Comparison of the temperature dependence of the intensity of each band for an inert and a polar solvent shows that the polarity of the molecules of the medium has a definite influence on the magnitude of the observed temperature effect, although this influence is not large. The temperature variations of intensity for most of the bands presented in the table increase more or less on going over to a polar solvent. The properties of the vibrations themselves--their sensitivity toward external disturbances--apparently play a very essential role in this. The result obtained is consistent with the data[2] on the temperature dependence of the intensity of infrared absorption bands in polar and nonpolar liquids. In view of the inaccuracy of the experimental data and the absence of a theory of the question under study, it would seem difficult to discuss the causes for the opposite conclusions concerning the role of the dipole moment which were drawn from study of the Raman spectra. It is possible that the difference in the origins of the vibrational spectra is manifesting itself here.

Furthermore, from a comparison of the temperature variations of the intensity of infrared absorption as a function of the solvent with the result of the influence of the same solvents on the intensity of the bands studied, it can be seen that there is a direct connection between the two phenomena. This is particularly marked for the 3025 cm^{-1} band of chloroform (see the Figure), whose negative temperature effect increases significantly in going from the inert solvent CCl_4 (a) to the polar solvent $SOCl_2$. Together with this, the above solvents differ greatly in the extent of their influence on the intensity of the above band. Studies of the influence of the nature of the solvent on the intensity of infrared bands, as already noted, have been carried out repeatedly.[6-10] Widely differing results have been obtained, in the course of which, as some authors point out,[9,11,12] there has also been observed in a number of cases, in agreement with out data, a marked increase in intensity on going from an inert to a polar solvent.

In spite of the fact that the polarity of the molecules of the medium, according to the experimental results, plays a certain role in the temperature variations of the intensity, the negative temperature effect in liquids is apparently controlled by intermolecular interactions of another kind. In this connection we must call attention to the evaluation carried out by Person[18] of the influence of the internal field, characterized by its dielectric constant or refractive index. The corresponding variations in intensity, connected with the temperature variation of the refractive index, are small however (about 3-5% for 100°C), and consequently are also not in a position to explain the observed facts completely. In the evaluation of this effect, it is possible that the limitations of the theoretical concepts used are manifesting themselves.[19,20]

The influence of the solvent on the intensity of the absorption bands and the connection of this phenomenon with the temperature variations of intensity are, as may be noted, similar to the effect of pressure in gases, investigated in reference 1. This is understandable, too, inasmuch as both phenomena characterize the sensitivity of the various vibrations and bonds in the molecule toward external disturbances. A simple calculation shows that the density of the substance in solutions at the concentrations used corresponds to very high pressures of the gas. Thus a 5% solution of chloroform corresponds to the vapor of this substance at a pressure of 15 atm, a 3% solution of acetone to 9.5 atm, etc. With respect to the magnitude of the intermolecular interactions, a solution (especially in an inert solvent) may be considered in a certain sense as the realization of a transitional case from almost isolated molecules (gas at low pressures) to an aggregation of strongly interacting identical molecules (pure liquid).

The result of a comparison of the experimental data on the temperature variations of intensity for gases, solutions, and liquids does not contradict the point of view just cited. Actually, if, for purposes of calculation, we use values of $(k_\infty)_{t_1}/(k_\infty)_{t_2}$ averaged* over all the bands studied for a series of substances, we obtain the following values for the relative variations in intensity:** 0.93 for gases, 1.03 for solutions in nonpolar solvents, 1.14 for solutions in polar solvents, 1.09 for nonpolar liquids, and 1.29 for polar liquids. One's attention is drawn to the fact that the value for the temperature variations in solutions assumes an intermediate place between the positive effect in gases and the markedly negative effect in the case of polar liquids.

*The averaging was carried out on the basis of the experimental results in references 1, 2 and the data of the present work: for gases, over 19 bands of 11 substances; for nonpolar and polar liquids, over 14 bands of 7 substances and over 18 bands of 6 substances respectively.

**The intensity of the band at the highest temperature investigated was everywhere taken as 1; the variations in intensity are reduced to an interval of 100°.

This result may be qualitatively explained if we assume that the two types of intermolecular interactions which exist in solutions--molecular collisions and the intermolecular interactions which are characteristic of the condensed state--lead simultaneously to opposite temperature variations of the intensity of infrared absorption bands. The first, a kinetic type of interaction which gives a positive effect,[1] is realized in pure form in gases at low pressures; the second type of interaction (a potential-force type), which leads to a negative effect,[2] prevails in liquids. For liquids and solutions, the qualitative considerations presented are consistent with the theory of the liquid state developed by Frenkel'.[21]

In explaining the influence of temperature or nature of the solvent on the intensity of infrared absorption bands in liquids and solutions, it is apparently wrong not to take into account also the possibility of a direct link between certain atoms or atom groups belonging to different molecules. Starting from this, one can explain the different sensitivity of various vibrations toward the temperature or nature of the solvent. In any case, it follows from the experimental data that it is not possible to explain the observed intensity variations completely by means of a single influence of the dielectric constant of the medium or by the polarity of the molecules. A more complete, systematic account of the forces of molecular interaction in the phenomenon studied is necessary. Accordingly, the present work is considered as part of a general investigation devoted to the study of the influence of temperature and solvent on the intensity of bands be-

longing to different forms of molecular vibrations.

In conclusion, I express my profound thanks to P. A. Bazhulin for his constant attention to the work and a series of valuable suggestions.

REFERENCES

1. V. N. Smirnov and P. A. Bazhulin. Opt. i Spektr. 7, 193 (1959).
2. P. A. Bazhulin and V. N. Smirnov. Opt. i Spektr. 6, 745 (1959).
3. L. M. Fishkova. Doklady Akad. Nauk SSSR 75, 523 (1950).
4. Ya. S. Bobovich. Doklady Akad. Nauk SSSR 98, 39 (1954).
5. A. I. Sokolovskaya and P. A. Bazhulin. Izv. Akad. Nauk SSSR, Ser. Fiz. 22, 1068 (1958).
6. D. Whiffen. Trans. Faraday Soc. 49, 878 (1953).
7. N. S. Bayliss, A. Cole, and L. Little. Australian J. Chem. 8, 26 (1955).
8. C. Huggins and G. C. Pimentel. J. Chem. Phys 23, 896 (1955).
9. H. W. Thompson, G. Steel. Trans Faraday Soc. 52, 1451 (1956).
10. E. E. Ferguson. J. Chem. Phys. 26, 1265 (1957).
11. M. R. Mander and H. W. Thompson. Trans. Faraday Soc. 53, 1402 (1957).
12. R. N. Jones, H. Forbes, and F. Mueller. Canad. J. Chem. 35, 504 (1957).
13. V. M. Chulanovskii, M. P. Burgova, G. S. Denisov, and E. L. Zhukova. Fiz. sb. L'vov. Univ. 1, 42 (1957).
14. C. La Lau. Conference on Molecular Spectroscopy, London (1958).
15. V. M. Chulanovskii and M. P. Burgova. Opt. i Spektr. 2, 330, 433 (1957).
16. R. E. Kagarise. J. Chem. Phys. 27, 827 (1957).
17. E. V. Biron. "Szhatie pri smeshenii normal'nykh zhidkostei." (Contraction on mixing normal liquids). SPB, 1912.
18. W. B. Person. J. Chem. Phys. 28, 319 (1958).
19. L. Onsager. J. Amer. Chem. Soc. 58, 1486 (1936).
20. S. R. Polo and M. K. Wilson. J. Chem. Phys. 23, 2376 (1955).
21. Ya. I. Frenkel'. "Kineticheskaya teoriya zhidkostei." (Kinetic theory of liquids), Izd. Akad. Nauk SSSR, 1945.

ON THE TEMPERATURE DEPENDENCE OF THE INTENSITIES OF VIBRATIONAL ABSORPTION BANDS OF GASES IN THE CASE OF FERMI RESONANCE

M. P. Lisitsa and V. L. Strizhevskii

Received 17 February 1959

The question of the temperature dependence of the intensities of vibrational absorption bands in the presence of resonance interaction of energy levels has been considered. It has been shown that the theory developed leads to conclusions which agree satisfactorily with experiment.

Studies previously carried out on the temperature dependence of the intensities of two composite vibrations of gaseous carbon tetrachloride[1] have qualitatively confirmed the correctness of the theory.[2] However, complete quantitative correspondence was not established: the theory led to a more rapid increase of the integrated absorption with an increase in temperature.

Of all the possible factors responsible for the observed discrepancy, the most important is the presence of resonance interaction between the vibrational levels*

*Here, and below, quantities referring to unexcited states are designated by the index "0".

$E^0_{\nu_1+\nu_2}$ and $E^0_{\nu_1+(\nu_3+\nu_4)}$, transitions to which give bands corresponding to the vibrations referred to above. In this connection, it might be expected that calculation of such an interaction would permit the establishment of not only qualitative, but also quantitative agreement between theory and experiment. This note is devoted to the results of carrying out such a calculation.

In the adiabatic approximation, the motion of the nuclei of polyatomic molecules takes place (as is known[3]) in a field with potential energy.

$$U(Q) = U_0 + \frac{1}{2}\sum_s \nu_s^2 \sum_i Q_{si}^2 + V, \qquad (1)$$

where ν_s are the frequencies of the normal vibrations, Q_{si} are the normal coordinates (the index "i" appears when degeneracy is present), U_0 is the part of the potential energy not dependent on Q, and V are anharmonic terms containing powers of Q higher than the second. If we consider V as a slight perturbation, it may be neglected in the zeroth approximation. It was for just this case that, in reference 2, formulas were obtained for the temperature dependence of the intensities of intramolecular vibrations, which manifest themselves particularly in infrared absorption spectra. The influence of the V term increases substantially in the presence of accidental degeneracy, when two vibrational levels either coincide completely or else are located sufficiently near each other. If the wave functions of such levels have the same symmetry, then Fermi resonance arises, in consequence of which there appears a splitting of the absorption band into two components and an increase in the intensity of the higher order vibration (the order may be determined, for example, by the number of quanta absorbed by the molecule in the phototransition which leads to the formation of the given absorption band).

Since the unexcited energy levels correspond to the levels of noninteracting harmonic oscillators, it is not difficult to understand that, if there are precisely coincident or closely-placed levels corresponding to some particular energy value, closely-placed levels will also be observed for higher values of the energy. This indicates that resonating levels are located in groups, with a different number of them in each group.

In reference 1 the case of resonance of the levels $E^0_{\nu_1+\nu_2}$ and $E^0_{\nu_3+(\nu_1+\nu_4)}$ of carbon tetrachloride was described.* In this case, those equidistant levels for which

*$\nu_1 = 459\ cm^{-1}$, $\nu_2 = 784\ cm^{-1}$, $\nu_4 = 314\ cm^{-1}$.

the vibrational quantum numbers of the oscillators with frequencies ν_1, ν_3, and ν_4 are $v_1 + n$, $v_3 - n$, and $v_4 + n$ are joined into resonating groups; by assigning different triads of numbers v_1, v_3, and v_4 ($v_i \geq 0$, $i = 1, 2, 3$), we shall obtain different groups. Within each group, on transition from one level to another n takes on all possible integral positive and negative values, for which none of the numbers $v_1 + n$, $v_3 - n$, and $v_4 + n$ becomes less than zero. The number of levels in each group is determined by the relation

$$m = v_3 + 1 + s(v_1, v_4). \tag{2}$$

where

$$s(v_1, v_4) = \begin{cases} v_1 & \text{if} \quad v_1 \leq v_4 \\ v_4 & \text{if} \quad v_1 > v_4. \end{cases} \tag{3}$$

Let there be, in the general case, a group consisting of m levels, to which correspond energies E_i^0 and wave functions u_i^0. The latter are fixed as products of the wave functions of linear oscillators. Since the distances between the levels of a single group are assumed to be small compared with the distances between different groups, we are considering the case of relative degeneracy described in reference 3, and we may take advantage of the general formulas set forth there. The presence of closely-placed levels leads to the conclusion that the experimentally observed picture is the result of the superposition of a series of closely-placed absorption bands of different intensities, grouped into unsymmetrical broad bands. Only at sufficiently low temperatures, when most of the molecules are in the ground state (which forms a one-level group), will the recorded bands be approximately symmetrical. (By their appearance, they are due to transitions from the ground state to states of the first group of excited levels.) Thanks to just this, it was possible in reference 1 to resolve the resonance doublet $\nu_1 + \nu_3$ and $\nu_1 + (\nu_1 + \nu_4)$ at room temperature into two fully symmetrical components. At higher temperatures, such resolution was unsuccessful, so that the comparison of theory and experiment was carried out for the integrated absorption of the whole doublet without resolution of the latter into its component parts.

According to reference 3, the integrated absorption coefficient

$$S = \sum_j S_j, \tag{3}$$

where S_j is the integrated coefficient of absorption by molecules in the states of the jth group of energy levels. For the case of thermal excitation, and under such conditions that the difference in population of the levels of the jth group may be neglected, we shall have

$$S_j = \bar{A}_j \left\{ \sum_{i=1}^{\bar{m}} \sum_{l=1}^{m} |p_{\bar{i}l}^0|^2 (\bar{E}_i^0 - E_l^0) + \sum_{i,\, i'=1}^{\bar{m}} \sum_{l=1}^{m} p_{\bar{i}l}^0 p_{\bar{i}'l}^{0*} \nu_{\bar{i}\bar{i}'} - \sum_{i=1}^{\bar{m}} \sum_{l,\, l'=1}^{m} p_{\bar{i}l}^0 p_{\bar{i}l'}^{0*} \nu_{ll'} \right\}, \tag{4}$$

where

$$\bar{A}_j = \frac{4\pi^2}{3\hbar c} n_j, \quad n_j = n \frac{\exp\left(\frac{-\bar{E}_j}{kT}\right)}{\sum_l \exp\left(\frac{-E_l}{kT}\right)}, \tag{5}$$

$\bar{E}_j$ is the average energy of the jth group of levels,*

$$p_{\bar{i}l}^0 = \int u_{\bar{i}}^{0*} p_{\bar{x}}(Q)\, u_l^0\, dQ,$$

$$p_{\bar{x}}(Q) = \int \varphi_{\bar{i}}^{0*}(\xi, Q)\, \hat{p}_{\bar{x}}\, \varphi_l^0(\xi, Q)\, d\xi,$$

$\varphi_l^0(\xi, Q)$ is the wave function of the ground electronic state, dependent on the electronic coordinates ξ and on the coordinates Q of the nuclei as parameters; $\hat{p}_x$ is the operator for projecting the dipole moment on the direction of the light vector of the incident electromagnetic wave.

In Eq. (4), the first component determines the integrated absorption without taking account of the V terms, which are lower by more than two orders of magnitude with respect to Q. The temperature dependence in this case is described by the formulas obtained in reference 2. In those cases where the V terms may not be neglected (in the case of resonance, for example), the form of the temperature dependence of the integrated absorption will differ somewhat from the previous one.

Generally, resonance is observed for tones of different order. Their appearance in the absorption spectrum is dependent on different terms in the expansion of the dipole moment (averaged over the electronic coordinates) in powers of the normal coordinates

$$p_x(Q) = p_0 + \sum_i \left(\frac{\partial p_x}{\partial Q_i}\right)_{Q=0} Q_i + \frac{1}{2} \sum_{ij} \left(\frac{\partial^2 p_x}{\partial Q_i \partial Q_j}\right)_{Q=0} Q_i Q_j + \ldots, \tag{6}$$

the higher terms in this series being responsible for the appearance of the higher order lines. For each level i of the initial group of states, there will always be found such a level i of the final group that the transition $E_i - E_i'$ arises from taking account of the lowest terms of expansion (6). The corresponding components in the first sum of relation (4) will predominate over the remaining components of the same sum, which, together with the terms of the second and third sums, may be referred to quantities of the next lower order of magnitude and, in a first approximation, omitted. This last implies that the temperature dependence of the over-all intensity of resonating vibrations is determined for the most part by the temperature dependence of the intensity of that vibration corresponding to the highest order tone in the absence of resonance. Allowance for quantities of the next lower order of magnitude would lead to additional terms with another, steeper temperature dependence. Thus, the temperature factor in the case of infrared absorption spectra changes[2] by a factor of the type $(1 - e^{-h\nu/kT})^{-1}$ on proceeding to terms of the next lower order of magnitude in expansion (6). If we assume that the ratio of adjacent terms in expansion (6) is a quantity of the order of 10 (the latter originates in a comparison of the experimentally observed integrated intensities of vibrational absorption bands corresponding to tones whose orders differ by unity[4]), then for a frequency $\nu \approx 10^3$ cm^{-1} the additional terms would become substantial only at $T \lesssim 10000°$. Accordingly, in carrying out a comparison of the experimental data with the theory, one may use the formulas obtained in reference 2, which describe the temperature dependence of only one component, the more intense one. One must remember that these formulas, on account of the presence of reconance, determine the temperature dependence of the integrated absorption of the whole doublet, since the absorption of the weaker component increases at the expense of a reduction in the intensity of the stronger, while the natural absorption* of the former, as was shown above, may be neglected.

[2]Quantities which refer to the final state are marked by a bar.

*This would exist in the absence of resonance.

Therefore, in determining the integrated absorption (necessary for comparison with theory) from experimental data, it is proper to measure the area enclosed between the frequency axis and the whole curve of the observed doublet; i.e., to take the sum of the integrated absorption coefficients of both bands.

If the precision of the measurements allows one to take into account the influence of terms of the next lower order of magnitude, this gives us, in principle, the possibility of calculating some of the constants in expansions (1) and (6). In various specific cases, the corresponding formulas will appear different.

In conclusion, we present a comparison, by means of the method cited above, of theory and experiment for the case of the resonance of the carbon tetrachloride vibrations with frequencies $\nu_1 + \nu_3$ and $\nu_1 + (\nu_1 + \nu_4)$. The temperature dependence of the more intense vibration with the frequency $\nu_1 + \nu_3$ (no resonance!) is determined by the factor[3]

$$f(T) = \left[\left(1 - e^{-\frac{h\nu_1}{kT}}\right)\left(1 - e^{-\frac{h\nu_3}{kT}}\right)\right]^{-1}. \qquad (7)$$

Then, for the integrated absorption coefficient at temperature T we may write

$$S_T = S_{T_0} \cdot \frac{f(T)}{f(T_0)}, \qquad (8)$$

where T_0 is some fixed temperature.

Comparison of the S_T values calculated according to (8) with the data of reference 1 leads to the results presented in the table (the value of S_{T_0}, determined at a temperature of 293°K, equals 1104 cm^{-2}). Inasmuch as the experimental errors in reference 1 were as much as 10%, the difference between theoretical and experimental

Temperature Dependence of the Integrated Absorption of the Resonance Doublet $\nu_1 + \nu_3$ and $\nu_1 + (\nu_1 + \nu_4)$ of Carbon Tetrachloride

T°K	S_T calc. (cm^{-2})	S_T exptl. (cm^{-2})	$\frac{\lvert\Delta S_T\rvert}{S_T}$ exptl. (%)
338	1 169	1 109	5.4
378	1 234	1 168	5.5
408	1 288	1 223	5.3
438	1 345	1 268	3.8
473	1 416	1 503	5.8

data presented in the last column may properly be considered small, and the agreement of theory and experiment entirely satisfactory. In view of the errors of measurement already referred to, there is no sense in carrying out a more precise calculation of the temperature dependence of the integrated absorption; i.e., to take into account terms of a lower order of magnitude.

REFERENCES

1. M. P. Lisitsa and V. N. Malinko. Opt. i Spektr. 6, 694 (1959).
2. M. V. Vol'kenshtein, M. A. El'yashevich, and B. I. Stepanov. "Kolebaniya molekul." (Vibrations of molecules), GITTL, Moscow-Leningrad, 1949.
3. V. L. Strizhevskii. Ukr. Fiz. Zhur. (in press).
4. M. P. Lisitsa and V. N. Malinko. Opt. i Spektr. 4, 455 (1958).

OPTICAL INVESTIGATION OF THE MOLECULAR STRUCTURE OF S-TRIAZINE DERIVATIVES. V. INFRARED ABSORPTION SPECTRA OF SALTS OF OXY- AND AMINO-DERIVATIVES OF S-TRIAZINE

E. N. Boitsov and A. I. Finkel'shtein

Received 26 February 1959

Absorption spectra of acid and base salts of amino-oxy derivatives of s-triazine have been obtained in the region 3-15 μ. Questions of the molecular structure of salts of oxy- and amino-derivatives of s-triazine are considered.

In the present work, acid and base salts of amino-oxy derivatives of s-triazine were obtained and their structure is shown. In the literature accessible to us there is only one work in which the spectrum of melamine hydrochloride[1] is presented without any interpretation. Investigation of the absorption spectra of aqueous solutions of amino-oxy derivatives of s-triazine in the ultraviolet region has shown that the character of the absorption changes to a significant degree depending on the pH of the medium.[2-4]

The authors link the changes which take place in the absorption spectra with the presence of tautomeric transformations. For example, for cyanuric acid and melamine in acidic and basic medium these transformations assume the following character:

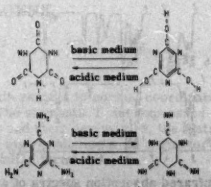

The results obtained in the investigation of the Raman spectra[5] of cyanuric acid are also interpreted on the assumption of tautomeric transformations.

In this connection, however, it must be taken into account that according to ultraviolet absorption spectra, one may not judge directly concerning the changes taking place in the structure of the molecules. Vibrational spectra of these compounds in various media have not been investigated, except for the work[5] mentioned above, which of course cannot give a full solution of the problem.

Inasmuch as obtaining absorption spectra of aqueous solutions of amino-oxyderivatives of s-triazine in the infrared region is difficult in consequence of their low solubility, the study of the molecular structure of their solid acid and base salts offers great interest.

We obtained the following substances for our investigation: the trisodium salt of cyanuric acid, the disodium salt of ammelide, the monosodium salt of ammeline, and the monohydrochlorides of melamine, ammeline, and ammelide.

The method of obtaining the salts just enumerated is described by Beilstein.[6]

The absorption spectra of the substances cited were

Fig. 1. Infrared absorption spectra of amino-oxy derivatives of s-triazine. a—trisodium cyanurate; b—melamine hydrochloride; curve 1—concentration 1%; curve 2—concentration 0.33%.

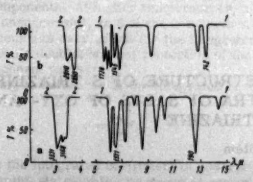

Fig. 2. Infrared absorption spectra of amino-oxy derivatives of s-triazine. a—disodium salt of ammelide; b—ammelide hydrochloride; curve 1—concentration 1%; curve 2—concentration 0.33%.

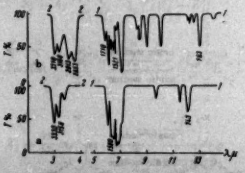

Fig. 3. Infrared absorption spectra of amino-oxy derivatives of s-triazine. a—monosodium salt of ammeline; b—ammeline hydrochloride; curve 1—concentration 1%; curve 2—concentration 0.33%.

Absorption Frequencies of Amino Derivatives of s-Triazine (cm^{-1})

Compound	N-H stretching vibrations of the amino group	N-H deformation vibrations of the amino group	Stretching vibrations of the C=O group	N-H stretching vibrations of the ring	Vibrations of the triazine ring
Melamine	3333 3125	1660	—	—	1560 810
Cyanuric acid	3338 3122	1665	1695	2928	1535 784
Ammeline	3336 3128	1665	1721	2930	1560 773
Ammelide	—	—	1721	2907	1490 789

obtained on samples pressed with KBr according to the method given in reference 7, with the help of an IKS-12 spectrophotometer (NaCl prism, region 3-15 μ). The spectra of all the salts studied are presented in Figs. 1-3 (T = transmission, in %).

The vibrational spectra of amino-oxy derivatives of s-triazine have not been fully interpreted. However, it has been shown in the works of a series of authors[8, 9] that many frequencies are characteristic for these compounds and change insignificantly in the case of various derivatives. In the table are presented the principal functional groups of the amino-oxy derivatives of s-triazine and the absorption frequencies which correspond to them. For the N-H bonds, the most intense bands were taken.

Consideration of the absorption spectra of base salts of amino-oxy derivatives of s-triazine shows that in these substances the frequency corresponding to the C = 0 group disappears. The increase in the frequencies which refer to ring vibrations in the base salts as compared with the neutral molecule indicates an increase in the bond order in the ring. In the region of stretching vibrations of N-H bonds, the frequencies corresponding to vibrations of the N-H bonds of the s-triazine ring disappear. The frequencies belonging to vibrations of the amino group change insignificantly.

Using supplementary conventional symbols,[10] the transition from the neutral compound to the corresponding salt may be schematically represented in the following way:

for cyanuric acid

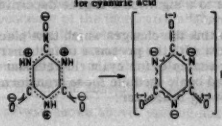

(I)

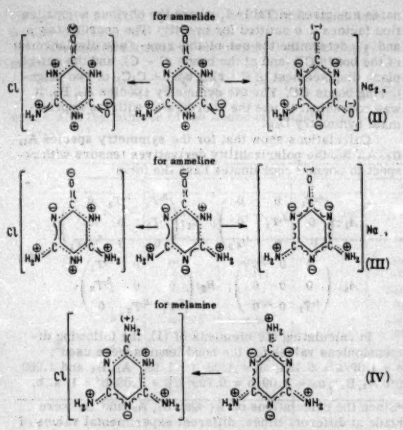

(II) (III) (IV)

The interpretation of the infrared absorption spectra of the acid salts is difficult on account of the presence of a large number of frequencies in the region of the stretching and deformation vibrations of N-H bonds. However, in this case also one can make some conclusions about the structure of the acid salts according to their vibrational spectra.

First of all, we note that the frequency around $\nu = 1700\ cm^{-1}$ indicates the presence of a C = 0 group in the acid salts of ammeline and ammelide.

In the region of N-H deformation vibrations, an increase in the number of bands is observed, which testifies to the presence of a series of different N-H bonds (for example, NH_2, $=NH_2^+$, NH, etc.). In the region of stretching vibrations of N-H bonds, two intense bands, strongly displaced toward the long-wavelength region, appear together with the existing frequencies of the amino group $\nu_1 = 3333\ cm^{-1}$ and $\nu_2 = 3125\ cm^{-1}$. A similar frequency shift is observed in aniline hydrochloride[11] and in the hydrogen chloride salts of amino acids.[12] In the case of ammelide, there are only the two strongly displaced absorption bands, which testifies to the formation of either the group NH_2^+ or NH_3^+. Taking into account the charge distribution in the neutral molecule (the ring nitrogen atoms carry a partial negative charge) and the results of investigation,[13] in which it was shown that the proton attaches itself to a nitrogen atom having a multiple bond, it is proper to consider that the formation of the acid salt of ammelide takes place at the expense of the attachment of a proton to a ring nitrogen atom.

In ammeline and melamine, which have more than one amino group, there arise, together with the persisting frequencies of the unchanged NH_2 group, two additional frequencies whose values are close to the values of the NH frequencies in the ammelide salt. Hence it follows that the formation of the mono-salt of ammeline and melamine affects one of the amino groups for the most part and proceeds analogously to the process described in the case of ammelide. The considerations expressed are confirmed by the lowering of the frequencies corresponding to ring vibrations, which indicates a reduction of the bond order in the ring. Schematically (using the supplementary conventional symbols), the transition from the compound to the corresponding acid salt is shown in schemes II-III.

REFERENCES

1. A. Roosens. Bull. Soc. Chim. Belg. 59, 377 (1950).
2. E. Agallidis, H. Fromherz and A. Hartmann. Ber. 71, 1391 (1931).
3. I. K. Dixon, N. T. Woodbery, and G. W. Costa. J. Amer. Chem. Soc. 69, 599 (1947).
4. I. N. Malkina and A. I. Finkel'shtein. Zhur. Fiz. Khim. 32, 5 (1958).
5. M. Ito. Bull. Chem. Soc. Japan 26, 339 (1953).
6. F. Beilstein. "Handbuch der organischen Chemie," Vol. XXVI, Berlin, 1937.
7. A. I. Finkel'shtein, A. M. Fisher, F. A. Malachevskaya, and B. T. Rabovskii. Opt. i. Spektr. (in press).
8. A. I. Finkel'shtein. Opt. i Spektr. 5, 3, 264 (1958).
9. R. Newman and R. M. Badger. J. Amer. Chem. Soc. 74, 3545 (1952).
10. A. I. Finkel'shtein. Zhur. Fiz. Khim. 31, 1659 (1957).
11. D. N. Shigorin, Ya. L. Daniushevskii, and Ya. L. Gol'dfarb. Izv. Akad. Nauk SSSR, Ser. Khim. 20, 120 (1956).
12. L. Bellamy. "Infrakrasnye spektry molekul." (Infrared Spectra of Molecules), IL, Moscow (1957).
13. N. Sheinker and V. M. Reznikov. Doklady Akad. Nauk 102, 109 (1955).

INTENSITIES AND DEPOLARIZATION IN RAMAN SPECTRA OF MOLYMETHYLBENZENES I. GENERAL THEORY. TOLUENE

M. A. Kovner and B. N. Snegirev

Received 10 January 1959

The tensor elements T of the polarizability derivatives with respect to normal coordinates were calculated for all 38 vibrations of the toluene molecule. The elements T are expressed by means of atomic masses, bond lengths, bond polarizabilities and their derivatives, the matrix elements L of normalized coefficients of vibration modes, and matrix elements L^{-1}. The formulas for T are very complex, and are given therefore in a tabular form.

1. In our previous paper[1] the bond polarizabilities in benzene and their derivatives with respect to the bond lengths were calculated. This permits the systematic evaluation of the intensities in the spectra of the substituted benzenes. As in reference 1, the calculations are based on the valence-optical theory suggested by Wolkenstein and further developed in detail by Wolkenstein and El'iashevich.[2, 3] The basic method[2] of calcula-

tion of the tensor elements T of the polarizability derivatives with respect to normal coordinates enables one to express these elements in terms of the matrix elements L of the normalized coefficients of the vibration modes. Ferigle and Weber[4] have suggested a formula by means of which the elements T are expressed through the elements of the matrix L^{-1}. In the present paper the elements T are expressed through L and L^{-1} which permits the necessary checking of the calculation of T, a more complete utilization of the results of the solution of the mechanical problem, and in many cases facilitates the determination of the electro-optical parameters from the experimental intensities data, as is particularly apparent in the article by Yoshino and Bernstein.[5]

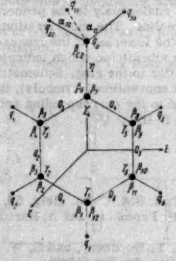

The figure depicts the geometric model of the toluene molecule assumed by us, and the internal vibrational coordinates. The symmetry coordinates of the symmetry species A_1, B_1, A_2, B_2, of the group C_{2v}, based on the vibrational coordinates, and the numbers of these coordinates are given in Table 1, where the obvious normalization factors are omitted for brevity. The coordinates ρ and χ_{ij} determine the out-of-the-ring-plane displacement of the bonds CH (and of the bonds C – C), and the out-of-plane displacement of the ring bonds C_iC_j of two neighboring bonds CC. For the symmetry species A_2, B_2, it was convenient to use the coordinates with the approximate symmetry D_{2h}.

Calculations show that for the symmetry species A_1, B_1, A_2, B_2, the polarizability derivatives tensors with respect to normal coordinates have the form

$$A_1:\begin{pmatrix} {}^{A_1}T_1 & 0 & 0\\ 0 & {}^{A_1}T_2 & 0\\ 0 & 0 & {}^{A_1}T_3\end{pmatrix};\quad B_1:\begin{pmatrix} {}^{B_1}T_1 & {}^{B_1}T_2 & 0\\ {}^{B_1}T_2 & 0 & 0\\ 0 & 0 & {}^{B_1}T_1\end{pmatrix};$$
$$A_2:\begin{pmatrix} 0 & 0 & {}^{A_2}T_1\\ 0 & 0 & 0\\ {}^{A_2}T_1 & 0 & 0\end{pmatrix};\quad B_2:\begin{pmatrix} 0 & 0 & {}^{B_2}T_1\\ 0 & 0 & {}^{B_2}T_2\\ {}^{B_2}T_1 & {}^{B_2}T_2 & 0\end{pmatrix}. \qquad (1)$$

In calculating the elements of (1), the following dimensionless values for the bond lengths were used*: $\sigma = 1.09/a = 0.784$; $\sigma_H = 1.09/b = 1$ for A_1, B_1 and 1.009 for A_2, B_2*; $\sigma_0 = 1.09/b = 0.709$; $\sigma'_H = 1.09/b' = 1$; a, b, b_0, b′ are the equilibrium lengths of bonds CC, C-$H_{a.r.}$, C-C, C-$H_{methyl.}$, respectively. The valency parts of the tensors (1) are as follows:

*Since the calculations of A_1 and B_1, A_2 and B_2 were made at different times, different experimental values of b were used, namely 1.09 A and 1.08 A.

$$({}^{A_1}T_1)_k^{val.} = \sqrt{2}\,\alpha'_{Q2}L_k^1 + \frac{1}{2\sqrt{2}}\left[(3\alpha'_{Q1}+\alpha'_{Q9})(L_k^2+L_k^3)+(3\alpha'_{\rho 1}+\alpha'_{\rho 2})(L_k^4+L_k^5)\right] + \alpha'_{\rho 2}L_k^6+\alpha'_{Q20}L_k^7+\frac{1}{3\sqrt{3}}\left(4\alpha'_{\rho 1}+5\alpha'_{\rho 2}\right)^{CH_3}L_k^{13},$$

$$({}^{A_1}T_2)_k^{val.} = \sqrt{2}\,\alpha'_{Q1}L_k^1 + \frac{1}{2\sqrt{2}}\left[(3\alpha'_{Q2}+\alpha'_{Q1})(L_k^2+L_k^3)+(3\alpha'_{\rho 2}+\alpha'_{\rho 1})(L_k^4+L_k^5)\right] + \alpha'_{\rho 1}L_k^6+\alpha'_{Q10}L_k^7+\frac{1}{3\sqrt{3}}\left(\alpha'_{\rho 1}+8\alpha'_{\rho 2}\right)^{CH_3}L_k^{13};$$

$$({}^{A_1}T_3)_k^{val.} = \sqrt{2}\,\alpha'_{Q3}(L_k^1+L_k^2+L_k^3)+\sqrt{2}\,\alpha'_{\rho 3}\left(L_k^4+L_k^5+\frac{1}{\sqrt{2}}L_k^6\right) + \alpha'_{Q30}L_k^7+\frac{1}{3\sqrt{3}}\left(4\alpha'_{\rho 1}+5\alpha'_{\rho 2}\right)^{CH_3}L_k^{13},$$

$$({}^{B_1}T_1)_k^{val.} = \frac{2\sqrt{2}}{3\sqrt{3}}\left(\alpha'_{\rho 1}-\alpha'_{\rho 2}\right)^{CH_3}L_k^{13},$$

$$({}^{B_1}T_2)_k^{val.} = \frac{\sqrt{3}}{2\sqrt{2}}\left[(\alpha'_{Q1}-\alpha'_{Q9})(L_k^2-L_k^3)+(\alpha'_{\rho 1}-\alpha'_{\rho 2})(L_k^4-L_k^5)\right] + \frac{2}{3\sqrt{3}}\left(\alpha'_{\rho 1}-\alpha'_{\rho 2}\right)^{CH_3}L_k^{13},$$

$$({}^{A_2}T)_k^{val.} = 0,\quad ({}^{B_2}T_1)_k^{val.} = -\frac{2\sqrt{2}}{3\sqrt{3}}\left(\alpha'_{\rho 1}-\alpha'_{\rho 2}\right)^{CH_3}L_k^9;$$
$$({}^{B_2}T_2)_k^{val.} = \frac{2}{3\sqrt{3}}\left(\alpha'_{\rho 1}-\alpha'_{\rho 2}\right)^{CH_3}L_k^9, \qquad (2)$$

where k is the number of normal vibration; and α'_{Q1}, $\alpha'_{\rho 1}$, $\alpha'_{Q\rho 1}$, $\alpha_{q1}^{CH_3}$ are polarizability derivatives of bonds CC, $CH_{ar.}$, C-C, $CH_{methyl.}$, with respect to the direction of these bonds. On the basis of general considerations about the structure of the electron shell of the toluene molecule, we have assumed that the bond polarizabilities in

Table 1. Symmetry Coordinates

Symmetrical Vibrations

No	A_1	B_1	No	A_2	B_2
1	Q_8+Q_{12}	Q_1-Q_6	8	τ_1	$\beta_8-\beta_{11}$
2	Q_1+Q_6	Q_2-Q_4	9	τ_4	$\beta_1-\beta_{12}$
3	Q_2+Q_4	q_9-q_{10}	10	$\beta_4+\beta_9$	$\beta_6-\beta_7$
4	q_9+q_{10}	q_8-q_{11}	11	$\beta_3+\beta_{10}$	$\alpha_{13}-\frac{1}{2}\alpha_{23}-\frac{1}{2}\alpha_{12}$
5	$q_{11}+q_{12}$	$\tau_3-\tau_5$	12	$\beta_{C3}+\beta_{C2}+\beta_{C1}$	$\beta_{C3}-\frac{1}{2}\beta_{C2}-\frac{1}{2}\beta_{C1}$
6	q_1	$\tau_6-\tau_8$	13	$q_{23}+q_{22}+q_{11}$	$q_{23}-\frac{1}{2}q_{22}-\frac{1}{2}q_{11}$

Antisymmetrical Vibrations

No	A_2						No	B_2					
	ρ_1	ρ_2	ρ_3	β_5	β_6	β_7		ρ_1	ρ_2	ρ_3	β_5	β_6	β_7
1	0	−1	−1	0	1	1	1	−1	−1/2	1/2	1	1/2	−1/2
2	0	−1	1	0	−1	1	2	1	−1	1	−1	1	−1
							4	1	1	1	1	1	1
							5	1	−1/2	−1/2	1	−1/2	−1/2
	x_{23}	x_{22}	x_{21}	x_{13}	x_{12}	x_{11}		x_{23}	x_{22}	x_{21}	x_{13}	x_{12}	x_{11}
3	1/2	−1	1/2	1/2	−1	1/2	3	−1	1	−1	1	−1	1
							6	1	0	−1	1	0	−1
							7	$\alpha_{23}-\alpha_{13}$					
							8	$\beta_{C3}-\beta_{C1}$					
							9	$q_{23}-q_{11}$					

CH_{ar}, have an axial symmetry, but that this is not true for the CC, CH_{ar}, and C-C bonds.

Deformational parts of elements (I) can be represented by

$$({}^{\tau}T_l)_k^{def.} = \sum_{\lambda}^{n_\tau} {}^{\tau}f_\lambda \sum_{i}^{n_\tau} {}^{\tau}a_{\lambda l i} ({}^{\tau}L^{-1})_{i_1}^{k} \qquad (3)$$

where λ is the number of the linear combination of bond polarizabilities ${}^{\tau}I_\lambda$; the values of ${}^{\tau}I_\lambda$ are given in Tables 2-5; l is the number of the symmetry coordinate; in the symmetry species τ = A_1, B_1, A_2, B_2, the number of independent symmetry coordinates m_τ = 13, 13, 3, 9, and the number of various linear combinations of bond polarizabilities n_τ = 3, 4, 2, 4; the values ${}^{\tau}a_{\lambda l i}$ are given in Tables 2-5, where $\varepsilon = m_H/m_C = 1.088/12 = 0.0906$ (1.088

Table 2. The Values of ${}^{A_1}a_{\lambda l i}$

i	1			2			3		
λ	1	2	3	1	2	3	1	2	3
$A_1 p_k$ / l	$\alpha_{Q1}-\alpha_{Q2}$	$\alpha_{q1}-\alpha_{q2}$	$(\alpha_{q1}-\alpha_{q2})^{CH_3}$	$\alpha_{Q1}-\alpha_{Q2}$	$\alpha_{q1}-\alpha_{q2}$	$(\alpha_{q1}-\alpha_{q2})^{CH_3}$	$\alpha_{Q1}-\alpha_{Q2}$	$\alpha_{q1}-\alpha_{q2}$	$(\alpha_{q1}-\alpha_{q2})^{CH_3}$
1	$3\alpha_0/\sqrt{2}$ 0.151	$3\varepsilon/\sqrt{2}$ 0.192	0	$-3\alpha_0/\sqrt{2}$ −0.151	$-3\varepsilon/\sqrt{2}$ −0.192	0	0	0	0
2	$-3\alpha_0/2\sqrt{2}$ −0.075	$-3\varepsilon/2\sqrt{2}$ −0.096	0	$3\alpha_0/2\sqrt{2}$ 0.075	$3\varepsilon/2\sqrt{2}$ 0.096	0	0	0	0
3	$-3\alpha_0/2\sqrt{2}$ −0.075	$-3\varepsilon/2\sqrt{2}$ −0.096	0	$3\alpha_0/2\sqrt{2}$ 0.075	$3\varepsilon/2\sqrt{2}$ 0.096	0	0	0	0
4	$-3\alpha_0/2\sqrt{2}$ −0.075	0	0	$3\alpha_0/2\sqrt{2}$ 0.075	0	0	0	0	0
5	$-3\alpha_0/2\sqrt{2}$ −0.075	0	0	$3\alpha_0/2\sqrt{2}$ 0.075	0	0	0	0	0
6	$3\alpha_0/2$ 0.106	0	0	$-3\alpha_0/2$ −0.106	0	0	0	0	0
7	$3\alpha_0/2$ 0.106	0	$8\varepsilon/9$ 0.080	$-3\alpha_0/2$ −0.106	0	$-16\varepsilon/9$ −0.161	0	0	$8\varepsilon/9$ 0.080
8	$15\alpha_0\delta^2/2\sqrt{3}$ 0.241	$3\alpha_0/2\sqrt{3}$ 0.062	0	$-15\alpha_0\delta^2/2\sqrt{3}$ −0.241	$-\sqrt{3}\alpha_0/2$ −0.062	0	0	0	0
9	$15\alpha_0\delta^2/\sqrt{3}$ 0.241	$3\alpha_0/2\sqrt{3}$ 0.062	0	$-15\alpha_0\delta^2/2\sqrt{3}$ −0.241	$-\sqrt{3}\alpha_0/2$ −0.062	0	0	0	0
10	$-3\alpha_0/2\sqrt{6}$ −0.044	$-3(1+\varepsilon)/\sqrt{6}$ −1.336	0	$3\alpha_0/2\sqrt{6}$ 0.044	$3(1+\varepsilon)/\sqrt{6}$ 1.336	0	0	0	0
11	$-3\alpha_0/2\sqrt{6}$ −0.044	$-3(1+\varepsilon)/\sqrt{6}$ −1.336	0	$3\alpha_0/2\sqrt{6}$ 0.044	$3(1+\varepsilon)/\sqrt{6}$ 1.336	0	0	0	0
12	0	0	$-4(3+8\varepsilon)/9\sqrt{6}$ −0.676	0	0	$8(3+8\varepsilon)/9\sqrt{6}$ 1.352	0	0	$-4(3+8\varepsilon)/9\sqrt{6}$ −0.676
13	0	0	$-8\varepsilon/9\sqrt{3}$ −0.048	0	0	$16\varepsilon/9\sqrt{3}$ 0.093	0	0	$-8\varepsilon/9\sqrt{3}$ −0.046

Table 3. The Values of ${}^{B_1}a_{\lambda l i}$

i	1				2			
λ	1	2	3	4	1	2	3	4
$B_{1\alpha} p_{\alpha\beta}$ / l	$\alpha_{Q1}-\alpha_{Q2}$	$\alpha_{q1}-\alpha_{q2}$	$\alpha_{Q61}-\alpha_{Q62}$	$(\alpha_{q1}-\alpha_{q2})^{CH_3}$	$\alpha_{Q1}-\alpha_{Q2}$	$\alpha_{q1}-\alpha_{q2}$	$\alpha_{Q61}-\alpha_{Q62}$	$(\alpha_{q1}-\alpha_{q2})^{CH_3}$
1	0	0	0	0	$3\sqrt{3}\alpha_0/2\sqrt{2}$ 0.130	$3\sqrt{3}\varepsilon/2\sqrt{2}$ 0.166	0	0
2	0	0	0	0	$-3\sqrt{3}\alpha_0/2\sqrt{2}$ −0.130	$-\sqrt{3}\varepsilon/2\sqrt{2}$ −0.055	$-\sqrt{3}\alpha_0/\sqrt{2}$ −0.078	0
3	0	0	0	0	$3\sqrt{3}\alpha_0/2\sqrt{2}$ 0.130	0	0	0
4	0	0	0	0	$-3\sqrt{3}\alpha_0/2\sqrt{2}$ −0.130	0	0	0
5	0	0	0	0	$15\alpha_0\delta^2/2\sqrt{2}$ 0.295	$\alpha_0/2\sqrt{2}$ 0.025	$\alpha_0/\sqrt{2}$ 0.036	0
6	0	0	0	0	$-15\alpha_0\delta^2/2\sqrt{2}$ −0.295	$-3\alpha_0/2\sqrt{2}$ −0.075	0	0
7	0	0	0	0	$\varepsilon(\varepsilon-5\alpha_0\delta^2/2\sqrt{2}$ −0.073	$[2(1+\varepsilon)+\varepsilon\alpha]/2\sqrt{2}$ 0.796	$-\varepsilon\alpha_0/\sqrt{2}$ −0.036	0
8	0	0	0	0	$-\alpha_0(1-5\varepsilon)/2\sqrt{2}$ 0.073	$[\varepsilon\alpha-2(1+\varepsilon)]/2\sqrt{2}$ −0.746	0	0
9	0	0	0	0	$-\varepsilon\alpha(2+5\varepsilon)/2\sqrt{2}$ −0.140	$-[4(1+\varepsilon)+\varepsilon\alpha]/2\sqrt{2}$ −1.587	0	0
10	0	0	0	$16\varepsilon/9$ 0.114	$\alpha_0(2\alpha_0+5\varepsilon/2\sqrt{2}$ 0.134	$-\varepsilon\alpha/2\sqrt{2}$ −0.025	$\varepsilon\alpha_0(4\alpha_0+\varepsilon)/\sqrt{2}$ 0.164	$-\sqrt{2}\varepsilon\alpha_0/9$ −0.010
11	0	0	0	$-2(15+16\varepsilon)/9\sqrt{3}$ −2.110	0	0	$-2\sqrt{2}\varepsilon\alpha_0/\sqrt{3}$ −0.105	$2\sqrt{2}(8+\varepsilon)/9\sqrt{3}$ 1.105
12	0	0	0	$2[4(1+3\alpha_0)\varepsilon-3]/9\sqrt{3}$ −0.240	$\sqrt{6}\varepsilon\alpha_0/4$ 0.031	0	$\varepsilon\alpha_0(1+6\alpha_0)/\sqrt{6}$ 0.137	$[21-\varepsilon(1+3\alpha_0)]/9\sqrt{6}$ 0.940
13	0	0	0	$-16\sqrt{2}\varepsilon/9\sqrt{3}$ −0.132	0	0	$-2\alpha_0/\sqrt{3}$ −0.074	$2\varepsilon/9\sqrt{3}$ 0.012

is the "spectroscopic" mass of hydrogen atom[2]) and $\varepsilon_H = m_H/m_H = 1$.

2. We now express $({}^{\tau}T_t)_k^{def.}$ in terms of the matrix elements ${}^{\tau}L$:

$$({}^{\tau}T_t)_k^{def.} = \sum_{\lambda}^{n_\tau} {}^{\tau}f_\lambda \sum_{s}^{n_\tau} {}^{\tau}X_{\lambda st} \cdot {}^{\tau}L_k^s. \qquad (4)$$

The coefficients ${}^{\tau}X_{\lambda st}$ can be found by the following method. It follows from the relation $LL' = A$ (A is the matrix of kinetic coefficient, prime indicates the transpose of the matrix), which was pointed out by Crawford and Fletcher,[6] that $L = A(L^{-1})'$ and

$${}^{\tau}L_k^s = \sum_{l}^{n_\tau} {}^{\tau}A_{sl}\,({}^{\tau}L^{-1})_l^k. \qquad (5)$$

Combining (3), (4), and (5), we obtain

$$\sum_{l}^{n_\tau}\sum_{s}^{n_\tau} {}^{\tau}X_{\lambda sl}\,{}^{\tau}A_{sl}\,({}^{\tau}L^{-1})_l^k = \sum_{l}^{n_\tau} {}^{\tau}a_{\lambda l}\,({}^{\tau}L^{-1})_l^k. \qquad (6)$$

One obtains from (6) the equation system for determining ${}^{\tau}X_{\lambda st}$:

$$\sum_{s}^{n_\tau} {}^{\tau}X_{\lambda sl}\,{}^{\tau}A_{sl} = {}^{\tau}a_{\lambda l};\quad l = 1, 2, \ldots, n_\tau. \qquad (7)$$

The matrix elements ${}^{\tau}A_{sl}$ are calculated by means of the formulas in reference 2. All ${}^{\tau}X_{\lambda st}$ not shown below are equal to zero. For $\tau = A_1$, A_2 the solution of (7) is elementary; the result is

$${}^{A_1}X_{121} = {}^{A_1}X_{131} = -{}^{A_1}X_{122} = -{}^{A_1}X_{133} = \frac{\sqrt{3}}{2};$$

$${}^{A_1}X_{3,\,10,\,1} = {}^{A_1}X_{3,\,11,\,1} = -{}^{A_1}X_{3,\,10,\,2} = -{}^{A_1}X_{3,\,11,\,2} = -\sqrt{\frac{3}{2}};$$

$${}^{A_1}X_{3,\,12,\,1} = -\frac{{}^{A_1}X_{3,\,12,\,2}}{2} = {}^{A_1}X_{3,\,12,\,3} = -\frac{4}{3\sqrt{6}};$$

$${}^{A_1}X_{111} = -\frac{\sqrt{3}\;\varepsilon_0(\sigma+\sigma_H)}{[\varepsilon(\sigma+\sigma_H)^3+\sigma_H^3]};$$

$${}^{A_1}X_{221} = {}^{A_1}X_{111} + \sqrt{3}.$$

For the symmetry species B_1, B_2, that include rotation, the solution of (7) is very difficult, and it is therefore necessary to make use of the condition that the momentum is equal to zero, explicitly. The formulas for its projections are exceedingly cumbersome and cannot be reproduced in this paper. Applying the method suggested, and already used in reference 2, we have obtained the following values of ${}^{B_1}X_{\lambda st}$ and ${}^{B_2}X_{\lambda st}$:

$${}^{B_1}X_{4,\,11,\,1} = -\frac{4}{3\sqrt{3}};\quad {}^{B_1}X_{122} = -{}^{B_1}X_{133} = \frac{1}{\sqrt{2}};$$

$${}^{B_1}X_{3s2} = \frac{{}^{B_1}N_{s1}}{z},$$

$$z' = z + \frac{6}{\varepsilon_0^3} + \frac{23}{\varepsilon\sigma_0^3} + \frac{15}{\sigma_0^3}.$$

Table 4. The Values of ${}^{A_2}a_{\lambda 1t}$

t	1		1		t	1		1	
λ	1		2		λ	1		2	
t \ Asλ	$s_{Q1}+s_{Q2}-2s_{Q3}$		$s_{q1}+s_{q2}-2s_{q3}$		t \ Asλ	$s_{Q1}+s_{Q2}-2s_{Q3}$		$s_{q1}+s_{q2}-2s_{q3}$	
1	$-\sqrt{3}\,\varepsilon\sigma_0(\sigma_H+\sigma)$	−0.220	$\sqrt{3}\,[(1+\varepsilon)\sigma_H+\varepsilon\sigma]\,\sigma_H$	2.047	2	0	0	0	0
					3	0	0	0	0

Table 5. The Values of ${}^{B_2}a_{\lambda 1t}$

t	1				2				
λ	1	2	3	4	1	2	3	4	
$B_{2s\lambda}$ \ t	$2s_{Q3}-s_{Q1}-s_{Q2}$	$2s_{q3}-s_{q1}-s_{q2}$	$s_{Q01}+s_{Q02}-2s_{Q03}$	$(s_{q1}-s_{q2})C\Pi_1$	$s_{Q1}+s_{Q2}-2s_{Q3}$	$s_{q1}+s_{q2}-2s_{q3}$	$s_{Q01}+s_{Q02}-2s_{Q03}$	$(s_{q1}-s_{q2})C\Pi_1$	
1				$-8\sqrt{2}\,\varepsilon\sigma_0/9\sqrt{3}$	$-\varepsilon\sigma(3\varepsilon+\sigma_0+2\sigma_H)/\sqrt{3}$	$2\sigma_H[(1+\varepsilon)\sigma_H+\varepsilon\sigma]/\sqrt{3}$	$\varepsilon\sigma_0(2\sigma_0+\sigma)\sqrt{3}$	$-\varepsilon\sigma_0/9\sqrt{3}$	
	0	0	0	−0.046	−0.208	1.265	0.081	−0.004	
2				$8\varepsilon\sigma_0/9\sqrt{3}$	$-\varepsilon\sigma(\sigma_H-\sigma_0)\sqrt{6}$	$\sigma_H[(1+\varepsilon)\sigma_H+\varepsilon\sigma]\sqrt{6}$	$-\varepsilon\sigma_0(2\sigma_0+\sigma_H)\sqrt{6}$	$\varepsilon\sigma_0/9\sqrt{6}$	
	0	0	0	0.033	−0.009	0.570	−0.119	0.003	
3						$-2\sqrt{2}\,\varepsilon\sigma\sigma_H$	$2\sqrt{2}\,\varepsilon\sigma\sigma_0$		
	0	0	0	0	0	−0.203	0.142	0	
4				$-8\varepsilon\sigma_0/9\sqrt{3}$	$-\varepsilon\sigma(\sigma_0-\sigma_H)\sqrt{6}$	$-\sigma_H^2(1+\varepsilon)\sqrt{6}$	$2\varepsilon\sigma_0/\sqrt{6}$	$-\varepsilon\sigma_0/\sqrt{6}$	
	0	0	0	−0.033	0.009	−0.453	0.037	−0.003	
5				$-8\sqrt{2}\,\varepsilon\sigma_0/9\sqrt{3}$	$-\varepsilon\sigma(\sigma_0-\sigma_H)\sqrt{3}$	$-\sigma_H[(1+\varepsilon)\sigma_H+2\varepsilon\sigma]\sqrt{3}$	$\varepsilon\sigma_0(2\sigma_0+3\sigma)\sqrt{3}$	$-\varepsilon\sigma_0/9\sqrt{3}$	
	0	0	0	−0.046	0.012	−0.765	0.139	−0.004	
6						$-4\varepsilon\sigma\sigma_H/\sqrt{3}$	$4\varepsilon\sigma\sigma_0/\sqrt{3}$		
	0	0	0	0	0	−0.165	0.116	0	
7				$-2(15+16\varepsilon)/9\sqrt{3}$			$2\sqrt{2}\,\varepsilon\sigma_0\sqrt{3}$	$-2\sqrt{2}\,(6+\varepsilon)/9\sqrt{3}$	
	0	0	0	−2.110	0	0	0.105	−1.105	
8				$2[3-4\varepsilon(1+3\sigma_0)]/9\sqrt{3}$	$-\sqrt{3}\,\varepsilon\sigma\sigma_0/\sqrt{3}$		$\varepsilon\sigma_0[1+8\sigma_0]\sqrt{6}$	$[21-\varepsilon(1+3\sigma_0)]/9\sqrt{6}$	
	0	0	0	0.340	−0.082	0	0.137	0.940	
9				$16\sqrt{2}\,\varepsilon_0/9\sqrt{3}$			$-2\varepsilon\sigma_0/\sqrt{3}$	$2\varepsilon/9\sqrt{3}$	
	0	0	0	0.131	0	0	−0.074	0.012	

Table 6. The Values of $^{B_1}X_{3\lambda 2}$

s	$^{B_1}N_s$	$1/\alpha$	$1/\alpha_1$	$1/\alpha_2$	$1/\alpha_1\alpha_2$	$1/\alpha_1^2$	$1/\alpha_2^2$	$1/\alpha$	$1/\alpha_1\alpha_2$	$1/\alpha^2$	$\frac{1}{\alpha_1^2}+\frac{1}{\alpha_2^2}$	$1/\alpha\alpha_1$	$1/\alpha\alpha_2$	$1/\alpha^2$	1	$^{B_1}X_{3\lambda 2}$
1	$\sqrt{6}/4$	2	3	3	4	1	1	0	0	0	0	0	0	0	0	0.014
2	$-\sqrt{6}/4$	10	15	15	20	5	5	0	0	0	0	0	0	0	0	−0.069
3	$-\sqrt{6}/2$	2	3	1	1	0	0	0	0	0	0	0	0	0	0	−0.002
4	$-\sqrt{6}/2$	2	3	1	1	0	0	0	0	0	0	0	0	0	0	−0.002
5	$-\sqrt{2}/4$	120	12	102	4	0	0	42	63	141	7	28	21	78	48	−0.356
6	$-\sqrt{2}/4$	88	12	74	4	0	0	42	29	63	1	4	3	34	48	−0.184
7	$\sqrt{2}/2$	14	−3	13	−1	0	0	14	0	0	0	0	0	0	16	0.013
8	$-\sqrt{2}/2$	18	3	15	1	0	0	14	0	0	0	0	0	0	16	−0.016
9	$\sqrt{2}/2$	10	3	8	1	0	0	7	0	0	0	0	0	0	8	0.008
10	$\sqrt{3}/2$	90	3	78	1	0	0	35	48	108	6	24	18	60	40	0.550
11	$-\sqrt{6}/9$	18	15	18	18	0	0	7	0	0	0	0	0	0	8	−0.009
12	$\sqrt{6}/9$	18	15	18	18	0	0	35	0	0	0	0	0	0	40	0.014
13	$-2/\sqrt{3}$	6	5	6	6	0	0	0	0	0	0	0	0	0	0	−0.012
z	1	96	18	84	14	0	0	140/3	48	108	12	48	36	80	160/3	

Table 7. The Values of $^{B_2}X_{3\lambda 2}$

	s	$^{B_2}N_s^a$	$1/\alpha$	$1/\alpha_H$	$1/\alpha_3$	$1/\alpha\alpha$	$1/\alpha\alpha_H$	$1/\alpha\alpha_3$	$1/\alpha^2\alpha_3$	$1/\alpha$	1	$^{B_2}X_{3\lambda 2}$
$a_{3\lambda 2}$	1	$-\sqrt{3}$	12	6	6	21	5	8	9	2	2	0.375
	2	$\sqrt{3/2}$	12	6	6	21	5	8	9	2	2	−0.283
	3	$\sqrt{3}/4$	22	13	9	39	11	12	17	3	3	−0.148
	4	$-\sqrt{3/2}$	12	6	6	21	5	8	9	2	2	0.289
	5	$-\sqrt{3}$	12	6	6	21	5	8	9	2	2	0.400
	6	$\sqrt{3}/4$	32	20	12	57	17	16	25	4	4	0.264
	7	$-\sqrt{2/3}a$	6	1	5	6	0	6	0	0	7/3	5/3	0.014
	8	$-\sqrt{2/3}\sqrt{3}a$	12	2	10	12	0	12	0	0	70/3	74/3	0.020
	9	$2/\sqrt{3}a$	6	1	5	6	0	6	0	0	0	−1	−0.012
	s	$^{B_2}N_s^d$	$1/\alpha$	$1/\alpha_H$	$1/\alpha_3$	$1/\alpha\alpha$	$1/\alpha\alpha_H$	$1/\alpha\alpha_3$	$1/\alpha^2\alpha_3$	$1/\alpha$	1	$^{B_2}X_{3\lambda 2}$
$d_{3\lambda 2}$	1	1	0	0	0	0	0	0	0	0	0	
	2	$\sqrt{3/2}$	8	8	0	7	7	0	0	0	0	
	3	$1/\sqrt{2}$	8	8	0	7	7	0	0	0	0	
	4	$-\sqrt{3/2}$	12	6	6	9	7	2	0	0	2	
	5	$-\sqrt{3}$	8	8	0	7	7	0	0	0	0	
	6	$3\sqrt{3}/4$	8	8	0	7	7	0	0	0	0	
Γ	γ_1		36	18	18	63	15	24	27	6	6	6
	γ_2		18	15	3	15	14	1	0	0	0	1
	γ_3		18	3	15	24	1	23	6	6	6	5
	γ_4		6	1	5	6	0	6	0	0	35/3	37/3

j, and z are linear combinations of simple functions of ε and of various σ, given in the first row of Table 6, with the coefficients shown in that table. The factors $^{B_1}N_s$ are given in the second column, and the calculated values of $^{B_1}X_{3\lambda 2}$ in the last column.

For λ = 2,4

$$^{B_1}X_{\lambda 2} = -{}^{B_1}X_{3\lambda 2} + \Delta_{\lambda 2}; \quad \Delta_{272} = \Delta_{2,10,2} = -\Delta_{288} = -\Delta_{2\,12} = \frac{1}{\sqrt{2}};$$

$$\Delta_{4,11,2} = 3^{-1}\Delta_{4,12,2} = \frac{\sqrt{6}}{9}.$$

The remaining $\Delta_{\lambda 2}$ are equal to zero.

$$^{B_1}X_{471} = -\frac{4}{3\sqrt{3}}; \quad {}^{B_1}X_{3\lambda 2} = -\frac{\left(\frac{^{B_1}N_s^{(a)}a_s}{\sigma} + \frac{^{B_1}N_s^{(d)}d_s}{\sigma_H}\right)}{\Gamma},$$

where

$$\Gamma = \frac{\gamma_1}{\sigma} + \frac{\gamma_2}{\sigma_H} + \frac{\gamma_3}{\sigma_3} + \gamma_4;$$

The values for c, d, γ_1, γ_2, γ_3, γ_4, N, are given in Table 7 which is similar to Table 6. $d_7 = d_8 = d_9 = 0$.

For λ = 1, 2, 4

$$^{B_2}X_{\lambda 2} = \left(-\frac{\lambda^2}{6} - \frac{\lambda}{2} + \frac{11}{3}\right). \quad {}^{B_2}X_{3\lambda 2} + {}^{B_2}\Delta_{\lambda 2}.$$

The $^{B_2}\Delta_{\lambda 2}$ values are given in Table 8.

Table 8. The Values of $^{B_2}\Delta_{\lambda 2}$

s \ λ	1	2	4
1	$-\sqrt{3}$	0	0
2	$\sqrt{3/2}$	$\sqrt{3/2}$	0
3	$1/\sqrt{2}$	$1/\sqrt{2}$	0
4	$-\sqrt{3/2}$	$-\sqrt{3/2}$	0
5	$-\sqrt{3}$	$-\sqrt{3}$	0
6	$3\sqrt{3}/4$	$3\sqrt{3}/4$	0
7	0	0	$-\sqrt{2}/3\sqrt{3}$
8	0	0	$2/\sqrt{6}$
9	0	0	0

By direct substitution of the values from Tables 2-8 into (7) one can see that they satisfy Eq. (7). Numerical calculations of intensities and depolarization, and comparison of these quantities with the experimental data will be given in the next paper.

REFERENCES

1. M. A. Kovner and B. N. Snegirev. Opt. i Spektr. 5, 239 (1958).
2. M. B. Wolkenstein, M. A. El'iashevich and B. I. Stepanov. "Kolebaniia molecul." (Vibrations of molecules), 2, GITTL, Moscow, 1949.
3. M. B. Wolkenstein. "Stroenie i fizicheskie svoistva molecul." (Structure and physical properties of molecules), Izd. AN USSR, 1955.
4. S. M. Ferigle and A. Weber. Canad. J. Phys. 32, 799 (1954).
5. T. Yoshino and H. J. Bernstein. J. Mol. Spectroscopy 2, 241 (1958).
6. B. L. Crawford and W. H. Fletcher. J. Chem. Phys. 19, 141 (1951).

ABSORPTION SPECTRA OF CRYSTALS OF SOME THIAZINE AND OXAZINE DYES

N. M. Melankholin

Received 26 February 1959

Absorption spectra of crystals of three dyes were studied: thionine blue, toluidine blue, and Capri blue. Characteristic absorption curves were obtained, corresponding to vibrations parallel to the different axes of the optical indicatrix of the crystals studied. Certain peculiarities were established which appear in the absorption spectra and were found earlier in other dyes. Anomalous dispersion of the axes of the indicatrix was discovered in crystals of Capri blue. An attempt was made to explain the observed shift of the absorption bands with a change in the wave normal.

For a number of years the laboratory of crystal optics of the Institute of Crystallography has been occupied with the investigation of the absorption spectra and other physical properties of dye crystals. The results of the investigation have already been published in part in a series of works.[1-3]

In the present article are set forth the data obtained by us for two thiazine dyes—thionine blue and toluidine blue—and one oxazine dye—Capri blue. The absorption curves of all crystals investigated were obtained with the help of a photoelectric microspectrophotometer constructed by us.[4] This apparatus makes it possible to carry out measurements on crystals with a diameter down to 0.02 mm in a polarized light beam with an aperture of about 9 deg (in air).

For the measurements crystals were chosen, as far as possible, with a symmetrical orientation; that is, oriented so that one of the planes of symmetry of the optical indicatrix was parallel to the surface of the slide. For each crystal, absorption curves corresponding to vibrations parallel to two principal axes of the optical indicatrix were measured in polarized light. The optical orientation of the crystals was determined by the conoscopic figure and checked by the dichroic colors. A difference in the dichroic colors for the same character of the conoscopic figures helped in distinguishing the different orientations from one another.

The determination of the optical orientation was often highly complicated; this is explained, first, by the prevalence of oblique orientations among crystals grown on the slide, and, second, by the indecipherability of the conoscopic figures, which resulted from the small thickness of the samples suitable for study and the high dispersion of the axes of the indicatrix and the optic axes.*

*The dispersion of the axes of the indicatrix was detected by the presence of dispersion in the angles of extinction; the latter reaches 30 deg for thionine blue[3] and 25 deg for Capri blue.

Consequently, it was not always possible to establish reliably the orientation of the vibrations corresponding to the absorption bands found. It must be noted that, in the presence of dispersion in the axes of the indicatrix and for a constant position of the polarizer with respect to the crystal studied, to speak of parallelism between the vibrations of the polarizer and any axis of the indicatrix can only be conditional, implying only some average orientation of this axis over the spectrum.

In view of the impossibility of an exact determination of the thickness of the crystals studied and the poor quality of their surfaces, absorption coefficients were not calculated, and all the absorption curves presented below have been plotted according to optical density values.

All the crystals studied were obtained by means of slow evaporation of drops of an aqueous solution of the dye, placed on the surface of a microscope slide. In order to slow down evaporation, the preparation was put in a loosely closed vessel.

THIONINE BLUE

In the preparations of thionine blue O

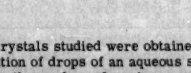

made by us, there were obtained variously-oriented platelike crystals, many of which have symmetrical orientations. To this category belong, first of all, crystals which show dichroism from dark blue-violet to a pale bluish color and are oriented perpendicular to the acute

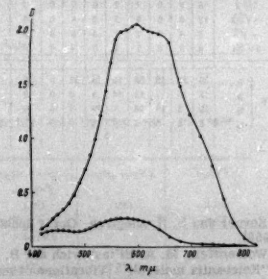

Fig. 1. Absorption curves of a crystal of thionine blue. Direction of observation: parallel to the N_g axis of the indicatrix.

bisectrix N_g. For these absorption curves were obtained, corresponding to vibrations approximately parallel to N_m and N_p (Fig. 1). Vibrations parallel to N_m (violet-blue tint) are very strongly absorbed (on the absorption curve there are observed three bands, close together and very intense, with maxima at 570, 598 and 640 mμ).

The absorption curve of vibrations parallel to N_p (pale-bluish tint) is characterized by a very washed-out, weak band with a maximum around 575 mμ and a second, hardly noticeable band located around 450 mμ.

Crystals with dichroism from dark-blue or blue to purple also have a symmetrical orientation. They are oriented approximately perpendicular to the obtuse bisectrix N_p. The absorption curve of vibrations parallel to N_g (purple color) in these crystals is characterized by one sharp absorption band at 544 mμ (Fig. 2). The absorption curve of vibrations parallel to N_m (dark-blue color) has a sharp intense absorption band around 585 mμ and also a less pronounced intense band around 630 mμ. On the curve there can also be seen traces of absorption bands around 450 and 680 mμ.

In some crystals which have the same dichroic colors, the absorption curve corresponding to the blue color has the same appearance as in Fig. 2, but the absorption band on the curve for the purple color is located at 560 mμ (instead of 545). These crystals lie on the slide at some oblique orientation which could not be precisely determined.

At a somewhat different oblique orientation, a rosy-red color is observed in place of purple, and on the corresponding absorption curve one can clearly see three overlapping intense bands around 520, 545, and 590 mμ, and also weaker and indistinct bands around 450, 620, and 700 mμ. Some other oblique orientations of thionine blue

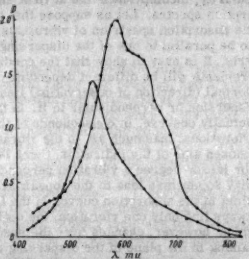

Fig. 2. Absorption curves of a crystal of thionine blue. Direction of observation: parallel to the N_p axis of the indicatrix.

crystals were also studied, for which somewhat different positions of the absorption bands were obtained. Thus, for example, in the absorption spectrum for a purple color one narrow band at 535 mμ was sometimes obtained, and for a blue color a wide band at 612 mμ.

TOLUIDINE BLUE

The toluidine blue of the JG company

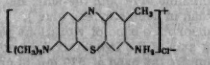

used by us for making our preparations gives crystals of a needle-like habitus or aggregates of such crystals on the slide. In all our attempts at crystallizing it, crystals in only one orientation were always obtained, showing dichroism from violet-rose to blue. Conoscopic investigation showed that in these crystals the N_gN_m plane of the indicatrix is parallel to the surface of the slide. This made it possible to measure absorption curves for them which corresponded to vibrations parallel to N_g and N_m. The first curve (rose-violet color) is characterized by a broad band of very intense absorption with a maximum at 582 mμ; the shoulder in the absorption curve on the short-wave side of the band indicates the presence of a second maximum around 540 mμ (Fig. 3). Weak traces of washed-out bands around 700 and 760 mμ are also noticeable on the curve. This curve corresponds to absorption by vibrations perpendicular to the long axis of the crystal.

The absorption curve of vibrations parallel to N_m (pale-blue color) has a very washed-out, weak absorption band around 640 mμ. Apparently there is also a second, even more washed-out band with a maximum around 600 mμ. We have not yet succeeded in obtaining absorption curves for other directions of vibration.

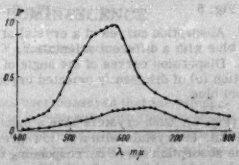

Fig. 3. Absorption curves of a crystal of toluidine blue. Direction of observation: parallel to the N_p axis of the indicatrix.

CAPRI BLUE

The crystals of Capri blue GON

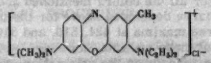

grow principally in the form of dendrites of various orientations. However, we did not succeed in finding among them a single crystal with a symmetrical orientation

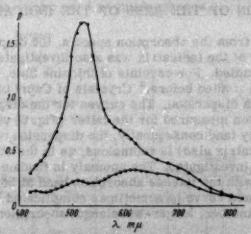

Fig. 4. Absorption curves of an obliquely oriented crystal of Capri blue.

favorable for measurements. Consequently, all the absorption curves determined by us refer to various oblique orientations.

Crystals with dichroism from pale-blue to dark purple (in thick crystals to black with a metallic luster) are most frequently encountered. As the absorption curves of such crystals show, two different orientations, which can also be distinguished by the tint of their metallic luster, are characteristic of them. Most such crystals give a curve, for the purple color, with one sharp band of intense absorption at 525 mμ.

The absorption curve corresponding to the considerably weaker blue color has three maxima at 430, 510,

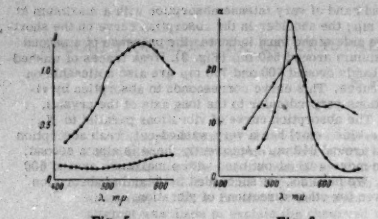

Fig. 5 Fig. 6

Fig. 5. Absorption curves of a crystal of Capri blue with a different orientation.
Fig. 6. Dispersion curves of the angle of extinction (α) of differently oriented crystals of Capri blue.

and 610 mμ (Fig. 4). Such crystals have a metallic luster with a green tint. In crystals with a yellow-green metallic luster, the absorption curve corresponding to the purple color has a broad intense band with a maximum at 565 mμ; a weak trace of a band at 525 mμ can also be noticed on it. The absorption curve for the bluish color has one weak, very washed-out absorption band around 620 mμ (Fig. 5).

In the Capri blue preparations, there are also commonly encountered crystals with dichroism from brown-yellow, yellow-green, or bluish-green to black. The absorption curve for all the colors mentioned above repeats the absorption curve described above for the blue color and also has three maxima at 424, 510, and 610 mμ. The relative height of these maxima, however, varies greatly, apparently in dependence on the orientation, which also produces the difference of the colors.

DISPERSION OF THE AXES OF THE INDICATRIX

Aside from the absorption spectra, the dispersion of the axes of the indicatrix was also investigated in the crystals studied. For crystals of thionine blue, it had already been studied before.[1] Crystals of Capri blue also showed high dispersion. The curves for the dispersion of the extinction measured for the latter (Fig. 6) show that this quantity (and consequently, the dispersion of the axes of the indicatrix also) is anomalous, as in the other dyes previously investigated. The anomaly is fundamentally connected with the intense absorption band at 565 mμ, but the dispersion curve is sometimes complicated by the influence of another, longer-wavelength absorption band.

DISCUSSION OF THE RESULTS

In this way, as a result of the investigation of crystals of a series of dyes, characteristic absorption spectra have been established for light vibrations which are differently oriented with respect to the crystallographic axes. We did not succeed in growing all the crystals in all the orientations needed for such an investigation. However, the results obtained for thionine blue have confirmed once again the fact that certain unusual peculiarities in the absorption spectra, which have not been observed up to the present in weakly absorbing crystals, are characteristic of dye crystals. In the investigation of the absorption spectra of crystals of methylene blue and some other dyes,[2] along with absorption bands corresponding to vibrations parallel to the principal axes of the optical indicatrix, there had already been discovered further special absorption bands corresponding to some obliquely oriented vibrations. The same peculiarity, as was shown above, is found in crystals of thionine blue, in which the absorption bands at 535 and 560 mμ are observed only at oblique orientations and are absent in absorption spectra which correspond to the two symmetrical orientations studied.

Another peculiarity (also discovered earlier) in the absorption spectra of dye crystals resides in the fact that the position of the absorption bands for vibrations which are more or less parallel to some principal axes of the optical indicatrix changes with a change in the direction of the wave normal. Such a property was also discovered in the case of crystals of thionine blue, in which, for vibrations parallel to N_m, the fundamental absorption band has a maximum at 598 mμ in the case of observation along N_g and at 585 mμ in the case of observation along N_p.

Taking into account that dye crystals show a more or less marked dispersion of the axes of the indicatrix, we may express the following supposition about the nature of this peculiarity, incomprehensible at first sight, in their absorption spectra. Let us suppose that we are studying the absorption spectrum of vibrations which are assumed to be parallel to one of the dispersing axes of the indicatrix. It is easy to show that the conditions of the measurements will be different depending on whether the wave normal (direction of observation) lies in the plane of dispersion or perpendicular to it. In the latter case, we actually observe, in consequence of the dispersion, two vibrations, inasmuch as, to the vibration parallel to the chosen axis of the indicatrix, there is added to a greater or lesser degree a vibration perpendicular to it, which may sometimes lead to the appearance of additional maxima in the absorption curve. In the former case we always find only one vibration, the optical orientation of which, however, changes over the spectrum while remaining in the plane of the dispersing axes. As was shown above, for such obliquely oriented vibrations the appearance of special absorption bands is possible, bands which are absent in the absorption spectra of vibrations oriented along the axes. These bands, superimposed on the absorption bands of vibrations parallel to the chosen axis, may produce an apparent shift in them.

Thus, when an "obliquely oriented" absorption band and significant dispersion of the axes of the indicatrix are present in the crystal, the absorption curves measured for one and the same direction of vibration at different directions of the wave normal may appear different.

The following experimental data bear witness in favor of the above-presented arguments:

1. The shift of the absorption band increases with increasing dispersion of the axes of the indicatrix (for example, in thionine blue both the shift and the dispersion are greater than in neomethylene blue[2]).

2. The absorption band of vibrations parallel to the nondispersing axis of the indicatrix does not undergo a shift (for example, the band at 570 mμ in crystals of neomethylene blue).

A final clarification of the peculiarities in the optical properties of dye crystals can only be given by a corresponding theory, which has not yet been devised. However, even the first (still few, up to the present time) theoretical works in the field of the crystal optics of strongly absorbing crystals often lead to new and unexpected results, showing that such crystals differ essentially in their optical properties from weakly absorbing ones.[3]

It would be of unqualified interest to measure the absorption curve for vibrations exactly parallel to the dispersing axis of the indicatrix. For this the requirement would be to turn the crystal (or the analyzer of the apparatus) gradually, in the process of measurement, in accordance with the dispersion of the chosen axis. Such measurements have not yet been carried out on account of experimental difficulties. It must be noted, however, that in such a method of measurement, the vibration studied, while keeping a constant optical orientation, would change its crystallographic orientation over the spectrum.

REFERENCES

1. N. E. Vedeneeva and E. N. Slavnova. Tr. Inst. Kristallogr. Akad. Nauk SSSR No. 7, 135 (1952).
2. N. M. Melankholin. Opt. i Spektr. 3, 104 (1957).
3. N. M. Melankholin. Kristallografiya 2, 48 (1957).
4. N. M. Melankholin and B. H. Grechushnikov. Tr. Inst. Kristallogr. Akad. Nauk SSSR No. 12, 186 (1956).
5. F. I. Fedorov. "Optika anizotropnykh sred." (Optics of anisotropic media), Izd. Akad. Nauk SSSR, Minsk, 1958.

VITRIFICATION OF POLYMERS AND LUMINESCENCE

E. V. Anufrieva, M. V. Volkenstein, and T. V. Razgovorova

Received 3 March 1959

In the investigation of luminophore-polymer systems it has been observed that the temperature dependence of the intensity of the luminosity for auramine (a molecule with flexible structure), and certain dyes with a rigid structure, changes at a point corresponding to the temperature of vitrification of the polymer T_g, that is, the luminescing molecule introduced into the polymer is a sensitive indicator of the mobility of the macromolecule.

INTRODUCTION

The vitrification of low-molecular liquids and polymers is a kinetic relaxation process, and amounts to the fixing of the equilibrium structure at the temperature of vitrification T_g. As a consequence of the large increase in the time of relaxation in the vicinity of T_g, no further reorganization of the structure at $T < T_g$ can be brought about under the conditions of the experiment. Thus, vitrification is determined by the mobility of the molecules or their individual fragments.[1-3] There exists a number of methods for the study of the mobility of the macromolecules in polymers. Among them are the methods of dielectric loss, nuclear paramagnetic resonance, ultrasonic absorption, etc.

The study, by means of luminescence, of the mobility of the macromolecules in polymers and the vitrification of polymers is the purpose of the present report. It is well-known that the intensity of the luminosity of luminophores, consisting of molecules having a flexible skeleton, depends strongly on the viscosity of the medium, decreasing with a decrease in the viscosity.[4-6] This is explained by the transformation of the excitation energy to the internal rotation degree of freedom (e.g., in such luminophores as the diphenyl- and triphenylmethane series of dyes, cyanides, etc.). During the vitrification of a polymer a sharp increase in viscosity occurs, i.e., a decrease in the mobility of the macromolecules or their individual fragments. Luminophores, introduced into the polymer by one method or another, should sense these changes. Actually, as we have shown for polyvinyl butyral,[7] the temperature function of the intensity of luminosity of a flexible luminophore (auramine, Michler's ketone), introduced into this polymer, undergoes a sharp break at 70°C, which coincides with the T_g for polyvinyl butyral as determined by other methods.

In the present work, a number of different polymers with flexible luminophore molecules introduced into them, were studied. Polymers into which rigid luminophore molecules were introduced were examined in order to study the effect of the structure of the luminescing molecule on the temperature function of the intensity of luminosity in a temperature range including T_g. It should be emphasized that the effect of the viscosity of the medium on luminescence has been previously studied for liquid solutions only at $T > T_g$. Meanwhile, it is precisely the temperature range which includes T_g that is of most interest.

EXPERIMENTAL PROCEDURE

The temperature dependence of the intensity of luminescence of polymer-luminophore systems was measured in a range including T_g of the polymer. Molecules with a flexible structure—auramine—and molecules with a rigid structure—rhodamine B, rhodamine G, rhodanyl orange, and safranin—were used as luminophores.

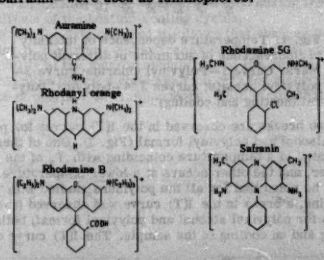

Luminescence was excited by the 436 or 365 mμ lines of the mercury spectrum. The temperature function of its intensity was recorded at the fluorescence band maximum (excited by a UM-2 monochromator) and band maximum of total luminosity. A FEU-19 photomultiplier served as the receiver. For best stabilization of the conditions of excitation, the relative intensities of luminosity, I/I_0, were determined, where I is the intensity of luminosity of the film being studied, and I_0 is the intensity of luminosity of the same film at T = 20°C. Fluorescence spectra were also measured for the systems at different temperatures above and below T_g. The spectra were measured with an apparatus consisting of a UM-2 mono-

chromator and a FEU-19 photomultiplier. A temperature range from 20 to 120°C was studied. The thermal cuvette, into which the samples were placed,[7] was connected to an ultrathermostat.

Temperature dependence curves for the intensity of luminosity were obtained during heating and cooling of the samples, which were prepared as films of 20-30μ thickness. The luminophore was introduced into the polymer either by mutual dissolving of the polymer and dye, followed by removal of the solvent, or by absorption of the dye from a solution of the polymer film. The luminophore concentration was 0.5-5%.

EXPERIMENTS WITH LUMINOPHORES CONSISTING OF MOLECULES WITH FLEXIBLE STRUCTURE

Of the luminescing compounds with flexible skeleton we chose auramine, which was introduced into all of the polymers studied: polyvinyl acetate, polyvinyl formal, polyvinyl alcohol, polystyrene, polyvinyl chloride, and polymethyl methacrylate. The temperature function of the intensity of luminosity I(T) in the range including T_g of the polymer is presented in Fig. 1. As is evident from the figure, the temperature function of the intensity of luminosity of the polymer, for all the cases studied, undergoes changes at T_g. With an increase in temperature, quenching of the luminescence appears to be more intense in the $T > T_g$ region.

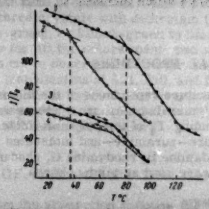

Fig. 1. Temperature dependence of intensity of fluorescence of auramine in different polymers. Curve 1—Polyvinyl chloride; curve 2—polyvinyl acetate; curves 3, 4—polyvinyl butyral (heating and cooling).

Two breaks are observed in the I(T) curves for polyvinyl alsohol and polyvinyl formal (Fig. 2). One of them is situated at a temperature coinciding with T_g of the polymer, and the other occurs at a lower temperature. It should be noted that for all the polymers studied with auramine, a break in the I(T) curve was observed (two breaks for polyvinyl alcohol and polyvinyl formal) both on heating and on cooling of the sample. The I(T) curve obtained during cooling repeats that obtained during heating (polyvinyl alcohol, polyvinyl formal), or passes below it (polyvinyl butyral, polyvinyl acetate). In the later instance, the decrease in intensity was associated with irreversible physicochemical changes occurring in the luminescing compounds at $T > T_g$.

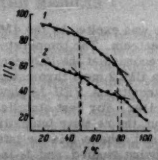

Fig. 2. Temperature dependence of intensity of fluorescence of auramine in different polymers. Curve 1—Polyvinyl formal; curve 2—polyvinyl alcohol.

During transition through T_g, the fluorescence band is shifted only very little (by 2-3 mμ) into the short-wavelength region (polyvinyl butyral, polyvinyl acetate) and into the region of long wavelengths (polyvinyl alcohol, polyvinyl formal). Thus, during transition through T_g, changes in the spectra are observed which are of the same order as those observed on substitution of one solvent for another. These changes indicate an alteration in the nature of the intermolecular interaction at T_g.

As is known, a decrease in the intensity of luminescence or discharge, i.e., quenching of luminescence, occurs with an increase in the probability of nonemission transitions from the excited to the normal state. The mechanism of nonemission transitions of a molecule to the normal state is perhaps different. Internal deactivation of the excited electronic state (transformation of electronic energy to vibrational energy as a result of the interaction of the motion of electrons and vibrations of the nuclei) is possible. Photochemical reactions can take place during the excited electronic state. The number of such reactions is large for complex molecules, since numerous changes in their molecular structure are possible, and are brought about by the accumulation of vibrational energy at the corresponding degrees of freedom. Finally, transitions without the emission of light can be brought about by the presence of interaction with the surrounding medium at the expense of a transfer of electronic energy to the solvent molecules.

In molecules with a flexible skeleton, the transformation of electronic energy to energy of torsional vibrations of large fragments of the molecule relative to one another, around the single bond which binds them, is the decisive mechanism of nonemission transitions. The probability of such a process is higher, the lower the viscosity of the medium.[4-6] It is true that until now the relationship of the discharge of flexible luminescing compounds to the viscosity of the medium had been studied for viscosities not exceeding 10^3 poises. Moreover, it was found that the viscosity is the decisive factor in changing the intensity of luminosity, but besides this factor, there also exists an additional thermal quenching.[5]

The quenching of the luminescence of auramine in poly mers above T_g is probably determined by the transformation of electronic energy to vibrational-rotational energy, as a result of the rotation of the benzene rings of the auramine molecule relative to one another, i.e., by the same mechanism which causes quenching of the luminescence of molecules with a flexible skeleton in low-viscosity media. Actually, the mobility of the macromolecules, and the related probability of rotational motions of the luminescing molecules changes above T_g. The intensity of luminosity of auramine in such media is determined, not by the macroviscosity, which above T_g is still quite large ($< 10^{13}$ poises), but by the local viscosity. The change in mobility of fragments of the macromolecules in the mass changes substantially with the local viscosity of the mass.

The equilibrium between the intermolecular bonds forming and dissociating is fixed by vitrification. This effect is quite clearly expressed for hydrogen bonds, as Zhurkov and Levin[8] showed by the method of infrared spectroscopy, in their investigations of polyvinyl alcohol and other vitrifying substances containing hydroxyl groups. The change in intermolecular interaction as a result of such fixing has also been successfully studied by the method of polarimetry.[9, 10]

Thus, the structure of vitrified polymers (or substances consisting of small molecules) is characterized by the presence of relatively stable intermolecular bonds, which form the modes of certain molecular networks. The luminophore molecules are included in this network. (In particular, auramine forms hydrogen bonds with polyvinyl alcohol.) At the same time, fragments of the macromolecules between the nodes retain a certain mobility up to some characteristic temperature, appreciably below T_g. Proceeding from this the local viscosity most immediately surrounding the luminophore can be much altered. It is possible to imagine that the appearance of the second break in the I(T) curve below T_g, for polyvinyl alcohol and polyvinyl formal, was related to the liquidation of this residual mobility as a result of cooling.

It should be noted that the presence of residual mobility in individual portions of the macromolecules is demonstrated by a number of kinetic methods, and also by the method of spectroscopy. Zhurkov and Levin[8] showed, in particular, that free hydroxyl groups appear in polyvinyl alcohol at 50-55°C. We observed the second break in the I(T) curve in the same temperature region. The vitrification of polyvinyl alcohol occurs at a higher temperature (80°C).

Other possible mechanisms of nonemission transitions to the normal state (photochemical reaction in the excited state, and transfer of electronic energy to solvent molecules) can contribute to the change in the intensity of luminosity of auramine in polymers above T_g, but are not the decisive source of the appearance of the break at T_g. The irreversible decrease in the intensity, which is observed above T_g, very significantly for polyvinyl butyral and polyvinyl acetate (Fig. 1), but which is absent in other polymers (polyvinyl alcohol, polyvinyl formal), can be attributed to some photochemical process. It is unlikely that a photochemical reaction in high-viscosity media can produce changes which are reversible with temperature. (No reversible reaction could occur under the conditions of a decrease in mobility of the macromolecules in the medium.) As regards the other factor—the reaction of auramine with the medium and the transfer of electronic energy to solvent molecules, i.e., polymer molecules—it also cannot be the decisive cause of the break in the I(T) curve at T_g of the polymer, since the presence of the break does not depend on the nature of the polymer.

Also supporting our concepts of the mechanism for the quenching of the luminescence of auramine in polymers above T_g, are data which we obtained for other luminescing molecules having a flexible structure.[7] In the investigation of the systems, crystal violet-polyvinyl alcohol and polyvinyl butyral, and Michler's ketone-polyvinyl butyral, we observed a break in the I(T) curve at T_g of the polymer. It could be imagined that, in all these instances, the transformation of electronic energy to vibrational-rotational energy, i.e., the flexibility of the skeleton of the luminescing molecule, is the source of the intense quenching of the luminescence above T_g of the polymer.

EXPERIMENTS WITH LUMINOPHORES CONSISTING OF MOLECULES WITH RIGID STRUCTURE

In order to establish whether the flexibility of the skeleton of the luminescing molecule is the decisive factor in the quenching of luminescence above T_g of the polymer, we studied the temperature dependence of the intensity of luminescence of systems of polymer-luminescing molecules with rigid skeletons. Such molecules produce an intense luminosity in low-viscosity media.

The temperature dependence of the intensity of luminescence I(T) of the following systems was studied:

Polyvinyl alcohol-rhodamine B
Polyvinyl alcohol-rhodamine G
Polyvinyl alcohol-rhodanyl orange
Polyvinyl butyral-rhodamine B
Polyvinyl butyral-rhodanyl orange
Polyvinyl formal-rhodamine B
Polyvinyl formal-rhodanyl orange
Polymethyl methacrylate-rhodamine B.

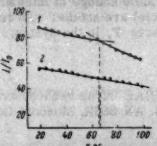

Fig. 3. Temperature dependence of the intensity of fluorescence of rhodanyl orange in different polymers. Curve 1—Polyvinyl alcohol; curve 2—polyvinyl butyral.

It was found that the presence of a break in the I(T) curve at T_g of the polymer is determined by the choice of luminescing compound and polymer. Thus, a sharp break in the I(T) curve of rhodamine B in polyvinyl butyral is observed in the I(T) curve for rhodamine B in polyvinyl alcohol at T_g of polyvinyl alcohol, and in polyvinyl formal at T_g of this polymer. The I(T) relationship of rhodanyl orange in polyvinyl butyral was not measured at T_g of polyvinyl butyral, whereas a break was observed at T_g in the I(T) curve of rhodanyl orange in polyvinyl alcohol and polyvinyl formal (Figs. 3 and 4). The I(T) dependence of safranin in polyvinyl butyral and in polyvinyl formal at the T_g of these polymers also changes (Fig. 5). It should be noted that a break in the I(T) curves of these systems is observed both during heating, and during cooling of the sample, and also during frequent repetitions of the heating-cooling cycles.

From the data obtained it follows that changes occurring in a polymer during transition through T_g (change of mobility of the macromolecule) affect the luminescence of molecules having a rigid skeleton only for a certain choice of polymer and luminophore. This means that

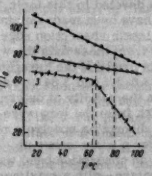

Fig. 4

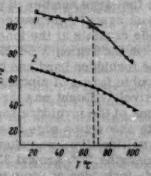

Fig. 5

Fig. 4. Temperature dependence of intensity fluorescence of rhodamine B in different polymers. Curve 1—Polyvinyl alcohol; curve 2—polyvinyl formal; curve 3—polyvinyl butyral.

Fig. 5. Temperature dependence of intensity of fluorescence of safranin in different polymers. Curve 1—Polyvinyl butyral; curve 2—polyvinyl formal.

above T_g the quenching of luminescence is determined by the nature of the interaction of luminophore molecules and polymer macromolecules. It can be imagined that in these instances the quenching of luminescence is brought about as a result of a transfer of the electronic energy of the luminescing molecule to the macromolecule, i.e., in systems with rigid luminescing molecules, intermolecular deactivation of the excited electronic state occurs. Photochemical reactions in the excited state, which lead to irreversible physicochemical changes in the luminescing compound (irreversible change in intensity during the heating-cooling cycle) are another source of the quenching of luminescence above T_g in the systems considered.

REFERENCES

1. P. P. Kobeko. "Amorfyne veshchestva." (Amorphous Materials), Izd. AN SSSR, Moscow-Leningrad, 1952.
2. G. O. Jones. "Glass." London, 1956.
3. M. V. Volkenstein and O. B. Ptitsyn, Zhur. Tekh. Fiz. 26, 2204 (1956).
4. P. P. Feofilov. Doklady Akad. Nauk SSSR 45, 387 (1944).
5. M. D. Galanin. Tr. Fiz. Inst. Akad. Nauk 5, 382 (1950).
6. J. Oster and Y. Nishijima. J. Amer. Chem. Soc. 78, 1581 (1956).
7. E. V. Anufrieva, M. V. Volkenstein and T. V. Razgovorova. Opt. i Spektr. 4, 414 (1958).
8. S. N. Zhurkov and B. Ya. Levin. Doklady Akad. Nauk SSSR 67, 89 (1948); Doklady Akad. Nauk SSSR 72, 269 (1950).
9. N. M. Bazhenov, M. V. Volkenstein and I. A. Bolotina. Zhur. Tekh. Fiz. 25, 1861 (1955).
10. I. A. Bolotina, N. M. Bazhenov and M. V. Volkenstein, Zhur. S. Sogomonyants. Fiz. Tverkogo Tel 1, 133 (1959).

STUDY OF THE ABSORPTION SPECTRUM OF ZINC SULFIDE

N. A. Vlasenko

Received 19 January 1959

We have studied the absorption spectrum of vacuum-evaporated zinc sulfide films from 200 to 600 mμ. We observed an absorption maximum in the 325 mμ region and strong long-wave absorption reaching to 550 mμ; the latter is absent in the absorption spectrum of zinc sulfide crystals, and disappears from films after they are heated in sulfur vapor or in a vacuum. We also studied the temperature dependence of the zinc sulfide absorption spectrum over the range 110-500°K. The temperature coefficient of the spectral shift is different for different spectral regions: it is -2.2×10^{-4} ev/deg around 250 mμ, and -4.4×10^{-4} ev/deg around 340 mμ. The absorption maximum at λ = 325 mμ becomes deeper and sharper and shifts towards the short wavelength region as the temperature falls. We discuss our results.

INTRODUCTION

A knowledge of the intrinsic absorption spectrum is important in constructing the energy level diagram of a substance and for understanding the physical nature of its electrical conduction, photoconductivity, and luminescence.

The date presently available on the zinc sulfide absorption spectrum are incomplete and contradictory, despite the large number of papers devoted to this topic.[1-12] In most cases[1-8] measurements have been made on zinc sulfide crystals at the long wavelength absorption edge only (in the region λ > 325 mμ); from these data the width of the forbidden band has been obtained for the hexagonal and cubic forms of zinc sulfide (3.6-3.7 and 3.64 ev respectively). Doubt was thrown on the validity of determinations of the forbidden band width from the long wavelength absorption edge when the absorption spectrum of zinc sulfide films was studied over a wider range of wavelengths.[9-12] Around 330 mμ an absorption band was found—forbidden at room temperature—with a maximum absorption coefficient of ~ 10^5 cm^{-1}; on the short wavelength side of this band a sharp increase in absorption was observed, up to ~ 10^6 cm^{-1}. Coogan[12] suggested that this band is due to excitons. However, in the spectrum of zinc sulfide films there is also additional strong longwave absorption which is not observed for crystals, according to the data of Coogan[12] and Hall[11]. Doubt therefore arises as to whether the band at 330 mμ and the additional long wavelength absorption of films is not the result of superimposing on the intrinsic zinc sulfide absorption edge the absorption of some impurity introduced in the process of preparing the films. Hall[11] makes this same suggestion. Shalimova[10] also concluded that the absorption band at 334 mμ, which she observed in films of sublimed zinc sulfide, was due to impurity. In addition to this band, Shalimova observed two absorption maxima of unknown origin at wavelengths 284 and 313 mμ.

In view of this disagreement in both the experimental data and their interpretation, it is interesting to study the absorption spectrum of pure zinc sulfide over a wide spectral range at different temperatures, and to explain the nature of its long wavelength region. Our paper is devoted to this.

PREPARATION OF SPECIMENS AND METHOD OF MEASUREMENT

It is possible to study the intrinsic absorption over a wide spectral range only if rather thin layers are used. The specimens were prepared by vacuum evaporation of pure zinc sulfide (phosphor quality) produced by the "Krasnyĭ Khimik" plant. Glass and quartz plates were used for the base. Before evaporation onto the base, the zinc sulfide was heated in vacuum to drive off possible chloride and sulfate impurities. Both evaporation and heating were carried out under a 5×10^{-5} mm Hg vacuum; the evaporating dish was made of tantalum sheet. The evaporating rate varied from 200 to 2000 A/min.

When measuring absorption in thin films interference must either be allowed for or excluded, since in sub-

stances like zinc sulfide, with a high refractive index, interference can cause serious distortion of the absorption spectrum—particularly at its long wavelength edge (see, for example, reference 7, Fig. 5). To exclude interference in the weak absorption region ($\lambda > 335$ mμ) we used the method that we suggested earlier.[13] In the strong absorption region ($\lambda < 335$ mμ) the absorption coefficient was determined by the usual method of comparing the transmission of two specimens of different known thicknesses. The thickness of the specimens was so chosen that their transmission did not exceed 10-20%, so that the error which arose from neglecting interference was small in this case (3-5%). The transmission was measured with an SF-4 spectrophotometer. The film thickness was determined interferometrically with an accuracy up to 1-2% by using lines of equal chromatic order. The error in measuring the absorption coefficient did not exceed 2% in the first case and 5% in the second.

For studying the temperature dependence of the absorption we used an optical Dewar flask with potassium chloride windows, and an oven for heating the specimen; the Dewar flask (or the oven) with the specimen was placed in the cell compartment of the SF-4.

RESULTS OF THE MEASUREMENTS

Figure 1 shows the results of measuring the absorption coefficient K for films of pure zinc sulfide at room temperature (curve 1) in the 220-600 mμ region. The region from 350 to 600 mμ is shown separately on an enlarged scale on the right-hand side of the Figure. Our spectrum agrees well with similar measurements made by Coogan[12] and Hall.[11] The Figure shows that strong absorption ($\sim 10^4$ cm^{-1}) begins at 365 mμ, passes through a broad maximum of $\sim 10^5$ cm^{-1} at 325 mμ, and grows sharply to 7×10^5 cm^{-1} as the wavelength decreases to 220 mμ. The long wavelength absorption tail reaches far into the visible region (at $\lambda \approx 500$ mμ the absorption coefficient is 10^2 cm^{-1}), but the function K (λ) varies monotonically; this is contrary to the results obtained by Coogan[12] who found several maxima in this region. The absorption is low (between 5 and 10%) in the long wavelength region ($\lambda > 365$ mμ) and varies from specimen to specimen; however, we could not find any definite relationship between the absorption and the evaporation conditions or specimen thickness. In the short wavelength region, the absorption does not depend on the evaporation conditions or specimen thickness.

We decided to investigate the variation of the absorption spectrum with heat treatment of the films, in order to elucidate the nature of the absorption maximum around 325 mμ and the long wavelength absorption which is observed in films but absent in zinc sulfide crystals. The films were heated in a vacuum or in sulfur vapor in a quartz tube.

Annealing the specimens at temperatures below 400°C had little effect on their absorption, but heating the films to a higher temperature changed the long wavelength absorption considerably. The change in the absorption spectrum was identical for heating in a vacuum or in sulfur vapor, but varied with the period and temperature of the annealing treatment. Figure 2 shows the absorption spectrum of unannealed films (curve 1) and of films annealed in a vacuum (or sulfur vapor) at 550°C for 2 min (curve 2), 15 min (curve 3), and 2 hr (curve 4). Figure 1, curve 2, shows the absorption over a wider spectral range of specimens after prolonged annealing. The long wavelength absorption of films ($\lambda > 330$ mμ) is greatly reduced, approaching the absorption of zinc sulfide crystals in this region, while the absorption in the

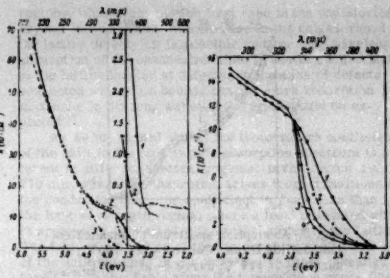

Fig. 1

Fig. 2

Fig. 1. Absorption spectrum of pure zinc sulfide films. Curve 1—at room temperature; curve 2—after prolonged annealing; curve 3—theoretical.

Fig. 2. Absorption spectrum of zinc sulfide films. Curve 1—Unannealed film; curve 2—annealed at 550°C in a vacuum for 2 min; curve 3—annealed at 550°C in a vacuum for 15 min; curve 4—annealed at 550°C in a vacuum for 2 hr.

region 270-330 mμ increases slightly with annealing; in the shorter wavelength region the absorption does not change. The maximum at 325 mμ becomes sharper after annealing. The change in the absorption becomes slower as the annealing time is increased and after a certain time, which is fixed for a given temperature, the change almost ceases. For example, at an annealing temperature of 550°C, this time is 2-3 hr. Figure 2 shows that with each successive annealing the greatest reduction in absorption occurs at the same region (around 345 mμ); consequently, the additional absorption is in the form of a band with a maximum at ~345 mμ. After prolonged annealing in a vacuum, the zinc sulfide films darken and continuous absorption appears, with a broad maximum at about 420 mμ, stretching to the red region, and becomes stronger as the heating continues. The film darkening is accompanied by the appearance of slight conductivity and is due, apparently, to dissociation of the zinc sulfide.

X-ray examination* of the zinc sulfide films prepared by evaporation in a vacuum showed that the films had a cubic structure both before and after heat treatment. The lines on the x-ray photograph of the annealed films were very diffuse, but annealing narrowed them greatly. An estimate of the crystal dimensions (or rather the dimensions of the regions of coherent scattering) before and after annealing the films gives orders of magnitude of 10^{-7} and 10^{-6} to 10^{-5}, respectively.

*I. V. Smushkov carried out these examinations, and the author is very grateful to him.

Results of an investigation of the temperature variation of the absorption spectrum of unannealed and annealed zinc sulfide films are given in Figs. 3 and 4, respectively. The absorption was measured at −155°C (curve 1), 17°C (curve 2), and 240°C (curve 3). In the region $\lambda < 280$ mμ the spectrum shifts almost parallel to itself toward the long wavelength region as the temperature increases, and the shift is directly proportional to the temperature; the temperature coefficient is -2.2×10^{-4} ev/deg. The absorption maximum at 325 mμ shifts

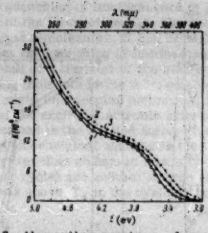

Fig. 3. Absorption spectrum of unannealed zinc sulfide films. Curve 1—at −155°C; curve 2—at +17°C; curve 3—at +240°C.

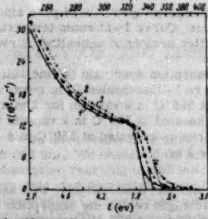

Fig. 4. Absorption spectrum for annealed zinc sulfide films. Curve 1—at −155°C; curve 2—at +17°C; curve 3—at +240°C.

toward the short wavelength region with reduction in temperature, and also becomes much sharper and increases in value (see curve 1, Fig. 4). The temperature coefficient of the shift in the long wavelength absorption edge of annealed specimens is -4.4×10^{-4} ev/deg. The temperature shift of the long wavelength absorption tail of the unannealed films is similar. Figure 5 shows the variation with wavelength of the difference between the absorption coefficients of unannealed and annealed films. These curves have a maximum which, as the temperature falls, increases in value, becomes sharper, and shifts towards the short wavelength region.

DISCUSSION

The absorption of zinc sulfide in the region $\lambda <$ 270 mμ is independent of the conditions of preparation of

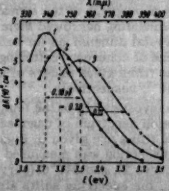

Fig. 5. The difference between the absorption coefficients of unannealed and annealed films (ΔK) plotted against wavelengt. Curve 1—At −155°C; curve 2—at +17°C; curve 3—at +240°C.

the specimens and their heat treatment; this absorption is obviously due to transitions from the valence band to the conduction band. It follows from theoretical considerations[14] that at the long wavelength edge, the absorption coefficient is proportional to $(E - E_G)^n$, where E is the energy of the photon absorbed, E_G is the width of the forbidden band, and for optically allowed transitions n is 0.5 or 1.5, depending on the approximation chosen for the electron wave function. The experimental data obtained agree well with the function $(E - E_G)^{1.5}$ in the 230–270 mμ region (the dashed curve 3 in Fig. 1), where $E_G = E_{G0} - \beta T = 3.64$ ev; here E_{G0}, equal to 3.77 ev, is the width of the forbidden band at 0°K, obtained from the temperature variation of the conductivity of zinc sulfide crystals,[5] β is the temperature coefficient of the change in width of the forbidden band (see the Table), and T is the temperature in °K.

β (10^{-4} ev/degree)	T° K	K (cm^{-1}), λ(mμ)	Author and reference
−4.6	77—300	50, > 340	Van Doorn[9]
−8.5	1073	50, > 340	Van Doorn[9]
−3.0 *	300	100, > 330	Piper[7]
−7.0	290—400	$5 \cdot 10^3$ > 330	Piper et al.[7]
−3.8 **	97—291	$5 \cdot 10^3$ > 350	Coogan[13]
−2.2	110—500	$3 \cdot 10^3$, 250	Data of
−2.9	110—500	$1.5 \cdot 10^3$, 290	present
−4.4	110—500	$3.0 \cdot 10^3$, 340	paper

Note. One asterisk indicates a value obtained from a combination of optical absorption data and the temperature variation of conductivity; two asterisks indicate measurements made on unannealed zinc sulfide films obtained by evaporation in a vacuum.

In the region $\lambda > 270$ mμ a marked deviation from this function is observed, due to the presence in this region of an absorption band with a maximum at 325 mμ, which is forbidden at room temperature and which grows in value, becomes sharper, and shifts toward the short wavelength region as the temperature is reduced. Coogan[13] observed anomalous dispersion of the refractive index in the region of this band.

This absorption region cannot be explained completely by nonvertical transitions between bands, the prohibition on which has been removed by lattice vibrations, or the presence of lattice defects, since firstly, the observed absorption coefficient is much too great for "forbidden" transitions, and secondly, the temperature variation of the absorption spectrum does not correspond to these transitions.[14]

Neither can the absorption band with a maximum at 325 mμ be attributed to impurities, as Hall[11] and Shalimova[10] suggest, for the following reason. The absorption coefficient in this band is of the order of 10^5 cm^{-1}. For this value of absorption coefficient to be produced by an impurity, the concentration would have to be about 10%. The only possible impurity in our case is a stoichiometric excess of one component, but then we would expect the change in absorption that occurs when the specimen is heated in a vacuum to be considerably different from the change that occurs with heating in sulfur vapor; it is well known (see, for example, reference 15) that heating in a vacuum leads to an excess of the metallic component, while heating in sulfur vapor restores the stoichiometric composition of sulfides. Since the change in the absorption spectrum does not depend on whether the specimen is heated in sulfur vapor or in a vacuum, we must reject this explanation.

The absorption band observed is apparently due to excited states in the lattice. In ionic crystals, an electron transition from the negative ion to a neighboring positive ion is attributed to the first excited state in the lattice.[16, 17] This is the interpretation of the first absorption maximum observed in the ultraviolet spectrum of

alkali halides. Similar, but broader absorption maxima are observed in several other substances (for example, in silver halides[17] and alkaline earth oxides[18, 19]).

The temperature dependence of the zinc sulfide absorption band with a maximum at 325 mμ is the same as the temperature dependence of the first absorption maximum of alkali halides. The observed experimental growth in the magnitude and sharpness of the band with fall in temperature is typical of exciton absorption.

Photoconductivity is observed in zinc sulfide in the region of this band,[4] while in alkali halides conductivity is not produced by absorption in the first exciton band. Seitz[17] has suggested that the energy corresponding to the first excited state of the lattice may be greater than the energy of nonvertical transitions (u) from the valence band to the conduction band (see Fig. 6). Due to this effect, it is possible that if the valence band is sufficiently wide, the energy of an exciton transition (e) differs little from the smallest energy of the optically allowed transitions between bands (a), and the prohibition on nonvertical transitions is removed, for example, by the presence of a lattice defects. In this case, which apparently occurs in zinc sulfide, absorption of light in the exciton band could give rise to conductivity.

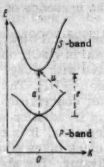

Fig. 6. Energy state diagram.

We will consider the nature of the additional long wavelength absorption of unannealed zinc sulfide films, which disappears after prolonged heating and is absent in crystals. A similar absorption additional to that occurring in monocrystals is observed in thin films of many substances: lead sulfide, lead selenide, and lead telluride.[20] This absorption cannot be explained by light scattering by the crystals constituting the film, as Coogan[12] suggested, since scattering should not disappear after the film is heated, but should increase due to the increase in crystal dimensions.

Since the long wavelength absorption observed in films is absent in crystals, it must be supposed that it is related to some lattice defects which arise in the process of forming the film. Judging from the value of the absorption coefficient, the concentration of defects in the films should be very great (10^{21} cm^{-3}). Repeating the argument given above for the absorption band in the 325 mμ region, we can show that the defects cannot be either foreign impurities or a stoichiometric excess of one component. The following defects are possible in films: (1) dislocations, a large concentration of which is possible due to the screw-dislocation mechanism of film growth[21]; (2) grain boundaires, which become important when the grain dimensions are of the order of tens of angstroms.

The similarity between the temperature dependence of the absorption band at 325 mμ in annealed films and that of the additional absorption in unannealed specimens, and the connection between the increase in absorption in the region 270-330 mμ on annealing and the decrease in the additional absorption, both suggest the identical nature of the transitions responsible for these absorption regions, which occur in the first case in the undistorted crystal lattice and the second case in the neighborhood of the lattice defects. It is possible that the long wavelength absorption of the unannealed films is due to excited states of the lattice located at defects. In the case of defects connected with grain boundaires, an extra absorption maximum in the long wavelength region would be expected.[22]

As we mentioned above, the temperature coefficient of the shift in the zinc sulfide absorption spectrum is different in different spectral regions: in the region $\lambda <$ 270 mμ, where the absorption arises from transitions in the conduction band, the coefficient is much less than in the long wavelength region, where a band is located which is apparently connected with excited states of the lattice. The table gives values of the temperature coefficient β of the shift obtained in our work and by other investigators[4, 5, 7, 12]; the Table gives the temperature range (the second column) in which the temperature dependence was measured and the region of the absorption spectrum (the third column) in which the temperature coefficient was determined. The discrepancy in the data in the Table is due to the different regions of the absorption spectrum at which different investigators determined β; as Fig. 4 shows, when the temperature changes the spectrum does not shift parallel to itself. All earlier determinations of the temperature coefficient of the shift in the absorption edge refer to the spectral region $\lambda >$ 330 mμ, while they are treated as a temperature change in the width of the forbidden band; however, in this region the absorption is not, basically, due to transitions between bands. It is therefore useless to compare these values[7] with the theoretical temperature variation of the width of the forbidden band[23] and the wide discrepancy is not surprising.

In conclusion the author thanks K. D. Sinel'nikov for his interest in and attention to the work, and I. N. Shklyarevskii and V. K. Miloslavskii for valuable discussions.

REFERENCES

1. F. A. Kroeger and J. E. Hellingman. J. Electrochem. Soc. 93, 156 (1948).
2. D. C. Reynolds and S. J. Czyzak. Phys. Rev. 79, 543 (1950).
3. R. H. Bube. Phys. Rev. 90, 70 (1953).
4. W. W. Piper. Phys. Rev. 92, 23 (1953).
5. C. Z. Van Doorn. Physica 20, 1155 (1954).
6. M. N. Alentsev and E. I. Panasiuk. Opt. i Spektr. 5, 2 (1958).
7. W. W. Piper, D. T. F. Morple, and P. D. Johnson. Phys. Rev. 110, 323 (1958).
8. E. F. Gross and L. G. Suslina. Opt. i Spektr. 6, 115 (1959).
9. E. Mollwo. Reichber. Phys. 1, 1 (1944).
10. K. V. Shalimova. Doklady Akad. Nauk SSSR 80, 587 (1951).
11. J. F. Hall. J. Opt. Soc. Am. 46, 1013 (1956).
12. C. K. Coogan. Proc. Phys. Soc. 70 B, 845 (1957).
13. N. A. Vlasenko. Uch. Zap. Khar'kovsk. Univ., Tr. Fiz. Otd. 7, 321 (1958).
14. H. Y. Fan. Rep. Progr. Phys. 19, 107 (1956); or Usp. Fiz. Nauk 66, 2, 315 (1958).
15. A. A. Bundel' and A. I. Rusanova. "Mat. Soveshch. po luminestsentsii." (Mathematical Conference on Luminescence), Tartu, 1957, p. 30.
16. N. Mott and R. Gurney. "Electronic Processes in Ionic Crystals."
17. F. Seitz. Rev. Mod. Phys. 23, 328 (1951).

18. R. Sproul and V. Taylor. "Semiconducting Materials."
19. J. Nelson, Phys. Rev. 99, 1902 (1955).
20. A. F. Gibson. Proc. Phys. Soc. 63 B, 756 (1950).
21. F. C. Frank. Advanc. Phys. 1, 91 (1952).
22. I. E. Tamm. Z. Physik 76, 849 (1932).
23. H. Y. Fan. Phys. Rev. 82, 90 (1951).

THE INFLUENCE OF AN ACTIVATOR ON THE STABILITY OF F-CENTERS

I. A. Parfianovich and E. I. Shuraleva

Received 7 February 1959

The optical bleaching curves of F centers in pure NaCl crystals and in crystals activated with copper or nickel at 680-760°C were studied after the crystals had been colored by exposure to x rays. It was shown that the bleaching rate increases with increasing activator concentration. The change in the additional absorption spectrum produced by illumination with F light was also investigated. An analysis of the results obtained is presented, leading to a more precise understanding of the mechanism of F-center stability in pure and activated crystals.

In crystals colored by ionizing radiation, it is possible for an electron released from an F center to either recombine with a trapped hole or to localize once more in one of the trap levels, including anion vacancies. The question of the bleaching mechanism of F centers is of great interest from the standpoint of studying the kinetics of electronic and hole processes in crystal phosphors and semiconductors, but up to the present it has not been sufficiently studied. There are isolated data in the literature relating to the stability of F centers in alkali halide crystals. The first observations on F-center bleaching were presented by Przibram,[1] who found that not all the F centers in photochemically colored crystals had the same stability. F-center stability in crystals colored at low temperatures has been studied by Casler, Pringsheim, and Yuster.[2] Along with these papers the mechanism of thermal bleaching of F centers has been discussed by Markham,[3] Mador and Wallis et al.,[4,5] attempted to describe the kinetics of optical bleaching of F centers. All the authors listed studied the thermal and optical stability of F centers in alkali halide crystals grown from fusion. The activating impurities were not purposely introduced into these crystals. Our observations show that F-center stability is extremely sensitive to the presence of impurities in the crystals. It was in this connection that a detailed study of the influence of the activator on F-center stability was undertaken.

During the progress of the experiments special attention was paid to the purity of the basic material. It should be noted that synthetic crystals cannot be considered sufficiently pure. For example, according to the data of Duerig and Markham,[6] synthetic crystals contain various random impurities that can change in quantity from one sample to another. These concentrations are such that they cannot be detected by the optical absorption method. The thermal luminescence method has a great advantage in this relationship, and utilizing it it is possible to establish the presence of extremely minute quantities of activator impurities. Using this method it can be shown that natural rock salt crystals compare very favorably to synthetic ones with respect to purity.

As the basic material we used natural NaCl crystals that had not been subjected to any treatment. We also used samples activated with nickel or copper at temperatures of 680-760°C. In order to take into account the heat treatment of the crystals during activation the experiments were also carried out with pure samples into which no activator had been introduced.

The crystals were photochemically colored at room temperature using 50 kv x rays from a tungsten electrode tube. The optical measurements were carried out on spectrophotometers of the SF-4 and SF-2 types.

Detailed studies made by one of us[7] on optical bleaching showed that the bleaching rate of F centers depends to a large degree on the presence of an activator and its concentration.

Figure 1 shows the optical bleaching curves of F centers in a pure crystal of NaCl, one that had been heated, and one activated with nickel (the concentration of nickel is 3×10^{-4} mol. % Ni). The values of the relative changes in F-center concentration are plotted on the ordinate and the time of irradiation with light of 465 mμ wavelength is on the abscissa. It is clear from the figure that the F-center bleaching takes place most rapidly in the presence of an activator. The stability of the centers in the heated crystal is also changed, although to a lesser degree.

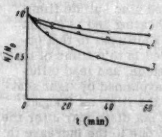

Fig. 1

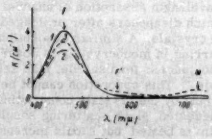

Fig. 2

Fig. 1. The optical bleaching of F centers in different samples. Curve 1—a pure crystal; curve 2—heat treated; curve 3—activated with nickel.

Fig. 2. Absorption of an x-rayed, pure NaCl crystal. Curve 1—immediately after x-ray irradiation; curve 2—after exposure to F light; curve 3—after irradiation with light at λ = 580 mμ.

Measurements conducted on NaCl samples containing different amounts of nickel indicated that the F-center bleaching rate increases with increasing activator concentration. A similar picture is observed with the presence of other activating impurities. For example it is quite evident from the data on the copper-activated NaCl crystal shown in the table.

Here K_m, K'_m, and K''_m correspond respectively to the absorption coefficients at the maximum of the F band after x-ray irradiation, after exposure to light at λ = 465 mμ, and after irradiation with light in the region of the F′ band. All three crystals had approximately the

Table 1. The Influence of an Activator and Heat Treatment on the Optical Stability of F Centers and the Recapture of Electrons

Crystal	K_m	K'_m	$K_m - K'_m$	$\frac{K_m - K'_m}{K_m}$ (%)	K''_m	$K'_m - K''_m$	$\frac{K'_m - K''_m}{K_m - K'_m}$ (%)
NaCl (pure without any treatment)	2.26	1.88	0.38	16.8	2.16	0.28	74
NaCl (heat treated)	2.24	1.70	0.54	23.0	1.89	0.19	35
NaCl (Cu) (0.06 mol. % Cu)	2.46	0.44	2.02	82.0	0.44	0.0	0.0

same initial F-center concentration. It is evident from the data in the table that, as was the case with NaCl (Ni), the F band in NaCl (Cu) is bleached most rapidly. The F centers in this crystal are bleached approximately five times faster than in the pure crystal under the same conditions.

For the purpose of clarifying the F-center bleaching mechanism, we studied the change in the additional absorption spectrum produced by exposing the x-rayed crystals to light in the F-band region. These observations enable one to follow the transformations of electron centers and also the changes originating from hole centers.

To begin with we will look at the data pertaining to a pure crystal. The absorption spectrum of such an x-rayed crystal in the visible region is shown in Fig. 2. As seen from a comparison of curves 1 and 2, the optical bleaching of F centers leads to an enhancement of the M band and the development of a broad new band on the long wavelength side of the F band. A study of its characteristics indicates that this is an F′ band. Bleaching of the F′ band and restoration of the F band is observed when the crystal is irradiated with light at $\lambda = 580$ mμ (curve 3). It follows from these experiments that the conversion of certain electron centers into others takes place in a pure natural crystal; the decrease of the F band is compensated by the growth of the long wavelength F′ and M bands, and inversely their bleaching restores the F band.

Quantitative data characterizing the conversion of electron bands in a pure crystal are shown on the first line of Table 1. It is seen from the data that the F band is restored to 74% by optical bleaching of F′ centers. It should be noted that in the given example, the restoration of the F band is less complete than it might have been. This result is due to the fact that a fraction of the electrons went over into the M level in this experiment.

The absorption spectrum of a pure natural NaCl crystal in the spectral interval from 210 to 800 mμ (curve 1) is shown in Fig. 3. Here the hole V band is

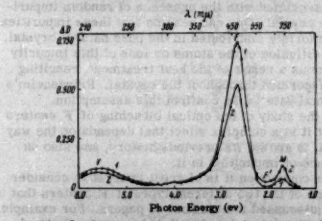

Fig. 3. Absorption spectrum of a pure NaCl crystal. Curve 1—immediately after x-ray irradiation; curve 2—after exposure to light at $\lambda = 465$ mμ.

clearly seen as well as the F and M electron bands. One can assume according to data given in references 8 and 9 that this band includes the two bands V_2 and V_3. The behavior of V_2 and V_3 centers with respect to their recombination with free electrons has to be considerably different according to the models of both Seitz[10] and Varley.[11] This is due to the fact that the V_3 centers carry an excess of negative charge while V_2 centers are electrically neutral.

Curve 2 of Fig. 3 indicates that the bleaching of the F band is accompanied by a slight attenuation of the V band. This is to be expected if one assumes that the hole centers in a pure crystal that has been x-rayed at room temperature are primarily V_3 centers. Accordingly, the transition of one kind of electron centers to others with negligible losses is possible. In this respect a purely photochemically colored crystal acts in just the same way as an additively colored one. In it only a small part of the F band is subject to true bleaching. Consequently the whole mechanism of optical bleaching of the F band can be described in the following way. At the beginning, conduction electrons for the most part recombine with V_3 hole centers. After that, since the V_3 centers are converted to V_2 centers as a result of recombinations, only the transformation of the F band to other electron bands is possible. However, as shown by the experiment, it is not possible to completely convert the F centers to F′ and M centers. There are a number of reasons for this. In the first place, electrons freed from F centers localize repeatedly at the same levels. Secondly, the number of M levels is probably more limited than the number of F levels. And thirdly, light in the F-band region also bleaches the F′ and M bands. The attenuation of the F′ band takes place as a consequence of its overlapping the F band, and probably the M centers are bleached owing to closeness of the location of the F and M centers. The data obtained by Lambe and Compton[12] during an investigation of F-center luminescence confirms the existence of such a distribution of F and M centers.

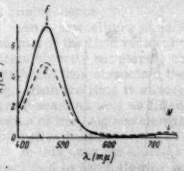

Fig. 4

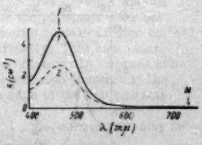

Fig. 5

Fig. 4. The absorption of the x-rayed phosphor NaCl (Ni) (8×10^{-4} mol. % Ni) in the visible region. Curve 1—immediately after x-ray exposure; curve 2—after illumination with light at $\lambda = 465$ mμ.

Fig. 5. The absorption of the x-rayed phosphor NaCl (Cu) (0.06 mol. % Cu). Curve 1—immediately after x-ray exposure; curve 2—after illumination with light at $\lambda = 465$ mμ.

Thus it is seen that the high optical stability of F centers in pure crystals depends not only on the properties of the holes but also on the electron centers that are products of the transformation of F centers.

We now turn to the experiments with activated crystals. As previously mentioned, the F band is optically bleached more rapidly in activated crystals than in pure crystals. This is evident in Figs. 4 and 5. The figures show the absorption curves in the visible spectral region

for the x-rayed phosphors NaCl (Ni) (8×10^{-4} mol. % Ni) and NaCl (Cu) (0.06 mol. % Cu) prior to (curve 1) and after exposure to F light (curve 2). Even though the duration of the exposure to bleaching light in these experiments was shorter by a factor of 15 than that used for the pure crystal (Fig. 2), the F-band change is significantly greater. The activator not only speeds up the F-center bleaching but it also affects the recapture of electrons in levels of the host material. It is less probable that electrons freed from F centers will localize in the F′ and M levels in activated crystals (Fig. 4). In the presence of appreciable activator concentration electrons are not recaptured at all in these levels (Fig. 5).

The results included on the last line of the table show that in the NaCl (Cu) crystal (0.06 mol. % Cu) along with considerable F-band bleaching, absolutely no restoration takes place after light in the F′ band acts on the crystal. The fact that the activator, and not the thermal treatment of the crystal, plays the primary role in this process is quite clear from a comparison of the data on the second and third lines of the same table. Data for a heat-treated crystal are given on the second line and show that it is closer to the pure crystal in its properties than to the activated one. The thermal treatment introduces some changes that are reflected less in the bleaching rate and to a large degree have their effect on F band restoration.

Let us turn to the absorption curves shown in Fig. 6 and Fig. 7 with the aim of making the mechanism of F-band bleaching in the presence of an activator more precise. Figure 6 pertains to the phosphor NaCl (Cu) (0.008 mol. % Cu) and Fig. 7 to NaCl (Ni) (4×10^{-4} mol. % Ni).

The F and M bands in the NaCl (Cu) (Fig. 6) are almost completely destroyed by optical bleaching. A very small fraction of the electrons freed from these centers transfer to activator capture centers (the bands at λ_m = 235 and 290 mμ). In addition to this a considerable reduction of the hole band at λ_m = 340 mμ is noted. The changes in the V band are not observed because of overlapping by the electron band at λ_m = 235 mμ.

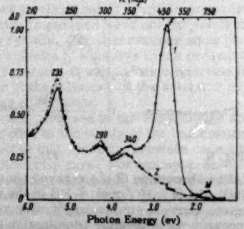

Fig. 6. The absorption spectrum of a crystal of NaCl (Cu) (0.008 mol. % Cu). Curve 1—immediately after x-ray irradiation; curve 2—after exposure to light at λ = 465 mμ.

The bleaching of the F band in NaCl (Ni) (Fig. 7) leads to the formation of a weak F′ band, the growth of "atomic" bands at λ_m = 276 and 308 mμ, and almost no change in the M band. Here, attenuation in the V band is clearly observed and a change in the region of λ_m = 340 mμ is also noted, though to a lesser degree.

It follows from Figs. 6 and 7, which reflect a large body of experimental data, that reduction in the optical stability of F centers depends on the same conditions that also increase the sensitivity of the crystals to coloring. Actually, both the formation of a relatively large number of V_3 centers in activated crystals and the appearance of hole centers (the band at λ_m = 340 mμ) create favorable conditions for the recombination of electrons with trapped holes. The probability of the recombination of electrons with localized holes becomes more and more significant as the concentration of the activator is increased. But the probability of recapture in the F band, as well as the F′ and M bands, decreases. Activator trapping centers that draw off part of the electrons also play a well-known role in the optical bleaching process. In the phosphors under consideration (Fig. 6 and Fig. 7) this was a negligible fraction of the electrons.

An analysis of the experimental data cited allows one to understand in more detail the mechanism responsible for the difference in the stability of F centers in pure and activated crystals. The reason for the high stability of F centers in pure crystals is connected with the fact that in these crystals the x-ray irradiation produces primarily hole centers with extremely low effective cross section for recombination.

The introduction of an activator creates favorable conditions for the production of a type of hole centers with which electrons can recombine at room temperature without requiring additional energy of activation. One can

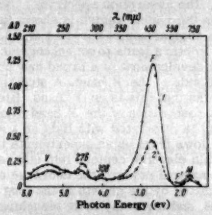

Fig. 7. Absorption spectrum of an NaCl (Ni) (4×10^{-4} mol. % Ni) crystal. Curve 1—immediately after x-ray irradiation; curve 2—after exposure to light at λ = 465 mμ.

assume that the presence of such centers is also the primary reason for the decrease in the optical stability of F centers in activated crystals. The direct role of the activator as an electron acceptor in this process is apparently insignificant, especially when its concentration is low.

The effect of heating on F-center stability may possibly be associated with the presence of random impurities in the crystal. One can assume that these impurities are not uniformly distributed in the pure natural crystal, but that a diffusion of the atoms or ions of this impurity takes place as a result of the heat treatment, resulting in their dispersion throughout the crystal. Pringsheim's experimental data[13] also confirm this assumption.

Thus the study of the optical bleaching of F centers shows that it is a complex effect that depends on the way the crystal is grown, its previous history, and also on the presence of impurities in it.

In this connection it is of great interest to consider the question of the two different types of F centers that have been discussed in a number of papers. For example, Oberly,[14] using data related to the photoconductivity of colored alkali halide crystals, arrived at the conclusion that two types of F centers exist, which he calls "soft"

and "hard." The first of these can be bleached and contributes to the photoconductivity, the second is not susceptible to bleaching. There are different points of view[9,10] on the nature and the very existence of "hard" and "soft" centers. We reached the conclusion that the differences in the optical stability of F centers depend not on their nature but on their environmental conditions. As was pointed out earlier centers having extremely great optical stability are produced in natural NaCl crystals by the action of x rays. However these are not any special kind of "hard" F centers. These "ordinary" F centers are not bleached at room temperature because the recombination of free electrons with V centers requires a quantity of activation energy which cannot be provided under the given conditions. Other hole centers appear in the presence of an activator and it becomes possible to bleach the F band. In such crystals the F centers produced have the properties of "soft" centers but structurally the "soft" and "hard" centers cannot be distinguished from each other.

REFERENCES

1. K. Przibram. Wien. Ber. 135, 202 (1926); Z. Physik 68, 403 (1931).
2. R. Casler, P. Pringsheim and P. Yuster. J. Chem. Phys. 18, 1564, 1887 (1950).
3. J. Markham. Phys. Rev. 86, 433 (1952); J. Chem. Phys. 57, 762 (1953).
4. I. Mador, R. Wallis, M. Williams and R. Herman. Phys. Rev. 96, 617 (1954).
5. R. Herman and R. Wallis. Phys. Rev. 99, 435 (1955).
6. W. Duerig and J. Markham. Phys. Rev. 88, 1043 (1952).
7. E. I. Shuraleva. Opt. i Spekt. 2, 396 (1957).
8. J. Alexander and E. Schneider. Nature 164, 653 (1949).
9. H. Dorendorf and H. Pick. Z. Physik 128, 166 (1950).
10. F. Seitz. Revs. Modern Phys. 26, 7 (1954).
11. J. Varley. Nature 174, 886 (1954).
12. J. Lambe and W. Compton. Phys. Rev. 106, 684 (1957).
13. P. Pringsheim. Z. Physik 144, 31 (1956).
14. J. J. Oberly. Phys. Rev. 83, 228 (1951); Phys. Rev. 84, 1257 (1951).

INITIAL STAGES OF THE RISE OF LUMINESCENCE IN PHOSPHORS WITH LEVELS OF SEVERAL KINDS

(See reference 1 devoted to the initial stages of decay.)

V. V. Antonov-Romanovskiĭ

Received 30 January 1959

We consider the kinetics of phosphor luminescence in the initial stage of excitation buildup for the "quasi-linear" case. We assume recombination to be negligible, and all free charges to be thermal.

The kinetics of phosphor luminescence are more complex for the buildup than for the decay stage due to the presence of two additional processes, namely, ionization and liberation of trapped charges by the exciting radiation itself. Furthermore, these processes can lead to the appearance of charges with energy exceeding the thermal energy (optical electrons and holes) and therefore capable of having values for the effective capture and recombination which are different from those of the thermal charges. This circumstance, and in particular the variation of the ratio of thermal to nonthermal carriers during excitation, further complicates the kinetics of luminescence.

An overwhelming number of free charges may be thermal if the light incident on the phosphor does not ionize directly but merely creates certain excited states, which can then dissociate thermally. This can occur, e.g., when the light is absorbed directly by capture centers (vacant as well as filled) and also possibly in the region of the long wavelength edge of the fundamental absorption band.

In this case the kinetics of phosphorescence may be described by the following equations:

$$\frac{dn_i^+}{dt} = -\frac{\sigma_{ai}^- n_i^+}{\sum_1^{\bar{n}} \sigma_{ak}^- n_k^+ + \sum_1^{\bar{n}} \sigma_k^- (\nu_k^- - n_k^-)} \left[\sum_1^{\bar{n}} w_k^- n_k^- + \sum_1^{\bar{n}} \varkappa_k^+ (\nu_k^+ - n_k^+) E \right] - w_i^+ n_i^+$$

$$+ \frac{\varkappa_i^+ (\nu_i^+ - n_i^+)}{\sum_1^{\bar{n}} \varkappa_{ak}^+ n_k^- + \sum_1^{\bar{n}} \varkappa_k^+ (\nu_k^+ - n_k^+)} \left[\sum_1^{\bar{n}} w_k^+ n_k^+ + \sum_1^{\bar{n}} \varkappa_k^- (\nu_k^- - n_k^-) E \right] + \varkappa_i^+ (\nu_i^+ - n_i^+) E = 0, \quad (1)$$

$$\frac{dn_i^-}{dt} = -\frac{\varkappa_{ai}^+ n_i^-}{\sum_1^{\bar{n}} \varkappa_{ak}^+ n_k^- + \sum_1^{\bar{n}} \varkappa_k^+ (\nu_k^+ - n_k^+)} \left[\sum_1^{\bar{n}} w_k^+ n_k^+ + \sum_1^{\bar{n}} \varkappa_k^- (\nu_k^- - n_k^-) E \right] - w_i^- n_i^-$$

$$+ \frac{\sigma_i^- (\nu_i^- - n_i^-)}{\sum_1^{\bar{n}} \sigma_{ak}^- n_k^+ + \sum_1^{\bar{n}} \sigma_k^- (\nu_k^- - n_k^-)} \left[\sum_1^{\bar{n}} w_k^- n_k^- + \sum_1^{\bar{n}} \varkappa_k^+ (\nu_k^+ - n_k^+) E \right] + \varkappa_i^- (\nu_i^- - n_i^-) E = 0, \quad (2)$$

$$w_k^{\mp} = w_{T,k}^{\mp} + w_{E,k}^{\mp}, \quad w_{E,k}^{\mp} = \varepsilon_k^{\mp} E, \quad (3)$$

Here E is the intensity of the exciting light, $w^+_{T_j,\,k}$ and $w^+_{g_j,\,k}$ are the probabilities of ejection of trapped charges per unit time by heat and by exciting light respectively. The quantities χ_0, α^+_k and χ^+_k are proportional to the coefficients of absorption of the exciting light by the host substance (in the region of edge absorption) and by filled and vacant traps respectively. The other quantities have the same meaning as in reference 1. When E = 0, Eqs. (1) and (2) become the corresponding decay[1] equations I (1) and I (2).*

*The symbol I is used before the number of any formula from reference 1.

In spite of the greater complexity of the buildup equations, they turn out to be quasi-linear in the initial stages and hence are easily solvable when conditions I(5) and I(6) are satisfied and the recombination term is neglected. The electrons and holes then move almost independently of each other. Thus, in this case, we need consider the motion of charges of one sign only, e.g., of electrons.

Let the trap depths be appreciably different from each other and let the ejection of charges proceed essentially thermally so that formulas I(7) and I(8) hold, and for t = 0 all $n^+_k = 0$. As in the case of decay, we may assume that only one or two types of traps are particularly effective at any given moment. We denote them by (j − 1) and j. (The numbering of trap types is carried out in order of increasing depth.)

Let us denote by τ_i the average lifetime of an electron on a level of the ith type. (In this case $\tau_i \sim 1/w_i$.) Then, as in the decay case, for the time interval

$$\tau_{j-2} \ll \vartheta \ll \tau_{j+1}, \tag{4}$$

the electron system (2) may be reduced to the following much simpler one:

$$\frac{dn_i^-}{d\vartheta} = -w_i^- n_i^- + \frac{c_i^- \nu_i^-}{(S^-)_{j-1}^m}\left[(T^-)_i^* + (K^+)_i^{m^+} + K_0\right] + \chi_i^- \nu_i^- E = 0, \quad (i < j-1), \tag{5}$$

$$\frac{dn_i^-}{d\vartheta} = -w_i^- n_i^- + \frac{c_i^- \nu_i^-}{(S^-)_{j-1}^m}\left[(T^-)_i^* + (K^+)_i^{m^+} + K_0\right] + \chi_i^- \nu_i^- E, \quad (i = j-1,\ j), \tag{6}$$

where

$$S_j^+ = \sum_p \alpha_p^+ \nu_p, \quad T_j^+ = \sum_p w_p n_p, \quad K_j^+ = \sum_p \chi_p^+ \nu_p E, \quad K_0 = \chi_0 \nu_0 E. \tag{7}$$

We do not write the equations for $i > j$ since deeper traps will only capture electrons. Accordingly we make $(T^-)_i^m = (T^-)_i^*$. The vanishing of dn_i/dt for shallower traps ($i < j - 1$) indicates that (for $\vartheta \gg \tau_{j-2}$) their population reaches a quasi-stationary state, i.e., the increase in the number of electrons almost balances the decrease.

Summing all equalities (5) and expressing $(T^-)_i^{*-2}$ by other quantities, we finally obtain from (6) the expressions

$$\frac{dn_{j-1}^-}{d\vartheta} = -w_{j-1}^- n_{j-1}^- + \frac{c_{j-1}^- \nu_{j-1}^-}{(S^-)_{j-1}^m}\left[w_{j-1}^- n_{j-1}^- + w_j^- n_j^-\right] + e_{j-1}, \tag{8}$$

$$\frac{dn_j^-}{d\vartheta} = -w_j^- n_j^- + \frac{c_j^- \nu_j^-}{(S^-)_{j-1}^m}\left[w_{j-1}^- n_{j-1}^- + w_j^- n_j^-\right] + e_j, \tag{9}$$

where

$$\left.\begin{aligned} e_{j-1} &= \frac{c_{j-1}^- \nu_{j-1}^-}{(S^-)_{j-1}^m}\left[(K^+)_1^{m^+} + K_0 + (K^-)_1^{j-2}\right] + \chi_{j-1}^- \nu_{j-1}^- E, \\ e_j &= \frac{c_j^- \nu_j^-}{(S^-)_{j-1}^m}\left[(K^+)_1^{m^+} + K_0 + (K^-)_1^{j-2}\right] + \chi_j^- \nu_j^- E. \end{aligned}\right\} \tag{10}$$

Equations (8) and (9) differ from the analogous decay equations I(17) and I(18) by the presence of the constant terms c_{j-1} and c_j, which, according to (7), are proportional to E. The first term on the right-hand side of Eqs. (8) and (9) represents as before the thermal decrease of electrons, while the second one represents the thermal increase. The quantity

$$\frac{c_i^- \nu_i^-}{(S^-)_{j-1}^m}\left[(K^+)_1^{m^+} + K_0\right]$$

in $c_j (i = j - 1, j)$ denotes the rate of increase of n_i^- due to the ionization by the exciting light of luminescence centers of all kinds and of the basic lattice. The quantity

$$\frac{c_i^- \nu_i^-}{(S^-)_{j-1}^m}(K^-)_1^{j-2}$$

is determined by the transfer of electrons by the exciting light from the lower band to shallower levels ($i < j - 1$) and their subsequent thermal transfer to the upper band. The reason for this is that when $\vartheta \gg \tau_{j-2}$ (see above) the population of these levels has already reached a quasi-stationary state, while there is practically no returning of electrons from these levels to the lower band (recombination with free holes).

Since the system of equations (8) and (9) differs from the system I(17) and I(18) only by the presence of constant terms, their solution can be represented in the form of solutions of the decay equations, with a constant term added to each of these. If we set $n_i^- = 0$ at $\vartheta = 0$, we obtain the solution in the form

$$n_{j-1}^- = \frac{e_{j-1} - \lambda_j n_{j-1,\,\infty}^-}{\lambda_{j-1} - \lambda_j}\left(1 - e^{-\lambda_j \vartheta}\right) + \frac{\lambda_{j-1} n_{j-1,\,\infty}^- - e_{j-1}}{\lambda_{j-1} - \lambda_j}\left(1 - e^{-\lambda_{j-1}\vartheta}\right), \tag{11}$$

$$n_j^- = \frac{e_j - \lambda_j n_{j,\,\infty}^-}{\lambda_{j-1} - \lambda_j}\left(1 - e^{-\lambda_j \vartheta}\right) + \frac{\lambda_{j-1} n_{j,\,\infty}^- - e_j}{\lambda_{j-1} - \lambda_j}\left(1 - e^{-\lambda_{j-1}\vartheta}\right), \tag{12}$$

where λ_{j-1} and λ_j are determined from I(22) and I(23) while

$$\left.\begin{aligned} n_{j-1,\,\infty}^- &= \frac{1}{w_{j-1}^-}\left[e_{j-1} + (e_{j-1} + e_j)\frac{c_{j-1}^- \nu_{j-1}^-}{(S^-)_{j+1}^m}\right], \\ n_{j,\,\infty}^- &= \frac{1}{w_j^-}\left[e_j + (e_{j-1} + e_j)\frac{c_j^- \nu_j^-}{(S^-)_{j+1}^m}\right]. \end{aligned}\right\} \tag{13}$$

If we take into account the fact that Eqs. (8) and (9) hold only for the time interval (4), which starts not from zero but from a time when the phosphor is already somewhat excited, we should, strictly speaking, set as the initial condition $n_i^- = n_{i,\,0}^-$ at $\vartheta = \vartheta_0$. However, we may set $n_i^- = 0$ (approximately) at $\vartheta = 0$ on the basis of the following consideration: Though the initial ϑ_0 is appreciably larger than τ_{j-2}, it is nevertheless appreciably smaller than τ_{j-1}. Hence it is small compared with the duration of the interval (4). As a consequence, the initial $n_{i,\,0}^-$ is appreciably smaller than the amount of light sum which will be stored during the entire time interval (4).

Using Eqs. I(22) and I(23) and the fact that $w_i^-/w_{i-1}^- \ll 1$, we obtain from Eqs. (11) and (12)

$$n_{j-1}^- = \frac{c_{j-1}}{\lambda_{j-1}}(1 - e^{-\lambda_{j-1}\vartheta}) + \frac{w_i^- n_{i,\infty}^-}{\lambda_{j-1}} \cdot \frac{c_{j-1}^- \gamma_{j-1}^-}{(S^-)_{j-1}^{m^-}}(1 - e^{-\lambda_j \vartheta}), \quad (14)$$

$$n_j^- = -\frac{c_{j-1}}{\lambda_{j-1}} \cdot \frac{c_j \gamma_j}{(S^-)_j^{m^-}}(1 - e^{-\lambda_j \vartheta}) + n_{j,\infty}^-(1 - e^{-\lambda_j \vartheta}). \quad (15)$$

As long as none of the constants c_{j-1} and c_j are equal to zero, we obtain from Eqs. (14) and (15), to a first approximation,

$$n_{j-1}^- \approx c_{j-1}\vartheta \text{ and } n_j^- \approx c_j \vartheta, \quad (\tau_{j-1} \ll \vartheta \ll \tau_{j-1}). \quad (16)$$

Such a result is to be expected since at the start of excitation the traps mainly capture electrons. The proportionality between n_{j-1}^- and n_j^- and the excitation time ϑ represents merely the condition of instantaneous excitation of traps of the $(j-1)$ and j types.

During the next time interval when $\tau_{j-1} \ll \vartheta \ll \tau_j$, the first terms in (14) and (15) are constant since $\exp(-\lambda_{j-1}\vartheta) \ll 1$ and only the second terms continue to increase linearly.

$$n_{j-1}^- = \frac{c_{j-1}}{\lambda_{j-1}} + \frac{w_j^- n_{j,\infty}^-}{\lambda_{j-1}} \cdot \frac{c_{j-1}^- \gamma_{j-1}^-}{(S^-)_{j-1}^{m^-}} \lambda_j \vartheta$$

$$\text{and } n_j^- = -\frac{c_{j-1}}{\lambda_{j-1}} \cdot \frac{c_j^- \gamma_j^-}{(S^-)_j^{m^-}} + n_{j,\infty}^- \lambda_j \vartheta,$$

$$(\tau_{j-1} \ll \vartheta \ll \tau_j). \quad (17)$$

Thus the rate of increase of n_{j-1}^- and n_j^- varies.

It may be shown that in the "correct" case, when all trap characteristics except depth differ little from each other, the coefficients of ϑ, i.e., the rates of increase of n_{j-1}^- and n_j^- during different time intervals, satisfy the following inequalities ($\lambda_{j-1} \gg \lambda_j$):

$$c_{j-1} \gg \frac{w_j^- n_{j,\infty}^-}{\lambda_{j-1}} \cdot \frac{c_{j-1}^- \gamma_{j-1}^-}{(S^-)_{j-1}^{m^-}} \lambda_j \text{ and } c_j < n_{j,\infty}^- \lambda_j. \quad (18)$$

Accordingly we represent schematically in the figure the variation of n_{j-1}^- and n_j^- with the time ϑ. A change in the behavior of both curves occurs at the instant $\vartheta \sim \tau_{j-1}$.

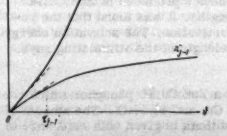

Thus, for $\vartheta > \tau_{j-1}$ the rate of increase of n_{j-1}^- is abruptly slowed down while the rate of increase of n_j^- is appreciably, though not as abruptly, accelerated. If the filling of the levels of the $(j-1)$ type stops being proportional to the excitation time ϑ, this proportionality is still achieved approximately with regard to the filling of the levels of the j type, but obviously with another (larger) angular coefficient than before. (This is the case when we may already neglect the constant term in the expression for n_j^-, but still have $\vartheta \ll \tau_j$.) The time τ_{j-1} is therefor critical with regard to the breakdown of proportionality, which is practically permanent for n_{j-1}^- and temporary for n_j^-.

The results obtained can be easily generalized for the whole initial period of luminescence buildup when other kinds of traps begin to take part (actively). We shall limit ourselves to a qualitative description of the kinetics of the buildup in view of the complexity of the corresponding mathematical calculation.

For $0 \ll \vartheta \ll \tau_1$, all the n_i^- increase proportionately to ϑ. For $\tau_1 \ll \vartheta \ll \tau_2$ this is true only for the concentrations n_i^- with $i \geq 2$, though with an increased slope. The increase in slope is in general different for levels of different types, because even though the increase in the concentration of free electrons increases the "feeding" of the traps to the same degree, the extent to which these traps are supplied directly by electrons from the filled band excited by light remains unchanged. The filling of levels of the first kind is sharply slowed down here. The situation is repeated for $\tau_2 \ll \vartheta \ll \tau_3$. However, in this case it is the levels of the second kind which no longer fill the proportionality condition, etc.

The general mechanism of the process of increase is perfectly clear. The time τ_1 plays the role of a critical time ("age") after which both the proportionality of n_1^- to ϑ and its rapid rate of increase with ϑ disappear simultaneously. At the same time for $i < j$ all the n_i^-, which until then were increasing relatively slowly, begin to increase even more slowly ("sublinearly") while for $i > j$ all the n_i^- remain quasi-proportional to ϑ even though the coefficient of proportionality is increased. However, if we also take into account the time intervals due to the transitions, we may on the whole call the behavior of n_i^- for $i > j$ "superlinear."

We must specify that these statements apply to the so-called "correct" case (see above). Obviously all kinds of strange mechanisms are possible if the "correctness" is destroyed. (See, for example, reference 2.)

The formula for the intensity of luminescence during the initial buildup stages and the time interval (4) has form

$$I_i = \varphi_i \frac{\sigma_m^- n_i^+}{(S^-)_{j-1}^{m^-}} [w_{j-1}^- n_{j-1}^- + w_j^- n_j^- + (K^+)_1^{m^+} + K_0 + (K^-)_1^{j-2}]. \quad (19)$$

By means of Eqs. (14) and (15) it may be shown that the expression in brackets in Eq. (19) divided by $u(S^-)_{j-1}^{m^-}$, where u is the average velocity of the electrons, has the property described below. This expression

$$N^- = \frac{w_{j-1}^- n_{j-1}^- + w_j^- n_j^- + (K^+)_1^{m^+} + K_0 + (K^-)_1^{j-2}}{u(S^-)_{j-1}^{m^-}}, \quad (20)$$

which represents the concentration of free electrons, cannot increase superlinearly even if n_i^- does increase superlinearly. Since the conductivity is exactly proportional to N^-, this means that insofar as the average lifetime of the free electron does not change, the photoconductivity cannot increase more rapidly with time than linearly. However, the brightness I_i, as opposed to N^-, can increase even more sharply than quadratically provided that n_i^- increases superlinearly in the interval of time (4) while N^- increases linearly.

At the very start of excitation, when $\vartheta \ll \tau_1$ (here $j = 1$), N^- almost instantaneously assumes the value

$$N_0 = \frac{(K^+)_1^{m^+} + K_0}{u(S^-)_1^{m^-}}. \quad (21)$$

[For $j = 1$, $(K^-)_1^{j-1} = 0$.]

Therefore, at the very beginning all the I_i increase as n_i^-, that is, proportionately to ϑ, provided that K^+ and K_0 are not zero. Later the dependence of I_i on ϑ becomes more complex due to the change in N^- at this stage. The rise of I_i is sharply slowed down for $\vartheta \sim \tau_1$, that is, when equilibrium is achieved between the popu-

lation of hole traps (of type 1) and the filled band. During decay, this instant corresponds to the appearance of external quenching. (See reference 1.)

According to (19), the intensities of two luminescence bands due to two different activators are in the same ratio as the concentrations of the corresponding ionized luminescence centers

$$\frac{I_1}{I_2} \sim \frac{n_1^+}{n_2^+}. \qquad (22)$$

This ratio is constant only at the very beginning when n_1^+, n_2^+, are proportional to the time t. Later n_1^+ and n_2^+ vary differently since they increase not only by hole capture from the general reservoir, i.e., the filled band, but also as a result of direct ionization by light, which in general is different for different centers.

In the case of luminescence buildup, we can derive an approximate formula for I_t, equivalent to I(25) in the decay case. Such a formula would hold not only during separate time intervals but during the whole initial buildup interval. We shall omit it due to the complexity of the derivation.

This finishes our study of the "linear" case of the initial period of excitation increase, when recombination may be considered to be negligibly small and all carriers may be considered to be thermal. In conclusion we shall note the following:

Thermal liberation of trapped charges is highly probable for the shallower traps and is hardly possible for the deeper ones. In the latter case optical liberation is certainly more probable. This will bring about the appearance of free charges with energy above thermal, provided, however, that the filled trap does not have a level of excitation from which the thermal liberation of a charge raised to that level is possible. Obviously, due to a sharp increase with temperature of the probability of thermal liberation of trapped charges, the number of trap types for which optical ejection would predominate over thermal ejection will, as a rule, diminish. The situation will be reversed for cooling.

We did not consider the case of the optical liberation of charges even under the assumption that the last stage of liberation renders these charges thermal. The reason for this was the following: The probabilities of optical liberation of charges from traps of different types will hardly differ as markedly from each other as in the case of thermal liberation. Since our method of investigation requires appreciable differences between the w_1^+, it is inapplicable when such differences do not exist. Furthermore, in view of the less marked difference between the w_1^+ for optical liberation, the series of deep levels may be approximately considered as equivalent to one type playing the role of the deepest one. This obviously makes our method entirely inapplicable. This case belongs already to the later stages of luminescence buildup.

Our method for studying the kinetics of buildup in the initial stages is also applicable in the special, rather unlikely, case when the majority of free charges is nonthermal. The only difference will be in the numerical values of the constants σ_{01}^+ and σ_1^+.

REFERENCES

1. V. V. Antonov-Romanovskii. Opt. i Spektr. 7, 376 (1959).
2. V. V. Antonov-Romanovskii. Opt. i Spektr. 7, 827 (1959).

INVESTIGATION OF THE THERMAL ACTIVATION ENERGY OF PHOTOSTIMULATED FLASHES IN Zns:Cu:Pb PHOSPHORS

V. L. Levshin and B. M. Orlov

Received 12 January 1959

A study was made of the development of luminescence in flashes produced in ZnS:Cu:Pb phosphors under the action of infrared rays of different wavelengths. It was found that the release of electrons from traps requires a preliminary thermal activation. The activation energy depends on the nature of the trap and is independent of the wavelength of the stimulating rays.

INTRODUCTION

It has been noted in several earlier works devoted to the study of the flash phenomenon that flash intensity increases strongly with a rise in temperature. Apparently the stimulation of trapped electrons requires that they be transferred into an active state. This can be accomplished at the expense of the thermal energy of the lattice.[1,2] However, a detailed study of this problem has not been carried out.

In this paper we set ourselves the problem of studying the amount of energy in a heat-activated flash for different trapping levels of the ZnS:Cu:Pb phosphors, the flash being stimulated by light of different wavelengths.

It is known that the ZnS:Cu:Pb phosphor has three luminescence bands, one in the blue and two in the green. The basic properties of this phosphor were described in references 2, 3, 4, 5, and others.

We used a ZnS:Cu:Pb phosphor which contained 5% Pb, 10^{-5} g/g Cu, and 4% NaCl. The amount of activators and other additions is given with reference to the ZnS content. Copper is introduced in the form of an alcohol solution of $CuCl_2$, lead as $PbSO_4$. The firing temperature was +1100°C, its duration 20 minutes. The firing was carried out in an evacuated bulb.

THE SYSTEMS OF TRAPPING LEVELS

We obtained a glow curve in order to ascertain the systems of trapping levels in the phosphor under investigation.

The phosphor was excited at −190°C and was heated to +140°C at a rate of 0.2°/sec. The glow curve is shown in Fig. 1a (solid line). The right wide of the curve is drawn with a magnification of 50. The phosphor was ex-

cited with the 365 mμ Hg line. The curve shows that the phosphor has two systems of trappings levels. One corresponds to the sharp peak at −125°C; the other gives a broad emission region between +30° and +140°C with a highly diffuse maximum between +50° and +80°C. The upper dotted curve in Fig. 1a represents the glow curve of a phosphor also excited at −190°C but subjected, still at −190°C, to a prolonged irradiation with 1.3μ radiation. This irradiation produces phosphorescence from the shallower system of levels. However, as may be seen from Fig. 1a, the deeper system of levels remains practically untouched. The action of 0.8μ light liberates phosphorescence from both systems of levels (lower dotted curve in Fig. 1a).

If we determine the glow curve of a phosphor excited at 20°C and irradiated at the same temperature by 1.3μ light, we find that both trapping levels are entirely evacuated. The activation energy imparted to the trapped electrons at +20°C turns out to be sufficient to permit their release by 1.3μ radiation. This is illustrated in Fig. 1b, where the solid line represents the glow curve taken immediately after excitation, and the dotted line, the glow curve after prolonged irradiation of the phosphor by 1.3μ radiation.

However, in this case the 1.3μ radiation does not bring about complete extinguishing of the phosphorescence of the phosphor. If, after irradiation with this light, and after the end of the flash, the phosphor is irradiated with 0.8μ radiation, another rather bright flash occurs. Thus, the glow curve in Fig. 1 is incomplete. The deepest trapping levels are not shown on it.

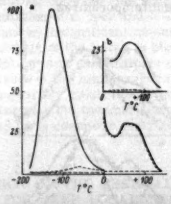

Fig. 1. Glow curves of the ZnS:Cu:Pb phosphor excited (a) at −196°C and (b) at +20°C. Solid line—curve taken immediately after excitation; small dashes—curve taken after prolonged irradiation with infrared radiation (1.3μ); large dashes—curve taken after the action of 0.8μ radiation.

A flash cannot be produced by infrared radiation of any wavelength after the excited phosphor has been heated to +180°C. It follows from this that the phosphor under consideration has at least one more deep system of localized levels.

STUDY OF THE THERMAL ACTIVATION ENERGY FOR THE FIRST SHALLOW SYSTEM OF LEVELS

To determine the energy of thermal activation of the flash corresponding to the release of electrons from any specified system of trapping levels, we must measure the flash intensities at different temperatures. The temperatures must be selected in such a way, however, that during the occurrence of the flashes electrons are released from only the system of levels being studied. In this case the intensity of luminescence of flashes corresponding to different temperatures is given by

$$I = I_0 e^{-E/kT}, \qquad (1)$$

where E is the activation energy and T the absolute temperature.

From Eq. (1) we obtain

$$\ln \frac{I}{I_0} = -\frac{E}{kT}. \qquad (1')$$

Thus the logarithm of the flash intensity is a linear function of the inverse temperature.

By means of Eq. (1′) we can determine the activation energy E from the slope of the curve $\ln I = f(1/T)$. However, since the abovementioned requirement that light act on only one selected system of levels is essential, we have to check whether it is satisfied for the given experimental conditions.

To study the flashes occurring when the shallowest system of levels (−125°C) is evacuated, we used temperatures between −196°C and −150°C. At each temperature, a prolonged pulse of stimulating rays was applied, and was made to act until the flash was fully developed. We measured the maximum intensity of the flash. The amount of energy radiated during one flash was vanishingly small, compared with the total light sum stored by the excited phosphor in the shallowest system of trapping levels. This was proved by comparing the area of the first peak of the glow curve obtained from a phosphor immediately after excitation with that of the glow curve obtained after the occurrence of a number of flashes (Fig. 2).

Figure 2 shows the following: No more than 10% of the light sum is emitted from the first system of levels when the phosphor is subjected to 1.3μ radiation during the entire flashing period (the number of flashes chosen was three times as large as was necessary for the determination of E). No more than 20% is emitted when 0.8μ radiation is used. Practically no electrons are released from the deep system of levels.

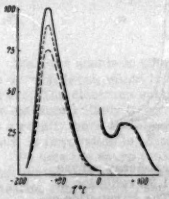

Fig. 2

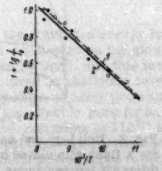

Fig. 3

Fig. 2. Glow curves of the ZnS:Cu:Pb Phosphor excited at −196°C. Solid line—curve taken immediately after excitation; small dashes—curve taken after a series of flashes stimulated by 1.3μ radiation; large dashes—curve taken after the same series of flashes stimulated by 0.8μ radiation.

Fig. 3. Linear dependence of the logarithm of the flash intensity on 1/T. 1—0.8μ radiation; 2—1.3μ radiation.

To study the activation energy of the first level, we carried out several series of experiments with flashes using light of different wavelengths for photostimulation. The validity of formula (1′) was confirmed in all cases. As an example, we show two straight lines in Fig. 3,

which correspond to photostimulation of the first system of levels under the action of light with $\lambda = 0.8\mu$ and 1.3μ. As seen in Fig. 3, the linear dependence of log I on 1/T is fulfilled quite satisfactorily. Both lines have the same slope, from which we find $E = 0.047$ ev as the activation energy.

Similar measurements were carried out at other wavelengths. These give the values for the activation energy for electrons of the first system of localized levels listed in Table 1.

Table 1

$\lambda\mu$	0.7	0.8	0.9	1.0	1.1	1.2	1.3	1.4	
$E_1 \cdot 10^3$ ev	35	47	31	50	39	31	47	30	$E_{1\,av.} = 0.039 \pm 0.002$ ev

The study was repeated with two similar phosphors obtained from different raw materials. For them we found $E_2 = 0.040 \pm 0.005$ and $E_2 = 0.037 \pm 0.002$ ev.

These results indicate that the appreciable fluctuations in the value of E for different wavelengths of the stimulating rays are not systematic in character and are apparently connected with experimental inaccuracies. We may conclude that for one system of levels, the activation energy is independent of the wavelength of the stimulating light. For the shallowest system of levels of the ZnS:Cu:Pb phosphor this value is 0.039 ± 0.002 ev.

The second important conclusion to be drawn from this first series of experiments is the establishment of the existence of inertia in the appearance of the flash in ZnS:Cu:Pb phosphors. The flash reaches the maximum corresponding to the intensity of the stimulating rays not immediately, but only after a rather appreciable time interval, which in our experiments was ~40 sec. Rebane[6] observed the same phenomenon of the flash inertia for a ZnS:Cu phosphor stimulated by 0.8μ radiation at room temperature.

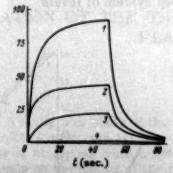

Fig. 4. Build-up and natural decay curves for a flash stimulated by 1.3μ radiation at different temperatures. (The stimulation affects a shallow system of levels.) Curve 1—(−150°); curve 2—(−165°); curve 3—(−185°); curve 4—(−195°C).

We made a special investigation of this phenomenon. Figure 4 shows the buildup of the flash under the action of 1.3μ radiation, (temperatures from −150°C to −195°C). It also shows the decay of radiation after photostimulation has been stopped. The shape of the build-up and decay curves agrees within the limits of experimental error, which indicates the presence of appreciable inertia in the process. The stored light sums determined from the build-up and decay curves agree within 10%. The inertia of the flash is a little less pronounced at room temperatures. This is true for all wavelengths of the stimulating infrared light.

It is known that the phenomenon of "pure flash" consists of the transfer of electrons from the localized levels into the conduction band and their immediate recombination with ionized centers. This process is of extremely short duration consisting of the time the electron spends in the conduction band and the duration of luminescence of the excited center.

The curves shown in Fig. 4 indicate the following: In ZnS:Cu:Pb phosphors there is, under the action of infrared rays, an initial transition of localized electrons to another system of shallow levels, from which thermostimulation proceeds. Thus, what we observe experimentally is not a flash but secondary phosphorescence. This circumstance does not interfere with the determination of the thermal activation energy of the flash, since if flash conditions have been established and there is no quenching, the number of electrons released from the phosphorescence levels by heat is equal to the number of electrons released from the initial trapping levels (the flash levels) by the infrared radiation.

STUDY OF LUMINESCENCE SPECTRA

Phosphors with several activators have different emission bands which appear in different proportions in fluorescence, phosphorescence, and in the photostimulated flash. The difference in the spectral distributions of these various types of luminescence must be taken into account when electrophotometric measurements are being carried out and when evaluating the share of energy for each process. On this basis we studied the emission spectra of all the indicated processes in the ZnS:Cu:Pb phosphors at different temperatures.

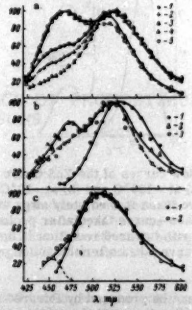

Fig. 5. Spectra of the luminescence of the ZnS:Cu:Pb phosphor at different temperatures. a—Fluorescence spectra: curve 1—+20°; curve 2—+50°; curve 3—+70°; curve 4—(−150°); curve 5—(−190°C). b—Phosphorescence spectra: curve 1—+20°; curve 2—(−150°); curve 3—(−190°C). c—Flash spectra: curve 1—+20°; curve 2—(−190°C). The dotted line represents blue radiation rising in a flash at low temperatures.

Figure 5a shows luminescence spectra of a phosphor which is being excited. It follows from Fig. 5a that blue luminescence with a maximum at 465 mμ is very pronounced at temperatures of −196° and −150°C. As the temperature is raised, the blue luminescence decreases

sharply. At +70°C it no longer exhibits a specific maximum but is shown only by a noticeable lengthening of the short wavelength slope of the luminescence spectrum.

The second emission maximum which is attributed to copper lies at −196°C near 520 mμ. This maximum increases slowly with increasing temperature and is displaced toward the red. At the same time there is a marked intensity increase on the long wavelength slope of the emission band. This may be explained by the development, with increasing temperature, of a new luminescence band with a maximum at about 550 mμ, which is apparently due to lead.

Figure 5b shows the phosphorescence spectra of the same phosphor. In the long wavelength region the spectral distribution curves are close in shape to the fluorescence spectra. In the short wavelength region, the luminescence is much weaker than under excitation. This can be explained by the way in which we conducted our experiment. Phosphorescence data were taken at a certain time interval after the end of excitation. Due to the more rapid decay of the blue radiation, it was weakened much more during the dark interval than during the green radiation. Hence it is represented more weakly in the phosphorescence spectrum which we obtained. It is also possible that added to this circumstance is the greater probability of recombination with the centers of blue luminescence for electrons raised into the conductivity band immediately after excitation, compared to electrons released from trapping levels, which cause phosphorescence.

Figure 5c shows spectra of the photostimulated flash at two temperatures. At −190° the spectra are composed of the green radiation of copper and lead, with a maximum near 520 mμ, and an insignificant amount of blue radiation. The percentage of the latter in the spectral distribution of the radiation is so insignificant that we may consider the spectrum of the luminescence practically invariant at the relatively small temperature variations required to determine the thermal activation of the flash. Any corrections for a change in distribution are superfluous.

DETERMINATION OF THE THERMAL ACTIVATION ENERGY FOR DEEP LOCALIZED LEVELS

As shown in Fig. 1, the glow curve in the temperature range from +20° to +140° represents a diffuse band without a definite maximum. This shape of the glow curve in the given temperature range indicates the complexity of its character. The ZnS:Cu:Pb phosphor obviously has several close-lying systems of localized levels. Hence the method for determining the thermal activation energy given above is inapplicable in this case: When the temperature of flashing is changed, the photostimulated electrons are released, not from one, but from several systems of trapping levels. Indeed, we obtained the following result from our experiments (carried out between +20° and +70°) for the determination of the energy of thermal activation using light of different wavelengths for photostimulation: The energy of thermal activation is a function of wavelength for the system of localized levels vacated at temperatures from +20° to +140°C. This is in direct contradiction with the result obtained for the system of shallow levels which corresponds to the first peak of the glow curve. We therefore tried to separate the electrons of the last (i.e., deepest) system from the total number of electrons trapped at deep levels. To accomplish this we kept the phosphor excited at +20° at that temperature for 0, 10, 30, and 90 minutes. During that time phosphorescence was decaying spontaneously. After that, the phosphor was thermostimulated. Figure 6 shows the shapes of the corresponding glow curves. The last glow curve with one maximum corresponds to the case where the phosphor was maintained at 20° for 90 minutes. It has the normal shape for an elementary glow curve for a system of levels of one depth (the case where repeated trapping of electrons has low probability).

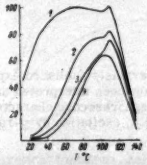

Fig. 6. Glow curves taken after keeping the phosphor excited at +20°C in the dark during various time intervals. (The heating rate was 0.45°/sec.) Curve 1—0; curve 2—10; curve 3—30; curve 4—90 min.

We also found that the phosphor has a system of deeper levels which do not manifest themselves on the glow curves. This system is not emptied by infrared in the region of 1.3μ. We may therefore apply the usual procedure for the determination of the thermal activation energy of photostimulation of the level corresponding to the lone peak of the lowest curve in Fig. 6, using different values of λ from the 1.3 region. In this case the electron will be released from one level only.

The same activation energy was obtained for all wavelengths used. (See Table 2.)

Table 2

λμ	1.1	1.2	1.3	1.4	
$E \cdot 10^2$ ev	18	19	19	19	$E_{av.} = 0.188 \pm 0.004$

We were unable to obtain the activation energy for the deepest level, which is not manifested on the glow curves. The electrons released by light from this level are extremely likely to be captured on shallower levels. As a result, there is a superposition of many processes, and it is impossible to obtain the effect in pure form.

We note the sharp peak corresponding to 110°C in the glow curves of Fig. 6. These curves were obtained with a heating rate of 0.45°/sec, which proved more favorable to making this peak apparent. The peak did not show at a heating rate of 0.2°/sec. (See Figs. 1 and 2.)

This peak should have become more and more sharply apparent with prolonged storage of the excited phosphor. This, however, was not observed. The peak disappeared completely with a 90 minute storage of the excited phosphor. We are dealing with a case here where the deeper localized levels are less stable than the shallower ones. It is possible that the departure of electrons from these levels is connected with nonradiative processes and with the development of thermal quenching.

REFERENCES

1. V. V. Antonov-Romanovskii, V. L. Levshin, Z. L. Morgenshtern, and Z. A. Trapeznikova, Izv. Akad. Nauk SSSR, Ser. Fiz. 13, 75 (1949).

2. G. R. Fonda. J. Opt. Soc. Am. 36, 382 (1946).
3. D. Pearlman, N. Nail, and F. Urbach. "Preparation and Characteristics of Solid Luminescent Materials." New York, 1948.
4. A. A. Cherepnev. Doklady Akad. Nauk SSSR 66, 621 (1948).
5. A. A. Cherepnev. Doklady Akad. Nauk SSSR 62, 767 (1948).
6. K. S. K. Revane. Tr. Inst. Fix. Astron. Akad. Nauk SSSR 7, 357 (1958).

STUDY OF LIGHT SUMS IN THE SrS:Eu:Sm PHOSPHOR. II

I. B. Keirim-Markus

Received 26 September 1959

Previously published experimental data on the study of light sums in the SrS:Eu:Sm phosphor have been interpreted theoretically. (See communication I.[1]) A detailed study was made of the phosphorescence characteristics caused by different means of phosphor excitation—photoexcitation, excitation by γ-rays, etc.

The previous communication[1] listed experimental data on the dependence observed between the exposure (γ-ray dosage) and the magnitude of the stored light sum. It was ascertained that the light sum is stored nonlinearly in the case of photoexcitation, while in the case of γ-ray excitation the light sum increases linearly with dosage over a broad range (up to dosages for which the light sum reaches 60-70% of its limiting value).

It has already been noted[2] that γ-ray excitation of a phosphor has its own special features comarable to photoexcitation. We shall consider this problem in more detail.

Let us compare the process of phorphor activation by γ-rays and by light in the activator absorption region. In the case of photoexcitation, the photons are absorbed by the luminescence centers and ionize them. In this process the hole is either captured by the Eu^{2+} ion or is localized at neighboring lattice points, while the electron migrates in the crystal and is captured by one of the traps. One absorbed photon does not form more than one electron-hole pair. The phosphor is excited uniformly throughout the volume (if we disregard the decrease in the intensity of the exciting light in the phosphor layer).

When irradiated by γ-quanta, the phosphor is excited under the action of fast secondary electrons, with the electron energy being transferred to the ions of the host substance as long as the activator concentration in the phosphor is not high. There are actually more than 10^4 SrS groups for each Eu^{2+} ion, and more than 10^3 for each Sm^{3+} ion.

We can estimate as follows the distance along the trajectory of the secondary electron between successive electron-hole pairs formed by it:

Let the phosphor be excited by γ-rays from Co^{60}. This causes the formation in the phosphor of fast Compton electrons with an average energy of about 500 kev. About 4 ev are used to ionize the SrS phosphor lattice. However, this number should be approximately doubled,[3] since part of the energy of the fast electron is wasted.

The Compton electron creates along its path about 6×10^4 electron-hole pairs. A 500 kev electron has about a 1 mm path length in the phosphor. Thus the average distance between pairs along the trajectory of a fast electron is about 1.5×10^{-8} cm or 25c, where c is the period of the SrS crystal lattice.

The electron-hole pairs formed migrate through the crystal—either as excitons or separately—until they are captured by some lattice defect. They must travel, on the average, a distance in excess of 2×10^{-6} cm, or 3000c, in order to be localized in an activator center. (The minimum distance between Sr ions is $c/\sqrt{2} = 4 \times 10^{-8}$ cm.) We obtain this path length on the assumption that the capture cross section of the hole (or exciton) by an ionized luminescence center is of the order of magnitude of c^2.

Thus, under the action of γ-irradiation, excitation channels are formed in the phosphor along the trajectories of the secondary electrons. Since we must take into account that electrons and holes migrate in arbitrary directions and are scattered many times, it is reasonable to assume a value between 10^{-4} and 10^{-5} cm as the effective channel radius. Hence one electron-hole pair occurs in a volume of $5 \times 10^{-14} - 5 \times 10^{-16}$ cm^3 containing $3 \times 10^4 - 3 \times 10^2$ Eu^{2+} ions and $3 \times 10^3 - 30$ Sm^{3+} ions. This means that the excitation accomplished in the channels is relatively weak.

As long as the channels do not overlap, i.e., for not too large dosages, the flash and afterglow brightness is obviously proportional to the number of channels or to the dosage. This is independent of the kinetics of the recombination processes in each of the channels.[3] From this point of view it is clear why the indications of the ILK dosimeters are proportional to the dosage over a very broad range (communication I, Fig. 13).

However, as stated above, the dependence between light sum and dosage remains linear even when the light sum reaches 0.6 of its limiting value. Since we arrived at the conclusion that the limit of the light sum storage is determined by the filling of deep traps, we must explain why the light sum yield does not vary when the concentration of unfilled electron traps is decreased appreciably.

Let us consider, therefore, how the yield of the light sum must change as it is being stored. Since only about 1% of the luminescence centers are ionized at full excitation, we shall assume that the conditions for the localization of holes do not change during the process of excitation. We shall also not explicitly take into account the possible capture of electrons by extraneous impurities.

Assume that the phosphor has ν deep traps with cross section σ_2. When the phosphor is excited by the dosage D, n luminescence centers with cross section σ_1 are ionized, and n deep traps are filled. While the electron is moving in the band, it may be captured by one of the ν-n traps or it may recombine with one of the n ionized luminescence centers. The probability that during a path length l an electron will be captured by one of the traps may be written as

$$\eta = \left(1 - e^{-(\nu - n)\sigma_2 l - n\sigma_1 l}\right) \frac{(\nu - n)\sigma_2}{(\nu - n)\sigma_2 + n\sigma_1} = \left(1 - e^{a(1 - x + bx)}\right) \frac{1 - x}{1 - x + bx},$$

where $a = \nu\sigma_2 l$, $b = \sigma_1/\sigma_2$, $x = n/\nu$.

Obviously η is equal to the yield of the light sum n to within a multiplying factor. Hence

$$\frac{dn}{dD} = \eta \quad \text{and} \quad D = \int_0^n \frac{dn}{\eta}.$$

For $n \to 0$, $\eta \to \eta_0 = 1 - e^{-a}$. As shown above, for incomplete excitation by γ-rays, the yield of the light sum is close to 0.1. Hence $1 - e^{-a} \sim 0.1$, that is, a takes on values greater than 0.1 or $l > 1/10\nu\sigma_x$.

According to experiment (communication I, Figs. 2 and 13) the light sum yield changes little as n/ν increases from 0 to 0.5 - 0.7. Let us see for what values of the parameters a and b this can occur.

The average path length l of the electron changes as the excitation of the phosphor proceeds. It remains constant only in the special case $b = \sigma_p/\sigma_x = 1$ insofar as each time a trap is filled an ionized luminescence center appears with the same cross section as the trap. In this case the expression for D is integrated in terms of elementary functions. It may be easily shown that

$$n = \nu(1 - e^{-bD}) \qquad (b = 1)$$

This relation does not agree with experiment, as may be seen in Fig. 13 (communication I).

Figure 1 shows graphs of the dependence of η on n/ν for different values of the parameters a and b. If $b > 1$, then l decreases with an increase in the light sum, hence a should also decrease. As shown in Fig. 1, for $b > 1$ the yield η cannot remain constant when n/ν increases. Thus the values $b > 1$ do not agree with the experiment either.

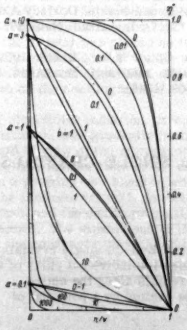

Fig. 1. Theoretical dependence of η on n/ν for different values of the parameters $a = \nu\sigma_x l$ and $b = \sigma_p/\sigma_x$.

For $b < 1$, l and a should increase as the light sum increases. In other words, if the light sum yield remains constant, then a point representing the yield in Fig. 1 should be displaced from the value η_0 to the right on a horizontal, moving from one curve to another corresponding to higher values of a. For weak excitation, however, when the concentration of vacant traps changes little, l and a should vary very slowly. According to Fig. 1, this behavior of η can be satisfied only for values $a > 3$ and $b < 0.1$, or $l > 3/\nu\sigma_x$ and $\sigma_p < 0.1\sigma_x$.

For $b = 0$ the expression for D can again be integrated provided we set a = const.

$$D = \frac{n}{\nu} + \frac{1}{a} \ln \frac{1 - e^{-a}}{1 - e^{-a(1 - n/\nu)}} \qquad (b = 0)$$

The dependence of light sum on dosage calculated from this formula is shown in Fig. 2. (Compare Fig. 13, communication I.)

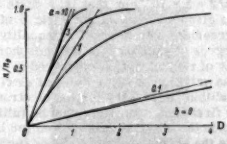

Fig. 2. Theoretical functional relation between the light sum and the dosage (exposure) for b = 0 for different values of the parameter a.

Thus the theory developed above agrees with experiment only when the recombination cross section σ_p is very small and $l > 3/\nu\sigma_x = 0.1$ mm assuming the value 10^{-17} cm^{-3} for ν, and 3×10^{-15} cm^2 for σ_x.

We shall defer the discussion of this rather unexpected result and consider the following: Phosphors of practical importance have a large light sum yield. This means that the parameter a (Fig. 1) is of the order of unity or more. Figure 1 shows that for values of a which are not too small and for $b > 1$, the light sum yield decreases as the traps are filled. It is practically zero when they are only partly filled.

Thus, if only part of the thermally stable traps are populated in such phosphors under conditions of practically complete excitation, this may be due not to the stimulating action of the exciting radiation[4] but to the interception of electrons by ionized luminescence centers.

The condition $b > 1$ or $\sigma_p > \sigma_x$ is often satisfied for thermal electrons.[5] It is valid in particular for the SrS:Eu:Sm phosphor as may be deduced from the following arguments.

Let us consider the kinetics of electronic processes occurring inside individual excitation channels in a phosphor irradiated by γ-rays. We can gauge it from the shape of the decay or thermal glow curves observed at dosages for which the channels do not yet overlap. According to Fig. 2 (communication I), the thermal glow curves correspond to kinetics of the first order for a dosage of 33 R, that is, for a degree of excitation which is at least 60 times less than complete. Hence we may draw the following conclusion for the SrS:Eu:Sm phosphor; the processes in the excitation channels in which thermal electrons take part obey first-order kinetics. Hence the shape of the decay and glow curves should be independent of γ-irradiation dosage, down to dosages as small as desired.

Since the processes in the channels obey first-order kinetics, the probability of recombination is much higher for thermal electrons than the probability of capture by traps ($\sigma_p n \gg \sigma_x(\nu - n)$). Since the excitation in the channels is weak ($n \ll \nu$), the recombination cross section σ_p for thermal electrons should be much larger than the capture cross section σ_x, that is, $b \gg 1$. This is due to the high concentration of vacant capture locations ($\nu - n \gg n$) in and around the channels. The estimate made above of the degree of excitation in the channels ($30n < \nu$) indicates that at least the relation $b \gg 30$ must be valid.

This result does not contradict the conclusions of the theory of diffusion.[5,6] The expression for the radius of the region within which thermal electrons are attracted by the ionized luminescence center

$$R_p = \frac{2e^2}{3\varepsilon kT}$$

gives $R_p \sim 10^{-6}$ cm. For neutral traps it is reasonable to set $R_t \sim c/2 = 3 \times 10^{-8}$ cm, that is, a value 30 times smaller. This gives a cross section ratio b of the order of 1000, in agreement with the above inequality.

As the degree of excitation of the phosphor increases, the probability of recombination compared to the capture probability can only increase for thermal electrons. Hence the conditions necessary for the electronic processes to satisfy first-order kinetics must be fulfilled all the more. Hence the thermal glow curves for large dosages also have the shape characteristic of the kinetics of this type (communication I, Fig. 2).

The same result should hold and is actually observed for photoexcitation (communication I, Fig. 2). A difference should be expected for very weak photoexcitation when the concentration of ionized luminescence centers is smaller than that produced by secondary electrons in the excitation channels. This may permit the realization of conditions which are necessary in order that processes in which thermal electrons take part obey the laws of second-order reactions. Even for more appreciable excitation these conditions will appear at later stages of afterglow or thermal luminescence. This is true not only after photoexcitation but also after the action of γ-rays.

We come back now to the problem of the dependence between the light sum and the dosage. If we consider that free electrons are formed in the phosphor under γ-ray excitation, then according to our analysis we should set $b \gg 1$. Indeed, it follows from our arguments that the path of the electron in the conductivity band exceeds 0.1 mm. It will obviously spend the major part of such a long path near the bottom of the band as a thermal electron, for which $b \gg 1$. A theoretical study of the experimental dependence between the light sum and the γ-ray dosage leads to the conclusion $b \approx 0$. In order to resolve this contradiction between experiment and theory, we may assume that the theory is inapplicable in this case. Since γ-ray excitation leads to the formation of excitons, which in their motion through the crystal are not localized at the ionized luminescence centers, but are reflected from them, we have $\sigma_p \approx 0$ and $b \approx 0$.

When the phosphor is excited by light with a frequency corresponding to the absorption region of the activator, optical electrons appear in the conductivity band. These traverse part of their path in the crystal as thermal electrons. Since $b \geq 1$ for them, the light sum yield keeps decreasing as the excitation of the phosphor proceeds. This is shown in Fig. 1. The relation between the light sum and the exposure should in this case be similar to $n = \nu[1 - \exp(-\eta_0 D)]$, which holds for $b = 1$. The experimental curve in Fig. 1 (communication I) does not contradict such a conclusion.

These are the possible explanations of the peculiarities observed when the phosphor is excited by γ-rays. However, the mechanism proposed may not be considered definitive.

The author expresses his deep appreciation to V. V. Antonov-Romanovskiĭ, who directed this work, and also to M. V. Fok.

REFERENCES

1. I. B. Keirim-Markus. Opt. i Spektr. 7, 384 (1959).
2. V. V. Antonov-Romanovskiĭ. Zhur. Eksp. i Teoret. Fiz. 21, 269 (1951).
3. M. D. Galanin, A. P. Grishin. Zhur. Eksp. i Teoret. Fiz. 30, 33 (1956).
4. V. V. Antonov-Romanovskiĭ. Doklady Akad. Nauk SSSR 58, 771 (1947); Izv. Akad. Nauk SSSR, Ser. Fiz. 13, 91 (1949).
5. Syui Syui-yun. Opt. i Spektr. 1, 264 (1956).
6. V. V. Antonov-Romanovskiĭ. Izv. Akad. Nauk SSSR, Ser. Fiz. 9, 369 (1945).

STUDY OF ELECTROLUMINESCENCE OF ZnS-Cu SINGLE CRYSTALS

V. E. Oranovskiĭ and B. A. Khmelinin

Received 18 February 1959

The properties of luminescent "striations" in electroluminescent ZnS-Cu single crystals were studied. Observation of the change in the shape of the light pulse for individual parts of a striation exposed to ultraviolet shows that excitation and emission results along the entire length of the striation. It was found that electroluminescence can be excited by a potential of 10^4 volts/cm.

In a previous work[1] it was noted that when the types of single crystals studied were excited electrically, luminescence was observed in the form of "striations" with more or less bright spots in them. In those experiments, however, we did not succeed in explaining whether the luminescence of the striations was independent of that of the spots, or whether their luminescence was actually scattered light which had originally been emitted by the spots. The basic problem of our work was to provide clarification of the properties of luminescent striations.

EXPERIMENTAL PART

The basic method of investigation was to observe the light pulses resulting from electro-excitation of individual sections of the striations, and to study the effect of ultraviolet light on the light pulses.

Excitation of luminescence was produced in the field at the edge of a condenser to which an alternating potential of 2000 volts and 1500 cycles was applied. The crystal was held near the edges of the condenser in such a way that it was not directly in contact with the plates. The striations were perpendicular to the plates.

Illumination with ultraviolet radiation was accomplished by passing the output of a dc quartz-mercury lamp and light filter through a special microscope objective. The diameter of the illuminated spot on the surface of the crystal was approximately 100μ; the spot could be moved continuously over the field of view of the microscope. The maximum effect on the electrolumines-

cence of a given type of crystal was caused by ultraviolet with a wavelength of $\lambda = 365$ mμ. The considerably weaker effect of other wavelengths, particularly 313 mμ, is probably due to the very rapid absorption of 313 mμ radiation by the base material, and the poor absorption of 404 mμ radiation by the copper.

To isolate individual small parts of the crystal for measurement, additional diaphragms of different forms and sizes were inserted in the plane of the field diaphragm of the microscope. A diaphragm with a circular aperture isolated a part of the field of view having a diameter of about 30-40 μ; a slit diaphragm isolated a part having a length of 100-400 μ and a width of 40 μ (magnified 160 times).

For the experiments, an electroluminescent crystal was selected which had comparatively very long striations (length about 1.2 mm), without spots.

Visual observation of these striations at different excitation voltages showed that they consisted of a series of adjoining sectors. The length of these sectors varied from 40 to 300 μ. Almost all the sector boundaries coincided with crystal defects visible in normal light, but the inverse was not true.

By using a photomultiplier and double beam oscillograph we obtained light pulse shapes for the individual parts of the striation. It was found that within the boundaries of each sector of a striation, the position of the maximum of the light pulse remained constant in phase relative to the excitation voltage. Variation of the frequency of the excitation voltage changed the phase of the light pulse.

The phase of the light pulse of neighboring spots was different. Eight different light pulse phases were observed along the longest striation. A series of measurements of differences in phase angle between their maxima gave: 26, 20, 70, 10, 170, 130, and 120 deg.

To study the action of ultraviolet light on the light pulse in detail, the crystal was placed so that two neighboring sectors of a striation were visible at the same time through the slit diaphragm. Therefore two light pulses were seen on the oscillograph in one half-cycle (Fig. 2a).

The spot of ultraviolet radiation, directed along the direction of a striation, was gradually brought to the center of the field of view of the microscope, while alternately moving it from one plate of the condenser to the other. When a position was found in which the action of the light on the luminescent striation was clearly visible, it was stopped and the oscillograph light pulse shapes photographed. The dimensions of the diaphragm, arrangement of the condenser plates, and the position of the light spot are shown in Fig. 1.

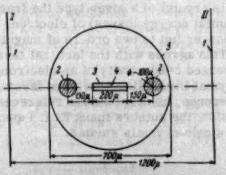

Fig. 1. Experimental scheme for determining the action of ultraviolet radiation on electroluminescence. 1—plate of the condenser; 2—spot of ultraviolet radiation; 3—slit diaphragm; 4—observed area of the "striation"; 5—boundary of the field of view.

In the test conducted in this manner, it was discovered that when the light spot was brought near a part of the striation from one direction, one of the light pulses sharply increased and the other almost vanished (Fig. 2b). When the spot approached from the reverse side, the first wave disappeared and the second was strengthened (Fig. 2c). Thus we find evidence for an inequality at opposite ends of the striations.

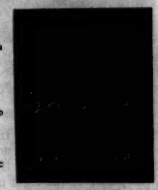

Fig. 2. Oscillogram of the light pulse and excitaton voltage. a—before switching on the ultraviolet; b—spot of ultraviolet radiation near condenser plate I; c—spot of ultraviolet radiation near plate II (cf. Fig. 1).

Shutting off the ultraviolet light led to restoration of the original light pulse picture.

The time elapsed from the moment the ultraviolet light is switched on until its action is fully evident can vary considerably. In general, in our experiment the picture changed very soon after the untraviolet light was turned on—in less than a second. Recovery after shutting off the light required considerably greater time—of the order of 10 seconds. However, in Fig. 3 an oscillogram is shown for the case when both the forward and reverse process developed almost at the same time. Recovery to the original picture, in this case, took approximately 15 seconds. In this group of oscillograms an interesting effect should be noted. Oscillogram (a) gives the original picture and (c) one of the stages of recovery after action of the light. From a comparison it can be shown that adjacent light pulses behave somewhat differently, not only while the ultraviolet light is shining, but also after it is turned off. The relative amplitudes of these neighboring light pulses reverse themselves by comparison with the original when the light is turned off.

Fig. 3. Oscillogram of the light pulse at different times. a—before switching on the ultraviolet; b—10 seconds after turning on the ultraviolet; c—5 seconds after turning off the ultraviolet.

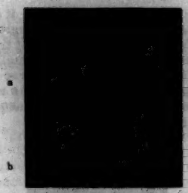

Fig. 4. Phase displacement of the light pulse due to the action of ultraviolet. a—before switching on of the untraviolet; b—during the exposure.

In a number of cases the ultraviolet light caused a change in the phase of the light pulse, in addition to increasing or decreasing its intensity. On the oscillogram of Fig. 4, (a) shows the phase of the light pulse relative to the excitation voltage before the light treatment, and (b) shows the same phase relationship when the ultraviolet light was brought to bear on the sector of the crystal next to that under observation. In all cases, the phase shift of the light pulse due to the ultraviolet light was in the direction of a phase angle earlier than the initial value. When photoluminescence prevented the obtaining of a light pulse curve on the oscilloscope, it was observed visually. Thus, it was noted that the part of the striation which was directly exposed to the ultraviolet spot was always quenched. It was also found that the electroluminescence of spots was less sensitive to the action of light, evidently because of the much greater intensity of the excitation and emission process in them.

The basic features of the effects described were repeated for other crystals and other striations.

DISCUSSION OF RESULTS

The influence of ultraviolet illumination of one sector of a striation on the electroluminescence of an adjacent sector of the single crystal can be explained by the migration of charge carriers produced by the exposure. Figure 5 shows a possible scheme of the charge distributions and the directions of motion. If we assume that in each part of a "striation" the processes of emission and excitation in electroluminescence occur in the same half-cycle, then in each case we can determine the sign of the charge carrier. Experiment shows that when the untraviolet spot was located near the condenser plate, while that plate was positively charged, quenching was observed. From the charge distribution scheme it is evident that holes enter the investigated region of the crystal under these conditions. For spot positions causing increased intensity of electroluminescence (flare-up) it is electrons which enter this region.

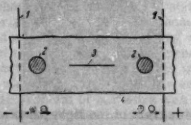

Fig. 5. Schematic diagram of the possible movement of charge carriers due to the action of ultraviolet. 1—plate of the condenser; 2—spot of ultraviolet radiation; 3—observed area of the "striation"; 4—crystal.

From oscillograms (b) and (c) (Fig. 2) it is seen that adjoining parts of a striation which give a light pulse in the same half-period react to injected charge carriers of the same sign in a directly opposite manner. In this section, the injection of holes produces a light pulse, while the injection of electrons produces quenching. This effect of holes and electrons may be explained in the following manner. Neighboring parts of a striation lie in parts of the crystal with different types of conductivity. When an electroluminescent state is established in a p-region, the overwhelming majority of luminescent centers are in an ionized state. Since the field carries off free electrons from the ionized centers, the intensity of luminescence is limited by the lack of electrons. An increase in the number of free electrons therefore produces an increase in the number of radiative recombinations. Penetration of electrons into an n-type region only causes increased conductivity and the screening of this area from the applied voltage, thus resulting in local quenching of the electroluminescence.

On the other hand introduction of a hole into an n-type region increases the number of ionization centers and produces an increase in the intensity of electroluminescence. Introduction of holes into a p-region where there is already an insufficiency of electrons and all the centers are already ionized, increases external quenching processes and thus diminishes the intensity of electroluminescence.

The existence of regions of p- and n-type conductivity in single crystals of ZnS-Cu probably involve the difference in the photoluminescence properties of these regions. Certain nonuniformity is actually observed, but as yet there is still no basis on which to state that it is actually connected with the presence of p- and n-type regions.

CONCLUSIONS

On the basis of the above account we may conclude that the luminescent striations depend on their own emission. There is some basis to assume that the separation of striations into parts corresponds to a division of the crystal into regions of n- and p-type conductivity.

It is also possible to hypothesize that spots develop on the intersection of striations with boundaries that divide the p- and n-regions.

The fact that the 1200 μ long striation spanned the entire distance between the condenser plates leads us to believe that a field of no more than 10^4 volts/cm is needed to maintain the electroluminescence process. This value shows that, at least in the direction of a striation, in a single crystal of a given type the free path (i.e., without substantial energy losses) of electrons may be considerably larger (up to two orders of magnitude) than the average. This agrees with the fact that there is considerably increased conductivity of an electroluminescent single crystal in the direction most favorable for electroluminescence, as described in reference 2.

In conclusion, the authors thank E. I. Panasiuk for preparing the single crystals studied.

REFERENCES

1. V. E. Oranovsky, E. I. Panasiuk, and V. T. Fediushin. Inzh. Fiz. Zhur. 2, 39 (1959).
2. A. Lempicki, D. R. Frankl, and V. A. Brophy. Phys. Rev. 107, 1238 (1957).

OPTICAL PROPERTIES OF METAL FILMS IN THE REGION OF ANOMALOUS SKIN-EFFECT

Van-Si-Fu, V. P. Silin, and E. P. Fetisov

Received 18 February 1959

The optical properties of conducting films are considered for the case in which losses due to diffusion scattering of electrons at the surface of the conductor are not negligible.

Experiments with thin films may be used to determine the optical parameters of conductors.[1] However, the theory of the optical properties of films has not yet taken into account the anomalous skin effect, which is found in many metals.[2-4]* The present article attempts to fill this gap.†

*Reference 3 is an exception. It treats the optical properties of surfaces in terms of a free electron model. However, it considers only the case of normally incident radiation.

†The properties of thin layers in general differ from those of massive specimens because of the granular structure of the former. We shall not attempt to explain the role of this structure here, but rather seek to investigate the part played by surface losses in determining surface conductivity, which in the case of metals is due to diffusion scattering of electrons at the surface.

In the case of the anomalous skin effect, we should not only use the equation

$$D = \varepsilon(\omega) E, \tag{1}$$

which is valid far from the surface, but should also make use of another equation relating surface current density to electric field.[5, 6]

$$i = \gamma(\omega)[n[En]], \tag{2}$$

where n is the external normal to the conductor surface. In Eqs. (1) and (2) the time dependence is assumed to be of the form $e^{i\omega t}$, which corresponds to a negative imaginary part of the dielectric constant $[\varepsilon(\omega) = \varepsilon_1(\omega) + i\varepsilon_2(\omega)]$. The volume absorption in the conductor is determined by the imaginary part of ε, but the surface absorption, which is connected with the diffusion scattering of electrons at the boundary of the conductor, is determined by the real part. Equation (1) is valid not only for an isotropic (e.g., polycrystalline) substance, but also for cubic crystals. Equation (2), on the other hand, holds only for isotropic bodies. For the case of cubic symmetry $\gamma(\omega)$ must be replaced by a surface resistance tensor having, in general, three independent components, which will be different for each different orientation of the conductor surface with respect to the crystallographic axes.

These macroscopic considerations are applicable if the distance in which the field changes appreciably is large in comparison with the smaller of the two parameters l and v/ω. Here l is the free path length of an electron, and v/ω is the distance traveled by an electron during one oscillation of the field. It should be noted that in the infrared region of the spectrum the conditions mentioned are fulfilled for metals. If the skin effect is normal, then, in massive bodies l is small in comparison with the skin depth, while in the region of the anomalous skin effect the reverse is true. However, in the latter case the distance traveled by an electron during one oscillation of the field is actually much smaller than the skin depth, so that Eqs. (1) and (2) may be used.

Maxwell's equations, applied together with Eqs. (1) and (2) and suitable boundary conditions, make it easy to find expressions for the complex reflection coefficient r and transmission coefficient t for light in the case of a plane parallel film, on both sides of which $\varepsilon = 1$. In this case, when the electric vector of the incident wave is perpendicular to the plane of incidence, we have

$$r_s = \frac{-e^{i\psi}\left[(\sqrt{\varepsilon-\sin^2\theta}+\xi)^2-\cos^2\theta\right]-e^{-i\psi}\left[(\sqrt{\varepsilon-\sin^2\theta}-\xi)^2-\cos^2\theta\right]}{e^{i\psi}\left[\sqrt{\varepsilon-\sin^2\theta}+\cos\theta+\xi\right]^2-e^{-i\psi}\left[\sqrt{\varepsilon-\sin^2\theta}-\cos\theta-\xi\right]^2}, \tag{3}$$

$$t_s = \frac{4\cos\theta\sqrt{\varepsilon-\sin^2\theta}}{e^{i\psi}\left[\sqrt{\varepsilon-\sin^2\theta}+\cos\theta+\xi\right]^2-e^{-i\psi}\left[\sqrt{\varepsilon-\sin^2\theta}-\cos\theta-\xi\right]^2} \tag{4}$$

Here θ is the angle of incidence, $\xi = 4\pi\gamma(\omega)/c$, $\psi = \sqrt{\varepsilon-\sin^2\theta}\,\omega d/c$, and d is the thickness of the film.

If the electric vector lies in the plane of incidence, then

$$r_p = -\frac{e^{i\psi}\left[(\varepsilon+\xi\sqrt{\varepsilon-\sin^2\theta})^2\cos^2\theta-\varepsilon+\sin^2\theta\right]-e^{-i\psi}\left[(\varepsilon-\xi\sqrt{\varepsilon-\sin^2\theta})^2\cos^2\theta-\varepsilon+\sin^2\theta\right]}{e^{i\psi}\left[(\varepsilon+\xi\sqrt{\varepsilon-\sin^2\theta})\cos\theta+\sqrt{\varepsilon-\sin^2\theta}\right]^2-e^{-i\psi}\left[(\varepsilon-\xi\sqrt{\varepsilon-\sin^2\theta})\cos\theta-\sqrt{\varepsilon-\sin^2\theta}\right]^2}, \tag{5}$$

$$t_p = \frac{4\varepsilon\sqrt{\varepsilon-\sin^2\theta}\cos\theta}{e^{i\psi}\left[(\varepsilon+\xi\sqrt{\varepsilon-\sin^2\theta})\cos\theta+\sqrt{\varepsilon-\sin^2\theta}\right]^2-e^{-i\psi}\left[(\varepsilon-\xi\sqrt{\varepsilon-\sin^2\theta})\cos\theta-\sqrt{\varepsilon-\sin^2\theta}\right]^2}. \tag{6}$$

From formulas (3)-(6) we may obtain expressions for all the observed magnitudes measured in optical experiments with metallic films. The complex coefficients may be represented in the form

$$r_s = \sqrt{R_s}\,e^{-i\alpha_s},\quad r_p = \sqrt{R_p}\,e^{-i\alpha_p},\quad t_s = \sqrt{T_s}\,e^{-i\beta_s},\quad t_p = \sqrt{T_p}\,e^{-i\beta_p},$$

where α and β determine the phase change of the reflected and transmitted waves, while R and T are the real coefficients of reflection and transmission, a knowledge of which allows the determination of the coefficient of absorption $A = 1 - R - T$.

In order to bring out the role of the surface resistance $\gamma(\omega)$, we shall consider several special cases. In these cases the imaginary part of γ will be neglected.

We consider first the case in which the volume absorption is negligibly small, so that $\varepsilon(\omega)\gamma$ may be assumed purely real. In the case where the thickness of the film is small in comparison with the depth of penetration of the field in a massive conductor, neglecting absorption is possible if the path length in the massive con-

ductor is also large in comparison to the film thickness. If the film thickness is large in comparison to the depth of penetration of the field, however, then the possibility of neglecting absorption corresponds to the usual case of anomalous skin effect, in which the free path is large compared to the depth of the skin-layer.

On the assumption that $\varepsilon(\omega) - \sin^2\theta < 0$, we have for the s-polarization

$$R_s = |(\varepsilon - 1 + \xi^2)\,\mathrm{sh}^2|\psi| + 4\xi^2(\sin^2\theta - \varepsilon)\,\mathrm{ch}^2|\psi|)|\,M_s, \tag{7}$$

$$T_s = 4\cos^2\theta(\sin^2\theta - \varepsilon)\,M_s, \tag{8}$$

$$A_s = 4\xi\cos\theta\,|2(\sin^2\theta - \varepsilon) + \mathrm{sh}^2|\psi|(\sin^2\theta - \varepsilon + |\cos\theta + \xi|^2)|\,M_s, \tag{9}$$

$$\beta_s = -\frac{\pi}{2} + \tan^{-1}\frac{2(\xi + \cos\theta)\sqrt{\sin^2\theta - \varepsilon}\coth|\psi|}{\sin^2\theta - \varepsilon - (\xi + \cos\theta)^2}, \tag{10}$$

$$\beta_s - \alpha_s = \frac{\pi}{2} + \tan^{-1}\frac{2\xi\sqrt{\sin^2\theta - \varepsilon}\,\mathrm{cth}|\psi|}{1 - \varepsilon - \xi^2}; \tag{11}$$

and, correspondingly, for the p-polarization

$$R_p = |[\varepsilon^2\cos^2\theta + (\sin^2\theta - \varepsilon)(1 - \xi^2\cos^2\theta)]\,\mathrm{sh}^2|\psi| + 4\varepsilon^2\xi^2(\sin^2\theta - \varepsilon)\cos^2\theta\,\mathrm{ch}^2|\psi|)\,M_p, \tag{12}$$

$$T_p = 4\varepsilon^2\cos^2\theta(\sin^2\theta - \varepsilon)\,M_p, \tag{13}$$

$$A_p = 4\xi\cos\theta(\sin^2\theta - \varepsilon)\{2\varepsilon^2\cos^2\theta + [\varepsilon^2\cos^2\theta + (\sin^2\theta - \varepsilon)(1 + \xi\cos\theta)^2]\,\mathrm{sh}^2|\psi|\}\,M_p, \tag{14}$$

$$\beta_p = -\frac{\pi}{2} + \tan^{-1}\frac{2(\xi\cos\theta + 1)\sqrt{\sin^2\theta - \varepsilon}\cos\theta\coth|\psi|}{-\varepsilon^2\cos^2\theta + (\sin^2\theta - \varepsilon)(1 + \xi\cos\theta)^2}, \tag{15}$$

$$\beta_p - \alpha_p = \frac{\pi}{2} + \tan^{-1}\frac{-2\varepsilon\xi\cos^2\theta\sqrt{\sin^2\theta - \varepsilon}\,\mathrm{cth}|\psi|}{\varepsilon^2\cos^2\theta + (\sin^2\theta - \varepsilon)(1 - \xi^2\cos^2\theta)}. \tag{16}$$

Here

$$M_s^{-1} = 4(\xi + \cos\theta)^2(\sin^2\theta - \varepsilon) + |\varepsilon - \sin^2\theta - (\xi + \cos\theta)^2|^2\,\mathrm{sh}^2|\psi|,$$

$$M_p^{-1} = 4(\xi\cos\theta + 1)(\sin^2\theta - \varepsilon)\varepsilon^2\cos^2\theta + |\varepsilon^2\cos^2\theta - (\varepsilon - \sin^2\theta)(1 + \xi\cos\theta)^2|^2\,\mathrm{sh}^2|\psi|.$$

As is clear from the formulas obtained, the dependence on surface resistance is quite essential. In particular, it is because of the presence of the surface resistance that the coefficient of absorption is different from zero, and that the phase difference of the incident and reflected fields is different from $\pi/2$. For the case $\varepsilon(\omega) - \sin^2\theta > 0$, the coefficient of absorption and the phase difference $\beta - \alpha$ are determined by the following formulas:

$$A_s = \frac{4\xi\cos\theta\,|2(\varepsilon - \sin^2\theta) - (\varepsilon - \sin^2\theta - |\cos\theta + \xi|^2)\sin^2\psi|}{4(\cos\theta + \xi)^2(\varepsilon - \sin^2\theta) + |\varepsilon - \sin^2\theta - (\xi + \cos\theta)^2|^2\sin^2\psi}, \tag{17}$$

$$\beta_s - \alpha_s = \pi + \tan^{-1}\frac{(\varepsilon - 1 + \xi^2)\tan\psi}{2\xi\sqrt{\varepsilon - \sin^2\theta}}, \tag{18}$$

$$A_p = \frac{4\xi\cos\theta(\varepsilon - \sin^2\theta)\{2\varepsilon^2\cos^2\theta - |\varepsilon^2\cos^2\theta - (\varepsilon - \sin^2\theta)(1 + \xi\cos\theta)^2|\sin^2\psi\}}{4\varepsilon^2\cos^2\theta(\varepsilon - \sin^2\theta)(1 + \xi\cos\theta)^2 + \sin^2\psi|\varepsilon^2\cos^2\theta - (\varepsilon - \sin^2\theta)(1 + \xi\cos\theta)^2|^2}, \tag{19}$$

$$\beta_p - \alpha_p = \pi + \tan^{-1}\frac{|\varepsilon^2\cos^2\theta - (\varepsilon - \sin^2\theta)(1 - \xi^2\cos^2\theta)|\tan\psi}{2\varepsilon\cos^2\theta\sqrt{\varepsilon - \sin^2\theta}}. \tag{20}$$

Formulas (7)-(20) become considerably simpler in the limiting cases of very thin films and massive conductors. In the latter case formulas (9) and (14) become

$$A_s = \frac{4\xi\cos\theta}{1 - \varepsilon + 2\xi\cos\theta + \xi^2},$$

$$A_p = \frac{4\xi\cos\theta(\sin^2\theta - \varepsilon)}{\varepsilon^2\cos^2\theta + (\sin^2\theta - \varepsilon)(1 + \xi\cos\theta)^2}. \tag{21}$$

When ξ and ξ^2 are small in comparison with ε, these formulas reduce to formulas (11) and (12) of reference 5.

We now consider the case of thin films, where

$$|\psi| = \frac{\omega}{c}d\,|\sqrt{\varepsilon - \sin^2\theta}| \ll 1. \tag{22}$$

We assume here that the imaginary part of ε, although small in comparison with the real part, is different from zero and makes a contribution, for example, to absorption in the film which is not negligibly small. We also assume the following inequalities:

$$|\varepsilon_1| \gg \xi, \quad |\varepsilon_1| \gg \xi^2, \quad |\varepsilon_1|\frac{\omega}{c}d \gg \xi. \tag{23}$$

The first of these inequalities is violated only near frequencies for which ε_1 goes to zero. The second inequality means that the frequencies considered are those for which the skin depth in a massive specimen is significantly larger than the distance traveled by an electron during a single oscillation of the field. The third inequality indicates that the thickness of the film is also large in comparison with this distance.

On making use of inequalities (22) and (23), we obtain from formulas (3)-(6) the following relations:*

*In deriving relations (24)-(29), we have kept only the principal terms. Thus we may consider these formulas as interpolations valid, for example, for arbitrary ε_1.

$$\beta_s = \tan^2\frac{\varepsilon_1 - \sin^2\theta + \cos^2\theta}{2\left(\frac{c}{\omega d}\right)(\cos\theta + \xi) - \varepsilon_2}, \tag{24}$$

$$\beta_p = \tan^{-1}\frac{1 + \varepsilon_1 + (1 - \frac{1}{\varepsilon_1})\tan^2\theta}{2\left(\frac{c}{\omega d}\right)(\sec\theta + \xi) - \varepsilon_2\left[\frac{\varepsilon_1^2 + \tan^2\theta}{\varepsilon_1^2}\right]}, \tag{25}$$

$$\beta_s - \alpha_s = \pi + \tan^2\frac{\varepsilon_1 - 1}{2\left(\frac{c}{\omega d}\right)\xi - \varepsilon_2}, \tag{26}$$

$$\beta_p - \alpha_p = \pi + \tan^2\frac{(\varepsilon_1 - 1)\left(\frac{\varepsilon_1 - \tan^2\theta}{\varepsilon_1}\right)}{2\left(\frac{c}{\omega d}\right)\xi - \varepsilon_2\left(\frac{\varepsilon_1^2 - \tan^2\theta}{\varepsilon_1^2}\right)}, \tag{27}$$

$$A_s = \frac{\cos\theta\left(2\xi - \varepsilon_2\frac{\omega d}{c}\right)}{\cos^2\theta + \left(\frac{\omega d}{2c}\right)^2(\varepsilon_1 - 1)^2}, \tag{28}$$

$$A_p = \frac{\sec\theta\left(2\xi - \varepsilon_2\frac{\omega d}{c}\right)\left(1 + \frac{1}{\varepsilon_1^2}\tan^2\theta\right)}{\sec^3\theta + \left(\frac{\omega d}{2c}\right)^2\left(\varepsilon_1 - \sec^2\theta + \frac{1}{\varepsilon_1}\tan^2\theta\right)^2}. \tag{29}$$

The formulas just written become especially simple in the case in which the real part of the dielectric constant is significantly greater than unity. In this case ξ and ϵ_2 enter into the combination

$$2\xi - \epsilon_2 \frac{\omega}{c} d. \qquad (30)$$

The second term of this simple combination corresponds to volume absorption, while the first is the sum of the surface losses on the two sides of the film. It should be noted that $2\xi \gg |\epsilon_2| (\omega d/c)$ for the case in which the free path length in a massive metallic specimen is significantly greater than the film thickness. This means that for thin films the skin effect may, in principle, be anomalous under conditions for which the normal skin effect would occur in a massive specimen. Moreover, in the case of large ϵ_1 the phase difference $\beta - \alpha$ is independent of the polarization and the angle of incidence; in the remaining formulas the change from s- to p-polarization corresponds to replacing $\cos\vartheta$ by $\sec\vartheta$. Hence with the aid of optical measurements on a film of a given thickness, when ϵ_1 is large, we may determine the real part of the dielectric constant and the film thickness. We cannot measure ϵ_2 and ξ separately, however, only in combination (30). The effect of surface resistance may be singled out, for example, by studying surfaces of various thicknesses if, of course, films can be prepared for which ϵ will be independent of thickness.

REFERENCES

1. G. V. Rozenberg. "Optika tonkosloinykh pokrytii." (Optics of Thin Coatings), GIFML, Moscow, 1958;
   O. S. Heavens. "Optical Properties of Thin Solid Films," London, 1955;
   H. Mayer. "Physik dünner Schichten." Stuttgart, 1950;
   H. Wolter. Handb. d. Phys. **24**, 461 (1956).
2. G. E. Reuter and E. H. Sondheimer. Proc. Roy Soc. **195**, 336 (1948).
3. R. B. Dingle. Physica **19**, 311, 348, 729, 1187 (1953).
4. V. L. Ginzburg and G. P. Motulevich. Usp. Fiz. Nauk **55**, 469 (1955).
5. V. P. Silin. Zhur. Eksp. i Teoret. Fiz. **35**, 1001 (1958). (See Soviet Phys.—JETP.)
6. V. P. Silin. Zhur. Eksp. i Teoret. Fiz. **36**, 1443 (1959). (See Soviet Phys.—JETP.)

THIN FILM OPTICS. V. THE PROPERTIES OF SILICON

M. P. Lisitsa and N. G. Tsvelykh

Received 17 February 1959

The coefficients T, R, and R′ were measured for amorphous layers of silicon of thicknesses $0 < d < 1200$ A, and for four wavelengths in the visible spectrum. On the basis of the experimental data curves were plotted of the dependence of the fractional absorption of light on the film thickness. The index of refraction was calculated for the thicker films. The question of aging was also partially studied.

FILM PRODUCTION AND METHOD OF MEASUREMENT

Wedge-shaped layers, which are convenient for studying the thickness dependence of optical parameters, were produced by thermal evaporation in vacuum. The conditions of condensation have been previously described by us.[1] Because of the high melting point of Si (1400° C), the choice of a material from which to evaporate is somewhat difficult since tungsten, tantalum, and molybdenum dissolve in molten silicon and form an alloy with it. As a result the evaporator material, as well as the silicon, would be condensed on the substrate. We convinced ourselves of this by comparing the optical properties of silicon layers evaporated from the above-mentioned metals and from a carbon crucible. This agrees with the conclusions of other work[2] that a silicon layer evaporated from a tantalum boat has twice the reflectivity in the far ultraviolet than when a crucible coated with Al_2O_3 or BeO is used. The increased reflectivity is caused by the above-mentioned solution of tantalum in silicon and the resulting evaporation, not only of the charge, but also of the evaporator material.

The carbon crucible which we used was a plane-parallel plate, 0.5 mm thick, and 5-6 mm wide. It was prepared from spectroscopically pure electrodes, and was first annealed in high vacuum so that the plate itself would not introduce contamination into the silicon layers. However, silicon carbide, which is formed at elevated temperatures, may be condensed on the substrate. To avoid this only a small part of the silicon on the carbon plate was evaporated.

The impurities in the initial material amounted to 0.2%. To decrease this the silicon was melted once in vacuum so that the more volatile impurities were driven off. All the layers studied were prepared from material subjected to this preliminary cleaning. On the basis of other work[3] (heating of a thin layer of Si to a temperature of 700° C for an hour in air did not lead to the appearance of an oxide film) we can be confident that, under the conditions of our experiment, the formation of an oxide film on the surface is unlikely.

The method of measuring the transmission coefficient T (light incident on the film side) and the reflection coefficients R and R′ (light incident on the substrate side) has been previously described by us.[4] Calculation of the influence of multiple reflections in the substrate was also done as in a previous manner.[5]

The error in the measurement of T did not exceed 5%. This reached 10% for R and R′ in one case.

TRANSPARENCY, REFLECTION, AND ABSORPTION

The optical properties of thin layers of silicon have still only been studied to a small extent. Until recently, only two works had been published in which some of the dependence of the optical properties on wavelength and film thickness had been explained. In one of these* results were given for five films of different density* in the

*Because of the absence of information on the layer thickness in reference 6, we were not able to compare our results with those in the cited report.

visible region of the spectrum. The experimentally determined coefficients T, R, and R′ were used to calculate n and χ. For this purpose the author used a graphical method developed by him.[7]

The second work was devoted to a study of the reflectivity of Si layers in the Schumann region[2] (the region of 1100-1700 A). The authors found a nonmonotonic dependence of the coefficient R on the thickness for very thin layers. In the case of thicker layers, having metallic luster, an increase in wavelength was accompanied by a smooth increase of R.

We describe below the results of our investigation.

All the wedge-shaped layers of silicon gave interference fringes for thicknesses d > 400 A. They became very strong if the wedge was coated with an opaque layer of silver or aluminum and examined in reflected light (from the underside).

Comparison of silicon and germanium layers[8] of comparable thickness shows that in the visible region the former is characterized by a much higher transparency. Taking into account the common structure of these layers,*

*Data on the structure of Si layers are given in reference 3. With the use of electron diffraction the authors showed that a homogeneous amorphous film is produced when silicon is deposited on a substrate whose temperature is kept below 600° C. If, however, the substrate temperature exceeds 600° C, then a crystalline film is obtained. Heating of the amorphous layer in vacuum at a temperature of 700° C led to crystallization. Thus, Si films, as also Ge films, prove to be amorphous when prepared under normal conditions.

and also the common structure and physical properties of single crystal samples of these materials, it is possible to hypothesize that this difference is connected with the width of the forbidden zone. Actually, if the true absorption edge of Si lies near the visible region,* and the

*The width of the forbidden zone is 0.78 ev for Ge and 1.12 ev for Si.[9]

absorption coefficient increases slowly at this edge, then in the case of Ge the last reaches its limiting value at a lower frequency. Such reasoning, naturally, only approximately indicates the nature of the effect, since complete parallelism in determining the optical properties of thin layers and bulk material is not possible. However, for thicknesses at which the layer becomes continuous and the interference effect is sufficiently clear, such a comparison is entirely justified.

Transmission curves obtained for four wavelengths are shown in Fig. 1. It is easy to see that with increasing

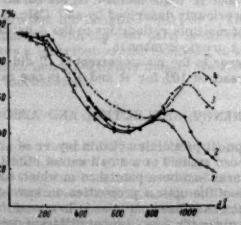

Fig. 1. Dependence of the transmission coefficient T on the thickness d of a silicon film for different wavelengths. Wavelength (in mμ): Curve 1—580; curve 2—640; curve 3—700; curve 4—760.

d the transmission gradually increases and forms a broad minimum near d ~ 600 A. The position of this minimum is different for different wavelengths. The displacement of it toward the region of greater thickness for increased λ indicates that its origin is primarily due to interference. At the beginning of the curves small oscillations can be noted, with one maximum near d ~ 220 A more prominent than the others. There is also a maximum in the region of greater thickness; and a tendency to form a minimum at the same thickness on the curve of R (Fig. 2).

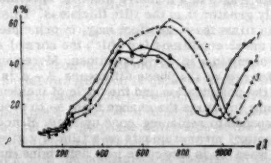

Fig. 2. Dependence of the reflection coefficient R on the thickness d of a silicon film for different wavelengths. Wavelengths are indicated in the caption of Fig. 1.

Such oscillations cannot be explained by the usual interference effect since they are observed for very small thickness. From the appearance the cause is apparently a resonance effect which was found, in part, by us when studying the optical characteristics of thin layers of other materials. A similar effect is not detected in the same thickness interval on the curve of R′ (Fig. 3). Together

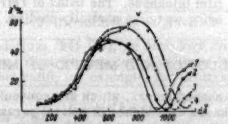

Fig. 3. Dependence of the reflection coefficient R′ on the thickness d of a silicon film for different wavelengths. Wavelengths are indicated in the caption of Fig. 1.

with the rest this case appears to be an additional verification of the hypothesis given by us earlier[5] concerning the effect of the form and surface granularity on the interaction of radiation with a two-dimensional collodion film. Note, finally, that for the introduction of very weak absorption in the thickness interval 0 < d < 400 the coefficient T decreases noticeably slower for a silicon layer than in the case of a germanium layer.

The general features of the dependence of the coefficients R and R′ on d (Figs. 2 and 3) are reminiscent of the corresponding curves for selenium and germanium layers. For example, a splitting of the first interference maximum into two components usually takes place; in the case studied it is clearly observed for only two wavelengths on the curve of R. In previous work[5, 8] we did not take the time to pursue the discovered splitting. Recurrence of the same effect for a new material eliminates any possible doubt of its existence. As a result it can be stated that the interference maximum somehow alters the subsidiary effect apparently connected with the structure of the layer. It is possible that there is still some granularity in the silicon layer at a thickness of 500-600 A

which is connected with the appearance of the (already referred to) high resonance extremum, the difference of which also leads to a splitting of the interference maximum. We regret that we do not have electron microscope data on the structure of the selenium layer. Until such data are obtained, the assumption expressed here concerning the granular structure of a 500-600 A layer of Si has no real basis.

Examination of Figs. 2 and 3 shows that after the first interference maximum (d > 750 A) all four curves occur in the usual order, i.e., with increased wavelength the maximum is displaced to higher values of d. There is no doubt that at that thickness the films are already continuous, and the movement of the curves is in complete agreement with the condition for interference. The differences in the values of the coefficients R and R′ should be noted. It R exceeds 10% in the first interference maximum, then R′ is practically zero, i.e., the system substrate-layer appears clear (the reflection from the free surface of the glass substrate is deducted and is not included in R′). This does not mean that a silicon film can be used for clearing purposes* since for a given thickness its absorptivity is considerable, and the clear part is narrowed, due to the high index of refraction.

*We speak here about the visible region of the spectrum.

We may conjecture about the value of absorption from the data on Fig. 4. In the interval of minimal thick-

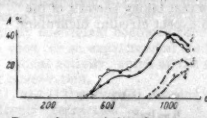

Fig. 4. Dependence of the absorption A on the thickness d of a silicon film for different wavelengths. Wavelengths are indicated in the caption of Fig. 1.

ness (0 < d < 420 A) it appears immeasurably small. In this respect the silicon layer is essentially different from the layers of germanium, selenium, and tellurium studied by us earlier. Comparison of all four curves shows an increase of A with decreasing λ. As we advance into the infrared region of the spectrum the energy absorbed rapidly decreases. Taking into account, furthermore, the high mechanical strength of a silicon film it can be stated that it is entirely possible to prepare reflecting multilayer films for use in the infrared region as well as clear ones.

REFRACTION CHARACTERISTICS (d > 1000 A)

To study the optical constants of thin layers of other semiconductors we used the experimental values of T, R, and R′ to calculate the indices n and χ. All the calculations were based on the applicability of Abeles relations.[10] Similar calculations in the present case are not practical since the relations mentioned are quite useless for thin layers of silicon. We can eliminate having to calculate n for relatively thick layers (d > 1000 A) by using another method. As shown in reference 11, the distribution of intensity in the interference picture, which gives the reflection of a monochromatic beam of light from a wedge-shaped layer, must obey the conditions

$$2nd_{max} + \delta = \left(k - \frac{1}{2}\right)\lambda, \qquad 2nd_{min} + \delta = k\lambda, \qquad (1)$$

where d_{max} and d_{min} are the respective thicknesses of the maximum and minimum, δ is the total phase shift for the reflection of light from the boundary air-layer and layer-backing, and k is the order of the interference.

If we assume that δ is the same for d_{max} and d_{min} (in the case of thick layers this assumption is entirely justified), then the value of the index of refraction which satisfies condition (1) can be calculated by the formula

$$n = \frac{\lambda}{4\left(d_{min} - d_{max}\right)}. \qquad (2)$$

The results calculated by the use of formula (2) are shown in the table. It is seen that for very small values

Index of Refraction for a Silicon Film Calculated Using Formula (2)

λ (mμ)	d_{max} (Å)	d_{min} (Å)	n
540	1020	1360	3.97
	1720	2240	2.8
	2900	3400	2.7
580	1150	1480	4.2
	1840	2380	2.84
	3060	3565	2.87
640	1160	1550	4.1
	2010	2615	2.6
	3305	3840	3.0
780	1190	1630	4.32
	2280	2980	2.71
	3640	4180	3.52

of d_{max} and d_{min}, n is substantially greater than the average and maximum values. In the last case it is sufficiently close, especially for the first three wavelengths. Hence, we may deduce that δ does not appear to be a function of thickness if d exceeds at least 1500 A. We can also note a general increase in the value of the index for increasing λ, and the fact that for thick layers its value is close to the value of n (~3.5) for single crystal silicon.[9]

AGING

In addition to studying the optical properties we partially investigated the question of aging of thin layers of Si, and found that spontaneous crystallization took place in a layer of d > 900 A after several days. (The film was in air at room temperature, but the free surface was coated with a layer of aluminum so that it was not in contact with the atmosphere.) The microcrystals of Si so produced lifted the metallic coating, generating, as a rule, a symmetrical mound in the form of a true circle or an ellipse. A microphotograph, obtained with an MII-4 micro-interferometer, permitted us to determine the heights of the mounds and thus establish the size of the single crystals in a direction perpendicular to the surface of the backing. It was shown that where the microcrystals were formed, their size exceeded the thickness of the film by one or two orders. The last circumstance indicates the great mobility of silicon atoms under the described conditions. In the course of time the crystal size increased so much that in their places of formation fracture of the metallic film took place. For small thickness (d < 900 A) crystallization did not take place, and the film remained amorphous.

CONCLUSIONS

1. The presence of a resonance effect for the interaction of light with thin layers of Si was found.

2. It was shown that the minimum thickness films of Si absorb very little visible radiation.

3. The over-all phase shift δ may change over a wide range of thickness up to d ~ 1500 a, taking into account a corresponding shift due to the reflection of light from the boundary dividing air-film and film-backing.

4. A layer of silicon is subject to spontaneous aging; in the course of time an amorphous phase changes to crystalline.

5. In general, the variation with thickness of the optical properties of an amorphous layer of silicon is similar to the behavior of amorphous layers of selenium and germanium.

REFERENCES

1. M. P. Lisitsa and N. G. Tsvelykh. Opt. i Spektr. 2, 674 (1957); Zav. lab. No. 9, 1072 (1956).
2. S. Kandare and D. Fabre. C. R. Acad. Sci. 242, 1150 (1956).
3. G. Hass and N. W. Scott. J. Phys. Rad. 11, 394 (1950).
4. M. P. Lisitsa and N. G. Tvelykh. Opt. i Spektr. 4, 373 (1958).
5. M. P. Lisitsa, V. M. Maevsky, and N. G. Tvelykh. Opt. i Spektr. 5, 179 (1958).
6. P. Cotton. J. Phys. Rad. 11, 390 (1950).
7. P. Cotton. J. Phys. Rad. 11, 321 (1950).
8. M. P. Lisitsa and N. G. Tvelykh. Opt. i Spektr. 5, 622 (1958).
9. A. F. Ioffe. "Fizika Poluprovodnikov." (Physics of Semiconductors), Izd. AN SSSR, 1957.
10. F. Abeles. Rev. Optique 32, 257 (1953).
11. K. D. Sinel'nikov, I. N. Shklyarevsky, and B. S. Skorobogatov, Uch. Zap. Kh. G. U. (Scientific Records of Kharkov State University) 64, 135 (1955).

THE PROPAGATION OF LIGHT IN ABSORBING MAGNETIC OPTICALLY ACTIVE ISOTROPIC MEDIA AND CUBIC CRYSTALS

B. V. Bokut' and F. I. Fedorov

Received 23 March 1959

We consider the propagation of plane electromagnetic waves in an optically isotropic medium with absorption, optical activity, and magnetic properties. We show that taking account of the magnetic terms in the optical activity of such a medium leads us to expect circular dichroism.

As is well known, the symmetry of crystals puts limitations on the electrical and magnetic activity tensors α and β.[1] In particular, for crystals having mutually perpendicular rotation-reflection axes or having inversion symmetry, the tensors α and β are zero. Therefore, of the five classes of cubic crystals, the didodecahedral, hexatetrahedral, and hexoctahedral cannot show optical activity. Optical activity is possible in cubic crystals of the tritetrahedral (T) and trioctahedral (O) classes, while the presence in these classes of mutually perpendicular axes of symmetry higher than the second order entails the scalar character of the tensors α and β.

In reference 2 the optical properties of active transparent crystals of cubic symmetry were studied, taking account of magnetic anisotropy. Since, in fact, most crystals are absorbing, it is of interest to study the laws of light propagation in optically active magnetic media, taking account of absorption.

In the present paper we will consider the optical properties of cubic crystals having absorption, optical activity, and magnetic properties. Invariance methods[1-3] will be used.

Maxwell's equations:

$$\left.\begin{aligned} \operatorname{rot} \mathbf{H} - \frac{1}{c}\dot{\mathbf{D}} &= \frac{4\pi}{c}\mathbf{I}, \\ \operatorname{rot} \mathbf{E} + \frac{1}{c}\dot{\mathbf{B}} &= 0 \end{aligned}\right\} \tag{1}$$

after substitution of the expression for a plane electromagnetic wave:

$$\left.\begin{aligned} \mathbf{E} &= \mathbf{E}_0 e^{i\eta}, \quad \mathbf{H} = \mathbf{H}_0 e^{i\eta}, \\ \eta &= \omega\left(t - \frac{1}{c}\mathbf{nr}\right) \end{aligned}\right\} \tag{2}$$

and application of the condition

$$\mathbf{I} = \varepsilon\mathbf{E} \tag{3}$$

take the form:[3-5]

$$\left.\begin{aligned} \mathbf{D} &= -[\mathbf{mH}] + i\tau\mathbf{E}, \\ \mathbf{B} &= [\mathbf{mE}]. \end{aligned}\right\} \tag{4}$$

where $\tau = 4\pi\sigma/\omega$ describes the absorption and m is the complex refraction vector $\mathbf{m} = \mathbf{m}' - i\mathbf{m}''$. For homogeneous waves, to which we confine ourselves, $\mathbf{m}' \parallel \mathbf{m}''$, and therefore the refraction vector becomes

$$\mathbf{m} = (n' - in'')\mathbf{n}, \quad (\mathbf{n}^2 = 1), \tag{5}$$

where n' is the refractive index, n'' is the extinction coefficient, and n is a unit vector parallel to the wave normal.

For plane waves in the optically active magnetic isotropic medium and cubic crystals, the equations of continuity have the form:[1, 2]

$$\left.\begin{aligned} \mathbf{D} &= \varepsilon\mathbf{E} + i\mathbf{k}\alpha[\mathbf{mE}], \\ \mathbf{B} &= \mu\mathbf{H} + i\mathbf{k}\beta[\mathbf{mH}]. \end{aligned}\right\} \tag{6}$$

where α and β are the coefficients of electrical and magnetic activity, respectively, and $k = \omega/c$ is the wave number in vacuum.

From (4) and (6), it follows that

$$\left.\begin{aligned} \varepsilon'\mathbf{E} + ip[\mathbf{mE}] + [\mathbf{mH}] &= 0, \\ \mu\mathbf{H} + iq[\mathbf{mH}] - [\mathbf{mE}] &= 0, \end{aligned}\right\} \tag{7}$$

where

$$\varepsilon' = \varepsilon - i\tau, \quad p = k\alpha, \quad q = k\beta. \tag{8}$$

Equations (7) differ from the corresponding equations in reference 2 only in the complex nature of the dielectric permittivity ϵ'. According to reference 2, Eqs. (7) yield expressions for the orientation of the vectors of the field and the complex refractive index in the following form:

$$\mathbf{E} = \pm i\,[\mathbf{nE}], \quad \mathbf{H} = \pm i\,[\mathbf{nH}]; \tag{9}$$

$$n = n' - in'' = \frac{1}{2(1-pq)}\left(\pm(\mu p + \varepsilon q) \mp i\tau q + \sqrt{[4\varepsilon\mu + (\mu p - \varepsilon q)^2 - \tau^2 q^2] - 2i\tau\,[2\mu + q(\varepsilon q - \mu p)]}\right). \tag{10}$$

This gives the refractive index and the extinction coefficient of both waves as

$$n'_{\pm} = \pm\frac{\mu p + \varepsilon q}{2(1-pq)} + \frac{\sqrt{\sqrt{[4\varepsilon\mu + (\mu p - \varepsilon q)^2 - \tau^2 q^2]^2 + 4\tau^2\,[2\mu + q(\varepsilon q - \mu p)]^2} + [4\varepsilon\mu + (\mu p - \varepsilon q)^2 - \tau^2 q^2]}}{2\sqrt{2}\,(1-pq)}, \tag{11}$$

$$n''_{\pm} = \pm\frac{\tau q}{2(1-pq)} + \frac{\sqrt{\sqrt{[4\varepsilon\mu + (\mu p - \varepsilon q)^2 - \tau^2 q^2]^2 + 4\tau^2\,[2\mu + q(\varepsilon q - \mu p)]^2} - [4\varepsilon\mu + (\mu p - \varepsilon q)^2 - \tau^2 q^2]}}{2\sqrt{2}\,(1-pq)}. \tag{12}$$

Therefore, along an arbitrary direction in optically active absorbing magnetic cubic crystals and isotropic media, two circularly polarized waves are propagated (9), the right-handed and left-handed waves having different velocities according to the two values of the refractive index (11), and different attenuations according to the two values of the extinction coefficient (12).

In the special case of a nonabsorbing medium ($\sigma = 0$) we get two unattenuated waves, circularly polarized, in agreement with reference 2. It is interesting to note that in the absence of magnetic activity ($\beta = q = 0$) that extinction coefficients for the two waves are identical, according to (12), although their velocities are different.

Therefore, for absorbing crystals, the magnetic terms of the optical activity acquire theoretical significance. Circular dichroism should be exhibited by cubic crystals if these terms are present and disappears if the magnetic activity coefficient becomes zero. In theory, this could be used for an experimental study of the magnetic part of optical activity, which up till now has resisted direct observation.

From (11) and (12), using (8), we find the value of the double circular refraction[3]

$$\Delta n' = n'_{+} - n'_{-} = \frac{k(\alpha\mu + \beta\varepsilon)}{1 - k^2\alpha\beta} \tag{13}$$

and the value of the double circular absorption

$$\Delta n'' = n''_{+} - n''_{-} = \frac{k\tau\beta}{1 - k^2\alpha\beta}, \tag{14}$$

which becomes zero if magnetic activity is absent. If we neglect the optical activity ($\alpha = \beta = 0$), we obtain from (11) and (12) the well-known expressions n' and n'' for absorbing isotropic media and cubic crystals:

$$\left.\begin{aligned} n' &= n_{10} = \sqrt{\frac{\mu}{2}\left(\sqrt{\varepsilon^2 + \tau^2} + \varepsilon\right)}, \\ n'' &= n_{20} = \sqrt{\frac{\mu}{2}\left(\sqrt{\varepsilon^2 + \tau^2} - \varepsilon\right)}. \end{aligned}\right\} \tag{15}$$

Neglecting terms containing the square of the electric and magnetic activity coefficients, their products, and higher powers (we consider them small), we convert (11)-(14) to the approximate formulas

$$n'_{\pm} = n_{10} \pm \frac{k}{2}(\alpha\mu + \beta\varepsilon), \tag{11'}$$

$$n''_{\pm} = n_{20} \pm \frac{k}{2}\tau\beta, \tag{12'}$$

$$\Delta n' = k(\alpha\mu + \beta\varepsilon), \tag{13'}$$

$$\Delta n'' = k\tau\beta. \tag{14'}$$

As is well known, the phenomenon of the rotation of the plane of polarization is explained as follows: two circularly polarized waves (right- and left-handed) with identical periods and amplitudes give a resultant linearly polarized wave; they correspond to the different indices of refraction. In the general case two circular waves can give a resultant wave with any polarization.[9] For the media that we are considering, the waves (2) which are circularly polarized in opposite directions have different amplitudes, since the absorptions (12) are not identical. Therefore, when light passes through optically active absorbing magnetic cubic crystals and isotropic media, the resultant wave should be elliptically polarized. The ellipticity of this wave will evidently be small, however, since it is determined by the magnetic activity coefficient.

The density of electric and magnetic energy in both waves is determined, as in reference 2, by the expressions

$$w_e = \frac{1}{16\pi}\left(\varepsilon \pm p n'_{\pm}\right)|\mathbf{E}|^2, \tag{16}$$

$$w_m = \frac{1}{16\pi}\left(\mu \pm q n'_{\pm}\right)|\mathbf{H}|^2, \tag{17}$$

where $n'_{\pm}$ is determined from (11'), where either the upper or the lower sign is used throughout in (16), (17), and (11').

To compare w_m and w_e we express $|\mathbf{H}|^2$ through $|\mathbf{E}|^2$. Using the formula for the inverse Hermitian matrix[3] we easily find:

$$|\mathbf{H}|^2 = \left(n'^2_{\pm} + n''^2_{\pm}\right)\frac{\mu^2 \mp 2q\mu n'_{\pm} + q^2\left(n'^2_{\pm} + n''^2_{\pm}\right)}{\mu^4 - 2q^2\mu^2\left(n'^2_{\pm} - n''^2_{\pm}\right) + q^4\left(n'^2_{\pm} + n''^2_{\pm}\right)^2}|\mathbf{E}|^2. \tag{18}$$

From (16), (17), and (18) we find the ratio of the energy densities

$$\frac{w_m}{w_e} = \frac{\left(n'^2_{\pm} + n''^2_{\pm}\right)\left[\mu^2 \mp 2q\mu n'_{\pm} + q^2\left(n'^2_{\pm} + n''^2_{\pm}\right)\right]}{\left(\varepsilon \pm p n'_{\pm}\right)\left[\mu^4 - 2q^2\mu^2\left(n'^2_{\pm} - n''^2_{\pm}\right) + q^4\left(n'^2_{\pm} + n''^2_{\pm}\right)^2\right]}. \tag{19}$$

As was also the case in reference 2, for a given $|\mathbf{E}|^2$, the electric and magnetic energies of the right- and left-handed waves depend on the corresponding refractive index. If we neglect the optical activity ($\alpha = \beta = 0$), we find from (19),

$$\frac{w_m}{w_e} = \frac{n'^2 + n''^2}{\varepsilon\mu}, \tag{20}$$

which agrees with the relationship obtained in reference 4 for absorbing isotropic media.

For the second special case, in which the medium does not absorb ($\sigma = 0$), expression (19) leads to the equality of the electric and magnetic energy of a plane wave, in agreement with reference 2.

The expression for the Umov-Poynting vector in isotropic media and cubic crystals having activity, absorption, and magnetic anisotropy takes the following form,

$$\mathbf{p} = \left\{\frac{c}{8\pi}\left(\frac{\varepsilon n'_{\pm} + \tau n''_{\pm}}{n'^2_{\pm} + n''^2_{\pm}} \pm k\mathbf{p}\right)|\mathbf{E}|^2 \pm \frac{w}{16\pi}\left(p|\mathbf{E}|^2 + q|\mathbf{H}|^2\right)\right\} \cdot \mathbf{n}. \tag{21}$$

Therefore, the energy flux vector lies in the direction of the wave normal but has a different magnitude for the right- and left-handed waves.

For nonabsorbing media ($\sigma = 0$), we obtain from (21),

$$\mathbf{p} = \frac{v_{\pm}}{16\pi}(\varepsilon|\mathbf{E}|^2 + \mu|\mathbf{H}|^2)\cdot\mathbf{n},$$

which agrees with reference 2.

REFERENCES

1. F. I. Fedorov. Opt. i Spektr. 6, 85 (1959).
2. F. I. Fedorov. Opt. i Spektr. 6, 377 (1959).
3. F. I. Fedorov. Opt. i Spektr. 2, 616 (1957).
4. F. I. Fedorov. Tr. Inst. Fiz. Mat. Akad. Nauk BSSR 2, 33 (1957).
5. F. I. Fedorov. "Optika anizotropnykh sred." (Optics of Anisotropic Media), Akad. Nauk BSSR, 1958.
6. M. Born. "Optika." (Optics), GNTIU, 1937.
7. K. Shefer. Teoreticheskaya Fizika. (Theoretical Physics), Vol. 3, chapter 2, GONTI, 1938.
8. B. V. Bokut' and F. I. Fedorov. Opt. i Spektr. 6, 537 (1959).

SHORT COMMUNICATIONS

THE TRANSITION PROBABILITY IN THE SCHUMANN-RUNGE BAND SYSTEM OF THE O_2 MOLECULE

L. M. Biberman, S. P. Erkovich, and V. N. Soshnikov

Received 3 February 1959

Keck, Camm, and Kivel[1] have measured the absolute radiation intensity of oxygen at 4100°K over the wavelength range 3000 to 5000 A. They compared their experimental data with an expression for estimating the radiation intensity given in reference 2. The authors of reference 1 concluded that the Schumann-Runge band system of the O_2 molecule has an oscillator strength $f = 0.015$, while from experiments on radiation absorption by cold O_2 it is known that $f = 0.016$ to 0.26.[3,4] These authors explained the discrepancy by the dependence of the electronic transition probability on the internuclear distance. Such a strong dependence would be of theoretical interest. However, very crude assumptions are used in reference 2 to derive the expression for estimating the radiation intensity, and these raise serious doubts: it is assumed that all transitions take place from the lower vibrational level of the upper electron state only; no account is taken of the effect of the Franck-Condon factors on the intensity distribution in the electronic vibrational band system.

In the present note we compare the experimental data of reference 1 with a more rigorous expression for the radiation intensity. We show that the value of the oscillator strength obtained there is incorrect.

Under the conditions of reference 1, equilibrium distribution of the molecules over the excited states prevailed and, for practical purposes, reabsorption was absent. We can therefore write the radiation intensity I_λ in the form:

$$I_\lambda = B_\lambda \sum_{v'}\sum_{v''} k_\lambda(v', v'')\cdot l, \qquad (1)$$

where B_λ is the black body emissivity, l is the thickness of the emitting layer, and $k_\lambda(v', v'')$ is the absorption coefficient for wavelength λ arising from the transition from vibrational level v'' of the lower electron state to the level v' of the upper. Summation takes place over all combinations v', v'' which contribute to the absorption at λ. Under the conditions of reference 1 overlapping of the rotational lines also occurs, so for $k_\lambda(v', v'')$ we can use the mean absorption coefficient for the given band; this quantity is determined by

$$\bar{k}_\lambda(v', v'') = \frac{1}{\Delta\nu}\int k_\lambda(\nu, v'')\, d\nu, \qquad (2)$$

where for $\Delta\nu$ we use the distance between the edges of the bands in which v'' is identical but v' changes by one unit.

Using the well-known expression for $\int k_\nu d\nu$ [5] and calculating for one O_2 molecule in the ground state, we get

$$I_\lambda = B_\lambda \cdot \frac{8\pi^3\nu^3 G'}{3\hbar\lambda}\left(1 - e^{-\frac{\omega''\hbar}{kT}}\right) R_e^2(\lambda) \sum_{v'} \frac{q(v', v'')}{\Delta\nu}\, e^{-\frac{E(v'')}{kT}}, \qquad (3)$$

where G' is the transition multiplicity, which is unity for $\Sigma \to \Sigma$ processes; $E(v'')$ is the energy of the lower vibrational state; $(1 - e^{-\omega''\hbar/kT})$ is the sum over the vibrational states calculated according to the harmonic oscillator approximation; $q(v', v'')$ is the Franck-Condon factor.

In expression (3) we take account of the fact that the electronic transition moment R_e may depend on the internuclear distance. We use the unique relation between the wavelength λ and the mean internuclear distance for the transition $v'' \to v'$ established in reference 6 (the so-called r-centroid).[7]

The Franck-Condon factors $q(v', v'')$ are calculated in reference 8 for $v' = 0, 1, 2, 3$ and $v'' = 0$ to 25; in addition, I. T. Yakubov has given us his calculations of $q(v', v'')$ for $v' = 4$ and 5. This is sufficient, since the sum on the right-hand side of (3) converges rapidly due to the presence of the exponential factor.

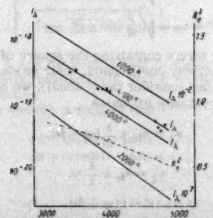

I_λ—radiation intensity at different temperatures for a single O_2 molecule in watts per steradian micron; R_e^2—square of the electron transition moment in atomic units. The experimental points are from the data of reference 1.

We have calculated the values of $R_e^2(\lambda)$ from (3), using the experimental values of I_λ (see the Figure). We find that $r_e^2(\lambda)$ decreases monotonically from 1 atomic unit at λ = 3000 A to 0.5 atomic unit at 5000 A. These values of $R_e^2(\lambda)$ correspond to an oscillator strength $f \approx 0.1$ to 0.2 which agrees well with the values of f measured by absorption and also with theoretical estimates,[5, 9] but not with the figures of reference 1.

Ditchburn and Heddle[10] have measured the oscillator strengths for individual bands of the Schuman-Runge system ($v'' = 0$, $v' = 0$ to 20). Nicholls,[11] using the appropriate Franck-Condon factors and the r-centroids, has obtained the variation of R_e^2 with internuclear distance in relative units [$R_e^2 \approx f_{v'v''}/q(v', v'')$].

The relationships for R_e^2 obtained by Nicholls and by us correspond to different internuclear distances and may supplement each other. However, we cannot make a comparison since the absolute values of R_e^2 obtained from the measurements of Ditchburn and Heddle for individual bands, and using the values of $q(v', v'')$ quoted by Nicholls, are improbably high ($R_e^2 \approx 50$ a.u., which corresponds to $f \approx 10$; an admissible value $f = 0.26$ was obtained in reference 10 because the ground state of the absorption was in a discontinuous spectrum, corresponding to photodissociation of O_2).

Using the values of R_e^2 that we have obtained, and the set of Franck-Condon factors, we can calculate from (3) the radiation intensity distribution in the Schumann-Runge system for the same wavelength interval 3000 to 5000 A at different temperatures. The Figure gives the curves. The slope of the curves varies little with temperature. Therefore the Schumann-Runge system can be used to estimate gas temperature only if absolute measurements are made.

The authors thank I. T. Yakubov who kindly made available the results of his calculations of the Franck-Condon factors.

REFERENCES

1. J. Keck, J. Camm, and B. Kivel. J. Chem. Phys. **28**, 723 (1958).
2. B. Kivel, H. Mayer, and H. Bethe. Ann. Phys. **2**, 57 (1957).
3. K. Watanbe, E. Inn, and M. Zelikoff, J. Chem. Phys. **20**, 1969 (1952).
4. R. Ditchburn and D. Heddle. Proc. Roy. Soc. **A220**, 61 (1953).
5. R. Mulliken and C. Rieke. Rep. Progr. Phys. **8**, 231 (1941).
6. P. Fraser. Canad. J. Phys. **32**, 515 (1954).
7. R. Nicholls and W. Jarmain. Proc. Phys. Soc. **A69**, 253 (1956).
8. W. Jarmain, P. Fraser, and R. Nicholls, Astr. J. **122**, 55 (1955); Astr. J. **119**, 286 (1954).
9. D. Ter-Haar. Proc. Roy. Soc. Edinb. **A63**, 381 (1952).
10. R. Ditchburn and D. Heddle. Proc. Roy. Soc. **A226**, 509 (1954).
11. R. Nicholls, Proc. Roy. Soc. **A69**, 713 (1956).

ON ECHELETTE THEORY

S. G. Rautian

Received 20 February 1959

One of the least developed topics of grating theory is the calculation of the energy distribution over the orders of the diffraction pattern. Two difficulties arise. Firstly, the grating period as a rule is of the order of a wavelength and so the distribution calculated by Kirchhoff's method may have a considerable error. Moreover, a rigorous solution can be obtained for normal incidence on a grating with rectangular grooves only.[1, 2] Extension of the method given in references 1 and 2 to echelettes of interest for spectroscopy is apparently impossible. For these Rowland's method must be used.[3-7]

The second difficulty arises from screening of the incident and diffracted wave by adjacent grooves; this difficulty arises even in the Kirchhoff theory. Neglect of this factor leads, in particular, to the absurd conclusion that the flux reflected from the grating is greater than the incident flux, for some angles of incidence.

In the present paper we consider one of the effects which results from taking account of this screening; we refer to double reflection within the groove. We will consider the following case as an example. Suppose the groove has a triangular profile and the angle between the groove walls is 90 deg (Fig. 1). We will designate the angle between the grating plane and the longer groove wall by δ. Suppose that a plane wave falls on the grating with the wave vector lying in the principal plane of the grating and making an angle ψ with the normal to the grating; we will restrict ourselves to the interval $-\pi/2 + \delta \leq \psi \leq \delta$.

From the point of view of geometrical optics we have

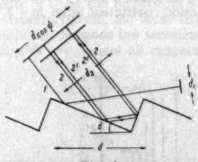

Fig. 1

the following situation. A section of the wavefront of width $d\cos\psi$ falls on a period d of the grating. Some rays reflected from one of the walls do not fall on the other (e.g., ray 1). Other rays are also reflected from the second wall and proceed in a direction opposite to that of the incident rays, since the angle between the groove walls is a right angle (rays 2 and 2'). The widths d_1 and d_2 of the fronts which undergo one and two reflections respectively can easily be calculated:

$$d_1 = d\cos(\psi - 2\delta) \text{ and } d_2 = 2d\sin\delta\sin(\delta - \psi)$$

$$\text{when } -\frac{\pi}{2} + 2\delta \leq \psi \leq \delta;$$

$$d_1 = -d\cos(\psi - 2\delta) \text{ and } d_2 = 2d\cos\delta\cos(\delta - \psi)$$

$$\text{when } -\frac{\pi}{2} + \delta \leq \psi \leq -\frac{\pi}{2} + 2\delta.$$

d_2 reaches its greatest value at $\psi = -\pi/2 + 2\delta$; in this case $d_1 = 0$ and $d_2 = d \sin 2\delta = d \cos\psi$, that is, all the rays undergo two reflections inside the groove.

The transition from geometrical optics to diffraction theory (using Kirchhoff's method), as is well-known, involves replacing a plane section of the wave front by an assembly of waves with amplitudes of the type a sin x/x, where a is the width of the initial "geometrical optics" part of the wave front, and x is a function of λ, a, and the angles. We will not write down the general expression for the diffracted wave and will only consider the intensity in the ψ direction, that is, the case of autocollimation. A simple calculation leads to the following formulas for the grating reflection coefficient* k_ψ:

*The function $k_\psi \cos\psi$ is an envelope of the magnitudes of the energy concentrated in the different orders. We have in mind the integrated flux of an order and not the "peak" value of the illumination at the principal maxima.

$$k_\psi = \frac{1}{d^2\cos^2\psi}\left[d_2 + d_1\frac{\sin x}{x}e^{ix}\right]^2,$$

where

$$x = \frac{2\pi}{\lambda} d\cos\psi\,\tan(\delta - \psi)$$

and $x = \frac{2\pi}{\lambda} d_1 \tan(\delta - \psi)$ when $-\frac{\pi}{2} + 2\delta \leqslant \psi \leqslant \delta$;

$$x = \frac{2\pi}{\lambda} d\cos\psi\,\cot(\delta - \psi)$$

and $x = \frac{2\pi}{\lambda} d_1 \cot(\delta - \psi)$ when $-\frac{\pi}{2} + \delta \leqslant \psi \leqslant -\frac{\pi}{2} + 2\delta$.

The quantity a is the phase difference between two waves; it must be borne in mind when considering their interference.

Figure 2 gives the reflection coefficients for various orders m, at wavelength λ = 5791 A with d = 1/300 mm and δ = 18 deg; the values were calculated from the above formulas. Using Rowland's theory we would have a considerable reflection coefficient when m = 3, 4, and −10.

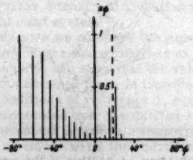

Fig. 2

Figure 2 shows that taking account of double reflection within the groove leads to a large number of intense orders with negative values of m. This conclusion of the theory is still valid qualitatively if the angle between the walls deviates from a right angle and if the walls are slightly deformed.

Figure 3a shows values of the reflection coefficient* that we measured for a GOI 600 groove/mm grating at λ = 5461 A (δ = 17 deg). Comparison with Fig. 2 shows a good qualitative agreement with the theoretical distribution. Similar results were obtained with this grating at other wavelengths and also with two GOI gratings with 300 and 200 grooves/mm. In addition, we reduced the data given in reference 8 for the energy distribution over the orders for a 300 groove/mm grating* and δ = 32.7 deg (λ = 5461 A). In this case also, as Fig. 3b shows, double reflection within the groove is important.

*In Fig. 3 the reflection coefficient is plotted in units of the maximum k_ψ with m > 0.

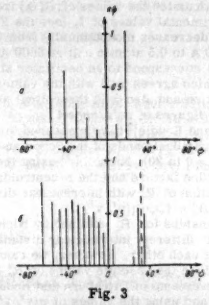

Fig. 3

*Unfortunately, the origin of the grating is not indicated in reference 8.

The groove walls deviate from plane at $d \gg \lambda$. This evidently explains why in the 200 groove/mm grating that we studied the reflection coefficients at λ = 5361 A did not exceed 20% (for negative values of m). However, for wavelengths $\lambda \sim d/3$, k_ψ reached 80% for this grating (as would be expected from the Rayleigh criterion).

Therefore we can attribute the large numbers of intense orders at m < 0,* observed by many spectroscopists, to double reflection within the grooves.

*In particular, a large concentration of energy in the high orders is recognized as the hallmark of certain GOI gratings.

It is very important that double reflection increases k_ψ at high diffraction angles. It is for this reason that it is possible to take advantage of the high angular dispersion of gratings at high values of ψ over a wide range of angles.

REFERENCES

1. L. N. Deriugin. Doklady Akad. Nauk SSSR 87, 913 (1952); Doklady Akad. Nauk 111, 1209 (1956).
2. L. N. Deriugin. Tr. MAI, No. 39, 26 (1954).
3. H. A. Rowland. Phil. Mag. 35, 397 (1893).
4. A. Sommerfeld. "Optics," 1955.
5. W. Friedl and B. Hartenstein, J. Opt. Soc. Am. 45, 398 (1955).
6. H. D. Hatcher and J. H. Rohrbaugh. J. Opt. Soc. Am. 46, 104 (1956); J. Opt. Soc. Am. 48, 704, 710 (1958).
7. S. G. Rautian. Opt. i Spektr. 2, 279 (1957).
8. T. A. Wiggins and G. D. Saksena. J. Opt. Soc. Am. 48, 429 (1958).
9. V. I. Malyshev and S. G. Rautian. Opt. i Spektr. 6, 550 (1959).

THE VERNIER EFFECT IN THE INTERFEROMETRIC MEASUREMENT OF THE THICKNESS OF THICK LAYERS

I. N. Shklyarevskii, E. T. Verkhovtseva, and G. N. Polyakova

Received 27 March 1959

In an earlier paper[1] one of us suggested a graphical method for calculating the thickness of thin films measured interferometrically. The case in which the layer being measured is of the order of several wavelengths was also considered there.

Suppose t_1 and t_2 are the thicknesses of the air gap between the interferometer plates and $t = t_1 - t_2 \approx k\lambda$ is the thickness of the film being measured (the step), where λ is the wavelength of the light and k is an integer. If the interferometer is placed in front of the slit of a spectrograph as previously described,[1] and illuminated by a parallel beam of white light, two systems of lines of equal chromatic order are formed at the focal plane of the camera lens. By varying the thicknesses t_1 and t_2 of the air gap, an mth-order line of one system can be brought into exact coincidence with an nth-order line of the second system of lines of equal chromatic order. The wavelength λ_0 of the coincident lines and their order of interference determine the layer thickness

$$t = \frac{m-n}{2}\lambda_0, \tag{1}$$

which in this case does not depend on the magnitude of phase changes.[1] The orders of interference of the coincident lines are determined by measuring the wavelengths of the (m + 1)th and (n + 1)th-order lines of the two systems.

As was noted in reference 1, a new coincidence of the lines of the two systems can be obtained after going through k lines of one system and (k + 1) lines of the other; that is, the so-called vernier effect is obtained. Tolansky[3, 4] started from this assumption in measuring the thicknesses of steps on a mica surface. He used simplified interference equations which did not take into account the phase changes occurring when light is reflected from metallized surfaces.

More detailed consideration of this point shows that an exact vernier effect would be possible only if the phase change were free from dispersion. Dispersion of the phase shift makes exact coincidence of later pairs of lines of the two systems impossible if one pair has been brought into coincidence.

For a pair of lines of the two systems to coincide, the following equations hold:

$$2t_1 - \frac{\delta_0\lambda_0}{\pi} = m\lambda_0$$

and

$$2t_2 - \frac{\delta_0\lambda_0}{\pi} = n\lambda_0, \tag{2}$$

where δ_0 is the phase change corresponding to wavelength λ_0. Equation (2) can be written as follows,

$$\frac{2t_1 - \frac{\delta_0\lambda_0}{\pi}}{m} = \frac{2t_2 - \frac{\delta_0\lambda_0}{\pi}}{n} = \lambda_0. \tag{3}$$

If there were no dispersion of the phase change, for a later pair of coincident lines this relation would hold:

$$\frac{2t_1 - \frac{\delta_k\lambda_k}{\pi}}{m+k+1} = \frac{2t_2 - \frac{\delta_k\lambda_k}{\pi}}{n+k} = \lambda_k. \tag{4}$$

It is not difficult to show that in the presence of phase change dispersion and the condition $\delta_k\lambda_k < \delta_0\lambda_0$, Eqs. (3) and (4) cannot be satisfied simultaneously for any ratio of the gap thicknesses t_1 and t_2. In fact, suppose

$$\frac{\delta_0\lambda_0}{\pi} - \frac{\delta_k\lambda_k}{\pi} = A, \tag{5}$$

then

$$\frac{2t_1 - \frac{\delta_0\lambda_0}{\pi} + A}{m+k+1} \neq \frac{2t_2 - \frac{\delta_0\lambda_0}{\pi} + A}{n+k}, \tag{6}$$

since

$$\frac{A}{m+k+1} < \frac{A}{n+k}. \tag{7}$$

Therefore, an exact vernier effect is impossible; or, if any pair of lines of the two systems coincide exactly, a later pair of lines cannot coincide exactly. It follows from (6) and (7) that the line with wavelength λ_k, corresponding to the gap of the greater thickness t_1, will be shifted towards the shortwave region relative to the line λ_k' which almost coincides with it and which corresponds to the gap of lesser thickness t_2. For coincident pairs of lines of lower orders (with wavelengths greater than λ_0) the shift in the lines will be opposite to this.

When no pair of lines can be brought into exact coincidence on the interferogram, the layer thickness can be calculated as follows. Suppose the wavelengths of lines that almost coincide are λ_0 and λ_0' respectively. Then

$$2t_1 - \frac{\delta_0\lambda_0}{\pi} = m\lambda_0$$

and

$$2t_2 - \frac{\delta_0'\lambda_0'}{\pi} = n\lambda_0'. \tag{8}$$

Since $\lambda_0' - \lambda$ is usually of the order of several Angstroms, neglecting the small difference

$$\frac{\delta_0'\lambda_0'}{\pi} - \frac{\delta_0\lambda_0}{\pi}, \tag{9}$$

we get from Eq. (8)

$$t = t_1 - t_2 = \frac{m\lambda_0}{2} - \frac{n\lambda_0'}{2}. \tag{10}$$

Neglecting the phase change difference (9) will give an error in the fifth place, which is quite negligible in measuring layers of several microns thickness.

We have measured the thicknesses of several thick layers of zinc sulfide. Since these layers are transparent in the visible region of the spectrum, the measurements were made in transmitted light. The Figure shows an interferogram of one of the specimens. The lines of equal

chromatic order in the upper part of the interferogram correspond to a lesser air gap between the interferometer plates, and the lines in the lower part correspond to a greater air gap. The vernier effect is clearly seen in the photograph—a rough coincidence of the lines occurs for every two lines of the upper system and for every three of the lower.

Wavelength λ (A)	Order of interference	Wavelength λ (A)	Order of interference	Layer thickness t (A)
5871.96	51	5874.48	68	49997.2
5550.9	54	5552.1	72	50001.3
5263.2	57	5263.16	76	49999.0
5003.86	60	5002.8	80	49996.2
				t_{mean} = 49998.45

The table gives the wavelengths of the almost coincident lines of the two systems, the corresponding orders of interference, and the values of the zinc sulfide film thickness calculated from Eq. (10). Averaging the results of these calculations, we obtain a mean value for the layer thickness of t_{mean} = 49,998.45 A. This differs insignificantly from the thickness t = 50,000.2 A calculated from Eq. (1) for λ = 5263.18 A (the corresponding lines of equal chromatic order almost coincide). We used the exact interference equations[3] to determine the orders of interference given in the Table for the lines of equal chromatic order.

Koehler[5] recently suggested a graphical method for calculating the thickness of thick films for the case where the vernier effect is not exact. We will only point out the unwieldiness of the method, leaving aside the question of the appropriateness of the Taylor series expansion of the phase change difference (taken with an incorrect sign, moreover[2]). The method requires measurements of the wavelengths of all the lines of equal chromatic order of both systems, the calculation of the corresponding wave numbers, and the construction of an auxiliary graph. In the method that we have suggested it is sufficient to measure the wavelengths of two or three pairs of almost coincident lines, and if any pair coincide exactly, it is sufficient to measure the wavelengths of three lines.

In conclusion, the authors thank K. D. Sinel'nikov for his interest in their work.

REFERENCES

1. I. N. Shklyarevskii. Opt. i Spektr. 5, 617 (1958)
2. I. N. Shklyarevskii. Zhur. Tekh. Fiz. 26, 333 (1956).
3. S. Tolansky. Usp. Fiz. Nauk 30, 103 (1946).
4. S. Tolansky, Phil. Mag. 36, 255 (1945).
5. W. F. Koehler. J. Opt. Soc. Am. 48, 55 (1958).

CANDOLUMINESCENCE AND SURFACE RECOMBINATION LUMINESCENCE OF PHOSPHORS IN THE ATMOSPHERE OF ACTIVATED GAS

A. N. Gorban' and V. A. Sokolov

Received 11 April 1959

In the preceding communication,[1] we presented experimental facts to show that candoluminescence of phosphors under the influence of flames is primarily due to the absorption by the phosphor of energy which is released due to the recombination on its surfaces of atoms and radicals of the flame.

In this connection, it was of interest to obtain the emission spectrum of the phosphor in an atmosphere of atoms and radicals of the particular gas, in the flame of which candoluminescence is observed. It was also desired to compare this luminescent spectrum of the luminor with its candoluminescence spectrum in the flame. We did this for the case of illuminating gas. To activate the gas, (i.e., to obtain atoms and radicals) we used a specially constructed gas discharge tube. This tube had a side-arm in the center, connected to the fore-vacuum pump. The side-arm had an enlarged section whose inner walls were coated with the phosphor being studied (Fig. 1). This excluded the possibility of the phosphor being excited by the ultraviolet radiation of the discharge. Furthermore, to absorb the light occurring during the discharge, the whole external surface of the discharge tube (with the exception of the enlargement in the side-arm) was covered with a black varnish.

The tube was evacuated and filled with illuminating gas. Then an electric discharge was excited in it (at a pressure of ≈ 0.1 mm Hg).

A noticeable part of the hydrogen atoms formed during the discharge (illuminating gas contains up to 40% of hydrogen) and of the radicals get into the side-arm while moving in the direction of the pump. This is due to their relatively long lifetime (τ ≈ 1 sec for hydrogen atoms). When the atoms and radicals recombine on the surface of the phosphor, they produce its luminescence,* which can be easily recorded with a spectrograph.

*It should be pointed out that the effect is observed only for relatively large dimensions of the discharge tube and of the electrodes, when the number of free atoms and radicals arising from the dissociation of the gas is sufficiently large.

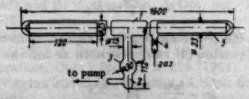

Fig. 1. 1—gas discharge tube; 2—side-arm; 3—enlargement (with the phosphor on its inner wall); 4—tube for filling the tube with gas; 5—aluminum electrodes. The dimensions are given in mm.

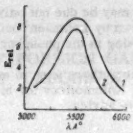

Fig. 2. Curve 1—luminescence spectrum of the Zns, CdS:Cu phosphor; curve 2—luminescence spectrum of the same phosphor in an activated gas atmosphere.

Figure 2 shows the spectrum thus obtained of the luminescence of the Zns, CdS:Cu phosphor (curve 2). It also shows the spectrum of luminescence of the same phosphor under the influence of a flame (curve 1). It is easily seen that these spectra are identical.

The following facts present additional arguments in favor of the surface recombination mechanism of candoluminescence: the existence of free atoms and radicals in the flame causing candoluminescence of the phosphor[1]; and the presence of phosphor luminescence (with identical spectral distribution) under the action of atoms and radicals of the same gas in the absence of a flame.

REFERENCE

1. A. N. Gorban' and V. A. Sokolov. Opt. i Spektr. 7, 556 (1959).

INFLUENCE OF CRUSHING ON THE OPTICAL AND ELECTRICAL PROPERTIES OF SOME ZnS ELECTROLUMINORS

E. V. Stauer and M. G. Rosenblat

Received 15 April 1959

It is known that crushing zinc sulfide phosphors brings about a decrease in the brightness of their luminescence under photoexcitation.[1] A study of the influence of crushing on the optical and electrical properties of the ZnS electroluminors is of both theoretical and practical importance.

We studied several electroluminors with the compositions ZnS:Cu, ZnS:Cu:Al, ZnS:Cu:Mn, and others. The properties of the basic powdered phosphor were compared with the properties of the same phosphor after it was milled for half an hour. The particle size was determined by means of an ocular micrometer. Their average size was decreased 2 to 3 times as the result of crushing.

The experiments were performed with an electroluminescent condenser filled with the phosphor mixed with a silicone oil. The thickness of the condenser was about 100μ.

Qualitatively similar changes in characteristics were observed for all phosphors when the particle size was made smaller. Crushing brought about a decrease in the intensity of both photoluminescence and electroluminescence of the phosphors. In our experiments the intensity of electroluminescence, B, as a function of the applied voltage, V, closely followed the law

$$B = B_0 \cdot e^{-\left(\frac{V_0}{V}\right)^{1/2}},$$

B_0 and V_0 being constants.

The values of B_0 and V_0 increase for the crushed phosphors as compared with the starting values. As the frequency of the applied field is increased, the intensity of luminescence increases faster for the crushed phosphors than for the unmodified variety. Thus, the higher the voltage and frequency of the applied electric field, the smaller the difference between the intensity of electroluminescence of crushed and uncrushed phosphors (Fig. 1). The same conclusions may be drawn from observations of brightness waves.

A shift of the spectrum of electroluminescence toward longer wavelengths is observed for certain phosphors after crushing. This shift is more pronounced at higher voltages. The temperature quenching of electroluminescence occurs at lower temperatures for the crushed than the unmodified phosphors (Fig. 2).

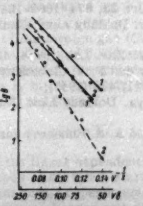

Fig. 1. The dependence of intensity of electroluminescence on voltage for the ZnS:Cu phosphor. Solid lines—original phosphor; dotted lines—crushed phosphor. Frequency: curve 1—10kc; curve 2—1 kc.

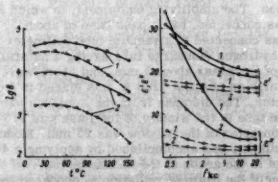

Fig. 2

Fig. 3

Fig. 2. The dependence of the intensity of electroluminescence of different phosphors on temperature. Curve 1—ZnS:Cu:Al; curve 2—ZnS:Cu.

Fig. 3. The dependence of the real and complex parts ε' and ε'' of the complex dielectric permittivity on the frequency f. Voltage: curve 1—100 volts; curve 2—50 volts.

Crushing of the electroluminors brings about a change in their electrical characteristics as well. The real and imaginary parts ε' and ε'' of the complex dielectric permittivity measured by means of the bridge proposed in reference 2 decrease for all frequencies and voltages. In phosphors showing a pronounced dependence of ε' and ε'' on applied frequency and voltage, this dependence becomes less pronounced (Fig. 3). When the temperature is changed, ε' and ε'' change less for the crushed than for the uncrushed phosphors.

In addition, crushing causes a marked decrease of both dark conductivity and photoconductivity of the phosphors. The ratio of photoconductivity to dark conductivity decreases somewhat with crushing.

All the changes in the properties of the electroluminors after crushing may be due not only to a change in particle size as shown by Lehmann[3] but also to the effect of deformations arising in the phosphor particles during milling.

In conclusion the authors wish to express their deep appreciation to F. I. Kolomoitsev for his interest in this work and his valuable advice.

REFERENCES

1. V. L. Levshin. Fotoliuminestsentsia zhidkikh i tverdykh veshchestv." (Photoluminescence of Liquid and Solid Substances), GITTL, 1951.
2. A. N. Ince and C. W. Oatley. Phil. Mag 46, 1081 (1955).
3. W. Lehmann. J. Electrochem. Soc. 105, 585 (1958).

OPTICO-ACOUSTIC EFFECT IN THE ULTRAVIOLET REGION OF THE SPECTRUM

Ya. I. Gerlovin

Received 18 April 1959

The optico-acoustic phenomenon, discovered by Bell, Tyndall, and Roentgen,[1] was made the basis of a method of gas analysis proposed in 1938, and of several subsequently developed procedures for determining certain molecular parameters of gases and vapors having absorption bands in the infrared.[2] Monatomic gases (and also nitrogen, oxygen, and hydrogen) do not absorb infrared radiation; the optico-acoustic phenomenon, therefore, does not occur in them. The effect may be expected, however, if these gases are irradiated by a discontinuous beam of ultraviolet radiation, which is strongly absorbed by them. The optico-acoustic phenomenon in the ultraviolet region should also occur in gases having infrared absorption bands. In fact, M. L. Veingerov and G. Ya. Turovskii are said to have observed the effect in a subjective manner in 1941, but further development of their work in this direction has not been forthcoming.

The author of this communication has observed the optico-acoustic effect in the ultraviolet region of the spectrum by means of an objective method—the use of an optico-acoustic detector—and has carried out an evaluation of the intensity of the effect in various gases.

The detector, provided with a resonance electrodynamic mierophone, was filled with the gas under investigation. The amplifying equipment, to which a microphone was connected, had a pass band of about 30 cps; its output was connected to a vacuum tube voltmeter. A half-kilowatt hydrogen discharge tube having a natural fluorite window, of thickness about 2 mm, and short-wave limit of transmission of about 1200 A, was placed in front of the detector. The distance from the luminous part of the discharge tube to the window of the flask was 110 mm, and the diameter of the window was 25 mm. Modulation of the radiation was accomplished by applying a 400 cps ac voltage to the anode of the discharge tube. (If the interruption of the beam of radiation is produced by use of a rotating disk, it is difficult to separate the ultraviolet radiation from the infrared emitted by the hot parts of the hydrogen lamp.)

The gases investigated were nitrogen, oxygen, and acetylene (the latter also absorbs in the infrared). When the flask was filled with nitrogen, the signal was 5 times the noise level, and with oxygen, it was 8 times the noise level; with acetylene it was 35 times the noise level. An increase in the optical speed of the apparatus should insure a considerable increase in the signal. The fact that the signal was caused by ultraviolet radiation, rather than infrared, was proven by the disappearance of the signal when the beam was interrupted by a thin plate of mica, which is transparent to infrared but opaque to ultraviolet radiation.

It may be concluded that the optico-acoustic effect in the ultraviolet region of the spectrum has application in the study of certain molecular parameters, and may also be used in the analysis of gas mixtures, the composition of which could not be previously determined by the optico-acoustic method.

REFERENCES

1. A. C. Bell. Phil. Mag. 2, 510 (1881);
W. C. Roentgen. Wied. Ann. 12, 155 (1881);
J. Tyndall. Nature 23, 374 (1880-1881)
2. M. L. Veingerov. Doklady Akad. Nauk SSSR 19, 687 (1938);
M. L. Veingerov. Zav. Lab. No. 4, 426 (1947);
M. L. Veingerov and P. V. Slobodskaya. Izv. Akad. Nauk, Ser. Fiz. 11, 420 (1947);
P. V. Slobodskaya. Doklady Akad. Nauk SSSR 120, 1238 (1958);
B. I. Stepanov and A. S. Rubanov. Inzh.-Fiz. Zhur. No. 4, 52 (1959).

EFFECT OF FOREIGN GASES ON THE ABSORPTION OF INFRARED RADIATION BY WATER VAPORS IN THE REGION OF AN INDIVIDUAL LINE IN BAND 2.7μ

K. P. Vasilevsky and B. S. Neporent

Received 23 April 1959

The investigation of the effect of foreign gases on the integral absorption was carried out by us for an individual line of water vapor at 4025 cm^{-1} (transition $v_2'' = 0$, $J'' = 5_{-5}$, $v_2' = 1$, $J' = 6_{-5}$). The dependence of the absorption in this line on the natural concentration of water vapor and on the length of path has been previously investigated by us,[1] and it was found that under the given experimental conditions the line absorption is accurately represented by the equations given by Laudenburg and Reiche[2] for lines of dispersion form; i.e., the integral absorption A is equal to

$$A = \int \left(1 - \frac{I}{I_0}\right) d\nu = 2\sqrt{S\gamma l} \qquad (1)$$

for $x = Sl/2\pi\gamma \gg 1$.

Here I_0 and I are the corresponding intensities of incident and transmitted light, $S = \int K_\nu d\nu = S^0 p_1$ is the integral intensity (strength) of the line, γ is its half width, p_1 is the vapor pressure of water, and S^0 is the strength of the line at $p_1 = 1$ atm. Assuming, in accordance with this, that the line has the dispersion form and maintains this upon the addition of the foreign gas, then it is possible to write, on introducing the relative effective optical collision diameter between molecules of water and of the foreign gas σ_{12},

$$\gamma = \gamma^0 (p_1 + \sigma_{12} p_2), \qquad (2)$$

where γ^0 is the width of the line when $p_1 = 1$ and the pressure of the foreign gas $p_2 = 0$.

We investigated the absorption of gas mixtures of H_2O and Ar, H_2O and N_2, and H_2O and CO_2 at water vapor pressure $p_1 = 0.00895$ atm (6.8 mm Hg std.) and at various total pressures of the mixtures up to 0.83 atm and at path lengths from 8.8 to 160.8 meters. The experiments were carried out with the help of a high resolution spectrometer and with multiple-passage cuvettes described in reference 2. The method of measurement is described in reference 1.

Figure 1 presents the results of measurements of integral absorption of the 4025.4 cm^{-1} line in the form of the dependence of A on $(p_1 l)^{1/2}$ for $p_1 = 0.00895$ atm and for pressures (p_2) of the foreign gas (CO_2) equal to 0, 0.057, 0.188, 0.386, 0.596, and 0.832 atm for curves 1–6, respectively. From the data presented it follows that the integral absorption A in the range from 0.07 to 0.9 cm^{-1} can be represented in the form

$$A = 2\sqrt{S^0 \gamma^0}\sqrt{p_1 l}. \qquad (3)$$

As a result of the linear dependence of γ on $(p_1 + \sigma_{12}p_2)$, the slopes of curves 1–6 are proportional to $(p_1 + \sigma_{12}p_2)^{1/2}$. An analogous dependency occurs with the use of the foreign gases nitrogen and argon. The curvature for A, 0.9 cm^{-1}, is a result of the overlapping of the line in question with its neighbors (see reference 1).

Let us use the previously-obtained data to obtain the quantities S^0 and γ^0. From curve 1 for $p_2 = 0$, it follows according to (1) that $S^0\gamma^0 = 0.0195$ $cm^{-2}atm^{-2}$ (at t = 20°C).*

*In reference 1 are presented several reduced values of the characteristic absorption of the line, since in treating the results no correction was made for the adsorption of water vapor by the walls of the cuvettes.

The foreign gases, by increasing the integral line absorption, permit the carrying out of measurements of absorption at low values of the parameter $x = Sl/2\pi\gamma$. In this case, according to reference 3,

$$A = 2\pi\gamma \cdot f(x) \simeq 2\pi\gamma \cdot x\left(1 - \frac{x}{2} + \frac{x^2}{4} - \ldots\right) \qquad (4)$$

and for $x < 1$

$$A \simeq 2\pi\gamma x = S^0 p_1 l \qquad (5)$$

and is independent of p_2. Accordingly, from Fig. 1 it can be seen that for a minimal path length l = 880 cm and large values of p_2 (0.386, 0.596, and 0.832 atm) the integral absorption remains almost constant and does not go below the value of 0.25 cm^{-1}. From Eq. (5) one can

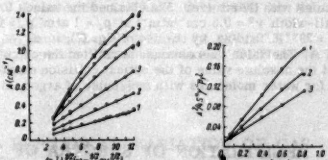

Fig. 1

Fig. 2

Fig. 1. Dependence of the integral absorption A of the water vapor line at 4025.4 cm^{-1} on $(p_1 l)^{1/2}$ at various pressures of foreign gas CO_2. Pressure of water vapor p_1 = 0.00895 atm; pressure of carbon dioxide: curve 1—0, curve 2—0.057, curve 3—0.188, curve 4—0.386, curve 5—0.596, curve 6—0.832 atm.

Fig. 2. Dependence of the quantity $A^2/4S^0\gamma^0 p_1 l$ for the 4025.4 cm^{-1} water vapor line on the pressure of foreign gas, p_2. Curve 1—CO_2, curve 2—N_2, curve 3—Ar

obtain an approximate value for S^0, and from the value of $S^0\gamma^0$ obtained above one can determine γ^0. Knowing the value of x, one can evaluate the magnitude of the correction terms in Eq. (4), and by the method of successive approximation one can obtain more precise values for the quantities S^0 and γ^0.

The values obtained by us for the 4025.4 cm^{-1} line of water vapor are $S^0 = 0.039$ $cm^{-2}atm^{-1}$, and $\gamma^0 = 0.5$ $cm^{-1}atm^{-1}$ (at t = 20°C).

Let us now consider the effectiveness of optical collisions. In the region of applicability of Eq. (1) we can

write, using Eq. (2),

$$A^2/4.5^2 p_1^0 p_1 l = p_1 + \alpha_{12} p_2. \qquad (6)$$

In Fig. 2 the data obtained by us are shown in a form corresponding to Eq. (6). The values of α_{12} used here are presented in the table below.

The effectiveness of optical collisions is obviously directly proportional to the pressure of the foreign gas, as is required for the broadening of the line in question to the given width, or for the attainment of the given value of A. If two different foreign gases x and y are introduced, starting from the known relationship for the half-width of a line[4]

$$\gamma_{ax} = \frac{N_x d_{ax}^2}{2c} \sqrt{v_a^2 + v_x^2} \quad (\text{cm}^{-1}), \qquad (7)$$

it is possible to obtain

$$\left(\frac{d_{ax}}{d_{ay}}\right)^2 = \frac{\gamma_{ax}}{\gamma_{ay}} \cdot \frac{(1 + m_a/m_y)^{1/2}}{(1 + m_a/m_x)^{1/2}}. \qquad (8)$$

Here d_{ax} and d_{ay} are the optical collision diameters for the absorbing molecules a with the foreign molecules x and y, m_a and m_x are the masses of the corresponding molecules, N_x is the density of the molecules of the foreign gas, v_a and v_x are the relative speeds of collision of the molecules, and c is the speed of light. An analogous method was used for the determination of relative optical collision diameters by Benesch and Elder.[5] The ratios of the optical collision diameters obtained by the use of Eq. (8) are presented in the table.

In the absence of foreign gases, the broadening of the line is determined by the collisions of the absorbing molecules with themselves. We obtained the values for the half-width $\gamma^0 = 0.5\ \text{cm}^{-1}\text{atm}^{-1}$ at $p_1 = 1$ atm, $p_2 = 0$, and $t = 293°K$, leading, by the use of Eq. (7), to $d_{H_2O-H_2O} = 12.7$ A. The value thus obtained permitted the calculation of the absolute value of the optical collision diameters for water molecules with molecules of argon, nitrogen, and carbon dioxide, as given in the table.

Optical Collision Diameters Between Molecules of "Water-X"

x	α_{H_2O-x}	$d_{H_2O-H_2O}/d_{H_2O-x}$	d_{H_2O-x} Å
H_2O	1	1	12.7
Ar	0.123	2.62	4.9
N_2	0.165	2.32	5.5
CO_2	0.239	1.88	6.8

Becker and Autler[6] investigated the absorption in water-oxygen mixtures in the centimeter spectral region. From their data on the dependence of the half-width of the 5_{-1}–6_{-3} line of water vapor on the partial pressure of oxygen, it is possible to obtain for $d_{H_2O-H_2O}$ the value of 5.6 A, and for $d_{H_2O-oxygen}$ the value 12.2 A, which is very close to our results for the line ($v_3'' = 0$, $J'' = 5_{-3}$, $v_3' = 1$, $J' = 6_{-3}$).

A more complete consideration of the experimental results concerning the effect of foreign gases on absorption, with reference to single lines and to groups of closely-spaced lines, will be presented by us in a forthcoming publication.

REFERENCES

1. K. P. Vasilevskii and B. S. Neporent. Opt. i Spektr. 4, 474 (1958).
2. B. S. Neporent, K. P. Vasilevskii, N. A. Lapina, and V. A. Fursenkov. Opt. i Spektr. 3, 289 (1957).
3. R. Ladenburg and F. Reiche. Ann. Phys. 42, 181 (1913).
4. V. Veiskopf. Usp. Fiz. Nauk 13, 552 (1933).
5. W. Benesch and T. Elder. Phys. Rev. 91, 308 (1953).
6. G. E. Becker and S. H. Autler. Phys. Rev. 70, 300 (1946).

REGISTRATION OF SPECTRA OF THE AURORA BOREALIS BY MEANS OF A RECORDING SPECTROMETER

I. G. Frishman

Received 25 April 1959

The successful application of photoelectric photometers[1–3] for measuring absolute values of intensities of the components in the spectra of the Aurora Borealis makes it possible to consider turning to photoelectric recording of their spectra.

The advantages thus obtained are obvious. The time necessary to record a spectrum, especially in the visible region, for which there exist photoelectric multipliers of high sensitivity, can be reduced to ten seconds. This permits us to investigate a number of problems related to the redistribution of energy in the spectra.

In comparison with spectrograms, the reduction of the photoelectrically recorded spectra entails much less work and time and gives higher accuracy, which is particularly important for mass measurements. With proper calibration, the spectrometer permits us to obtain intensity data directly in absolute units.

As far as we know, the only other attempt to record the spectra of the Aurora Borealis was made by Hunten,[4] and gave good results.

We built a simple spectrometer using a reflecting monochromator with a diffraction grating made in the experimental workshops of NIFI LGU. The optics of the monochromator consisted of a 70 × 80 mm, 600 lines/mm diffraction grating, used in the second order. The focal lengths of the mirrors of the collimator and the camera were 700 mm. The lengths of the entrance and exit slits were 16 mm. In the green region of the spectrum the monochromator had a dispersion of 11.4 A/mm. For slit-widths of 1 mm, the monochromator collected the radiation from 0.1 sq. deg of the sky.

An FEU-19-M photomultiplier, operated at 1300 volts, served as the radiation detector. The FEU was calibrated in absolute units; its sensitivity at 4278 A, for example, was 1.1×10^8 A/w. It could be cooled with solid carbon dioxide, but during the operation it became clear that the recording of spectra could also be accomplished without cooling. The spectra recordings shown below were obtained without cooling. In order to obtain the final results in absolute units we investigated the transmission of the optics of the monochromator as a whole for the total range of the registered spectrum. The maximal

transmission of the optics of the monochromator, corresponding to maximum concentration of the light by the grating for 5076 A, was 46%.

The current furnished by the FEU was amplified by means of a 238 cps resonant amplifier, this being the frequency of the chopper located in front of the entrance slit. The current amplification factor of the amplifier was 1.3×10^7. The recording of the amplified photocurrents was made by means of a POB-L oscillograph. The spectrum was scanned at 21.5 A/sec by means of a reversible motor and reducing gear (thus the spectrum of the Aurora Borealis in the region 3914-5577 A was recorded within 77 sec). The level of the signals at the output of the amplifier for the strong emissions turned out to be so high that the scanning speed could be increased at least five-fold. Since we had to check the possibility of recording weak emission spectra (in particular to attempt to record the line Hβ of hydrogen, which requires at least an hour using a spectrograph with photographic registration) we did not increase the scanning speed to its maximum.

Figure 1 represents a recording of the 5577-3914 A region of the spectrum of a diffuse emission scarcely visible to the eye. The absolute intensities of the emissions indicated on the photograph are 5577 A—13,

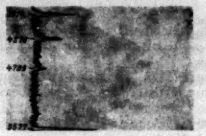

Fig. 1

4709 A—0.5, 4278 A—4, and 3914 A—17×10^{-4} erg/sec cm² sterad. Figure 2 shows a recording of the 3914—4708 A section of the spectrum of a diffuse arc of the Aurora Borealis situated in the southern part of the sky. One can see a weak peak at the position of the Hβ line in the spectrum. A similar peak was observed on later recordings of the spectrum of this arc, which confirms the registration of the Hβ emission line in the present case. The absolute intensity of the Hβ line in this case is equal to 8×10^{-5}, and that of the 4709 A band—5.7×10^{-4} erg/sec cm² sterad.

Fig. 2

Thus, the spectrometer permits us to record strong emission spectra much faster than the usual spectrographs. In order to be able to obtain reliable recordings of weak components of the spectrum, it is necessary to increase the surface of the grating used, and to make the slits as long as possible, because the light flux is proportional to the surface of the grating and the length of the slit at the exit of the monochromator, other conditions being equal.[5]

REFERENCES

1. S. F. Rodionov and L. M. Fishkova. Doklady Akad. Nauk SSSR 70, 1001 (1949).
2. I. G. Frishman. Opt. i Spektr 6, 323 (1959).
3. N. V. Dzhordzhio. Isv. Akad. Nauk SSSR, Ser. Geofiz. 692 (1957).
4. D. M. Hunten. Canad. J. Phys. 31, 681 (1953).
5. A. S. Toporets. "Monochromators," GTTI, Moscow, 1955.

SELECTIVE MODULATION OF RADIATION BY PERIODICAL VARIATION OF GAS TEMPERATURE

A. O. Sall'

Received 24 January 1959

For various research and control-measurement purposes, one may use a radiation source based on emission from a heated gas which radiates over a characteristic spectral interval. However, the window and walls of the chamber in which the gas is enclosed emit radiation in other spectral regions, which reduces the selectivity of such a source. In order to decrease the influence of

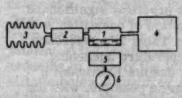

Fig. 1

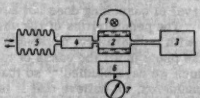

Fig. 2

radiation from the windows and walls of the chamber, the gas temperature may be varied periodically (e.g., by alternate compression and expansion of the gas), without essentially changing the window and wall temperatures of the chamber. If only the modulated flux is utilized, the influence of nonselective radiation from the window and walls of the chamber will be reduced considerably. This has been confirmed experimentally by using carbon dioxide subjected to periodic compression. The gas was contained in a chamber provided with a window which was transparent to the radiation. The interior surface of the chamber was chrome-plated and polished. The emission of the gas arising from its compression was registered by an optical-acoustic selective radiation detector.

Another method of modulation was also studied, consisting of periodic variation of the temperature of the emitting gas by filling the chamber alternately with heated and cooled gas. This is shown in Fig. 1, and is accomplished in the following way. The interior cavity of the emission chamber 1 is connected to a container 4 filled with gas, to a heater 2 used to heat the gas, and to a sylphon 3, the volume of which is periodically increased and decreased. The periodic variation of the gas sylphon volume is brought about by the operation of an electric motor. When the volume of the gas increases, the gas

from container 4 is drawn through chamber 1 and heater 2 to the sylphon. When the sylphon compresses, heated gas is expelled into chamber 4. Number 5 is the radiation detector, and 6 the recorder.

A selectively gas-modulated radiation flux may also be realized in the following way (see Fig. 2): the radiation flux from an incandescent nichrome helix 1 is passed through chamber 2. The chamber is connected to a container 3, filled with gas, and through heater 4 to sylphon 5. When the volume of the sylphon is varied periodically, heated and cooled gas (carbon dioxide) is alternately admitted to the chamber. The density of the radiation-absorbing gas filling the chamber varies periodically. As a result, the radiation flux passing through the chamber is modulated at a frequency equal to the frequency of gas exchange in the chamber. The modulated flux is recorded by a selective optical-acoustic detector 6, whose radiation-receiving chamber is filled with carbon dioxide, and is connected to a recorder 7.

The systems of Figs. 1 and 2 may be used to make a single-flux absorption gas analyzer. The emission chamber in this case is connected to the mains through which the gaseous mixture to be analyzed flows continuously. When the volume of the sylphon is varied periodically, the temperature of the gas mixture in the chamber varies, giving rise to a signal in the radiation detector. The magnitude of this signal indicates the concentration of the desired component in the mixture.

LETTERS TO THE EDITOR

ON THE ARTICLE BY M. G. KAMINSKII "CONTRIBUTION TO THE 'BALLISTIC' METHOD OF INVESTIGATION OF THE DECAY OF PHOSPHORESCENCE"

B. A. Pyatnitskii

Received 5 February 1959

The ballistic deflection, i.e., the maximum deflection of the armature of a galvanometer, and its subsequent return to zero depends on the duration and form of the current pulse.[3] One should distinguish between (1) a ballistic deflection from a short current pulse which ceases as the armature starts to move, but imparts an initial velocity, and (2) a ballistic deflection from a prolonged pulse, which continues through a part of the movement of the galvanometer armature.[3]

The ballistic deflection from a short current pulse is directly proportional to the quantity of electricity which has flowed through the winding. The ballistic deflection from a prolonged pulse of current is not proportional to the quantity of electricity which has flowed through the winding, but, with current decay curves of the form

$$I = I_0 f(t)$$

is directly proportional to the initial current strength I_0 and is expressed by the formula

$$A = \frac{qI_0}{K(\mu - \nu)} \left[e^{\mu t} \int_0^t f(t) e^{-\mu t} dt - e^{\nu t} \int_0^t f(t) e^{-\nu t} dt \right], \qquad (1)$$

where μ and ν are roots of the characteristic quadratic equation (known from the theory of the galvanometer), K is the moment of inertia, and q is the dynamic constant of the galvanometer.

The time t in formula (1) is counted from the moment of closure of the photoelement switch, so that I_0 is the initial photocurrent, proportional at t = 0 to the intensity of illumination at a given moment, i.e., at the end of that second of decay.

Formula (1) was obtained on the basis of a more general formula from a work of Diesselhorst[2]; it is the theoretical foundation of my method.

In all my work,[5-10] and also in the work of my colleagues,[11-13] it is not the light-sum L that is measured, but the intensity of illumination I, at the end of each second of decay. The light-sum, used in some of my papers[5,9] is not measured, but calculated according to well-known formulas. It follows from this that the photocurrent durations calculated by Kaminskii have no relation to my method in which ballistic deflection is proportional, not to the light-sum, but to the intensity of illumination at a given second of decay.

Thus formula (1) in Kaminskii's article corresponds essentially to my formula (1) which is a more general one. It embraces not only simple exponential decay, but also complex decays such as that described by Vavilov's law[14] and hyperbolic decay.

Furthermore, by analyzing his formula (1), Kaminskii obtains Table 1, from which he draws unfounded conclusions. We will contrast Kaminskii's data for the galvanometer at $T_0 = 12$, with his own table.

Influence of Temperature on Phosphorescence of Benzoic Acid[7]

	Temperature (°C)												
	−183	−172	−162	−143	−134	−121	−109	−91	−67	−57	−40	−23	−16	−7.5
I_0	363	234	151	110	100	91	85	85	68	85	54	44	22	15
α	0.47	0.50	0.48	0.49	0.47	0.48	0.48	0.54	0.57	0.61	0.65	0.75	0.83	0.93
τ_m	4.5	4.5	4.5	4.5	4.5	4.5	4.5	4.5	4.5	4.0	4.0	3.7	3.5	3.0
γ/γ_1	0.28	0.28	0.28	0.28	0.28	0.28	0.28	0.28	0.28	0.24	0.23	0.21	0.19	0.18

Note: Values of τ_m and γ/γ_1 are given also in reference 7.

It is clear from our table that over a considerable temperature range α is constant with temperature, while the initial value of intensity I_0 quickly begins to change with temperature. Thus, the temperature dependence of I_0 is shown at constant α, and thus also at constant γ. The small change of γ at the end of the temperature interval of quenching does not have practical significance.

The peculiarities of the variation of quantities α and I_0 with temperature, presented in Table 1 in reference 7, take place in all the cases of temperature quenching which we have studied[7-9] so that, despite Kaminskii's conclusion, we believe that it is quite possible, with the help of our method, to establish the dependence of the initial value of intensity upon temperature. Reference to my works[4, 10] was entirely inappropriate, since there is nothing in them about decay according to a sum-of-two-exponents law. It is shown in reference 4 that the decay of the phosphorescence of paraffin at the temperature of liquid air takes place according to the complex expo-

nential law of Vavilov,[14] which has a structure of the form $I = I_0 f(t)$, and the possibility of the appearance of decay according to such a law confirms my formula (1).

Finally, it should be noted that the basic formula (1) in Kaminskii's article confirms my method, but the conclusions drawn from formulas (1) and (2) are founded upon hypothetical, artificially chosen values, and not on my experimental data.

REFERENCES

1. M. G. Kaminskii. Opt. i Spektr. 6, 103 (1959).
2. N. Diesselhorst. Ann. Phys. 9, 712 (1902).
3. B. A. Pyatnitskii. Zhur. Eksp. i Teoret. Fiz. 9, 310 (1939).
4. B. A. Pyatnitskii. Zhur. Eksp. i Teoret. Fiz. 9, 1351 (1939).
5. B. A. Pyatnitskii. Doklady Akad. Nauk USSR 57, 711 (1947).
6. B. A. Pyatnitskii. Doklady Akad. Nauk USSR 64, 813 (1949).
7. B. A. Pyatnitskii. Doklady Akad. Nauk USSR 62, 59 (1948).
8. B. A. Pyatnitskii. Doklady Akad. Nauk USSR 68, 281 (1949).
9. B. A. Pyatnitskii. Izv. Akad. Nauk SSSR, Ser. Fiz. 15, 597 (1951).
10. B. A. Pyatnitskii and M. S. Fadeeva. Izv. Akad. Nauk SSSR, Ser. Fiz. 20, 520 (1956).
11. A. P. Vishnevskii. Doklady Akad. Nauk SSSR, 63, 503 (1948).
12. P. A. Teplyakov. Opt. i Spektr. 1, 896 (1956).
13. O. G. Zinov'eva. Doklady Akad. Nauk SSSR, 68, 265 (1949).
14. S. J. Vavilov. Soviet Phys. 5, 369 (1934).

ON THE ARTICLE ON L. A. BOROVINSKY

N. V. Kudryavtseva and A. F. Terpugova

Received 18 February 1959

In his article[1] Borovinsky questions the logical consistency of the method of the so called "metal model."

Using as an example a molecule having as a model a ring of radius R with a side piece of length l and a constant potential along its entire contour, Borovinsky shows that the solution*

*The same notation is used as that in Borovinsky's paper.

$$\cot \alpha\pi = 2 \tan \alpha \frac{l}{R} \qquad (1)$$

does not lead in the two special cases, $l \to 0$ and $R \to 0$ (or, equivalently, $l \to \infty$), to the solutions obtained for the free ring without a side piece or to the case of a potential well with two infinite walls, respectively. The absence of the indicated asymptotic transitions he considers as paradoxes which prove the inconsistency of the "metal model" method. In particular, Borovinsky states his doubt in the suitability of using the continuity conditions

$$\psi(x_{1p}) = \psi(x_{2p}) = \ldots, \qquad (2)$$

$$\left[\sum \frac{d\psi(x_i)}{dx_i}\right]_p = 0. \qquad (3)$$

for the wave functions at the branch points.

In Eqs. (2) and (3) and index i denotes the branch number and the index p, the branch point.

Without discussing the question of expediency of replacing the continuity conditions (2) and (3) by others, it will be shown that the cases of a free ring (with a constant potential) and that of a potential well are not special cases of a "ring with a side piece." The solution for these cases can therefore not be obtained mathematically from the solution for the "ring with a side piece" independent of the conditions for the joining functions. Indeed, reducing to infinity the length of the side piece with an infinite potential barrier at the end (i.e., $\psi = 0$ at the end of the piece), the model does not pass over to a free ring with a constant potential but into a ring with a node, since the infinite potential barrier is transferred from the end wall of the side piece to the point of the ring where the side piece is attached. It is clear that the solution for a ring with a node does not coincide with the solution for a free ring without any singular points. As can be readily shown, for a ring with a node we have

$$\cos \alpha\pi = 0.$$

The roots of the above equation are given by

$$\alpha = n + \frac{1}{2} \qquad (n = 0, 1, 2, \ldots),$$

which agrees with the solution found by Borovinsky for the "ring with a side piece" if we let l approach 0 in the limit.

The solution for the free ring can be obtained as a limiting case only if, at the end of the side piece, the condition $\nabla\psi = 0$ which agrees with Eq. (3) is imposed, instead of the condition $\psi = 0$.

In a similar way will the decrease to zero in the diameter of the ring (or, equivalently, the unlimited increase in the length of the side piece) lead to a potential well with only one infinite wall (and not two!), since from the side of the ring the condition $\nabla\psi = 0$ must be fulfilled, instead of the condition $\psi = 0$. The solution for this model is found to be

$$\cos \alpha \frac{l}{R} = 0,$$

which leads to

$$\alpha = \frac{R}{l} \pi \left(n + \frac{1}{2}\right)$$

where n = 0, 1, 2, 3..., and the asymptotic transition again takes place.

There are therefore no paradoxes in the results found by Borovinsky and consequently there are no inconsistencies in the method of the "metal model" of a molecule.

However, in order to reflect the reality correctly it is necessary to approach very carefully the very process of determining the proper model--the problem of boundary conditions, the shape of the potential distributions, etc. It is clear that the choice of the model cannot be determined entirely on the basis of theoretical considerations but must be supported by further experiments.

REFERENCE

1. L. A. Borovinsky. Opt. i Spektr. 4, 526 (1958).

REPLY TO N. V. KUDRYAVTSEVA AND A. F. TERPUGOVA

L. A. Borovinsky

Received 26 May 1959

Kudryavtseva and Terpugova state that there is a correct asymptotic transition as one passes to the limit $l \to 0$ for the model of the "ring with a side piece." To prove their point the authors introduce the model of the "ring with a node" as the asymptotic model for the "ring with a side piece" as $l = 0$. Thus, the model is so selected beforehand that as $l \to 0$ the correct asymptotic transition takes place. It is obvious that with this special choice of the model the desired result can be obtained.

The example we considered was intended to show that in the one-dimensional branched model the state of the electrons does not change continuously as the contour of the model is changed. Introducing the model of a "ring with a node" does not remove this inconsistency. Indeed, let us assume that an infinitely short side piece is attached at an arbitrary point along the contour of the model. This results in a "node" at the point of attachment of the side piece and in an abrupt change in the state of the electrons. Thus, the appearance of the node during the attachment of the side piece violates the requirement of continuity in the change of the states of the electrons. Consequently, the model with nodes not only does not remove the inconsistency of the metal model but, on the contrary, it gives an additional example of inconsistency.

In our article[2] it was pointed out that, if we decrease to zero the diameter of the ring (or increase the length of the side piece infinitely) the "ring with a side piece" must, in the limit, pass over to a model of a potential well with two infinite walls. Kudryavtseva and Terpugova object to this. It must be admitted that the stated requirement should have been substantiated. One can prove this by passing to the limit, i.e., by decreasing the ring diameter (or by increasing infinitely the length of the side piece) in a two-dimensional model of a corresponding configuration. However, it should be pointed out that the simple metal model without branches is used very successfully in computations of polyene chains containing ring systems at their ends, as for example, radicals of the form

It is in molecules of this form that the greatest alignment of C-C bonds takes place and consequently the greatest freedom of transfer of π-electrons along the linked chain. The application of the nonbranched metal model to chains of linked bonds with rings at their ends is based on the assumption that the presence of a ring at the end of a chain is, for sufficiently long chains, equivalent to an infinitely large potential barrier. Thus, the conditions we put forward are implicitly contained in a large number of articles devoted to computations of the spectra and other properties of molecules on the basis of the simple metal model. This, of course, does not deny the necessity to justify these conditions theoretically.

Even if we assume that when $R \to 0$ (or $l \to \infty$) the ring with a side piece passes over into a potential well with two infinite walls, an inconsistency is still found in the asymptotic transition of a branched metal model. This is pointed out in another paper.[3] In this and another article[3,4] we state, more specifically, our opinion on the conditions for joining the wave functions in a branched metal model and methods are indicated how to overcome the deficiencies of this model.

The letter of Kudryavtseva and Terpugova does not discuss all the paradoxes of the branched metal model. Therefore, even if we agree with their viewpoint on the questions they raised, their generalizing conclusion about the absence of inconsistencies in the method of the metal model is surprising.

REFERENCES

1. N. V. Kudryavtseva and A. F. Terpugova. Opt. i Spektr. 7, 451 (1959).
2. L. A. Borovinsky. Opt. i Spektr. 4, 526 (1958).
3. L. A. Borovinsky. Opt. i Spektr. 6, 267 (1959).
4. L. A. Borovinsky. Izv. Akad. Nauk SSSR 22, 1019 (1958).

OPTIKA I SPEKTROSKOPIYA

Volumes I through V

Some of the papers in the 1956 through 1958 volumes of "Optika i Spektroskopiya" have been translated. These are listed below, and information as to their availability can be obtained from the Office of Technical Services, U.S. Department of Commerce, Washington 25, D.C. or from the OSA Executive Office:

VOLUME I (1956)

Landsberg, G. S., Shatenshyteyn, A. I. and others.
Vibration Spectra of Diphenyl and Decadeutero-Diphenyl

Agranovich, B. M.
Theory of the Intrinsic Optical Activity of Molecular Crystals I. Classical Theory

Faydysh, A. N., Kucherov, I. Ya., and Terskiy, A. A.
Disturbances in the Transfer of Excitation Energy in Solid Solution of Naphthacene in Anthracene

Fedrov, F. I.
Optics of Magnetic Crystals. I. Equations of the Normals. II. Binormals and Biradials. Optical Surfaces. III. Uniaxial and Unirefractive Magnetic Crystals

Raskin, Sh. Sh.
On the Raman Spectra of Complex Compounds of Antimony Trichloride with Benzene and Some of its Deritives

Agranovich, V. M. and Faidysh, A. N.
Migration and Transmission of Electron Excitation Energy from the Base Material to the Impurity in Molecular Crystals in the Presence of Two Types of Excitons

VOLUME II (1957)

Rashba, E. I.
Theory of Strong Interactions of Electron Excitations with Lattice Vibrations in Molecular Crystals

Lushchik, Ch. B.
New Methods of Investigation of Relaxation Processes and Trapping Centers in Crystal Phosphors

Vasil'kovskiy, A. A.
Calculation of a Thin Multilayer Plate as a One-Layer Plate with an Effective Refraction Index

Kard, P. G.
The Analytical Theory of Optical Properties of Multi-Layer Dielectric Coatings

Kizel, V. A. and Stepanov, A. F.
Reflection of Light from a Liquid Surface and its Connection with the Process of Crystallization

Rozman, I. M.
Dependence of the Luminescence Yield of Plastic Scintillators with Tri-Phenylpyrazoline on Temperature

Andreyeshchev, E. A. and Rozman, I. M.
Luminescence Spectra of Plastic Scintillators with Triphenylpyrazoline

Gromov, V. A.
New Method of Exciting Spectra in an Atomic Beam

Leontovich, A. M.
Absorption Spectra of Crystals of Plutonium Salts

Agranovich, V. M.
Theory of the Intrinsic Optical Activity of Molecular Crystals, 2 Quantum Theory

Bakhshiyev, N. G.
A New Principle of Spectrometry

VOLUME III (1957)

Deigen, M. F. and Shul'man, L. A.
On the Theory of Electron Spin Resonance in F-Centers in Ionic Crystals (Continuum Model of F-Center -- "Smoothed Function")

Chayka, M. P.
Luminosite d'un Spectrometre a Interferometre Fabry-Perot

Ostrovskiy, Yu. I. and Penkin, N. P.
Relative f-Values of the Spectral Lines of Scandium

Shatalov, A. A.
Photochemical Conversion of Color Centers in Heated Alkali-Halide Crystals

VOLUME IV (1958)

Shirokshina, Z. V. and Suykovskaya, N. V.
Preparation of Infrared Transmitting Films

Batarchukova, N. R.
Comparative Investigations of the Metrological Qualities of the Spectral Lines of $^{206}_{Pb}$ and $^{114}_{Cd}$

Sevchenko, N. A. and Florinskaya, V. A.
Infrared Spectral Transmittance of Porous and Quartzoid Glasses

Galanin, M. D. and Chizhikova, Z. A.
On the Quenching of Luminescence of Organic Substances upon Excitation by a- Particles

Krylova, T. N.
Multilayer Dielectric Coatings with a High Coefficient of Reflectance on Glass Surfaces

Ivanov, A. P.
Theoretical Investigations of the Behavior of Luminescent Radiation of Dispersed Luminescent Particles

Gurevich, I. M.
Rayonnement d'un Tube d'Impulsion Puissant au Moment de l'Explosion

Sevchenko, N. A. and Florinskaya, V. A.
Reflection Spectra of Quartz Crystal Plates Cut at Different Angles to the Optical Axis within the 7-24 μ Wavelength Range

Tagirov, R. B.
A Method of Measuring the Reflection Coefficient of Mirrors

Tolstoy, N. A.
Possibility of Using Pulse Lamps for Studying the Relaxations of Luminescence and Photoconductivity

Royev, L. M., Filimonov, V. N. and Terenin, A. N.
Changes in the Infrared Spectra of Molecules Interacting with the Adsorption Centers of a Silica-Alumina Catalyst

Yeremenko, V. A.
Luminescence of Cadmium Sulfide Crystals

VOLUME IV (1958) – cont'd

Slyusarev, G. G. and Kulikovskaya, N. I.
Distribution of Light Energy Changed in the Diffraction Pattern by Variable Transmittance Filters

Toporets, A. S.
Absorption and Scattering of Light in Pigments

Lyzina, L. A.
Method of Precipitation of Solid Dye Layers from Solutions; Corrections Due to the Reflectance Made in Absorption Measurements of these Layers

Barchukov, A. I., Murina, T. M., and Prokhorov, A. M.
Microwave Spectrum and Rotational Constants of the C_2H_5Cl Molecule

Nikitin, V. A.
Relationship Between the Scanning Speed and the Resolving Power of a Spectral Instrument

Barchukov, A. I. and Basov, N. G.
Measurement of Frequencies and Intensities of Hyperfine Structure Lines of CH_3I ($J=0 \rightarrow 1$ Transition)

Irisova, N. A.
Radiospectroscopic Investigation of CH_3GeCl_3

Lubchenko, A. F. and Bashba, E. I.
On the Excitonic States of a Molecular Crystal Containing Different Molecules

Agranovich, V. M.
On the Capture of "Free" Excitons by Impurities in Molecular Crystals

Faydysh, A. N.
Experimental Proof of the Theory of the Transfer of Excitons by Diffusion

Kats, M. and Semenov, B. Z.
The absorption and Luminescence Spectra of Nickel-Activated Alkali Halide Crystals

Parfyanovich, I. A.
Interaction Between Electrons and the Activator in NaCl-Ni and NaCl-Cu Phosphors

Tarasova, L. I. and Feofilov, P. P.
Polarization of Luminescence and the Nature of Luminescent Centers in NaCl-Ag and KCl-Tl Crystals

Galanin, M. D.
On the Causes for the Dependence of the Luminescence Yield of Organic Substances on the Energy of the Ionizing Particles

Gerasimov, F. M., Tel'tevskiy, I. A. and others
Diffraction Gratings from the State Optical Institute

Basov, N. G. and Osipov, B. D.
Lines of Emission for the F=5/2-3/2, J=1, K=1 Transition of the Rotational Spectrum of the CH_3I^{127} Molecule

Barchukov, A. I. and Prokhorov, A. M.
Microwave Spectrum of the CH_3GeH_3 Molecule

Protas, I. R.
Plates for Vacuum Ultraviolet Photography

VOLUME V (1958)

Titushina, V. P. and Fabrikant, V. A.
Etude de la Divergence du Flux de Rayonnement de la Raie 2537 a d'une Decharge Dans le Mercure

Voyevodskiy, V. V., Molin Yu. N., and Chibrikin, B. M.
Spectra of Electron Paramagnetic Resonance of Cr-Aromatic Compounds with Various Substitutes

Sinel'nikov, K. D. and Ryazanov, A. N.
Resolving Power of Optical Systems Increased

Distler, G. I.
Infrared Polarisation Filters

Kovarskiy, V. A.
Theory of Non-Radiative Transitions in an F-Center

Belyanin, V. B.
Multiplet Splitting of the Ground Term of the Holmium Atom

Barchukov, A. I., Prokhorov, A. M.
Quadrupole Coupling Dipole Moment and Barrier of Internal Rotation of the CH_3GeH_3 Molecule as Determined from its Rotational Spectrum

Moroz, L. P.
Imaging of Separate Objects by an Aberrationless Optical System in a Field which is more or less Luminant than the Objects themselves

EDITOR'S NOTE

Comments on the scientific content of the translated Russian articles published in OPTICS AND SPECTROSCOPY are invited. They should be addressed as a Letter to the Editor of the Journal of the Optical Society of America and forwarded to the Editor of that journal, Dr. W. R. Brode, National Bureau of Standards, Washington 25, D.C.

TRANSLITERATION OF CYRILLIC CHARACTERS

used by the Optical Society of America

А	а	a	Р	р	r
Б	б	b	С	с	s
В	в	v	Т	т	t
Г	г	g	У	у	u
Д	д	d	Ф	ф	f
Е	е	e	Х	х	kh
Ж	ж	zh	Ц	ц	ts
З	з	z	Ч	ч	ch
И	и	i	Ш	ш	sh
Й	й	i	Щ	щ	shch
К	к	k	Ъ	ъ	″
Л	л	l	Ы	ы	y
М	м	m	Ь	ь	′
Н	н	n	Э	э	e
О	о	o	Ю	ю	yu
П	п	p	Я	я	ya

VOL. VII, NO. 4 OPTICS AND SPECTROSCOPY OCTOBER 1959

CONTENTS

The Classification of Secondary Radiation 285
B. I. Stepanov and P. A. Apanasevich
The Pressure Dependence of the Intensity of Certain Helium Lines 290
V. E. Yakhontova and M. I. Kliot-Dashinskii
Vibrational Spectrum and Structure of the Arsenic Trioxide Molecule 293
V. P. Cheremisinov
Calculation and Interpretation of Vibrational Spectra of Naphthenes. II. Methylcyclopropane and 1,1-Dimethylcyclopropane 296
L. M. Sverdlov and E. P. Krainov
Rotational Structure of the (1-1) and (0-1) Bands in the Spectrum of the Carbon Monochloride Molecule 300
Yu. Ya. Kuzyakov and V. M. Tatevsky
Study of the Temperature Dependence of the Intensity of Infrared Absorption Bands in Solutions 302
V. N. Smirnov
On the Temperature Dependence of the Intensities of Vibrational Absorption Bands of Gases in the Case of Fermi Resonance 305
M. P. Lisitsa and V. L. Strizhevskii
Optical Investigation of the Molecular Structure of s-Triazine Derivatives 307
E. N. Boitsov and A. I. Finkel' shtein
Intensities and Depolarization in Raman Spectra of Polymethylbenzenes. I. The General Theory. Toluene 309
M. A. Kovner and B. N. Snegirev
Absorption Spectra of Crystals of Some Thiazine and Oxazine Dyes 314
N. M. Melankholin
Vitrification of Polymers and Luminescence 318
E. V. Anufrieva, M. V. Volkenstein, and T. V. Razgovorova
A Study of the Intrinsic Absorption Spectrum of Zinc Sulfide 320
N. A. Vlasenko
The Influence of an Activator on the Stability of F Centers 324
I. A. Parfianovich and E. I. Shuraleva
Initial Stages of Luminescence Buildup in Phosphors with Levels of Several Kinds. 327
V. V. Antonov-Romanovskii
Investigation of the Thermal Activation Energy of Photostimulated Flashes in ZnS : Cu : Pb Phosphors 330
V. L. Levshin and B. M. Orlov
Study of Light Sums in the SrS : Eu : Sm Phosphor. II 334
I. B. Keirim-Markus
Study of the Electroluminescence of ZnS-Cu Single Crystals 336
V. E. Oranovskii and B. A. Khmelinin
Optical Properties of Metal Films in the Region of Anomalous Skin Effect 339
Van-Si-Fu, V. P. Silin, and E. P. Fetisov
Thin Film Optics. V. Properties of Silicon 341
M. P. Lisitsa and N. G. Tsvelykh
The Propagation of Light in Absorbing Magnetic Optically Active Isotropic Media and Cubic Crystals 344
B. V. Bokut' and F. I. Fedorov
The Transition Probability in the Schumann-Runge Band System of the O_2 Molecule 346
L. M. Biberman, S. P. Erkovich, and V. N. Soshnikov
On Echelette Theory 347
S. G. Rautian
The Vernier Effect in the Interferometric Measurement of the Thickness of Thick Layers 349
I. N. Shklyarevskii, E. T. Verkhovtseva, and G. N. Polyakova
Candoluminescence and Surface Recombination Luminescence of Phosphors in an Activated Gas Atmosphere 350
A. N. Gorban' and V. A. Sokolov
Influence of Crushing on the Optical and Electrical Properties of Some ZnS Electroluminors 351
E. V. Stauer and M. G. Rosenblat
An Optico-Acoustic Phenomenon in the Ultraviolet Region of the Spectrum 352
Ya. I. Gerlovin
Effect of Foreign Gases on the Absorption of Infrared Radiation by Water Vapours in the Region of an Individual Line in the Band at 2.7 μ 353
K. P. Vasilevsky and B. S. Neporent
Recording Spectra of the Aurora Borealis by Means of a Photoelectric Spectrometer 354
I. G. Frishman
Selectrive Modulation of Radiation by Periodic Variation of Gas Temperature 355
A. O. Sall'
On the Article by M. G. Kaminskii 'Contribution to the "Ballistic" method of Investigation of the Decay of Phosphorescence' 356
B. A. Pyatnitskii
On the Article by L. A. Borovinsky 357
N. V. Kudryavtseva and A. F. Terpugova
Reply to N. V. Kudryavtseva and A. F. Terpugova 358
L. A. Borovinsky